



## Durham E-Theses

---

### *Some new techniques in automated multiple-object fibre spectroscopy*

Lewis, Ian J.

#### How to cite:

---

Lewis, Ian J. (1991) *Some new techniques in automated multiple-object fibre spectroscopy*, Durham theses, Durham University. Available at Durham E-Theses Online: <http://etheses.dur.ac.uk/6204/>

#### Use policy

---

The full-text may be used and/or reproduced, and given to third parties in any format or medium, without prior permission or charge, for personal research or study, educational, or not-for-profit purposes provided that:

- a full bibliographic reference is made to the original source
- a [link](#) is made to the metadata record in Durham E-Theses
- the full-text is not changed in any way

The full-text must not be sold in any format or medium without the formal permission of the copyright holders.

Please consult the [full Durham E-Theses policy](#) for further details.

The copyright of this thesis rests with the author.  
No quotation from it should be published without  
his prior written consent and information derived  
from it should be acknowledged.

# **Some New Techniques in Automated Multiple-Object Fibre Spectroscopy**

by

**Ian J. Lewis**

February 1991

A thesis submitted to the University of Durham  
in accordance with the regulations for admission to the degree of  
Doctor of Philosophy



18 AUG 1992

to my parents

## **Acknowledgements**

I would like to thank Mike Breare and Ian Parry for their guidance and support during the last three years. I would also like to thank John Webster for his technical help and my fellow students for their support. Finally I would like to acknowledge many useful discussions with Peter Gray and Keith Taylor of the Anglo-Australian Observatory.

## Preface

The work reported in this thesis was carried out between 1987 and 1990 while the author was a research student under the supervision of Dr J.M. Breare in the Department of Physics at the University of Durham. None of the material contained has been submitted previously for a degree at this or any other University. Although the some of the work described is part of a collaboration, the author was responsible for the experimental results presented within. Certain results have appeared in the following papers:

Lewis, I.J., and Parry, I.R., Proc. SPIE, **1235**, 754, (1990)

Parry, I.R., and Lewis, I.J., Proc. SPIE, **1235**, 681, (1990)

# Some New Techniques in Automated Multiple-Object Fibre Spectroscopy

Ian J. Lewis

PhD Thesis

February 1991

## Abstract

Multiple-object fibre optic spectroscopy has for several years enabled extensive spectroscopic surveys of faint astronomical objects to be made. In the near future, large fields of view will become available at the prime foci of two UK telescopes, the William Herschel Telescope and the Anglo-Australian Telescope.

Multiple fibre spectroscopy is ideally suited to cover the large fields of view soon to be available at prime focus. In order to apply the technique of multiple fibre spectroscopy to these prime foci, the current technology used in automatic fibre positioners must be improved upon.

As part of this work, a full working instrument has been built to investigate the operational problems associated with an instrument working at prime focus. The technical results from two commissioning runs, and some examples of astronomical results are presented. This work also describes the development of robotic techniques that will enable the simultaneous use of up to 400 fibres, each located to an accuracy of better than  $10\ \mu\text{m}$  rms. This is easily within the tolerance required by the plate scale of the prime focus correctors planned for each telescope.

## Contents

<b>Chapter 1 Multiple Object Spectroscopy</b> . . . . .	1
<b>1.1 Introduction</b> . . . . .	1
<b>1.2 Slitless spectroscopy</b> . . . . .	2
1.2.1 Objective prism spectroscopy . . . . .	2
1.2.2 Multi-colour photometry . . . . .	3
1.2.3 Fabry–Perot interferometry . . . . .	4
<b>1.3 Longslit spectroscopy</b> . . . . .	4
<b>1.4 Multi-slit spectroscopy</b> . . . . .	6
1.4.1 The multiple slit technique . . . . .	6
1.4.2 The Low Dispersion Survey Spectrograph . . . . .	8
1.4.3 Other aperture plate multi-slit instruments . . . . .	9
1.4.4 Reusable multi-slit systems . . . . .	10
<b>1.5 Multiple fibre spectroscopy</b> . . . . .	11
1.5.1 Principles of fibre spectroscopy . . . . .	11
1.5.2 Aperture plate fibre systems . . . . .	13
1.5.3 Automated fibre systems . . . . .	16
<b>1.6 Extending existing techniques</b> . . . . .	19
<b>1.7 Providing a larger telescope field</b> . . . . .	20
<b>1.8 Future fibre fed spectrographs</b> . . . . .	22
<b>1.9 Summary</b> . . . . .	23
<b>Chapter 2 Description of the WHT Autofib Prototype (Autofib–1.5)</b> . . . . .	25
<b>2.1 Introduction</b> . . . . .	25
<b>2.2 Why build a prototype instrument</b> . . . . .	25
<b>2.3 New design features</b> . . . . .	28
2.3.1 Fibre probe design . . . . .	28
2.3.2 Fibre bundle preparation . . . . .	31
2.3.3 Pickup head design . . . . .	34
2.3.4 Sky and fibre viewing head . . . . .	35
2.3.3 Error tables . . . . .	38
<b>2.4 Overall description of Autofib–1.5</b> . . . . .	39
2.4.1 Mechanical design . . . . .	39

2.4.2	Control systems . . . . .	42
2.4.3	Electrical systems . . . . .	45
<b>2.5</b>	Configuration software . . . . .	51
2.5.1	Description of the observing procedure . . . . .	51
2.5.2	Fibre allocation algorithm . . . . .	53
<b>2.6</b>	Control software . . . . .	54
2.6.1	Overview . . . . .	54
2.6.2	Interactive control mode . . . . .	55
2.6.3	File or Automatic control mode . . . . .	56
2.6.4	Engineering control mode . . . . .	57
2.6.5	Instrument mimic display . . . . .	57
2.6.6	Measurements of offsets and errors during calibration . . . . .	59
<b>2.7</b>	Summary . . . . .	60
<b>Chapter 3</b>	Commissioning of Autofib-1.5 . . . . .	61
<b>3.1</b>	Introduction . . . . .	61
<b>3.2</b>	Commissioning, February-March 1989 . . . . .	62
3.2.1	Technical results . . . . .	62
3.2.2	Problems encountered during testing on the telescope . . . . .	63
<b>3.3</b>	Mechanical modifications, 1989-90 . . . . .	67
3.3.1	Mechanical changes to the fibre positioner . . . . .	67
3.3.2	Changes to the fibre module . . . . .	68
3.3.3	Multi-way fibre connectors . . . . .	69
<b>3.4</b>	Software changes, 1989-90 . . . . .	73
3.4.1	Configuration software . . . . .	73
3.4.2	Control software . . . . .	74
<b>3.5</b>	Commissioning, April 1990 . . . . .	75
3.5.1	Telescope setup . . . . .	75
3.5.2	X-Y Carriage . . . . .	78
3.5.3	Fibre module . . . . .	78
3.5.4	Reliability . . . . .	78
3.5.5	Positioning accuracy . . . . .	80
<b>3.6</b>	Application of the current work to Autofib-2 . . . . .	82
<b>Chapter 4</b>	Observing with Autofib-1.5 . . . . .	86
<b>4.1</b>	Introduction . . . . .	86
<b>4.2</b>	March 1989 . . . . .	86



4.2.1 Motivation of observations . . . . .	86
4.2.2 Technical setup . . . . .	87
4.2.3 The observations . . . . .	87
4.2.4 Example results . . . . .	88
4.3 Observations, April 1990 . . . . .	89
4.3.1 Astronomical results from the commissioning run, April 1990	90
4.3.2 The extent of massive dark halos, April 1990 . . . . .	97
4.3.3 Technical setup . . . . .	97
4.3.4 Target field acquisition . . . . .	98
4.3.5 Results . . . . .	99
4.4 Conclusions . . . . .	101
<b>Chapter 5 A new technique for automated fibre positioning . . . . .</b>	<b>102</b>
5.1 Introduction . . . . .	102
5.2 Description of the 2dF prototype . . . . .	103
5.2.1 Mechanical description . . . . .	103
5.2.2 Control of the prototype robot . . . . .	106
5.3 Testing of the 2dF prototype . . . . .	107
5.3.1 Centroiding accuracy . . . . .	107
5.3.2 Accuracy of the X-Y table . . . . .	108
5.3.3 Procedure for positioning fibres . . . . .	108
5.3.4 Overall positioning accuracy . . . . .	109
5.3.5 Speed of operation . . . . .	111
5.3.6 Problems for future work . . . . .	112
5.4 A new 2dF Prototype . . . . .	114
5.4.1 A new fibre probe design . . . . .	114
5.4.2 A new design of gripping robot . . . . .	115
5.4.3 Fibre retraction mechanisms . . . . .	118
5.4.4 Experimental setup . . . . .	122
5.4.5 Initial results . . . . .	124
5.5 Improvements and fine tuning . . . . .	127
5.5.1 A new centroiding software routine . . . . .	127
5.5.2 Fine tuning of the gripper release . . . . .	137
5.5.3 A new fibre placement procedure . . . . .	138
5.5.4 Results using the modified prototype . . . . .	139
5.5.5 Reliability . . . . .	141

5.6 Further work . . . . .	142
5.6.1 Reliability . . . . .	142
5.6.2 Operating speed . . . . .	144
5.7 Summary . . . . .	145
<b>Chapter 6 Handling large numbers of fibres . . . . .</b>	<b>146</b>
6.1 Introduction . . . . .	146
6.2 Specifying the problem . . . . .	147
6.3 Current techniques . . . . .	149
6.4 Description of the simulations for the 2dF facility . . . . .	150
6.5 Results for the fibre array geometry simulations . . . . .	153
6.5.1 Initial results for a simple case . . . . .	153
6.5.2 Pivot geometries . . . . .	156
6.5.3 Object priority distributions . . . . .	161
6.6 Design of the fibre probes . . . . .	161
6.6.1 Expected losses . . . . .	161
6.6.2 Results . . . . .	165
6.7 Simulations for the WHT prime focus instrument (Autofib-2) . . . . .	167
6.7.1 Differences between 2dF and Autofib-2 . . . . .	167
6.7.1 Results of the Autofib-2 simulations . . . . .	170
6.8 Summary . . . . .	172
<b>Chapter 7 Conclusions . . . . .</b>	<b>174</b>
7.1 Overview . . . . .	174
7.2 Design and operational experience . . . . .	175
7.3 Applications to future work . . . . .	176
<b>References . . . . .</b>	<b>177</b>
<b>Appendix A . . . . .</b>	<b>A-1</b>
<b>Appendix B . . . . .</b>	<b>B-1</b>

# 1 Multiple Object Spectroscopy

## 1.1 Introduction

Observing time on large optical telescopes is usually heavily over-subscribed. For example, moonless nights ('dark time') on UK telescopes is in particular demand, with applications for almost three times as much dark time as is available. Therefore, techniques that can offer an improvement in the 'data grabbing' capability of a given telescope have become very popular. Spectroscopy of astronomical objects accounts for a large fraction of telescope time awarded, and is possibly unique in that simultaneous observations of several objects are possible. Methods of obtaining more than one spectrum during a single exposure have enabled observations previously deemed to be uneconomic in telescope time to be undertaken, as well as making more efficient use of the telescope for routine observations. Multiple object spectroscopy (MOS) has particular applications in the gathering of large amounts of data for statistical purposes and in survey astronomy, for example galaxy redshift surveys and the collection of large numbers of stellar radial velocities for galactic astronomy.

Multiple object spectroscopy can be performed in a number of different ways, each with its particular applications and advantages, these techniques may be divided into four groups. Firstly, simple spectroscopy may be performed using the technique of slitless spectroscopy. This may be achieved using an objective prism,



or simply by imaging in several different colour bands (multi-colour photometry). A second technique that allows simultaneous observations of a few objects is longslit spectroscopy. This uses no special instrumentation, but is limited to small numbers of objects in crowded fields. It is to overcome some of the restrictions of longslit spectroscopy, that the technique of multi-slit spectroscopy has been developed. A further technique for multiple object spectroscopy, is that of multiple fibre spectroscopy, where optical fibres are used to couple the spectrograph to the telescope.

In this chapter, brief descriptions of these different approaches are given. The major advantages or disadvantages of the techniques and their possible use on future telescopes are discussed.

## **1.2 Slitless Spectroscopy**

### **1.2.1 Objective prism spectroscopy**

Objective prism spectroscopy probably involves the largest multiplexing gain of any MOS technique. A thin wedge prism covering the entire aperture of the telescope disperses all the point images in the focal plane into small spectra. Unfortunately, because of the difficulty in making large objective prisms, this technique is limited to small aperture telescopes. Objective prism spectroscopy has been particularly successful at the UK Schmidt Telescope in Australia and also at other Schmidt survey telescopes.

Within the large field of a Schmidt telescope, many thousands of spectra may be obtained in a single exposure. However, several difficulties limit the usefulness of the technique, for example, the detector has to cover such a large area that only photographic plates are used. Since the photographic emulsions in use have such a low Detective Quantum Efficiency (DQE) the spectra must be of low dispersion in order that the light available from a small aperture telescope is not spread out too

much. Thus the detector limits the dispersion and with it, the limiting magnitude to which the technique will work.

In order to extract the information contained within each spectrum on the photographic plate, it is necessary to digitise the plate in an automatic plate scanning machine. In the UK machines such as COSMOS at the Royal Observatory Edinburgh and APM at Cambridge have proved particularly successful. When observing crowded star fields, overlap of individual spectra may become a real problem, however, this may be alleviated somewhat by making two exposures of the same field and rotating the objective prism through  $90^\circ$  between them. A comparison of the two plates will then help untangle the spectra of objects in the field.

Since objective prism spectroscopy does not use a slit to cut out background sky, and the only available detector has a low sensitivity, this technique is limited to observations of reasonably pointlike sources. Even with this restriction on target objects, the resolutions offered are only suitable for object classification and low precision redshift work.

### 1.2.2 Multi-colour photometry

While this technique is not really spectroscopy, it can yield useful information about the colour balance of an object. Several images of a starfield are taken through different filters (U,B,V,R,I etc.), the spectral resolution being limited by the bandpass of the individual filters. Whilst it is impractical to perform spectral line identification (as the bandpass of the filters used are larger than any spectral line) this technique can be used for the identification of objects by colour excess, for example, quasars or white dwarfs. However, follow up spectroscopy will be required for a full identification of objects selected by this technique. The follow up spectroscopy may be of the traditional single object type, or for a large number of objects, use another MOS technique.

This technique may be used on any telescope with an imaging capability, the usable field size depending on the telescope design and the physical size of the detector.

### 1.2.3 Fabry–Perot interferometry (TAURUS)

For an extended astronomical object, where different parts of the image arising from the same emission lines can appear at different wavelengths due to doppler shifting of the emission lines, narrow band imaging techniques are required. In order to achieve this TAURUS (Taylor and Atherton, 1980, Atherton *et al*, 1982) utilises a Fabry–Perot etalon to form a very narrow pass band filter centred on the emission line under observation. Images are taken of the target field as the etalon is scanned throughout its free spectral range. In this way a data cube is formed, with x,y as spatial coordinates and the intensity at each wavelength along the z direction. From this data cube the velocity field of a whole image may be determined, which is particularly useful in obtaining the rotation curves of galaxies and the dynamics of planetary nebulae. This type of observation had previously required large amounts of conventional spectroscopic data. As might be expected, because of the large amount of information obtained in a single exposure, complex computer algorithms which require a large amount of computing power are used to analyse the data and remove any instrument effects. This interferometry technique may be adapted for almost any telescope, but has limited application given the very small spectral range available, being particularly useful for observing narrow emission lines such as [O III] and  $H\beta$  in extended images.

### 1.3 Longslit Spectroscopy

The Longslit spectrograph may be used for Multiple Object Spectroscopy. In this case, a conventional longslit spectrograph with a two dimensional detector and instrument rotator to be found at most large telescopes. By careful choice of

objects and slit position angle, the spectrograph slit can be placed so that light from more than one object enters the spectrograph simultaneously (figure 1.1) (Breare *et al*, 1987).

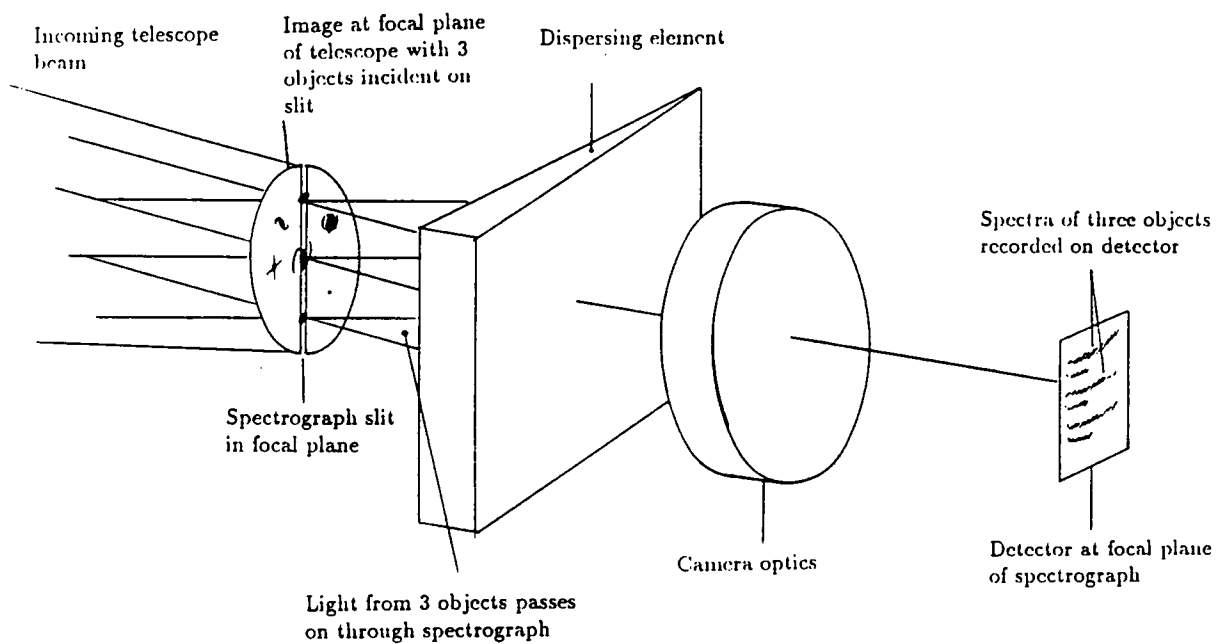


Figure 1.1 Schematic diagram of a longslit spectrograph (FOS) being used for MOS by aligning the spectrograph slit so as to include more than one object.

The usefulness of this technique will of course depend on the density of the objects in the field being observed, and also largely on the luck of the observer that

his chosen objects lie in a straight line. As this method uses no special techniques or instrumentation, it is an easy and inexpensive technique to implement, and can obtain the spectra of up to half a dozen objects at once. All the advantages of slit spectroscopy (limiting magnitude, sky subtraction) as well as spatial information about the objects are retained although care must be taken to avoid overlap of the spectra on the detector.

## 1.4 Multi-slit Spectroscopy

### 1.4.1 The multiple slit technique

This is a combination of the objective prism and longslit techniques, where the sky background has been reduced to a minimum by a mask with a small slit placed at the location of each chosen object (figure 1.2). A grism ( a coarse transmission grating ruled on a prism) or grating covering the whole field provides the dispersion required, the two dimensional result being imaged onto a detector by a fast camera. The field that may be covered by the spectrograph due to vignetting limits the maximum area that may be covered using this technique.

The aperture mask can be made in either of two ways:

- (a) by means of slits cut into a thin metal aperture plate for each object field,
- (b) or by the use of a reusable mechanical multi-slit unit.

Such designs retain many of the advantages of longslit spectroscopy in that they offer good sky subtraction, and the spatial information in the spectra can be used to optimise the extraction of the object signal (Robertson, 1986). In addition the problem of requiring that the target objects are aligned (as in the longslit case) is reduced, as there is much more flexibility in the location of the individual slits. Limitations of this technique include the off axis vignetting of the spectrographs. Hence, specially designed spectrographs with a very wide field of view are required.



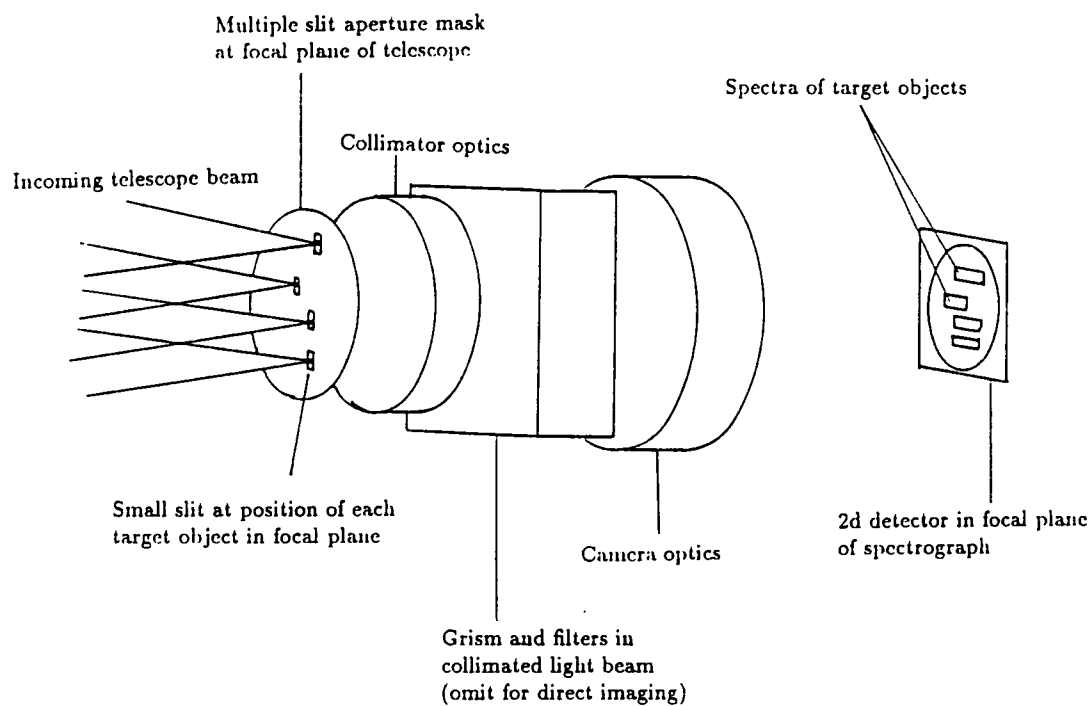


Figure 1.2 Schematic diagram of the multiple slit technique for MOS.

Of course the detector must be large enough to record all the spectra generated by the spectrograph, in practice this usually limits the number of spectra and the dispersion that may be used in any single exposure. Also note that in crowded fields, more than one aperture mask may be required in subsequent exposures to avoid overlapping of the spectra on the detector.

Re-configurable multi-slit devices for existing spectrographs have been described for several telescopes including the Isaac Newton Telescope (INT), William

Herschel Telescope (WHT) and Multiple Mirror Telescope (MMT). As these devices replace the existing slit arrangement with no change to the spectrograph, the field of view and range of dispersions available is dependant on the original spectrograph.

Several examples of dedicated aperture plate multi-slit spectrographs now exist at observatories worldwide. These include at the Anglo-Australian Telescope (AAT) the Low Dispersion Survey Spectrograph (LDSS), at the European Southern Observatory (ESO) the ESO Faint Object Spectrograph and Camera (EFOSC) and at the Canada-France-Hawaii Telescope (CFHT), ESSEFEM. These instruments are now briefly described.

#### 1.4.2 The Low Dispersion Survey Spectrograph

The Low Dispersion Survey Spectrograph (or LDSS) consists of a specially designed collimator/camera with a very large field (12 arcminutes). Image dispersion is obtained by inserting a grism between the collimator and camera. The fully transmitting modular design of LDSS allows a variety of detectors to be used at the external focus. The original LDSS is now a common user instrument at the AAT, whilst a second generation instrument (LDSS-2) is currently under construction for the WHT (Allington-Smith *et al*, 1990).

In theory, it is possible to use LDSS in an imaging mode (no grism) to obtain astrometric information for the production of the aperture plates. Unfortunately the only detector currently capable of covering the entire field of LDSS ( the Image Photon Counting System or IPCS) is unable to image at  $f/2$  without saturating, so plate manufacture following directly on from imaging is not practical. However, in the near future, a micro-channel plate (MCP) intensified IPCS which remains linear whilst receiving a much higher count rate may become available (Fordham *et al*, 1990). This should be able to image over the entire field without

saturating. As an alternative, large format CCDs able to cover the whole field of LDSS are becoming available.

Several techniques exist for the manufacture of aperture plates from astrometric data. Currently a photochemical etching process is used to obtain the accuracy required in the position and quality of the slits. Unfortunately this technique requires special observations consisting of a set of astrometric images of the target fields, several weeks before the LDSS observing run. This allows time to manufacture the aperture masks in plenty of time, but does not allow for any change in the planned observations. Other methods used elsewhere for aperture plate manufacture have included photographic masks (Dressler and Gunn, 1983) and mechanically punched plates (Fort *et al*, 1986) and most recently laser cutting. The latter techniques would enable real time mask manufacture directly after acquiring a direct image of the field.

LDSS is basically a slit spectrograph, and hence very good sky subtraction is possible. This enables observations of objects fainter than the night sky ( $B = 23.5$ ) at dispersions of 164 and 950  $\text{\AA mm}^{-1}$ .

#### 1.4.3 Other aperture plate multi-slit instruments

An instrument based on the multi-slit technique (ESSEFEM) has been built for the Canada-France-Hawaii Telescope (CFHT). This has a very similar design to LDSS, being based on a collimator/camera plus grism, but has a higher dispersion ( $48 \text{\AA mm}^{-1}$ ). To cover a field of 15 arcminutes, a photon counting system utilising four rapid scan CCDs is used. This means that the focal reducer can be used as an imaging device, with the output directly driving a punching machine (PUMA1) for the online production of aperture plates.

A third instrument, the ESO Faint Object Spectrograph and Camera (or EFOSC), offers similar dispersions to LDSS, but over a much smaller field (3.6

by 4.5 arcminutes ). This field is easily covered by a CCD detector and therefore when being used in a camera mode, EFOSC can provide astrometric data to drive a punching machine (PUMA2 ) (Dupin, Fort *et al*, 1987). Once aperture plates have been punched, EFOSC allows them to be loaded 11 at a time, thus providing almost uninterrupted observing.

#### 1.4.4 Reusable multi-slit systems

An alternative to aperture plate multi-slit spectroscopy is to have a system in which a series of slits are mechanically moved around the focal plane of the telescope. If the movement of these slits can be automated then we would have a reusable aperture plate thus enabling realtime decisions to be made about the observing program.

A manual multi-slit unit with 10 slits is available at the INT (Ellis *et al*, 1986) which covers a field of 4 by 1 arcminutes (using the Intermediate Dispersion Spectrograph). The position of the slits are chosen by a computer program which assesses the coordinates of all the objects in the field and their priority, and tries to find the 'best' position for the instrument rotator and each individual slit. However, even with large numbers of objects in the field of view of the spectrograph, it is difficult to configure more than two sets of objects that will optimally fill all 10 slits.

Movement of the slits to the positions indicated by the computer program is currently achieved manually, by placing the multi-slit unit on a XY Coradograph machine and measuring the position of each slit as it is moved into place using micrometer screws. The time taken to set up a field by an experienced observer is of the order of 30 minutes.

An automated version of this instrument has been described for the triple spectrograph (ISIS and FOS) of the WHT (Breare *et al*, 1986 ) which should

enable much more rapid slit configuration, however this will not remove all of the limitations of this type of device, for example the limited field size. Also, for small numbers of objects, configuration difficulties mean that some slits may not be used, thus reducing the overall multiplex advantage.

A further reusable multiple slit unit (FOGS) is in operation at the MMT (Geary *et al*, 1986). This instrument consists of 8 reflective slides in the focal plane of the telescope, each with a 18 by 1.5 arcsecond slit. The reflective surface of the slide is angled to allow off-slit viewing with a TV camera for alignment of the individual slits and for field acquisition. The individual slides can be moved longitudinally by 8 stepper motors in 50  $\mu\text{m}$  steps (approximately 0.2 arcsec). The spectrograph used with FOGS is a high efficiency, modular system giving moderate to low spectral resolution with a choice of 3 gratings, covering a field approximately 3 by 4 arcminutes.

## 1.5 Multiple Fibre Spectroscopy

### 1.5.1 Principles of fibre spectroscopy

Optical fibres were first used in astronomical spectroscopy to link the light obtained at a telescope focus to an off-telescope spectrograph (Hubbard *et al*, 1979). Obviously, if the light from a single object can be collected in this way, then the light from more than one object can be collected using individual fibres and distributed to separate spectrographs. Alternatively, if a two dimensional detector is available, several fibre outputs may be aligned along the slit of a single spectrograph (figure 1.3), each giving a spectrum with dispersion perpendicular to the slit axis.

The second method is the most practical way of using fibres to obtain the spectra of many objects simultaneously (although more than one spectrograph may be used when the number of fibres exceeds that which may be accommodated

along the spectrograph slit). The advantage of this type of MOS is that it can use a standard spectrograph (probably already in existence) that can be mounted either on or off the telescope. The usual method of holding the fibres at the spectrograph is to mount them in a block which holds the fibres in a line, this block then plugs directly into the spectrograph replacing the slit.

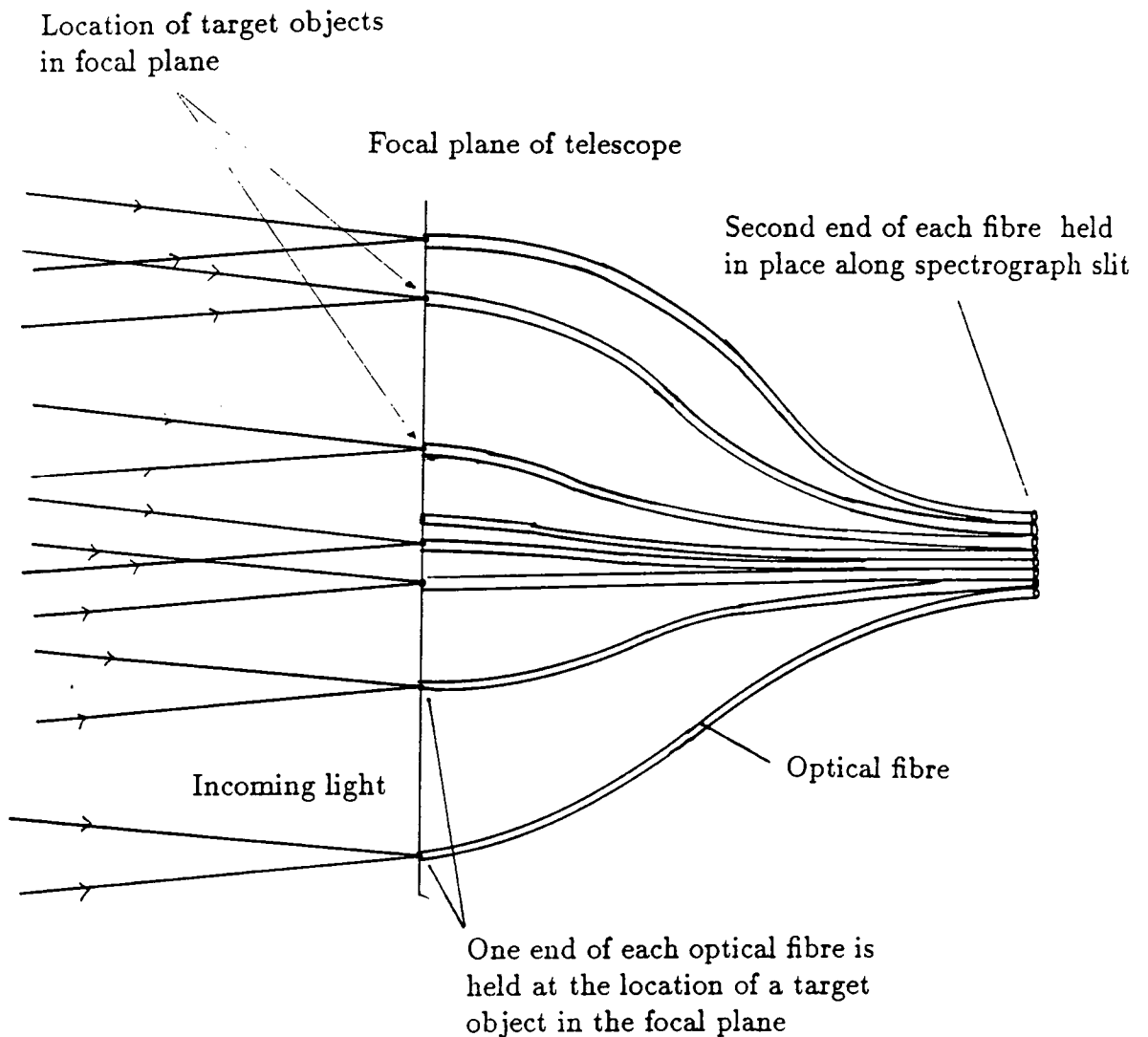


Figure 1.3 Schematic diagram of a multiple fibre feed for a spectrograph.

At the focal plane of the telescope, each fibre must be held at the location of an object for the duration of the observation. This creates problems because of the high positional accuracy required and the need to change the locations of the fibres for each different target field. Two main types of fibre location system have evolved, the aperture plate 'plug-in' type, and the automated fibre positioner type.

The limiting magnitude of fibre spectroscopy is currently determined by the accuracy of the sky subtraction. The inability to sky-subtract with sufficient accuracy (Ellis and Parry, 1987) limits observations to objects brighter than the night sky. This is because optical fibres scramble the image of object +sky, thus making it impossible to 'sky subtract' the spectrum in the same way as for a slit spectrograph. Therefore, separate fibres are dedicated to sample just the sky. However the 'sky' fibres are not sampling the same sky as in the object position, and positional variation in the sky background may then limit the sky subtraction. Also, any movement of the fibre due to changes in the telescope attitude may cause a variation in the fibre response. As not all the fibres may experience exactly the same effect, it will become very difficult to compare and subtract individual spectra. This, and other systematic errors (Parry and Carrasco, 1990) limit the signal to noise ratio for deep fibre spectroscopy.

### 1.5.2 Aperture-plate fibre systems

The aperture-plate method consists of a plate (often brass) held exactly in the focal plane with small holes drilled at the locations of the objects to be observed. Each fibre is terminated in a small ferrule which is simply plugged into the holes in the aperture plate by hand (figure 1.4). Of course a different aperture plate must be provided for each target field, which can prove expensive and time consuming

if the astronomer is observing large numbers of relatively bright objects during a night.

The aperture plates are drilled using astrometric data obtained from CCD images or by scanning photographic plates. As with LDSS, the reliance on pre-manufactured aperture plates means that observations must be very carefully pre-planned. Aperture plate fibre systems are currently available at several observatories, including FOCAP at the AAT (Gray, 1983, Gray and Sharples, 1985, Gray, 1986), OPTOPUS at the ESO (Lund and Enard, 1983, D'Odorico, 1985), NESSIE at Kitt Peak (Barden and Massey, 1988) and MEDUSA at Steward Observatory (Hill *et al*, 1980) all having 50–100 fibres.

A second variation on the aperture plate method (FLAIR) has been devised for use at the UK Schmidt Telescope (Watson, 1986). In its initial configuration, a heavily exposed positive copy of a Schmidt photographic plate is made. This copy has the property that it is transparent at each image on the plate. It is then a simple matter to glue the ends of the fibres onto the images of objects to be observed, thus eliminating the need for accurate astrometric data. Because of the large field of a Schmidt telescope, where thousands of images are formed, there is a possibility of several hundred or a thousand fibres linking the focal plane to one or more specially designed spectrographs.

A second version of FLAIR named PANACHE (Watson, 1988) has been designed to overcome some of the deficiencies of FLAIR. In this version the fibres are mounted on the front surface of the photographic plate, using a microprism to fold the light into the fibre which is taped to the surface of the plate. This allows more efficient coverage of the field area, as well as increased throughput of the light to the spectrograph. The number of fibres available is limited by the length of the spectrograph slit ( $\sim 70$  fibres using two small spectrographs) and the manpower required to set each field up on the glass plates.



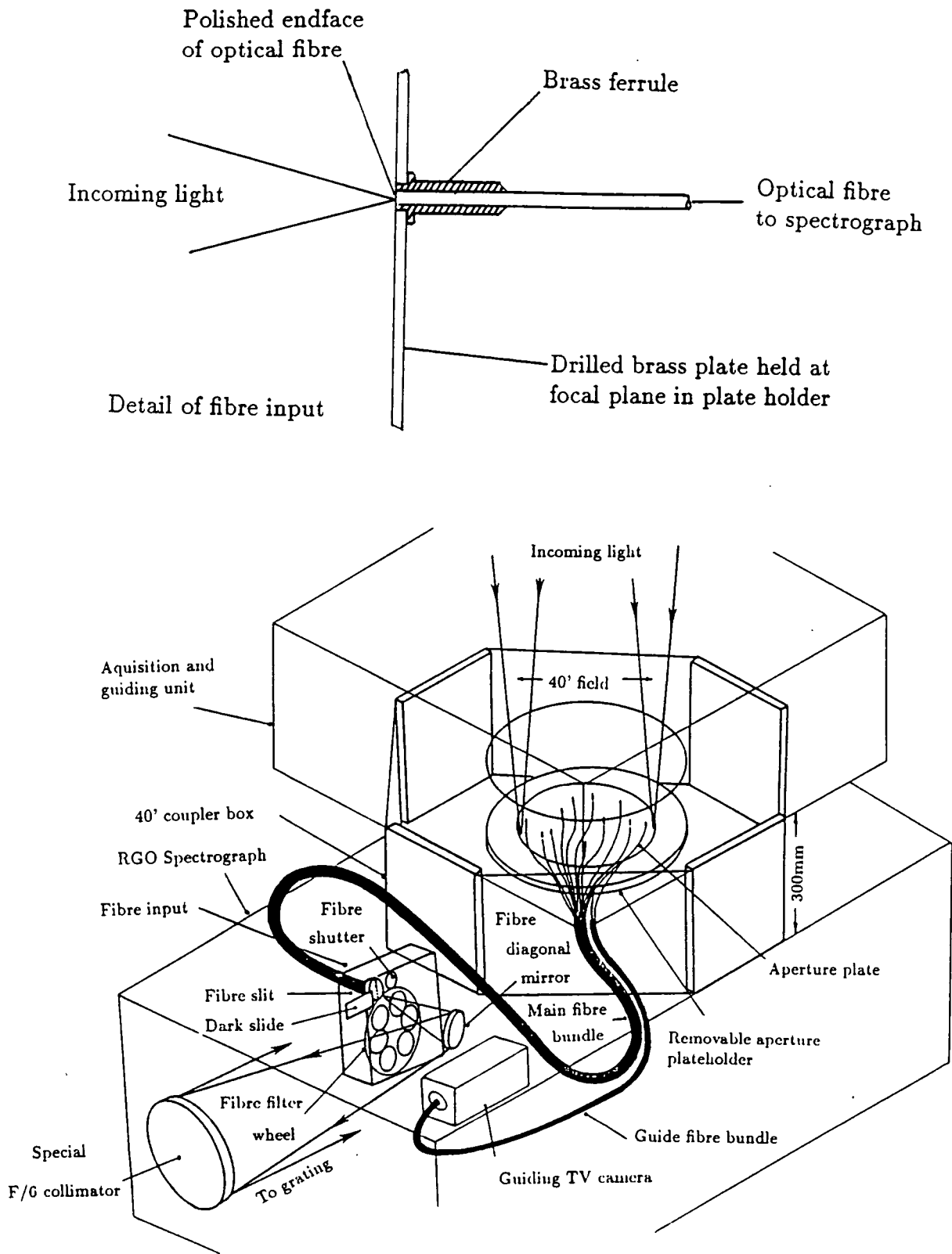


Figure 1.4 Schematic diagram of the AAO Fibre System (FOCAP), and detail of a single fibre termination.

### 1.5.3 Automated fibre systems

Automated fibre positioners such as those in operation at the Steward Observatories (MX) (Hill and Lesser, 1986, Hill and Lesser, 1987) and the AAT (AUTOFIB) (Parry, 1986, Parry and Gray, 1986, Parry and Sharples, 1988) only differ from the aperture plate type in the way that the fibres are positioned and held in place in the telescope focal plane. Fully automated systems allow much greater versatility during observing, allowing advantage to be taken of the current weather conditions, and provide much more accurate positioning by allowing for non-constant effects such as refraction in the atmosphere. In addition it is possible that a well engineered automatic fibre system will be more stable and less susceptible to systematic errors (due for example to fibre movement during an exposure) than a plug plate fibre system.

The MX spectrometer uses a robot positioner for each pair of fibres (one object and one sky) to move the fibres to the correct position, and then to hold them in place (figure 1.5). This requires two controlled degrees of freedom for each pair of fibres, and therefore rapidly becomes prohibitively expensive for large numbers of fibres. The main advantage of this system is that the time taken to reconfigure the field is extremely small, as each positioner can move simultaneously. Also it is possible to 'search' for objects whose coordinates are not accurately known.

AUTOFIB is a different solution to the same problem. All the fibres are moved individually by the same robot positioner, then held in place on a steel field plate by small permanent magnets (figure 1.6). Because only a single robot is used, it is possible to make it extremely fast, yet less expensive than a large number of MX positioners. Also it is possible to construct the instrument in two sections, one half containing the robotic positioner, and the other a 'fibre module' containing the fibres and field plate. This allows interchange of different fibre modules if it is

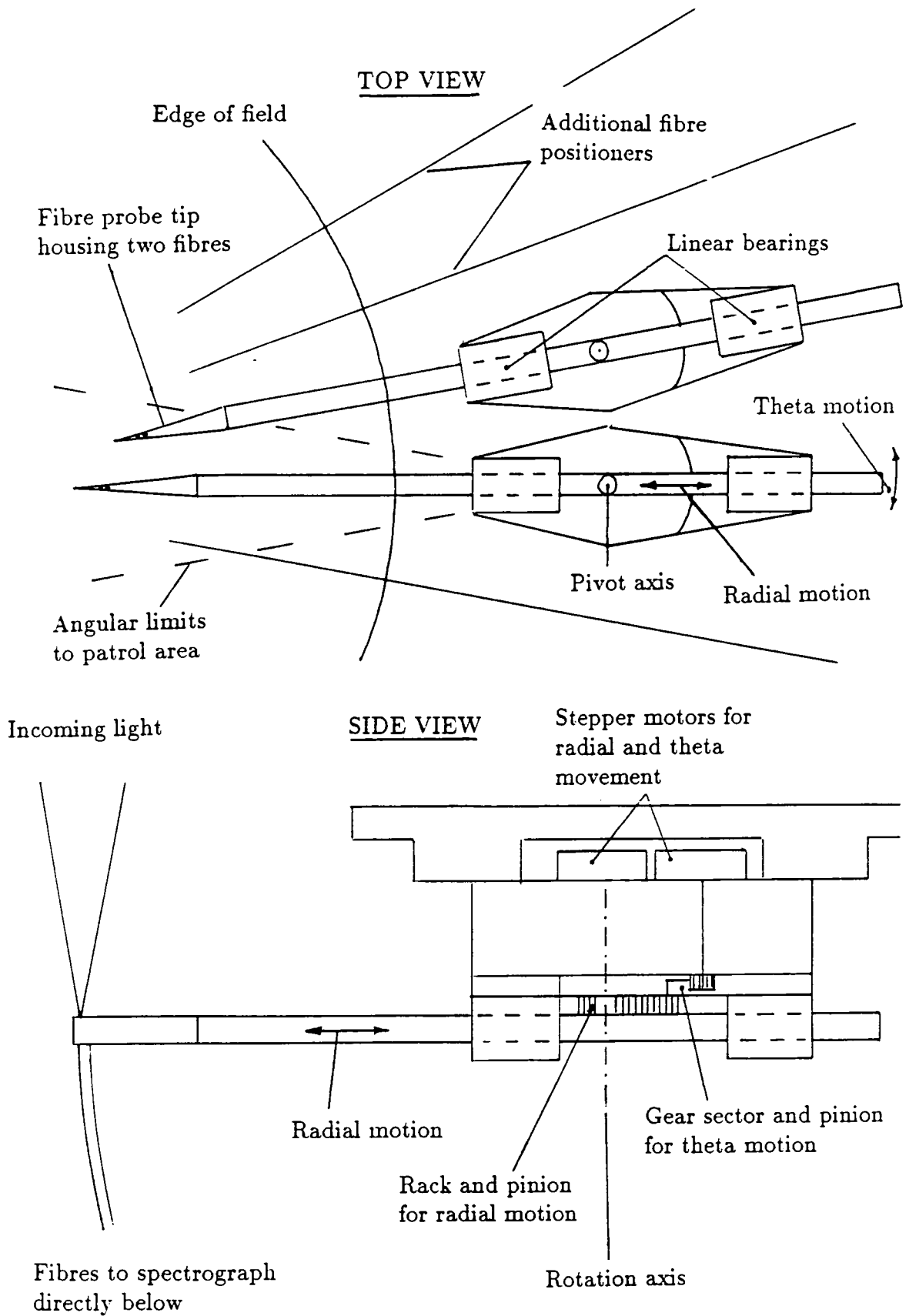


Figure 1.5 Schematic diagram of the MX Spectrometer.

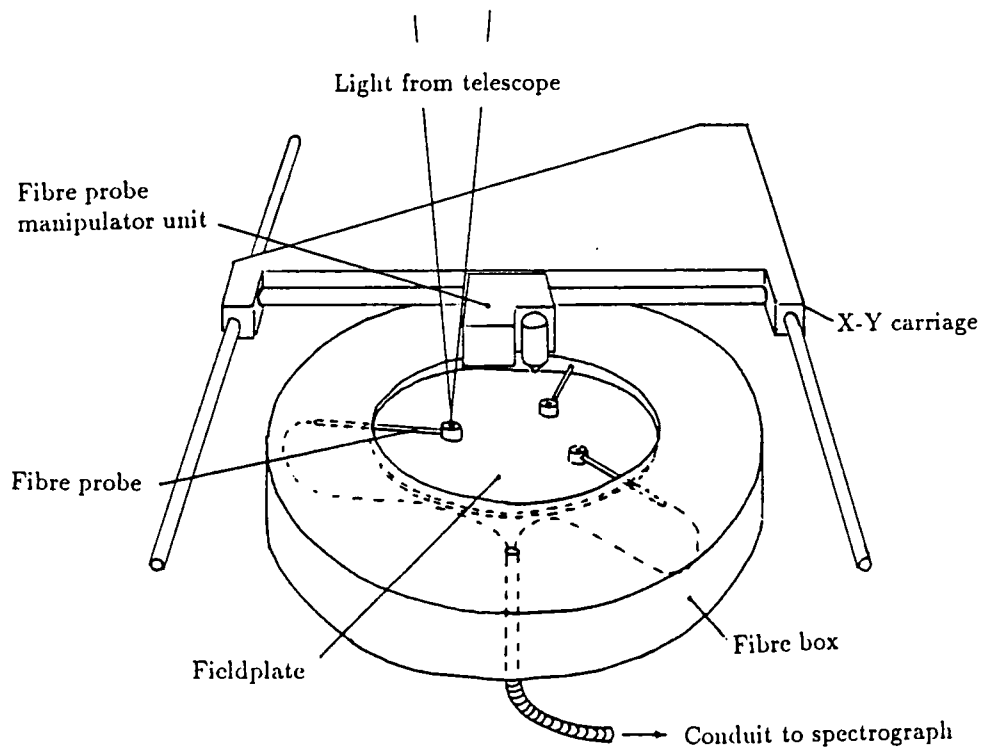


Figure 1.6 Schematic diagram of the Autofib concept of automated fibre positioner.

required to change the fibre size to match current seeing conditions, or to match the type of project: stellar or extragalactic.

Disadvantages of the Autofib concept include the fact that there are no dedicated sky fibres in close proximity to the object fibres. Furthermore, because a single positioner has to locate all 64 fibres, the time taken to reconfigure the field (approximately 6–10 minutes) is necessarily longer than that for MX. However, this is not unduly long when compared to the time taken to slew the telescope.

These disadvantages are to be weighed against large savings in cost and much greater versatility over MX. It will be a simple matter to increase the number of fibres at a later date simply by changing the fibre module half of the instrument and reprogramming the robot positioner.

Both the MX and Autofib concepts have proved popular at other observatories around the world. Instruments under construction based on MX include ARGUS at CTIO (Ingerson, 1988) and MEDISIS (Felenbok *et al*, 1988). Instruments based on Autofib include HYDRA at Kitt Peak (Barden and Rudeen, 1990), the Norris spectrograph at Palomar Observatory (Cohen *et al*, 1988, Hamilton, 1990) and AMOS at Lick Observatory (Craig *et al*, 1988, Brodie *et al*, 1990).

In comparing the manual and automated systems it should be remembered that the aperture plate systems can position fibres much closer together which is an advantage in very crowded fields. However, automated systems do not require such a long leadtime when planning observations (thus allowing last minute changes to the observing programme) and are much less expensive to support in the long term (a single brass plate can cost typically 200 A\$). A further long term advantage of an automated fibre system is that the fibres themselves are likely to last much longer as they are only handled by humans during their manufacture and not during day to day operation. Such protection of the delicate fibres is important as an instrument will undergo a large amount of possibly rough handling in the telescope environment.

## 1.6 Extending existing techniques

The preceding sections have described various methods for increasing the efficiency with which astronomical spectroscopic data may be obtained. However for many applications it is desirable that even more data is acquired. One way of achieving this (if the object density is high enough) is to develop the above techniques so as to increase the multiplex gain for the same field size. As already

mentioned some of the above techniques reach a limit where they no longer offer any improvement in crowded fields (eg LDSS).

Another alternative is to increase the size of the telescope field of view to include more objects. This is useful if the surface density of the objects is not particularly high. Again some of the techniques in previous sections encounter difficulties, for example, limitations on spectrograph design prevent much scaling up to cover a larger field. Also current detector size would limit the increase in field size that could be used (this is already a constraint at cassegrain).

These limitations can in some way be overcome by the use of a fibre feed to cover an extended field, with the fibres feeding a spectrograph (or two smaller ones) located off the telescope to reduce design difficulties. An increased multiplex gain would then arise by simply increasing the number of fibres to cover a larger field.

### **1.7 Providing a larger telescope field**

The field available at cassegrain at most telescopes is limited to less than 30 arcminutes by the off axis image quality, and vignetting due to geometrical constraints. The cassegrain focus of the AAT has a respectable field size of 40 arcminutes due to its unusual optical design, but with no prospect of increasing this any further.

If the prime focus is considered, the telescope beam is much faster ( $f/3$ , or faster for recent telescopes) and has much less severe geometrical constraints, meaning that the prime foci is capable of providing a much larger field than is available a cassegrain focus. However, a suitable Prime Focus Corrector (PFC) is required to provide good images over the complete field.

Prime focus correctors were originally used to provide a large useable field for astronomical photography, the AAT being provided with a PFC giving a full  $1^\circ$

field. However a complication arises if it is required that the PFC should provide a wide field for spectroscopy. This complication is caused by the refractive nature of the atmosphere, and is termed atmospheric dispersion, point images at the edge of the field being dispersed into small spectra. Typically when taking a photographic image, filters are used to limit the wavelength coverage and atmospheric dispersion of the pointlike images does not pose a problem. However when we are interested in obtaining spectroscopic data over a wide wavelength range, we find that the image of the star or galaxy is dispersed in wavelength so that the spectrograph slit or optical fibre only samples one particular part of the image. This will lead to inaccuracies in flux calibrating the resulting spectra, and in severe cases even prevent the astronomer from being able to assign a colour to the object (Taylor and Gray, 1990).

It is to prevent this difficulty that PFC's designed to provide a spectroscopic wide field may include an Atmospheric Dispersion Corrector (ADC) (Wynne and Worswick, 1986). However, this does not preclude the use of such a PFC for photographic use. An ADC consists of two rotating prisms, usually incorporated into the front elements of the corrector to reduce the number of air-glass interfaces. The prisms have their position angle set to exactly counteract the atmospheric dispersion of the images over the whole field. As the telescope tracks the field, the atmospheric dispersion changes and the ADC elements must be continually moved to provide the required correction.

The PFC design for the WHT provides a  $1^\circ$  field with an ADC and is therefore suitable for spectroscopic use. However the original  $1^\circ$  corrector at the AAT does not have an ADC and is therefore not particularly useful for spectroscopic purposes. A new corrector with ADC is currently under development for the AAT's prime focus. The constraints on image quality have been relaxed slightly to provide a full  $2^\circ$  field. The slight loss of image quality is not critical for spectroscopic purposes if an optical fibre feed is used, as the image is scrambled inside the fibre.

## 1.8 Future fibre fed spectrographs

Considering the large fields which will be made available at the WHT and AAT, the question arises as to what is the best way to provide for the acquisition of spectroscopic data? Some of the difficulties of applying existing techniques to a larger field have been mentioned already, but a fully automated fibre feed to a spectrograph has several distinct advantages, five of which are worthy of note.

- A fibre optic feed is essentially a field reformatter, and spectrographs can be designed to accept a relatively small line of fibres along the central slit rather than the entire field, whilst still retaining the ability to access the whole field.
- If a fibre fed spectrograph is bench mounted off the telescope, its mechanical design is greatly simplified and flexure problems eliminated, resulting in an extremely stable spectrograph.
- Since a fibre feed reformats the target field, the only constraint on the maximum surface density of objects that may be observed is that a fibre probe must be placed on each object.
- The number of available fibres and their size may be changed by using a different fibre module.
- The faster focal ratio of the prime focus telescope beam is much better suited to fibre spectroscopy than the slower cassegrain beam. This is because the beam suffers less focal ratio degradation (FRD) at faster focal ratios.

Of course, a fibre optic feed does have disadvantages as a prime focus instrument when compared to existing instruments at cassegrain. The smaller plate scale requires that smaller fibres are used, and these fibres must be positioned with much higher accuracy. If we wish to exploit the increased numbers of target objects in the larger field at prime focus, the number of fibres must be increased



significantly. This would limit the choice of fibre positioner to the AUTOFIB design, as it would be impossible to increase the number of fibres very much with the MX approach. Existing fibre positioners have less than 180 fibres, but up to 400 fibres are planned to cover the proposed  $2^\circ$  field of the AAT. However, there is currently no experience in handling such large numbers of fibres. This presents problems on two fronts, from the astronomer's point of view, as he has to decide on the optimum way of assigning the fibres to his target objects, and from the instrumentation side, as the fibres must be moved in the most efficient way without tangling, or loss of position.

Although the faster focal ratio at prime focus is better preserved after transmission through an optical fibre, the spectrograph must now be designed to accept a much faster focal ratio beam. Such design considerations are not trivial, and may require that the output beam of the fibre is converted using a microlens to a slower focal ratio before entering the spectrograph.

If a spectrograph is to be located off the telescope (as for the fibre spectrograph WYFFOS which is to be located on the Nasmyth platform of the WHT) then long (25–30m) fibres are required to reach from prime focus to the spectrograph, the operational and technical problems of such a system are as yet unknown (existing instruments have short (2–3m) fibres).

## 1.9 Summary

It is toward solutions to some of the problems mentioned above that current work proceeds. The work contained in this thesis forms part of the research and development of a fibre positioning system (Autofib-2) for the WHT and the fibre feed for the proposed  $2^\circ$  field for the AAT (a facility to be known as the 2dF).

In chapters 2,3 and 4, the design and operational considerations for a prime focus fibre system are described with application to a prototype instrument built as

a test bed and commissioned at the cassegrain focus of the WHT. The requirement for a high speed and high accuracy fibre positioning system is investigated in chapter 5. Chapter 6 contains an investigation into handling large numbers of fibres for future instruments. Finally, chapter 7 brings together the work of the previous chapters, and applies it to future instruments.

## **2 Description of the WHT Autofib Prototype (Autofib-1.5)**

### **2.1 Introduction**

The concept of a “pick and place” robot to manipulate optical fibres in the focal plane of a telescope has already been described in detail (Parry, PhD Thesis, Parry and Gray, 1986, Parry and Sharples, 1988). In this chapter I will give a brief overall description of an instrument (Autofib-1.5) built as a prototype for the common user instrument (Autofib-2) planned for the prime focus of the WHT, with more detail of the new features and modifications made to the original design. This description applies to the prototype instrument as it existed for a commissioning run in February 1989, subsequent modifications are detailed in chapter 3.

### **2.2 Why build a prototype instrument ?**

The Autofib system currently in use at the AAT (hereafter referred to as Autofib-1) works at a plate scale of  $150 \mu\text{m} / \text{arcsec}$ , likewise, the various fibre optic feeds of the Autofib type currently under construction at Lick, Palomar and Kitt Peak all work at fairly large plate scales ( $86$ ,  $400$  and  $150 \mu\text{m} / \text{arcsec}$  respectively). Experience with Autofib-1 at the AAT has shown that with the use of error tables it is possible to position the fibres into an observing ‘field’ with an accuracy of  $30 \mu\text{m}$  rms quite routinely, and by taking extreme care  $25 \mu\text{m}$  rms may be achieved. This accuracy represents less than  $0.2$  arc second for the cassegrain

systems mentioned, and only 0.33 arc second for the Lick prime focus system. This accuracy is of the same order as the reliability of the coordinates obtained during routine scanning of Schmidt Survey plates on measuring machines such as COSMOS and the APM. However, this accuracy will not be good enough for the new prime focus instrument for the WHT with its much smaller plate scale.

The prime focus corrector (PFC) design currently under construction for the WHT has a field of view of  $1^\circ$  (40 arcminutes unvignetted) with a plate scale of  $57 \mu\text{m} / \text{arcsec}$ . Thus the current performance of Autofib-1 would only place fibres to within 0.5 arcsec at the new plate scale. Clearly to achieve a satisfactory 0.2 arcsec rms positional accuracy, different techniques are required to handle the fibres to improve on the  $30 \mu\text{m}$  currently achieved. Another significant feature of the PFC design is that the back focal distance is only 110 mm. This imposes the additional constraint on the design of the fibre positioner that the robotic fibre handler must be thin enough to fit between the rear element of the corrector and the focal plane where the fibres are placed (figure 2.1).

Another issue requiring investigation is that of the closest approach of two fibres, or the minimum separation between two target objects that may be successfully acquired. This has long been an issue at the AAT where the 4mm diameter buttons housing the end of the fibre and prism of Autofib-1 impose a minimum separation of 27 arcsec. This minimum separation does not compare very favourably with the manual fibre system FOCAP (minimum object separation 19 arcsec) and for some projects FOCAP might be chosen in preference to Autofib-1 for this reason. A similar fibre probe design used at prime focus would impose an unacceptable limit for closest approach of over 70 arcseconds.

Considering that the corrector design will give a field of  $1^\circ$ , resulting in a large increase in the numbers of astronomical objects available as target objects, the operating speed of the robot should be increased. With such an increase, the

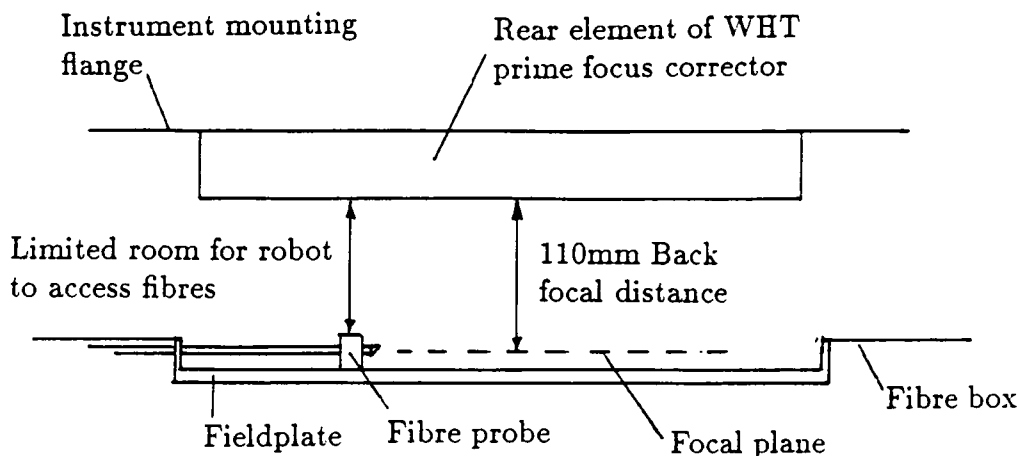


Figure 2.1 Relation of the fibre positioner to the prime focus corrector and telescope focal plane.

robot can handle many more fibres without unreasonably increasing the time to set up each field configuration. Also, if we are to greatly increase the numbers of fibres then we must pay some attention to the reliability of the Autofib positioning system, with particular attention to the elimination of pickup-putdown operation failures. As the new WHT instrument will be located at the more inaccessible prime focus (cf Autofib-1 at cassegrain at the AAT) the new instrument must have the ability to recover from an error state without manual intervention.

The new version of Autofib for the WHT prime focus (Autofib-2) must embody the operational requirements outlined above. In order to investigate the feasibility of some of these ideas, a prototype fibre positioner (Autofib 1.5) has been built for the cassegrain focus of the WHT, the prime focus not being available until 1992.

## 2.3 New design features

### 2.3.1 Fibre probe design

To try and alleviate some of the problems of working at a very small plate scale, the design of the fibre probes has been changed to reduce the minimum fibre to fibre separation to 1.5mm (7 arcsec at cassegrain and 30 arcsec at prime focus on the WHT). The fibre-microprism assembly now projects from the button by 6mm, the button merely acting as a handle for the robot to pick up the fibre (see figure 2.2). As on Autofib-1, the fibre is contained inside hypodermic stainless steel tubing and is terminated at the polished end by a micro-prism. Incoming light is then reflected through 90° and into the fibre which is held parallel to the focal plane. Once again, the fibres are held in position on a steel plate with small permanent SmCo magnets in the underside of the button. The microprisms do not have a silvered hypotenuse, as the f/11 cassegrain telescope beam is slow enough to be totally internally reflected, however for a fibre probe at prime focus, the prisms will have to be silvered to completely reflect the faster beam.

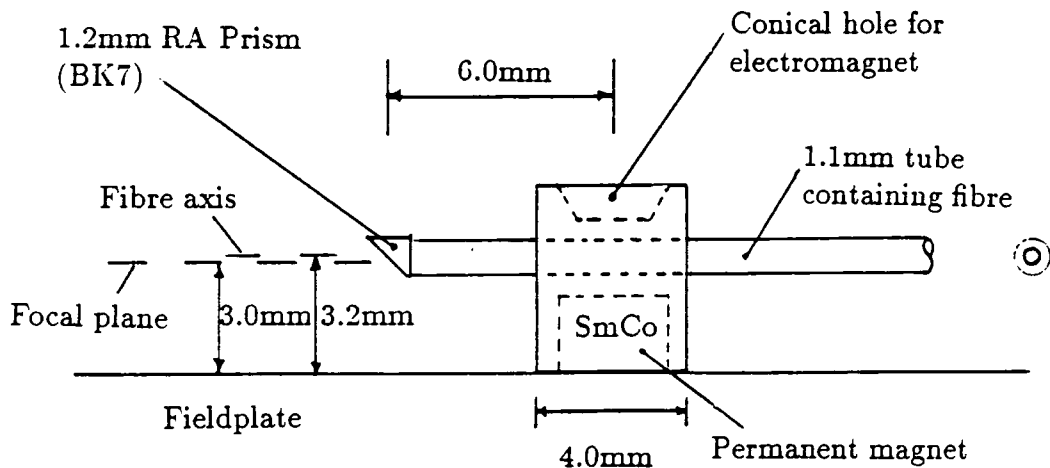


Figure 2.2 Design of the spectroscopic fibre probes

The fibre used in the construction of the fibre probes is Polymicro Technologies FHP 260  $\mu\text{m}$  core, 320  $\mu\text{m}$  outside diameter, this was an optical fibre manufactured specially to our specifications. This diameter fibre was chosen to exactly match the inside diameter of Gauge 23 hypodermic stainless steel tubing (a useful side effect of this high tolerance fit became apparent at a later stage, see section 3.3). Although this fibre is only 1.2 arcseconds in diameter at the cassegrain plate scale, it was felt that the prototype should be constructed using a small fibre size in terms of arcseconds because this would highlight any positioning errors more clearly.

A major consequence of the change in design of the fibre probe from that used in Autofib-1.5, is that the button position is no longer equivalent to the fibre position. As all of the fibre probes contain small manufacturing errors we cannot consider each one to be a straight line, so to avoid problems we introduce a new pair of coordinates, those of the fibre tip. The position of the fibre probe is then completely described by three pairs of coordinates: pivot, button and fibre tip. These three coordinates contain all the necessary information about the fibre probe, including any manufacturing errors.

The fibre-fibre anti-collision algorithm in the configuration and control software also increases in complexity slightly to allow for the protruding fibre. The instrument control software still requires both the button and fibre tip coordinates. The button coordinates when moving fibres, and the fibre tip coordinates when checking that the fibres are at their correct positions using the viewing head and CCD TV camera (section 2.3.4).

In addition to the spectroscopic fibres just described, a second set of 6 fibres (the guide fibres) are arranged around the fieldplate and feed a TV camera. These fibres can be placed at the locations of fiducial stars and are used to acquire and guide on the target field. The guide fibres follow the design of a coherent bundle of seven fibres used in Autofib-1. In order to improve the ability to acquire a

sufficient number of guide stars, the guide fibres are set at a slightly higher level to allow them to cross the spectroscopic fibres without collisions occurring. The guide fibres use a different design of microprism so that the guide fibre images are parfocal with the spectroscopic fibres (figure 2.3).

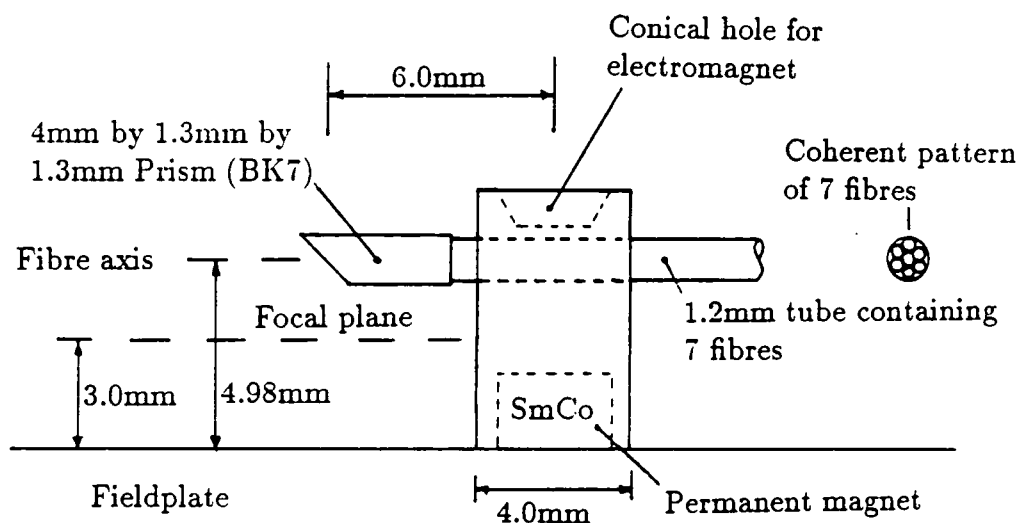


Figure 2.3 Design of the guide fibre probes

The fibre buttons were manufactured by an outside contractor, resulting in a batch of 200 individual buttons all supposedly to the required tolerance. As the fit of the conical tip of the electromagnet in the conical hole of the button lies at the heart of the mechanism whereby repeatability is achieved, exceptionally tight tolerances are required ( $\pm 0.025\text{mm}$ ). The size of the conical hole in the top of the buttons was measured for each button, and all 200 graded according to the size of the hole. In this way 66 buttons with the same sized hole were chosen from



the original 200. The conical tip of the electromagnet was then modified to fit the chosen button hole size.

### 2.3.2 Fibre bundle preparation

Each fibre probe consists of a 14m length of optical fibre terminated at both ends with a 25mm length of gauge 23 hypodermic stainless steel tubing. The tubing is held in place using Araldite epoxy resin as this had a reasonable pot life (approximately 30 minutes) before the glue became unworkable, and also gave good Focal Ratio Degradation (FRD) performance.

At one end of the fibre, a second tube 313mm long was glued outside the first. This outer tube protects the fibre from damage between the pivot and the prism and also acts to hold the fibre in a straight line between the pivot and button to allow the anti-collision software to predict the path of the fibre between the pivot and prism. The second end of the fibre was left with just a single tube in place, ready for polishing and to form part of the fibre 'slit' at the spectrograph. With all the hypodermic tubing glued in place, each end of the fibre was polished. To aid in the polishing process, a small polishing jig was designed to allow up to 20 fibres to be polished simultaneously on a automatic lapping machine (figure 2.4).

The procedure for polishing each group of 20 fibres was as follows. Firstly the rough ends of the tubes were trimmed to the same length and squared up using wet and dry abrasive paper, working from the coarsest to the finest (500 to 1200 grit). Next, each set of fibres were polished using a series of aluminium oxide lapping films, with grades from 30  $\mu\text{m}$  to 0.3  $\mu\text{m}$  . Approximately 10 minutes was spent on the coarser papers, increasing to 30 minutes for the finest ones. The polishing surface was lubricated at all times using a proprietary polishing fluid.

At each stage in the polishing process, the fibres were inspected under a specially designed microscope, the objective of which looked upwards at the newly



Figure 2.4 Photograph showing the polishing jig in use

polished face of the fibres as they were swung across from the lapping machine. A final check was made on the quality of the polished fibre before gluing the microprism in place.

After sliding the fibre button onto the longer of the stainless steel tubes (the fibre probe end), the tube and fibre was held in place in a jig by a magnetic clamp, and viewed from the side by a microscope (figure 2.5). Next, a small drop of UV curing adhesive (Vitalit 7105) was placed onto the polished fibre end and the prism placed onto the adhesive using tweezers. The prism was then aligned by looking through the microscope and nudging the prism using the tweezers, before fixing in place using a UV light. The prepared face of the fibre was finally checked

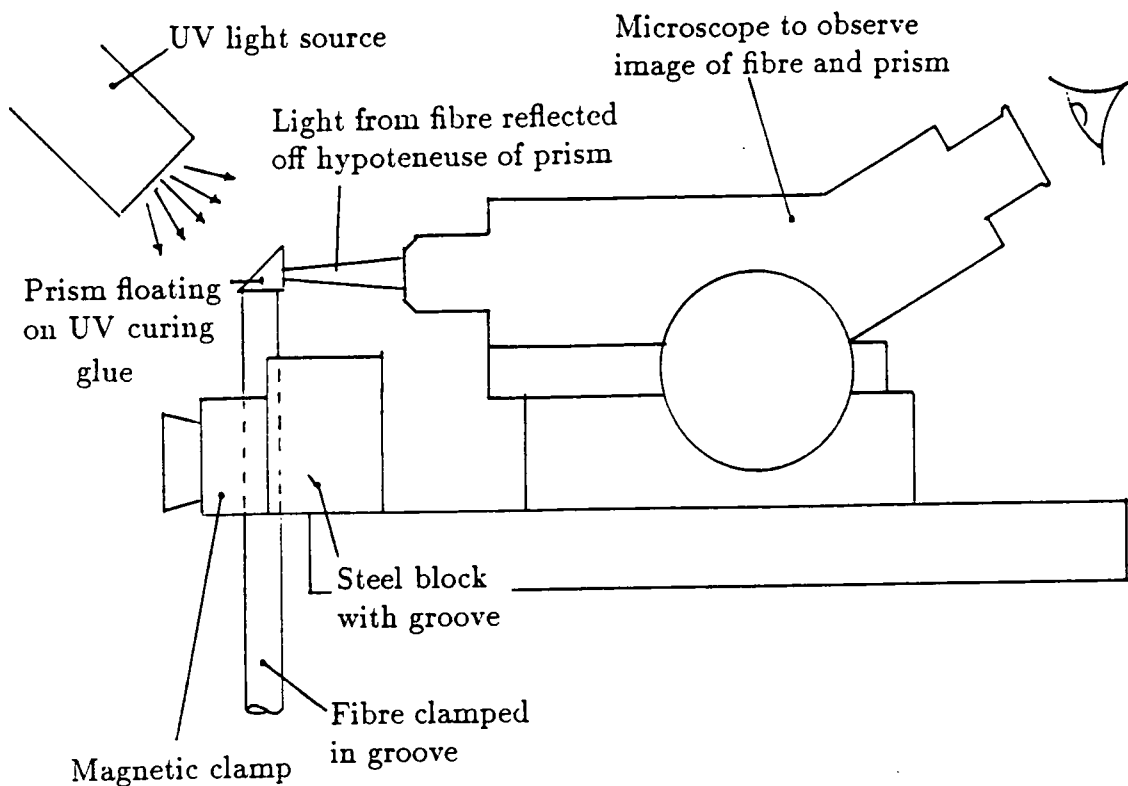


Figure 2.5 Assembly of the fibre probes

by rotating the fibre in the clamp and observing the polished fibre end through a reflection off the prism hypotenuse.

The final step in the preparation of the fibre probe was the fixing of the fibre button to the stainless steel tube. This was achieved by placing the button on a steel jig (the button being held in place by its SmCo magnet) and butting the prism against an end stop to set the protrusion of the prism from the button. Laser light was shone into the fibre from the slit end, and with the projected beam viewed on the ceiling of the lab, the long stainless steel tube could be twisted to ensure that the beam emerged perpendicular to the fieldplate. The tube was then fixed into the button using a second type of UV curing cement (Vitalit 4280).

### 2.3.3 Pickup head design

Although similar instruments to Autofib-1, currently being built in the USA, use gripper type devices to pickup the fibres, it was decided for reasons of simplicity to retain the basic idea of an electromagnetic pickup head, and to determine whether we are already at the limit of accuracy for the self-centering conical magnet design. In order to improve the reliability of the pickup and putdown operation which has caused some problems at the AAT, the electromagnet was redesigned to improve the magnetic flux obtained between the pole pieces. In addition, a pressure sensing device was added to the electromagnet to provide information about the success or failure of pickup thus enabling remedial action to be taken automatically. The pressure sensor works by constantly monitoring the pressure in a pipe that is sucking air through the pole pieces of the electromagnet. When a button is present on the electromagnet, the gap between the pole pieces is effectively sealed and the pressure in the tube drops. By checking the pressure at critical points during normal operation, the control software can determine if the pickup or putdown operation has been successful.

Because of the space limitations, the concept of the whole pickup head has been redesigned to make it more compact than that on the AAT instrument. To reduce the height of the pickup head to within the allowed back focal distance, the Z axis motor and lead-screw assembly is folded, with the motor parallel to the lead-screw. The motor is coupled to the lead-screw via a pair of spur gears (figure 2.6). The electromagnet is mounted on a crossed roller linear bearing, and is moved in Z by a spring loaded leadnut on the Z axis lead-screw. Two microswitches remove power from the Z motor in the event of the linear bearing running into the limits of its travel. A third microswitch removes power if the lead nut becomes overloaded. This will occur if the magnet is driven into the button too far and compresses the lead nut spring. In practice this automatic cutout is

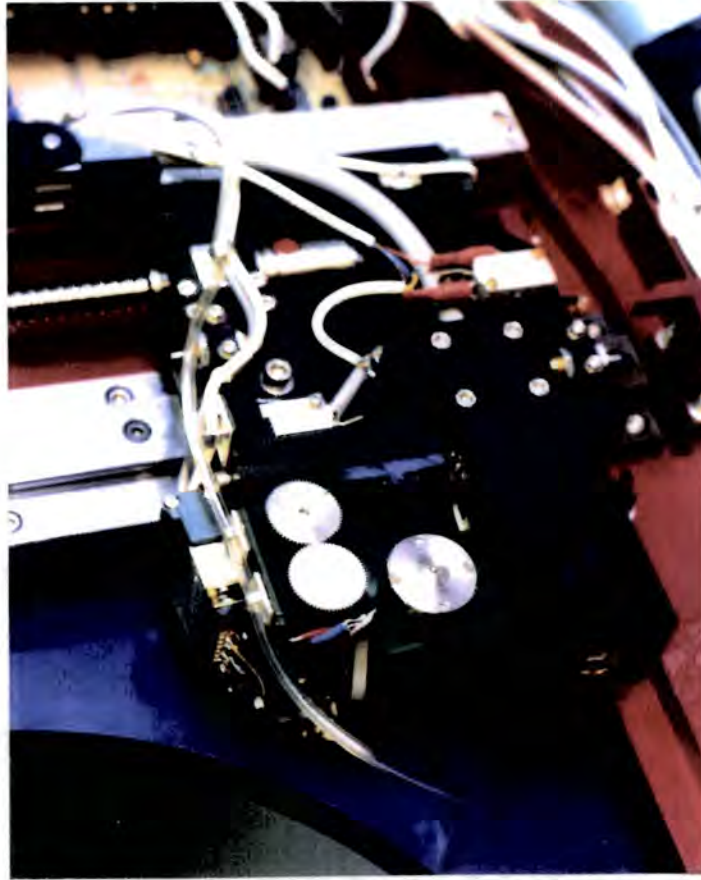


Figure 2.6 Photograph showing the new pickup head

used during pickup operations to ensure that the same force is always used to centre the button on the electromagnets conical tip.

#### 2.3.4 Sky and fibre viewing head

An improvement to Autofib-1 that was fitted during and after the instrument was commissioned, are TV cameras, one looking up at the sky, the other down at the fibres (which may be back illuminated from the spectrograph slit). The cameras can be used to measure the plate scale, measure error table values for the individual fibres, acquire fields, and check on the positional accuracy of the fibre placement. Unfortunately these cameras cannot cover the complete 40 arcminutes field of the AAT as they were fitted after completion of the instrument, and the X-Y carriage does not have enough travel to allow full access for the cameras. On

the WHT Prototype instrument a viewing head has been included that can cover the complete field of the instrument and that is capable of looking both at the sky and the back illuminated fibres simultaneously with a single TV camera. By ensuring that the images of the back illuminated fibre and star are parfocal then it follows that if the star image is in focus on the TV camera, the star will also be focussed in the plane of the fibres. In this manner the telescope focus may be adjusted using the viewing head. As the image of the viewing head is formed inside the positioner, where space would not allow a sensitive TV camera to be fitted, the image is brought to a more accessible point by a flexible coherent fibre bundle or image guide.

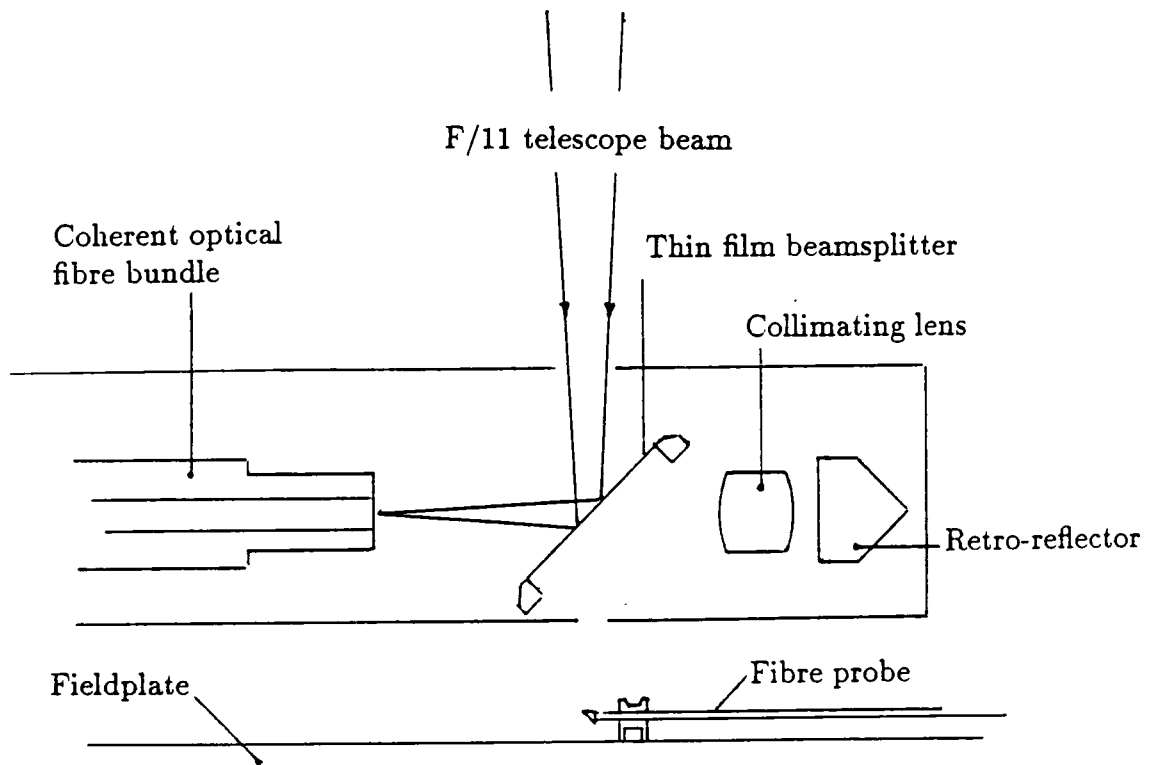


Figure 2.7 Viewing head with optical path for viewing the sky.

To avoid any ghost images, a thin film beam-splitter was chosen which transmits and reflects 50% of the incident light. The star light is directed onto the coherent fibre bundle with a single reflection in order to avoid losing too much light on faint images (figure 2.7).

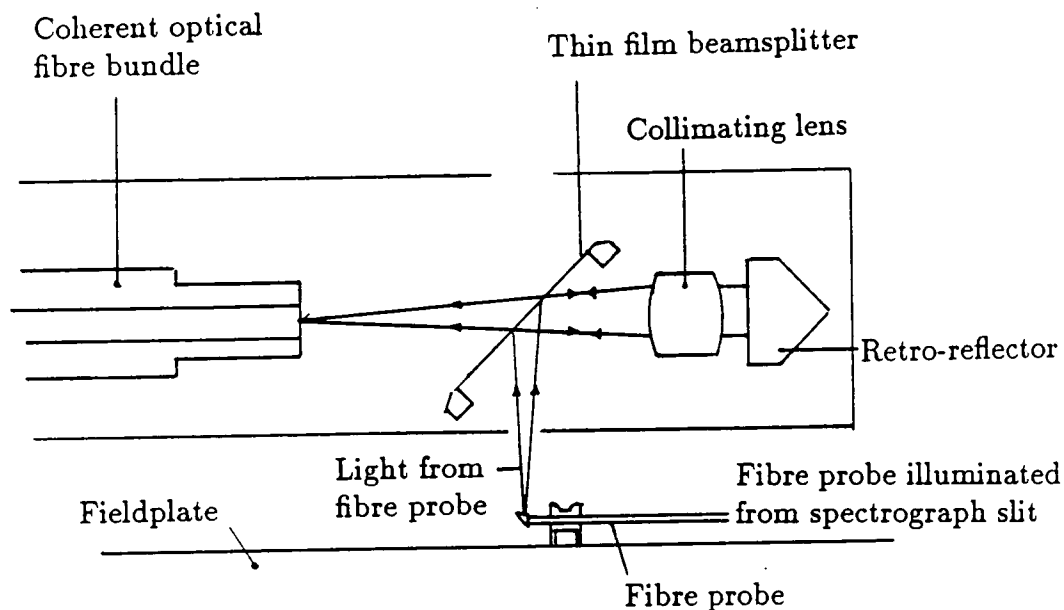


Figure 2.8 Viewing head with optical path for viewing a back illuminated fibre.

The back illuminated fibre illuminates the coherent bundle by a less efficient (and more tortuous) route as we can supply as much light as is required by artificial means. Light from the fibre is reflected from the beam-splitter through a collimating lens and onto a retro-reflector. The collimated light returns from the retro-reflector back through the lens and through the beam-splitter, onto the coherent bundle (figure 2.8). A retro-reflector is used in preference to a mirror

as it has the property that collimated incident light is returned in the same direction. Therefore, if the viewing head is moved when viewing a star and fibre simultaneously, the images of the star and fibre will move in the same direction.

### 2.3.5 Error tables

The AAT Autofib uses a system of lookup error tables to improve the accuracy with which fibres are placed in the focal plane. Each fibre probe has a unique error due to imperfections in the manufacturing process. This is tabulated as a x-y offset from an ideal fibre probe, this offset is added to the object position to obtain the required probe position. Placing a fibre at the corrected probe position should then place the fibre exactly over the object position. The error lookup table can be generated prior to observing, and should remain constant for a given set of fibres. In practice however, this system of correcting fibre positions only works to an accuracy of approximately 30  $\mu\text{m}$  rms. If a new error table is generated for every field to be observed ( i.e. a field specific error table ) the overall accuracy of fibre positioning improves to approximately 25  $\mu\text{m}$  rms.

The reason for this improvement can be seen in figure 2.9 by comparing the cartesian error offset to an error offset in the coordinate frame of the fibre ( $l,b$ ). Although the  $l,b$  error offset is the same for both cases a) and b), the resulting cartesian error offsets ( $dx,dy$ ) and ( $dx',dy'$ ) are very different. The change in the required cartesian error offset, if measured at one angle and used at another angle, may be as large as 6% for a change in angle of 20°. If a single error table value of ( $dx,dy$ ) is used for each fibre, then with typical manufacturing errors of 100-200  $\mu\text{m}$  , the error due to moving the fibre to a location other than that where the error table was measured would become significant.

As already mentioned, positioning accuracy may be significantly improved by the use of field dependent error tables. However, if this improvement is due to inaccuracies in the original error table, then the use of an  $l,b$  error table would



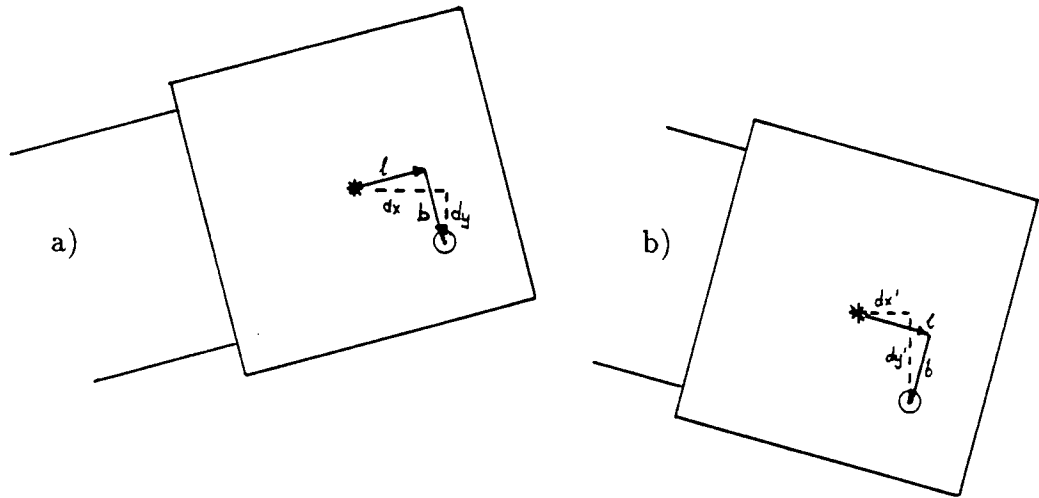


Figure 2.9 Comparison of error table schemes. A tip of a fibre probe is shown at its extreme angular limits. The star represents the location of the fibre in the prism for a perfect case, the circle the actual location of the fibre for a probe with a manufacturing error  $l, b$ .

avoid the need to generate a field specific error table. This simplification in the use of an error table is at the cost of an increase in the complexity of the software required to handle the error table corrections (namely the control and configuration software). The “ $l, b$ ” form of error table has been adopted for Autofib 1.5.

## 2.4 Overall description of Autofib-1.5

### 2.4.1 Mechanical design

In many respects the overall mechanical design of Autofib-1.5 is very similar to Autofib-1. The main part of the instrument consists of two subsystems stacked one on top of the other: namely the robot positioner mounted directly on the telescope, and secondly, the fibre module below. In addition to these, the control

electronics and the acquisition and guiding (A & G) TV interface are mounted in the telescope electronics racks.

The top half of the instrument is the "pick-and-place" robot which positions the fibres in the required locations one at a time. The robot consists of an X-Y table which carries the viewing head and an electromagnetic gripper which may be moved in the Z direction in order to lift a fibre above any others when being moved from one position to another.

The main support of the instrument is a 19 mm thick piece of aluminium toolplate which bolts directly to the telescope instrument mounting interface. All of the components of the X-Y table hang from this top plate, as do the six fibre module support legs.

The layout of the X-Y table has been redesigned from the Autofib-1 concept to help in reducing the thickness of the instrument to less than the back focal distance of the new prime focus corrector. In particular, the Y axis motor is at the opposite end of the Y axis compared to Autofib-1, and the large X axis motor is mounted into a hole in the top plate to reduce the height of the motor axis and ballscrew from the top plate. These design changes were not necessary for Autofib-1.5 which was to operate at the cassegrain focus, but it provided useful practice for Autofib-2 which is to operate within a limited space envelope at prime focus.

The X-Y carriage is constructed from standard machine tool components. Crossed roller recirculating linear bearings are used on both axes, their hardened steel tracks being linear to better than  $10 \mu\text{m}$ . Each axis is driven by a DC servo motor via a ballscrew. Preloaded double ballnuts convert the rotary motion to a linear one, whilst eliminating backlash entirely. The system is protected from end stop crashes by limit switches and mechanical shock absorbers.

The pickup head electromagnet moves in the Z direction on a small linear bearing with 30 mm travel. The Z axis is also DC servo driven (another departure from the Autofib-1 design), with a rotary incremental encoder on the motor. A simple leadscrew provides the coupling between the motor and linear bearing, a spring loaded leadnut ensures that the fibres are placed on the field plate with a controlled vertical pressure.

The lower half of the instrument is the fibre module, this consists of a mild steel field plate (on which the fibres are placed) which sits on three legs on kinematic seats for adjustment. This assembly is bolted firmly to a support frame which itself is bolted directly to the six fibre module support legs hanging from the fibre positioner.

The field plate consists of a disc of mild steel with a thin wall on a 600mm diameter around its periphery. Around this wall are 72 equi-spaced holes through which the 14m long fibres are passed. The holes act as pivots for the stainless steel tubes enclosing the first part of each fibre. The rest of the fibre loops back under the fieldplate to a conduit which protects all of the fibres as far as the spectrograph. The radius of the pivots has been deliberately chosen to be larger than that on the AAT Autofib in order to reduce the angle that the fibre makes with the fieldplate when being moved around by the robot. If this angle is large, the natural springiness of the fibre probe acts to lever the button from the pickup head. Experience with the AAT Autofib has shown that when the buttons are picked up from near the periphery of the field more pickup failures occur, as this is where the fibre-fieldplate angle is largest. Increasing the pivot radius reduces the angle at all points in the field. The whole fibre assembly (fibres and fieldplate) is contained within a disc shaped aluminium box for protection (figure 2.10). To aid with the initial loading of the fibres into the fibre module a thin ring of aluminium with a 4.2mm hole for each fibre button is attached to the fieldplate. This load

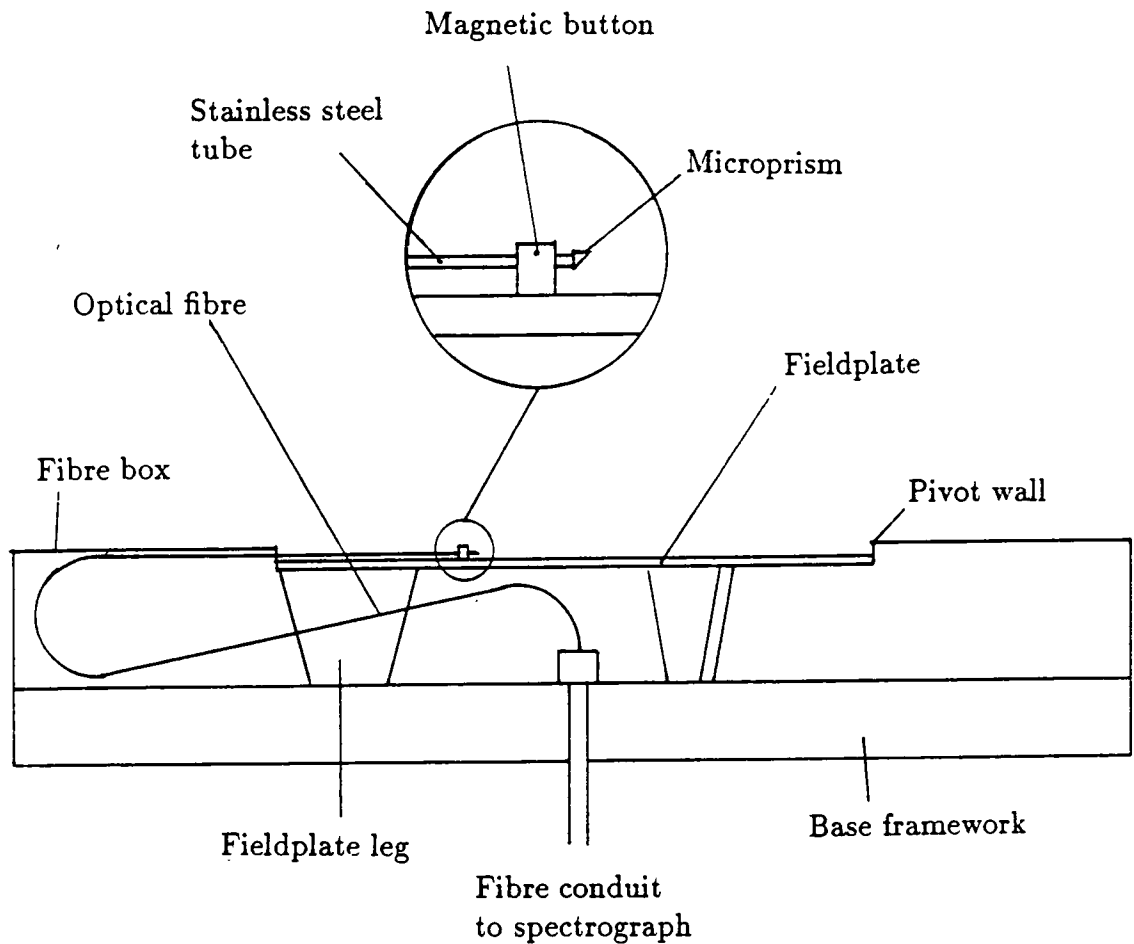


Figure 2.10 Schematic side view of fibre module

ring provides a reference point for loading each fibre, from which the fibre can be located using the viewing head system.

#### 2.4.2 Control systems

The instrument control computer is a Compac Deskpro 20/e, PC compatible, which controls the whole instrument in a stand alone mode, i.e. it does not interact with any other instrument or telescope control computer. Control of the 3 DC servo motors is by an intelligent 3 axis motor control card (Galil DMC430-10)

which fits into an expansion slot in the PC and uses the PC as a host computer. A second expansion card in the host PC is a general purpose input and output (I/O) card containing a 12 bit analogue to digital converter and an 8 bit digital to analogue processor for the monitoring of the status of various instrument functions and for basic control of some other functions.

Data files containing the positional information for every fibre for each target field are transferred to the PC from the Vax data reduction computer where they are generated by the configuration software (section 2.5) via an RS232 serial link. A VT200 emulator program is used to log on to the Vax while the instrument is in a 'safe' condition (during the day or, during a long exposure when the robot may be powered down as fibres are not being moved). Kermit file transfer software is then used to transfer the ASCII data files to the hard disk of the PC, ready for use from within the instrument control software.

The general purpose I/O card monitors and controls three functions of the robotic positioner. One channel of the analogue to digital (a/d) converter monitors the voltage generated by the pressure sensor in the pickup head, allowing the control software to decide if the fibre button is present on the electromagnet or not. The digital to analogue (d/a) processor is configured as an output device and by writing the appropriate number to the device the eight TTL output bits may be controlled. Two bits of the d/a processor are used to control the electromagnet and the the relay that switches power to the X and Y axis motors.

Communication between the host computer and the Galil card is by simple ASCII character instructions. The instructions are generated and sent by the software controlling the instrument which also performs all the necessary handshaking and checking. Direct communication is also possible using a diagnostic program, but in normal use it is not necessary to communicate with the Galil card in this manner.

The Galil card controls all motion of the robotic positioner, including velocity, acceleration of the movements of each of the three axes, and the stability of the feedback loop used to control the servoing of each motor. Positional feedback to the Galil card is provided by two linear optical encoders for the X and Y axes, and a rotary encoder (on the motor itself) for the Z axis. The encoders have a resolution of  $1 \mu\text{m}$  (X and Y axes) and  $1.25 \mu\text{m}$  for the Z axis.

The Galil controller is operated in a deadband mode. In this mode the controller constantly monitors the current encoder position and if the position error exceeds a deadband value, the motors are servoed to reduce the position error to within the deadband. The deadband is currently set to  $2 \mu\text{m}$ .

All of the encoders are of the incremental type, so an external datum point is used to define the origin of each axis. For the X and Y axes the TTL transition caused by the obscuration of an optoswitch provides the reference mark. This TTL transition is fed directly to the Galil card which has a 'find edge' command to move the X or Y axis in the correct direction to find the transition, thus enabling the origin to be found rapidly from any point in the robot's X or Y travel.

The external reference point used to define the origin of the Z axis encoder is the upper of two end of travel limit switches. The Z axis is driven very slowly into the upper limit switch, which automatically removes power from the motor to prevent any further motion in the same direction (but will allow movement in the return direction). When the Z axis times out because it is not moving, this position is defined as  $Z = -500$ . Next the Z axis is immediately moved in a downward direction to  $Z = 0$ , after which the control software prevents the pickup head from being allowed to travel to negative Z.

### 2.4.3 Electrical systems

Figure 2.11 shows a block diagram of the instrument and its control system. The instrument control computer remains in the telescope control room during observations, and is connected to the instrument and its electronics at the cassegrain focus by a standard 50-way twisted pair cable and four coaxial cables. These cables run from the control room to the telescope instruments via the building, telescope pier and finally the cassegrain cable wrap, a length of approximately 100 metres.

All TTL signals are sent between the host computer and the instrument using line drivers to convert the TTL level to an inverted pair of signals over a twisted pair of wires, thus making the signals less vulnerable to electrical noise. This is particularly important when the host computer is monitoring pulses from the encoders during movement of any of the motors, Noise on the encoder signal might be interpreted as extra pulses, causing the Galil card to stop the motion in the wrong place or, in the worst case, cause the motor to runaway violently.

Coaxial cables are used to carry the four analogue voltages to and from the instrument. The signal voltage from the pickup head pressure transducer is sent back to the general purpose I/O card in the host computer, and the Galil card sends three command voltages (X,Y,Z) to the servo amplifier over the remaining coaxial cables.

The servo amplifier is a pulse width modulated servo drive amplifier, which switches at 18 kHz to simulate voltages between  $\pm 24$  V. The voltage and current required for each motor are generated by the amplifier from the command voltage (from the Galil card). The output from the amplifier is carried by a heavily screened cable directly to the motors in the instrument.

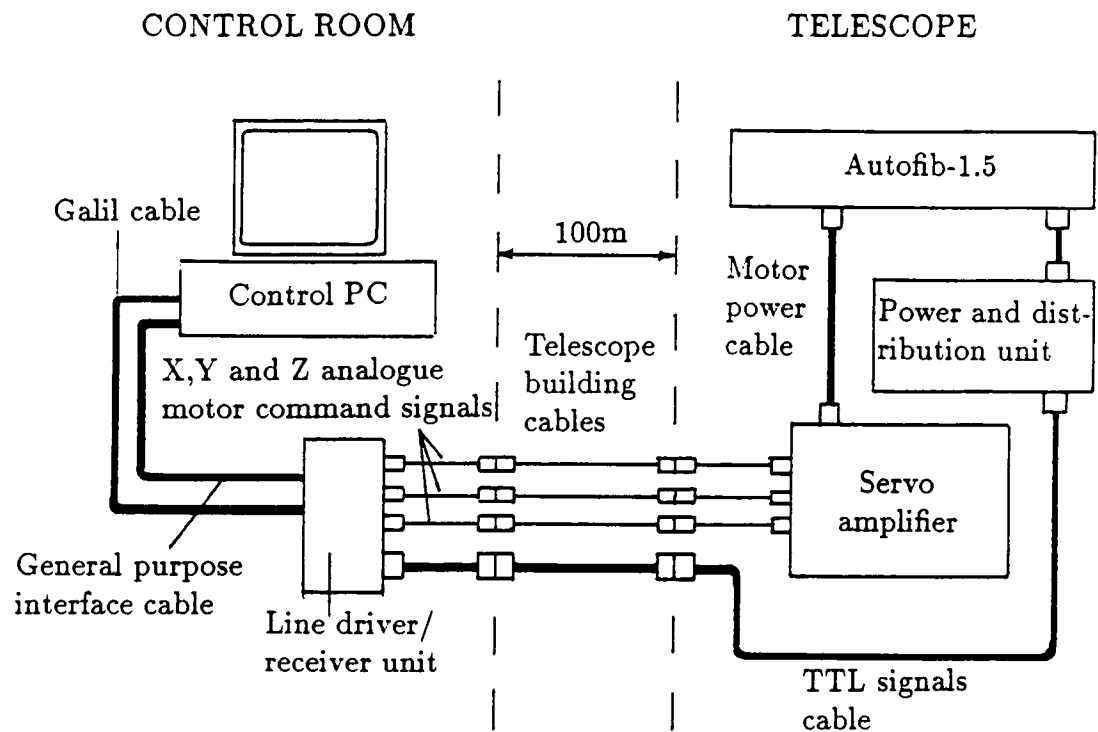


Figure 2.11 Block diagram of instrument control system.

The power and distribution box contains a multiple voltage power supply for the circuitry within the instrument. The 50-way cable from the host computer (via the telescope cables) is connected to this box and redirected to the instrument together with the required voltage supplies.

Within the instrument, the electrical systems may be divided into two sections:

Control related electrical systems,

Instrument protection devices.



## Control related electrical systems

The electronics for the X,Y linear encoders are supplied with the encoders, and provide TTL pulses for the Galil card. The only modification was to add a simple circuit to each encoder which sends each of the encoder pulses as an inverted pair of signals using a line driver. A matching line receiver circuit is used to reconvert the pulses at the control computer.

The output from the Z axis encoder is a pair of sine waves in quadrature. This has to be converted into a series of TTL pulses for the Galil card, which means that the pulses may be sent to the Galil card via a standard line driver circuit.

The electromagnet is switched on and off by the level of a TTL voltage (5 V is magnet on, 0 V is magnet off). The TTL voltage is fed to a circuit which uses it to switch a 24 V supply on or off. Due to the length of time required for the electromagnetic field to dissipate when the TTL voltage drops to zero volts, a simple circuit based on a Wien bridge is used to rapidly reduce the electromagnetic field and prevent any permanent magnetic field building up in the electromagnet core. This works by applying an exponentially decaying sine wave voltage across the electromagnet when it is switched off, starting at +24V and then switching rapidly between +Ve and -Ve whilst decaying (figure 2.12).

To sense the presence or absence of a fibre button on the electromagnet, air is sucked through the pole pieces of the electromagnet (figure 2.13). If a button is present the pressure in the tube drops as the gap between the pole pieces is effectively blocked. The pressure in the tube is measured relative to atmospheric pressure using a piezo-electric pressure sensor with a differential voltage output. This output voltage is then amplified using two 741 operational amplifiers to between 0 and 10 volts to give a easily measurable voltage change. This pressure signal is sent to the a/d converter in the host computer via a coaxial cable.

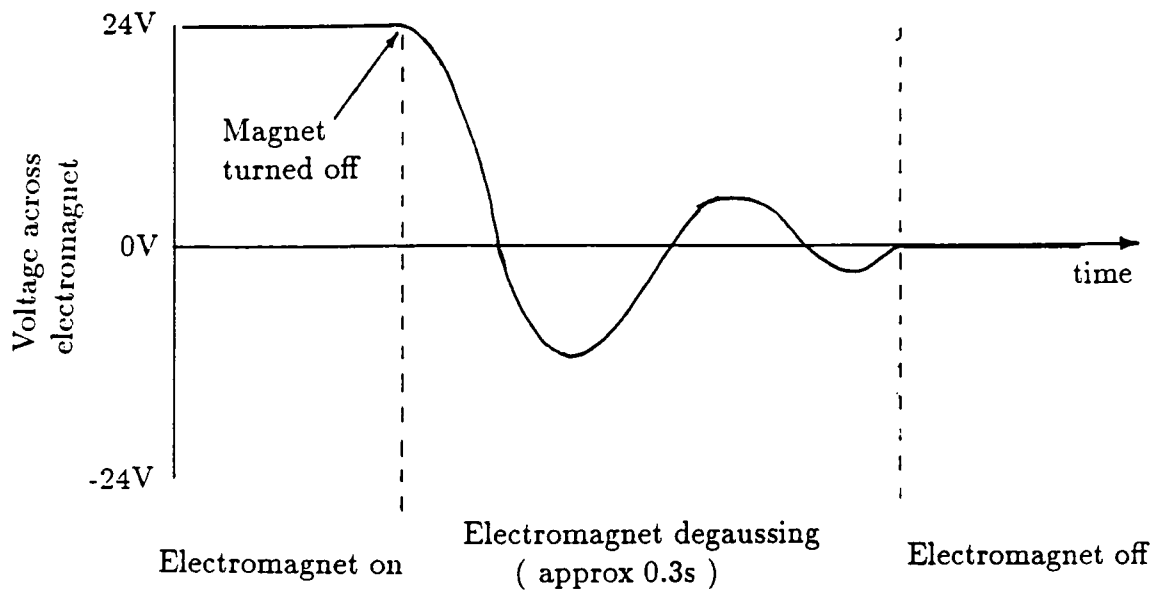


Figure 2.12 Voltage supply to electromagnet

#### Instrument protection devices

To allow the safe operation of the instrument, a number of protection devices have been designed into the electrical systems, particularly for the X and Y axes which are extremely powerful and could easily damage themselves if allowed to run out of control.

The power to both the X and Y axes is switched by a relay. The power to enable the relay passes around a loop which contains several safety devices in series. Any of these safety devices may break the loop and thus disarm the relay, removing all the power from the X and Y axes. The safety devices are shown in figure 2.14, and consist of four end-of-travel limit switches, and two enable or disable switches.

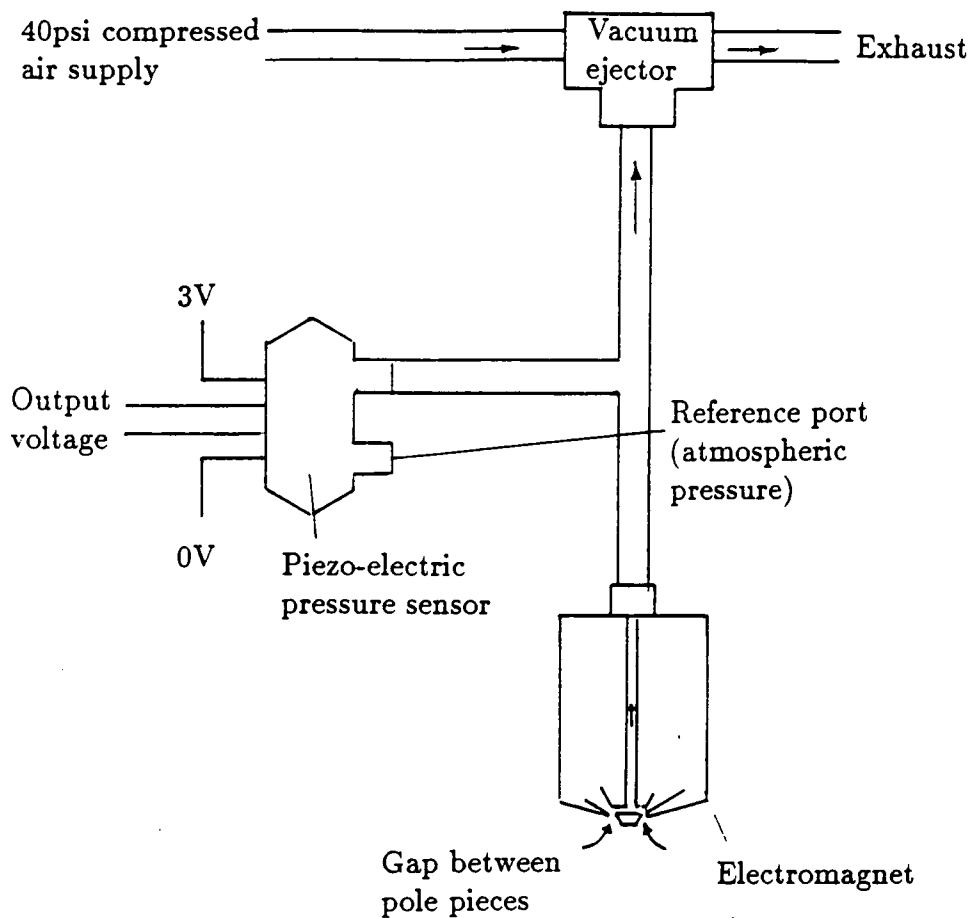


Figure 2.13 Pressure sensor arrangement for detection of a button on the electromagnet.

Under normal operating conditions all of the end-of-travel limit switches and the manual motor enable switch are closed. The motors are then enabled by raising a TTL level from the host computer. This signal is fed to a Darlington pair of transistors which switch on to complete the safety loop and thus arm the relay. Lowering the TTL signal will turn off the transistor pair and break the loop, disarming the relay and thus disabling the motors.

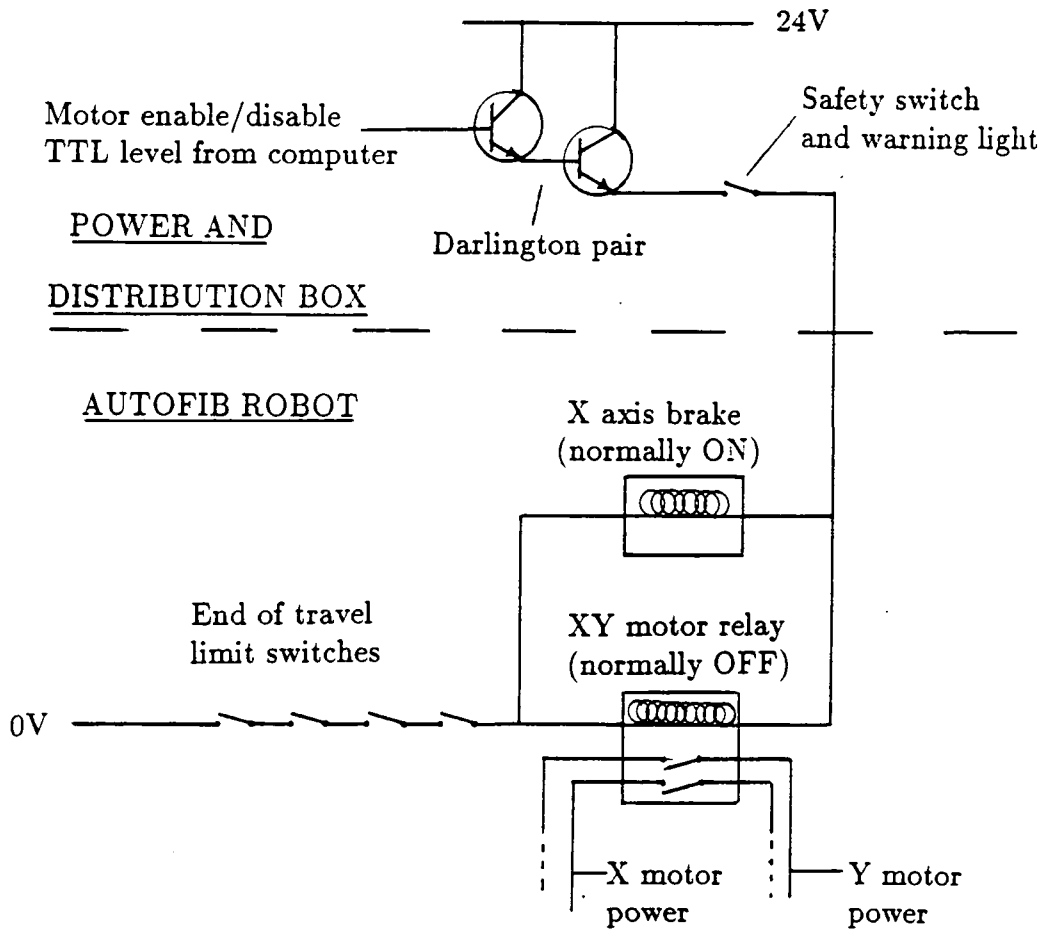


Figure 2.14 Electrical layout of safety devices

If an abnormal action occurs, and any of the X-Y limit switches are thrown open, again the safety loop is broken and the motors disabled. Once the motors have their power removed in this manner, any remaining momentum of the X-Y carriage is absorbed by the mechanical shock absorbers at the end of each axis. The manual motor enable or disable switch on the power and distribution box is used during the power up of the computer and electronics, the motors only being enabled at this switch when the computer and electronics have been switched

on and the control software is running. This procedure avoids damage to the instrument caused by stray voltages during the power up process.

## 2.5 Configuration software

### 2.5.1 Description of the observing procedure

The job of assigning fibres to target objects is performed by a piece of software on a Starlink Vax called CONFIGURE. This program deals with the allocation of specific fibres to each object, ensuring that the fibres do not collide or are moved outside of their physical limits.

The astronomer gives the program a file containing all the information about the target field, including the Right Ascension and Declination of the field centre, target objects and fiducial objects, as well as the equinox of the coordinates and epoch of the observation. Each object may also be assigned a priority (1.0 to 5.0) and have an associated comment for additional identification. This information is contained in a \*.FLD file (where \* represents the target field name). These positions are converted to x,y positions relative to the field centre. Any objects outside of the field of view of the telescope (17 arcminutes at cassegrain with the interim A & G box) are ignored. More detailed information about the configuration software and data file formats can be found in Appendix B.

The program assigns as many of the fibres as possible to target objects then allows the astronomer to alter the configuration interactively with the use of an IKON image display and mouse. This fine tune up of the configuration allows the astronomer to ensure that his highest priority target objects have been assigned fibres, and to assign any unassigned fibres to random positions to monitor the sky. Of course this random allocation of sky fibres has a major drawback in that it is possible to accidentally place a 'sky' fibre on a bright star or galaxy and lose a sky fibre. Therefore, if using an IPCS type detector, this would limit the exposure to

one for the brightest objects in the field, precluding the observations of the faint objects in the field. For this reason, a third type of 'object' is allowed in the input file, these are sky positions that have been checked against the survey plates to make sure that they correspond to blank areas of sky.

To aid in the acquisition of fiducial objects (guide stars are a very real problem when observing clusters of galaxies near the galactic poles) the astronomer may also vary the instrument rotator angle. As the guide fibres are only located at discrete intervals around the field and have a limited angle through which they can patrol, varying the rotator angle can bring a fiducial object within the range of a guide fibre.

Once happy with the fibre configuration, the astronomer may save the configuration and the program will produce two output files. The first is a log file used by the astronomer (the \*.LOG file, where \* is the field name). This contains the positions of the target objects in RA, Dec and in x,y relative to the field centre and any comments assigned to each object. In addition, some information is added by the program as it assigns a fibre to the object, this consists of the fibre number, and its position on the spectrograph slit. The \*.LOG file is the astronomers main reference when reducing the spectroscopic data. The log file also contains any relevant telescope information, such as the coordinates and equinox for the telescope and instrument rotator angle.

The second file (the \*.FIB file) contains no astronomical information, but consists only of the required positional information for each of the 72 fibres for that particular field. This file is downloaded to the instrument control computer via an RS232 serial link using Kermit software, ready for the field to be set up by the fibre positioner.

Ideally the astronomer should have prepared all of his target fields before observing, and downloaded all of the \*.FIB files to the control computer before

the nights observing. However, experience during commissioning has shown that preparing the field configurations only takes between 10 minutes and an hour, depending on the complexity of the field, and transferring the \*.FIB file to the PC takes just a few seconds. Therefore, the nights observing can usually be prepared during the preceding day.

Current practice with the FOCAP manual fibre system is to note the fibre number and hole number by hand as the fibres are plugged into the aperture plate. This information then forms the observers reference log and must be prone to observer error during a tiring and hectic observing run. By automating the process of generating the \*.LOG and \*.FIB files, the possibility of errors caused the observer making a mistake during the night are greatly reduced.

#### 2.5.2 Fibre allocation algorithm

This section contains a description of the algorithm used to assign fibres to objects in the configuration software for Autofib-1.5. A more detailed discussion of configuration algorithms in general can be found in chapter 6.

Once the computer program has been supplied with the list of target objects and has converted all of the coordinates (RA and Dec) to instrument coordinates (x and y in microns with origin at the centre of the array of parked fibres) it finds the median position of the target objects, and the number of the pivot nearest to the median point. The fibre residing in the nearest pivot is the first to be assigned to an object. The target objects are sorted into order of increasing distance from the median point, and the fibre tried on each object in turn. For each target object the following tests are performed,

1. Is the target object within the range of the fibre (defined by the length of the fibre in the fibre parameters data file).
2. Is the object within the angular range of the fibre.

3. Test that no other objects will be obscured by the act of placing a fibre on the current object.
4. If the above tests are passed, finally check that the fibre will not collide with any of the other fibres.

The first object that will satisfy all of the above constraints is assigned the 'nearest' fibre, and is deleted from the list of target objects. The \*.LOG file is now updated with the fibre number being added to the target object's record.

Subsequent fibres are now assigned in turn around the circle of pivots (from the 'nearest' to the 72<sup>nd</sup>, then from the 1<sup>st</sup> to the (nearest - 1)<sup>th</sup> fibre). All of the remaining unassigned target objects are arranged in order of decreasing non-radial angle  $\theta$  from the fibre being processed. The non-radial angle is defined as the departure of the fibre probe from the radial direction. When viewed from the fibre pivot, the non-radial angle decreases from left to right with the radial direction having a value of zero. The fibre is then tested against each target object in turn using the same tests (1...4) above. The first object that passes the tests is assigned the fibre being processed. The target object is then deleted from the working list of unassigned objects, and the \*.LOG file updated before starting with the next fibre.

## **2.6 Control software**

### **2.6.1 Overview**

The instrument control software is written in the C programming language (Kernighan and Ritchie) and runs on the PC compatible instrument control computer. This software performs a number of functions, chief amongst which is to protect the instrument from any incorrect commands issued by the astronomer



and likely to cause damage to the instrument. Other functions include the continuous updating of a mimic display, and the generation of sequences of commands for automatic target field configuration setup.

The control software receives data from two sources, fibre configuration data files over a RS232 serial link from the VAX, and simple commands from the control computer keyboard. The instrument may be operated in any one of three modes, Interactive, File (automatic) and Engineering. Under normal observing conditions only the File and Interactive modes are required, and will be described first.

### 2.6.2 Interactive control mode

The Interactive mode enables the instrument to be controlled using a limited set of two letter commands (and if necessary, numerical parameters), for example:

**EM** Enable motors,

**GO** Initialise encoders,

**VF n** Place viewing head at location of fibre n.

\* A full description of commands is given in Appendix A.

This mode is used on power up to initialise the instrument. After a fibre configuration has been set up (see below on the File mode of operation) the Interactive mode may be used to check on the locations of fibres and aid in acquiring the target field. In short, from the interactive mode it is possible to control any aspect of the instrument that does not involve handling the fibres. These are all perfectly safe commands in that it is almost impossible to issue a command that could cause damage to the instrument.

### 2.6.3 File or Automatic control mode

The file mode invokes a subprogram to generate and process the series of commands required by the robot to set up the next target field configuration. The astronomer provides the name of the configuration file (\*.FIB) for the target field (previously downloaded from the VAX). The control software then generates the sequence of commands required to move the fibres from the current configuration to the new configuration. It is usually possible to go directly from one configuration to the next without parking all of the fibres at some intermediate stage. However, very occasionally it might be necessary to park a single fibre temporarily during this process, a procedure which is performed completely automatically.

The algorithm used to achieve direct field to field movement of fibres is described below. A working copy of the current fibre configuration is made in memory. Each fibre is now tested in turn at its future location as defined by the new configuration file. If the anti-collision algorithm (the same as for the configuration software) will allow the fibre movement, the commands to perform the movement are written to a setup file (\*.STP) and the working copy of the configuration updated to show the fibre in its new location. If the fibre is not yet allowed to be placed at its new location, the next fibre is tried. Eventually one fibre will be allowed to move thus making room for another fibre and so on. In the unlikely event of no fibres being allowed to move to their future location, the first fibre is temporarily parked to free some room, and the process repeated. It is worthwhile noting that, of all the astronomical field configurations attempted so far, no fibre has had to be temporarily parked in order to move the fibres from one configuration to the next.

Once the new field has been set up, control is returned to the Interactive mode, so that the astronomer has control of the viewing head to help in field acquisition.

If an error occurs during the automatic field setup, an error flag is returned from the operation in progress, and no further commands will be processed until the error has been rectified. The field setup is automatically aborted and must be restarted from the command sequence generation stage once the error has been cleared.

#### 2.6.4 Engineering control mode

In normal operation of the instrument at the telescope, this mode of control should not be required. However, Engineering mode provides for complete low level control of the instrument during commissioning, and enables recovery of the instrument from a situation where an error has occurred. In Engineering mode all of the commands in Interactive and File mode are available as well as an extensive list of extra commands. These extra commands range from very low level ones controlling single functions of the robot (for example, **MG 0** or **1**, electromagnet off or on) to high level commands useful when calibrating the instrument (for example, **ER n**, measure the error table values for fibre n). Whilst movement of individual fibres is possible, extreme care is required to avoid damaging the fibres when using the low level commands as it is possible to circumvent the anti-collision checking. Safer operation of the instrument is possible using the higher level commands that perform all of the necessary anti-collision checking.

#### 2.6.5 Instrument mimic display

The VDU of the control computer forms the mimic display for the instrument with all necessary information displayed and continuously updated (figure 2.15). As commands are entered at the keyboard (or read from a command file in File mode) they are echoed on the mimic display, as are any messages during, or at

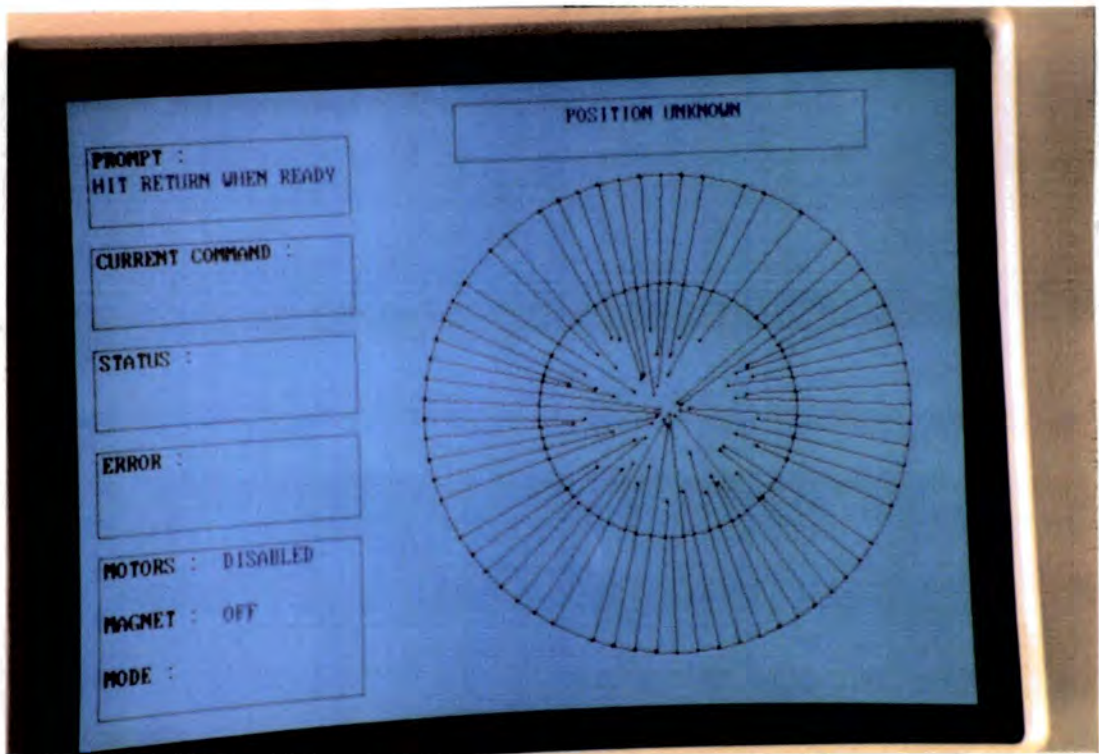


Figure 2.15 Photograph showing the control computer mimic display

the end of execution of a command. Should an error occur, an error message indicating the type of error is displayed.

The main feature of the mimic display is a representation drawn in red of the current configuration of all the fibre probes. As each fibre is picked up in preparation to be moved, it is redrawn in blue. As it is put down in its final position, the 'blue' fibre is erased and redrawn in red at the new location.

Surrounding the fibre configuration diagram are a series of 'windows'. Above the configuration diagram is the 'current position' window, which will show one of three sets of information.

1. Position Unknown. The encoders have not been initialised yet, no movement is allowed until this has been done.
2. X = xxx Y = yyy Z = zzz. Current x,y,z pickup head position.
3. X = xxx Y = yyy. Current x,y of the viewing head, note that z is an irrelevant coordinate for the viewing head.

The second option showing the current pickup head coordinates is the default position display. However, it is possible to toggle between the latter two position display formats, the usefulness of each will depend on whether it is the pickup head or the viewing head being used.

The remaining windows provide the astronomer with the feedback to his commands necessary to control the instrument. From the top, the first window gives a prompt message, telling the astronomer what sort of input the software is waiting for, or displaying a message indicating that it is busy carrying out a previous command. The second window shows an echo of the current command being executed, and is also occasionally used when it is necessary to provide large amounts of information. The third window provides information on the current status of the instrument, what action is currently taking place etc. A fourth window that should remain empty during normal operation is the error message display. The last display window provides information on the current status of the motors, electromagnet (enabled or disabled) and the current mode in which the instrument is being operated (File, Interactive or Engineering) and the field name if in File mode.

#### 2.6.6 Measurements of offsets and errors during calibration

From within the Engineering and Interactive modes it is possible to measure the x,y offsets of the fibre from their required (or expected) position. This is achieved by positioning the viewing head crosshair at the required position and

entering the command "JO". The astronomer may then move the viewing head using the cursor keys in steps of 10,30,100,300  $\mu\text{m}$  (F1,F2,F3 or F4 keys) to centre the fibre on the crosshair, the x,y offset is displayed on the screen.

This feature of the control software is used to locate fibres when they are initially loaded by hand (from within the command **LF n**, load fibre n), and in the generation of an error table (from within **ER n**). Another use of this feature is to measure the locations of stars in a target field. A comparison of their measured location with their predicted position would give information about the plate scale and map any distortions present across the field. By toggling the position display to show the viewing head position and centering the stars on the viewing head crosshair, the position of each of the stars may be noted down and used in STARLINK software (for example ASTROM) to determine the plate scale together with any non-linearities present and the also orthogonality of the X-Y carriage itself.

## 2.7 Summary

In this chapter I have described a prototype instrument for the William Herschel Telescope on La Palma. It includes design features relevant to the planned second generation fibre positioner (Autofib-2), and has been used as a test bed for these ideas. Whilst not destined to become a common user instrument, the WHT Prototype incorporates many of the requirements of such an instrument, with particular emphasis being placed on reliability, ease of use and full computer control where possible. The next two chapters present the results of the testing of the prototype instrument on the WHT, chapter 3 gives the technical results on the performance of the positioner, and chapter 4 the astronomical results.

## **3** Commissioning of Autofib-1.5

### **3.1** Introduction

This chapter presents the technical results from the commissioning of Autofib-1.5 at the cassegrain focus of the WHT. This work was carried out with the instrument at the telescope in late February and early March 1989 and again in April 1990. A series of modifications and improvements were made in the period between the commissioning runs.

The two commissioning runs served as a useful test of the accuracy of the robot positioner and enabled the evaluation of the reliability of the overall system. In particular, the new features incorporated into the design required extensive telescope testing. A secondary objective was to obtain operational experience with a fibre system at the WHT. The experience gained from this work will be folded back into the design for a common user instrument, Autofib-2. As a result of this work, an operational multiple fibre system was available at the WHT at least two years ahead of any other fibre instrument. The scientific applications of Autofib-1.5 are discussed in chapter 4.

## 3.2 Commissioning, February–March 1989

### 3.2.1 Technical results

#### Pickup head

The pickup head which had undergone several fundamental design changes from the Autofib-1 design as mentioned in chapter 2, worked very well with no pickup failures. The servo control of the Z axis, along with its compact design made for extremely fast operation (approximately 2.5 seconds for a single pickup or putdown operation). The pressure sensor in the pickup head was not utilised due to lack of time to commission it.

#### Viewing head

The viewing head was very successful, enabling the instrument to be operated from the control room with a minimum of manual intervention (even in the case of any abnormal operation of the instrument). When back illuminating the fibres from the spectrograph slit, the viewing head was used for a number of purposes:

- To locate the fibres reliably after some manual intervention such as initial placement in the load ring, or removal of the fibre module for cleaning.
- To check the fibre positions after setting up a field.
- To generate an error table in order to calibrate out the inaccuracies in the manufacture of each fibre.
- To check the alignment of fibre and target object when viewing the fibre and sky simultaneously.

In addition the viewing head proved exceptionally useful in the testing and calibration of the instrument on the sky, in particular:



- To enable a measurement of the cassegrain plate scale to be made.
- To assist with initial field acquisition when telescope pointing or guide fibre placement is not very accurate.

In addition to the above uses, the viewing head was used to guide the telescope by observing a star at the periphery of the field in such a position that the X-Y table would not obscure the field itself.

#### Other aspects

The redesigned fibre probe with projecting fibre tip worked very well (but see below for the guide fibres), as did the associated software, allowing close approach of the fibres and easing the difficult problem of assigning fibres to target objects (see chapter 6).

The electrical control of the instrument worked as planned, with no electrical noise problems. The length of the cables connecting the instrument to the control computer had no detrimental effects on the performance of the instrument.

The operational tests of the instrument progressed very well, from the configuration of the target fields on the VAX data reduction computer, to setting up the fibre configurations and acquiring the target field. Spectroscopic data was obtained on an open star cluster. This cluster was chosen because accurate positions of the stars were available to within 0.1 arcseconds (see chapter 4). Therefore, this cluster provided a very good way of assessing the fibre positioner performance as it eliminated any problems that might have been caused by poor astrometry.

### 3.2.2 Problems encountered during testing on the telescope

#### Servo loop control

A problem encountered early on in the testing was that the X axis servo

loop had a tendency to become unstable in certain circumstances. Whilst the X axis servo loop was stable with the telescope pointing at the zenith, as soon as the telescope was moved to zenith distances of greater than  $10^\circ$ , the X axis started juddering, and even stalling on occasions. This instability was caused by mechanical compliance between the X motor and its encoder due to a spring washer in the motor bearing. The problem was alleviated slightly by retuning the servo loops enabling the X axis to be moved safely at zenith distances of up to  $75^\circ$ , and by limiting the cassegrain instrument rotator angle so that the X axis was only ever loaded in a direction away from the motor, thus avoiding any compression of the spring washer.

A result of the retuning of the servo loops was that they did not exhibit good repeatability with the telescope at positions away from the zenith. The X-Y carriage would not go where it was told with the required accuracy (although the encoding told us where it was to  $1\ \mu\text{m}$  resolution). It should be noted that the Y axis which uses similar components does not suffer from these problems. With a slight mechanical modification and more time spent tuning the servo loops much improved performance should be achieved (section 3.3). However during the course of the commissioning run, there was not enough time for a full solution to be implemented.

There was another operational problem, which did not affect the operation of the instrument during observing, but caused trouble during the daytime when the instrument was unpowered. The X axis is driven by a high efficiency ballscrew. Unfortunately this ballscrew is so efficient, that if the telescope was moved away from the zenith during the day, the weight of the X carriage was enough to make it free-wheel along the ballscrew. As a result the instrument was left at one of the limit switches at the beginning of an observing period, meaning that some time was lost at the start of the night extricating the carriage from the limit switches so that normal operation could proceed.

## Positioning errors

The implementation of the error table mentioned above suffered a software bug. This seemed to cause the fibres to be placed with lower accuracy when using an error table, our best positioning accuracy was therefore achieved using a 'zero' error table containing zero values for  $l, b$  for each fibre. The overall positioning accuracy was estimated at 100–150  $\mu\text{m}$  rms, a figure dominated by the manufacturing errors of each fibre and the poor servo performance.

## Plate scale

An attempt was also made to determine the plate scale of the cassegrain focus using the viewing head to measure the positions of two known stars for inclusion into the configuration software when converting the RA and Dec of target objects to instrument  $x, y$ . Unfortunately our determination of 221.81  $\mu\text{m} / \text{arcsec}$  did not work as well as that of 221.46  $\mu\text{m} / \text{arcsec}$  used at the FLEX nasmyth focus. Reasons for this anomaly are that the seeing was rather poor (2.0-3.0 arcsec) and the low magnification of our viewing system did not allow very accurate centering of the star on the viewing system crosshair. Another reason for possible errors in the determination of the plate scale is movement of the star during the measuring procedure as the telescope mistracked, no autoguider being available with the interim A & G structure. The difference between the two plate scale determinations corresponds to approximately 1.5 arcseconds across the 15 arcminute field, which would cause a significant error in positioning the 1.2 arcsecond diameter fibres.

## Guide fibre design

The new guide fibre design was not very successful because of the error table problems mentioned above. The elongated prisms required to make the guide fibres parfocal with the spectrograph fibres made the guide fibre probe assembly rather difficult. This in turn caused large manufacturing errors for the guide fibres (up to

500  $\mu\text{m}$  ) which should have been removed by the software. Normally, poor guide fibre performance would make target acquisition very difficult indeed. However, it was still possible to acquire the field successfully using the viewing head, as only relatively bright star fields were being observed.

#### Back illumination of fibres

Although the viewing head worked very well, the methods of back illuminating the fibres to make them visible to the viewing head were inadequate. During daytime testing an intensified CCD TV camera was used to view the coherent image guide from the viewing head for calibration purposes. At night, when it was necessary to view the sky, a more sensitive Westinghouse TV camera was used. If it was required to back illuminate the fibres during the night, great care had to be taken to avoid damage to the TV camera. Proper remote controlled and interlocked illumination equipment must be provided for future systems. The simultaneous viewing of fibre and object was not as useful as had been hoped because, to protect the camera and be able to see the object, the fibre illumination had to be carefully matched to the magnitude of the object.

#### Long spectrograph fibres

There were operational problems associated with the design of the fibre module and the 14m long fibre feed from cassegrain to the nasmyth platform where the FLEX spectrograph was located during the commissioning run. Loading the fibres into the fibre module was a very difficult process, due mainly to the length of the fibres. During this process several fibres were broken. In total 57 fibres were available for use, two of which were too far off axis on the spectrograph slit to be seen by the spectrograph CCD. In addition the long conduit protecting the fibres from the fibre module to the spectrograph slit was particularly difficult to handle when mounting the fibre module onto the fibre positioner at the telescope. Also,

during the daytime the long fibre conduit was extremely vulnerable to accidental damage as it hung from the cassegrain focus to the nasmyth platform.

## Software

While the control software functioned extremely well, with only one bug discovered in the error table routines, a number of possible improvements were noted down (see section 3.4) that would make control of the instrument much easier, especially during the commissioning phase.

### **3.3 Mechanical modifications, 1989–90**

#### 3.3.1 Mechanical changes to the robotic positioner

The X axis of the X–Y carriage was redesigned during the period between the commissioning runs. This involved the addition of an extra thrust bearing to remove the load from the motor bearing and so avoid any compliance in the X axis. Although the Y axis showed no problems with compliance during the first commissioning run, this was probably because the mass of the moving part of the Y axis was much smaller. To avoid any future problems a thrust bearing was added to this axis as well.

An electromagnetic brake was added to the X axis so that when the instrument was unpowered, the X axis of the carriage was firmly clamped allowing no further movement. The act of powering up the instrument automatically releases the brake. This avoids any possibility of releasing the brake before the instrument is powered up or vice versa.

Once the modifications to the X–Y carriage were complete, the servo loops were retuned. The process of tuning the servo loops proved to be a much simpler process now that the compliance in the X axis had been reduced to a satisfactory level. As a result safe movement of the X–Y carriage was possible at all orientations

for both the X and Y axes, with the destination point being within 2  $\mu\text{m}$  of the desired position after the retuning process. Unfortunately it was still only possible to operate the robot at a quarter of its designed maximum speed, as the linkage between the motor and encoder still has a very small amount of compliance when operated at very high speed (due to twisting of the ballscrew during acceleration and deceleration of the X-Y carriage).

### 3.3.2 Changes to the fibre module

The fibre module was completely redesigned from its original form in 1989, to make loading the fibres and handling the fibre module a much simpler task. The fieldplate was remade in two separate parts, an outer ring made of aluminium with the pivots formed as slots in a thin wall at the outer edge, and a central thin disc of magnetic stainless steel. The resulting fieldplate is considerably lighter than the original mild steel version. The stainless steel tubes protecting the fibre probes are retained in their slots by a piece of PVC tubing which is slit along its length so as to clip onto the top edge of the wall, closing off the open end of each pivot slot. The maximum number of spectroscopic fibres was kept at 64, but the number of guide fibres was increased from 6 to 8 to make the acquisition of guide stars easier.

As before, after passing through the pivot wall inside the stainless steel tube, the bare fibre curls back under the fieldplate inside the aluminium box. However it now terminates at the base of the box in a multiple way fibre connector (section 3.3.3), the total length of the fibre to this point being only 1.5m. The slots in the pivot wall and the shorter length of the fibres made loading the fibres much easier than in the original design. At the base of the fibre module are two multi-way fibre connectors, one containing the 64 spectroscopic fibres, the other the output from the 8 guide fibres (a total of 56 individual fibres). The connection from the fibre module to the spectrograph is now made by a fibre optic 'cable'. This cable has the second half of the connector at one end to mate with the fibre

module, and the fibre slit for the spectrograph at the other end. Similarly for the guide fibre connector, the guide fibre cable joins the fibre module to the TV interface.

On the first commissioning run it was felt that the new design of guide fibre was not very successful due to manufacturing problems and gave no added advantage in the ability to acquire guide stars. Therefore the redesigned fibre module has eight guide fibres of the conventional design. The guide fibre probes are now the same height above the fieldplate as the spectroscopic fibres, consequently the guide fibres use the same prisms as the spectroscopic fibres.

### 3.3.3 Multi-way fibre connectors

High efficiency fibre connectors such as the AT&T ST Connector can achieve transmission losses as low as 0.2 dB. Unfortunately this type of connector is only available for the 50 and 100  $\mu\text{m}$  fibres used in the communications industry. It is not available commercially for non-standard fibre sizes or in a multiple fibre connector format. For these reasons it was decided to devise our own multi-way fibre connector.

The ST Connector relies on the butting together of the polished ends of the two fibres with very high positional accuracy to achieve low transmission losses. The positional accuracy is obtained through the use of very high tolerance ceramic ferrules. Having chosen a fibre whose outside diameter precisely matched that of the inside of a hypodermic stainless steel tube, small lengths of the tubing were used in a similar way to the ceramic ferrules, to ensure that the fibres align properly in the connector.

To make sure that the two halves of the connector aligned properly, the two matching faces were originally a single aluminium disc or 'blank'. Through the blank were drilled 64 1.1mm holes counter-bored slightly at each end. In a trial

blank, the positional uncertainty of the drilled holes at the point of entry was better than  $10\ \mu\text{m}$ , but was significantly worse ( $50\ \mu\text{m}$ ) at the point of exit due to the drill wandering slightly. Subsequent blanks (including the two used in the connectors) had their thickness reduced in the area of the drilling to try and reduce this effect. In addition, near the edge of the blank, two 3.0mm holes were drilled and reamed to take dowels, in order that the two halves as they would later become could be realigned properly.

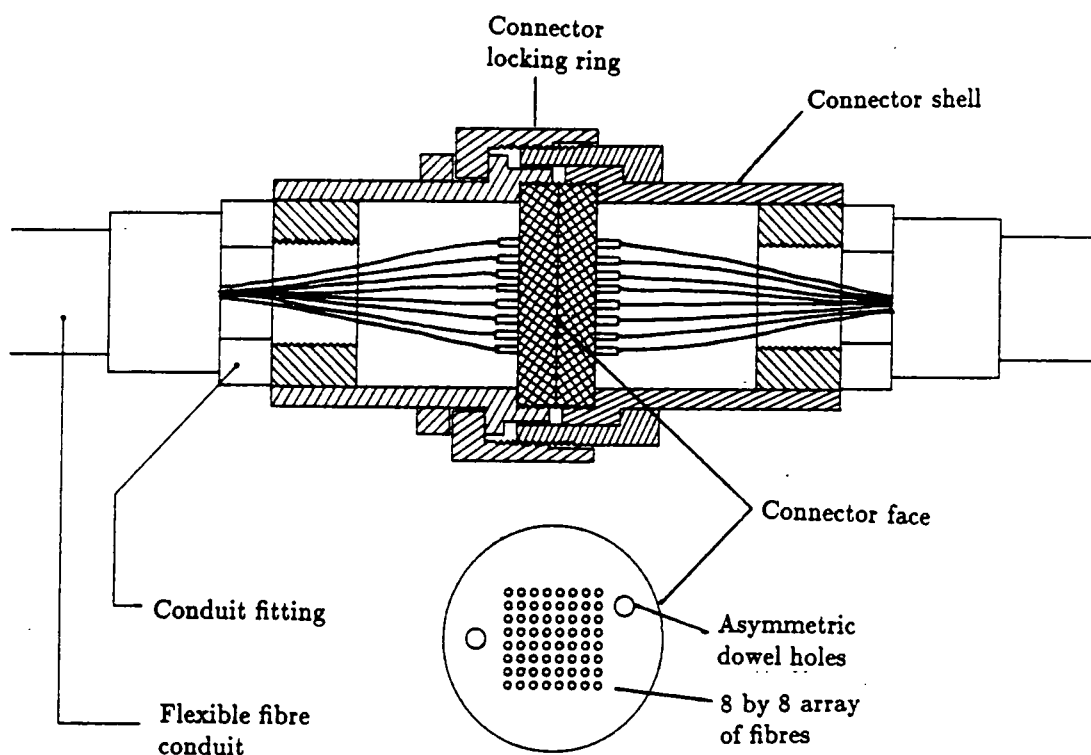


Figure 3.1 Schematic diagram of connector.

Once drilled, the blank was cleaned, and two sets of stainless steel tubes were epoxied into the 64 holes. Firstly a tube of outside diameter 1.1mm was glued



into each hole. Next, inside each of the first set of tubes, a slightly longer tube was glued. The second tube was of a size that exactly matched the fibre (and also the inside diameter of the 1.1mm tube). The second tube was longer to avoid introducing any epoxy to the inside of the highly toleranced second tube.

After the epoxy had hardened, the whole blank was sliced into two halves perpendicular to the tubes. This was followed by washing in an ultrasonic bath, after which fine wire was used to remove any dirt and swarf from the cutting process from the inside of the tubes.

The fibres were now epoxied into the tubes using a very low viscosity epoxy with a curing time of approximately 24 hours at room temperatures (TRA-BOND BA-F1135C). The low viscosity was necessary in order to get sufficient epoxy inside the high tolerance tubing. The long curing time was required so that all of the fibres could be inserted in their place and aligned together before the epoxy became unworkable. This process took 1-2 hours, after which the whole assembly was left to harden overnight.

Once the epoxy had hardened, the connector shell could be assembled around the aluminium disc to protect the delicate fibres, as they could no longer be replaced. The projecting fibres were then trimmed to within 0.5mm of the face of the connector using a sapphire cleaving tool.

The whole connector assembly provided protection for the fibres during the polishing process. This consisted of polishing the projecting fibre faces on five different grades of aluminium oxide paper (30,9,3,1,0.3  $\mu\text{m}$ ) supported on a piece of float glass until the fibres were flush with the connector face. Then the whole connector face was polished until the faces of the fibres were of a high optical standard and unmarked by scratches. The polishing process was performed by hand. Extreme care was required to ensure that the axis of the connector remained perpendicular to the polishing surface to avoid polishing the ends of the fibres at

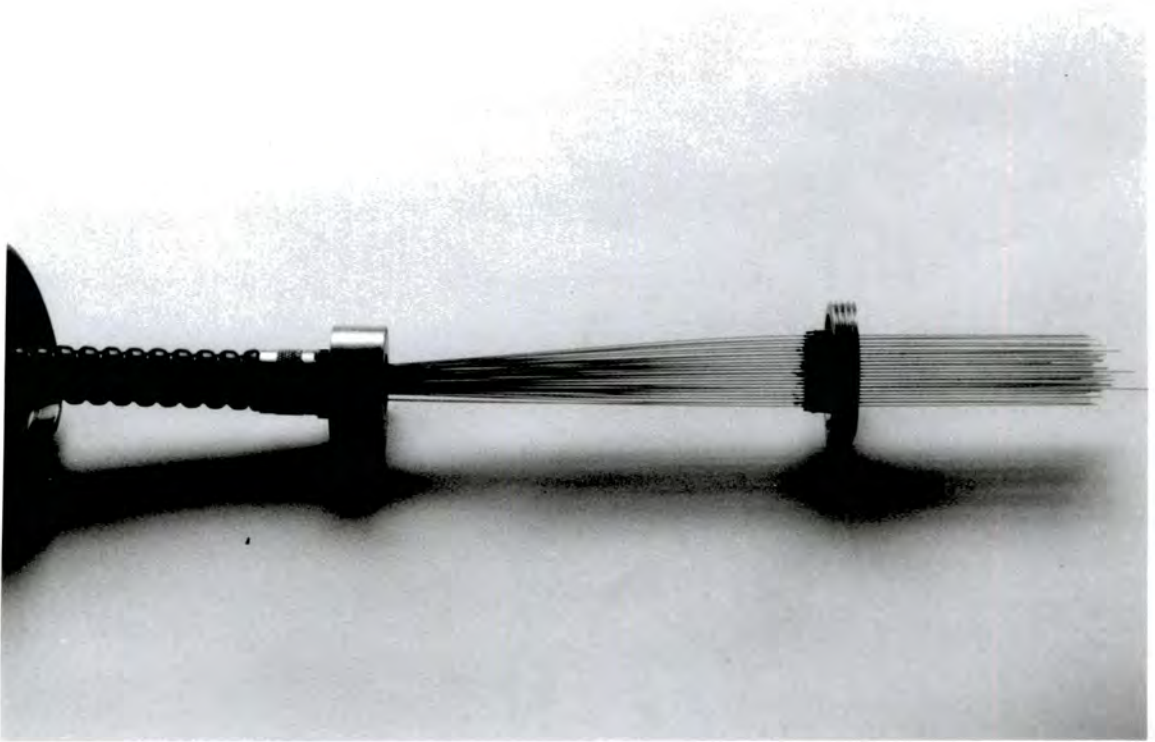


Figure 3.2 Photograph showing a partially assembled connector with fibres epoxied into the connector face.

an angle other than  $90^\circ$ . This was important as it would reduce the throughput and also increase the focal ratio degradation.

When both halves of each connector were prepared in this way the final stage was to fix dowel pins in the half of the connector on the fibre module. Two sets of perspex caps were provided to give some protection to the polished faces of the connectors during shipping and handling at the telescope. These simply screw into place using the existing locking ring threads.



Figure 3.3 Photograph showing one half of the completed and assembled connector.

### **3.4 Software changes, 1989–90**

#### **3.4.1 Configuration software**

As a result of exhaustive testing of the configuration software under observing conditions, a number of minor changes were made to its operation. A minor bug in the generation of the log file was eliminated and several changes made to the process of interactively modifying the field configuration to allow more flexibility. Because of the change to a new A & G box at the WHT during this period, a modification was made to the data written out to the log file so as to include information about the required instrument rotator angle. This was necessary as

the new instrument mounting flange bolt holes were offset from the ones on the interim A & G box.

### 3.4.2 Control software

As a result of the first commissioning run, several additional commands were added to those available in engineering mode which is the mode most often used during commissioning. These were all high level commands that made operations that originally used low level commands much simpler, as well as much safer for the fibres. These included the parking of individual fibres to the park circle with a single command with the necessary anti-collision checking, and the movement of a specified fibre to a given x,y location, again with the necessary anti-collision checking prior to any movement.

A major improvement made at the last moment before commissioning to the instrument control system was the inclusion of a video frame-grabber card for the analysis of the images of the back illuminated fibres. This was added as a result of work carried for the design study for the 2dF facility at the AAT (see chapter 5). A centroiding routine derived from that used in the AAT 2dF prototype is used to locate the image of the fibre relative to the centre of the CCD TV camera.

The software is now able to perform all of the original functions involving the measurement of fibre positions in two different ways. The first method is by nudging the X-Y carriage and lining the image up on a point determined using a software crosshair as before. The second method involves using the centroiding routine to determine the offsets automatically, a process taking approximately 0.7 seconds. The limitation of the automatic centroiding routine is that the whole image of the fibre must be visible to the TV camera for the offsets to be determined correctly. This does not always occur when initially loading the fibres, as the first approximation may not be accurate enough to fully include the fibre. For this reason the manual approach was retained.

In addition to making many routine operations easier, the addition of the frame-grabber generated several new possibilities for operation of the instrument. In particular, using experience gained from the 2dF work, a command to measure the position error of a fibre placement and automatically try and correct it when it is outside some tolerance was implemented.

### 3.5 Commissioning, April 1990

#### 3.5.1 Telescope setup

The instrument was again used at the cassegrain focus of the WHT, with the control electronics placed in the normal cassegrain electronics racks. The fibres were used to feed the FLEX spectrograph on the nasmyth platform. The whole instrument was controlled by the instrument control PC from the main WHT control room.

Major changes from the previous run in 1989 were made to the procedures used to enable the viewing of the back illuminated fibres and of the sky. When it was required to view the fibres, the coherent bundle from the viewing head was fed to a high magnification CCD TV camera and the video frame-grabber. During the night when using the viewing head to observe the sky, the coherent bundle was fed to a low magnification optical system and an intensified CCD TV camera. The high magnification day-time system has a field of view of approximately 3 arcseconds (limited by the CCD TV camera), and enabled centroiding of the fibre to within  $5 \mu\text{m}$  (limited by the size of the fibres making up the coherent bundle). The low magnification night-time system gave a field of view of 13 arcseconds (limited by the overall size of the coherent bundle) and a limiting magnitude of about 16. Note that this result was in itself limited by the poor transparency of the sky during the observing run (chapter 4). The change-over between the two viewing systems was achieved by manually swapping the coherent bundle between the two optical

systems, an operation carried out very simply with a repeatability of better than  $5 \mu\text{m}$ .

As before the 8 guide fibres were fed to a Westinghouse Integrating TV camera system bolted to the side of the fibre positioner, with TV display in the control room. Each guide fibre image consisted of a group of seven fibres arranged so that north for each guide fibre was orientated in the same direction on the TV display. This arrangement greatly simplified field acquisition because it was possible to see at once which direction the telescope should be moved to acquire the field.

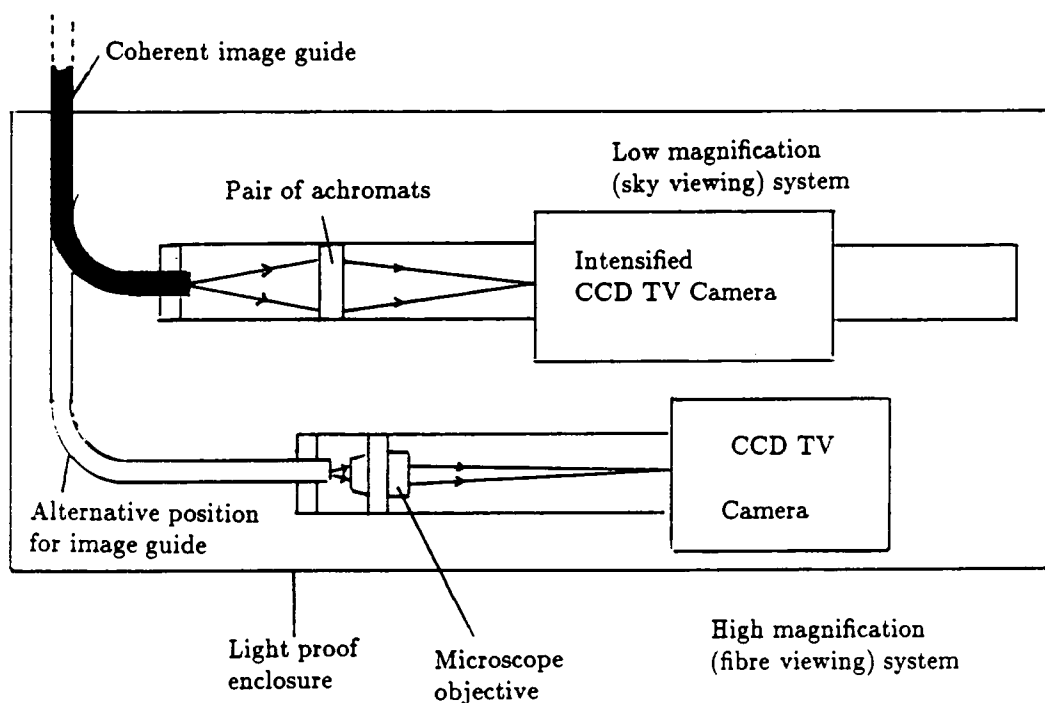


Figure 3.4 Diagram showing the optical arrangements for imaging the viewing head coherent image guide.

A new method of back illuminating the fibres that took advantage of the fibre connectors on the fibre module was tried successfully at the telescope. Two small torches, suitably modified to screw into the fibre module half of the connector, provided the illumination. This method of illumination was considerably more successful than that of illuminating the whole slit at the spectrograph, as it was much easier to evenly illuminate the  $8 \times 8$  array of fibres at the connector, than to illuminate a long slit at the spectrograph. Also the fibres are much shorter, only passing from the connector to the prism and this results in brighter and more evenly illuminated fibres for the viewing head to look at. The torches are connected in series by a mains power unit supplying 100 mA at 20V dc.



Figure 3.5 Photograph showing procedure for back illumination of the fibres.

### 3.5.2 X-Y Carriage

The X-Y carriage performed as expected from the lab tests, moving to the requested x,y position to within 2  $\mu\text{m}$  at all position angles of the telescope. The magnetic brake on the X axis successfully eliminated the mechanical runaway problem when the instrument was left unpowered.

### 3.5.3 Fibre module

Handling the new fibre module was extremely easy, only requiring two people to remove or mount it on the fibre positioner at the telescope. The absence of a fibre conduit at the rear of the fibre module made the handling procedure much safer with no chance of damage to the fibre bundle. Once the fibre module had been attached to the rear of the robot positioner, it was extremely simple to connect up the fibre cable connectors. A few drops of index matching fluid were added between the faces of the connector to reduce any reflection losses.

### 3.5.4 Reliability

In order to improve the ability of the control software to detect and enable remote correction of any pickup or putdown failures, the pickup head pressure sensor was used during the second commissioning run. Compressed air was fed to the instrument from a pump on the cassegrain floor at a pressure of 40psi. The pressure sensor worked extremely well, enabling the control software to differentiate between a missing or incorrectly placed button or a bad pickup caused by a slightly misplaced button.

Normally, field setups were performed with the telescope pointing at the zenith. During the lab testing before mounting the instrument on the telescope, and during seven nights of intensive use on the telescope, no pickup or putdown failures resulting in the misplacing of a fibre occurred. On three occasions however, during the first two nights on the telescope, the control software halted the



operation of the instrument. By careful use of the instrument in Engineering mode it was determined that the fibres were in fact at their correct locations, but that the pressure sensor was not showing a large enough voltage drop to convince the control software that the button was in fact present. By over-riding the pressure sensor, successful operation of the instrument continued for the rest of that night. Later inspection of the fibres revealed the cause of the problem to be contamination of the button which manifested itself in several ways

- Metallic swarf
- Rusty flakes of steel
- Blobs of dirty grease

Every one of the three pickup 'failures' was caused by a contamination of this sort. For the rest of the observing run, the fibre module was removed and thoroughly cleaned prior to each nights observing as a precaution. During this procedure several potentially troublesome items were removed from the fieldplate. No other failures of any type occurred during field setups, even when setting up a field at a zenith distance of  $60^\circ$  on one occasion as a test.

One point to note about the pressure sensor is that the stability of the air supply is critical for determination of the presence or absence of a fibre button on the electromagnet. The pressure seen by the piezo-electric sensor varies due to two things, firstly the pressure change due to the presence or absence of a fibre button on the electromagnet, and secondly due to any variation in the pressure of the compressed air supply. Although the air supply used was regulated, it was regulated with respect to atmospheric pressure, meaning that if the atmospheric pressure changed, it was necessary to adjust the air supply to obtain the correct voltages from the pressure sensor circuit. The output voltage was continuously monitored in the control room using a digital voltmeter across the coaxial cable

carrying the analogue pressure signal. This problem of air pressure stability could be avoided by monitoring the pressure sensor when there is no button present and using a pressure differential to test for the presence of a button. This was unnecessary during the time at the telescope since, when atmospheric pressure dropped sufficiently to require recalibration of the pressure sensor, the observing run was terminated by poor weather.

### 3.5.5 Positioning accuracy

The instrument was calibrated very roughly, with only a first approximation error table used during the second commissioning run. However, the positioning accuracy was easily good enough for operation of a fibre positioner at the cassegrain focus. The instrument could be operated in one of three ways, firstly a 'blind' setup of the fibres using only the error table to correct the fibre positions. This procedure achieved an overall accuracy of  $45 \mu\text{m}$  rms, limited chiefly by the inadequacy of the error table used. A second method was to set up the field as before, using the error table to get the fibres in almost the correct positions, then to automatically 'tweak' the position of each fibre using the 'correct fibre position' function (CF n). In this manner, a positional accuracy of  $26 \mu\text{m}$  rms was achieved. Unfortunately this method of operation requires the back illumination of the fibres for each field configured during the night, and takes twice as long as the blind method to reach the final configuration. These are costly time overheads that must be avoided if possible.

A third mode of operation to avoid the problems mentioned above, was to set each field up during the daytime using the second method (with automatic correction) then save the 'corrected' configuration to disk before starting the next field setup. During the night, the robot sets up each of the 'corrected' fields blindly. This process is equivalent to generating a field specific error table for each field, but we are still limited by the repeatability of the setup process. This mode of

operation was the one used most often during observations at the WHT in April 1990 and achieved positional accuracies of 35–40  $\mu\text{m}$  rms.

These results quoted above are the scatter of the positioning errors for all fibres around a zero error point for all the fibres. Results for individual fibres are much better, but exhibit small residuals that have not been removed adequately by the error table.

The main limitations to the overall positional accuracy seem to arise from two sources, the repeatability of the electromagnet pickup and release, and the effect of torsion causing the fibre to jump slightly as it was released. The first effect was estimated by repeatedly picking up and putting down a fibre at the same location, and measuring its position. This showed a repeatability of 15  $\mu\text{m}$  for a given fibre at a particular place in the field, provided the button or electromagnet did not become contaminated as previously discussed. However, when moved to a new point in the field, the initial pickup–putdown of the fibre probe was very poor, but subsequent operations were of the same high standard as in the previous location.

The second source of positioning error was a side effect of the success with which the magnet strength was increased to avoid pickup failures. The conical design of the fibre button has two purposes, firstly to automatically self centre the button on the electromagnet, and secondly to allow the button to swivel on the electromagnet as the fibre is moved around the field. The levering force for this rotation is provided by the stainless steel tube acting on the fibre pivot. Unfortunately, the electromagnet is now so strong, that while there is no longer any problem picking up the fibres, the levering force is not large enough to swivel the fibre button. Therefore, as the button is moved from one position to another, the fibre tube deforms like a spring. As the fibre button is released from the electromagnet, the fibre tube springs straight and the fibre pivots around the button, moving the prism slightly.

This effect could be reduced by introducing a rotation stage into the pickup head mechanism, to provide the angular movement. Alternatively, the fibre might be relaxed at its final position to ensure that it is at the correct location. Some evidence of this working may be seen in the results for the **CF n** command, as they are better than the positioning accuracy using the 'corrected' fields technique. This is because as a 'corrected' field is set up from the current field the fibres are being moved some distance, thus introducing the the effect we are trying to avoid. However, during an individual position correction, the fibre movement is quite small, and has the effect of relaxing the fibre slightly. As the accuracy was adequate for a cassegrain instrument, no attempt has been made to modify the pickup head to correct this problem.

### **3.6 Application of the current work to Autofib-2**

Autofib-2 will be like Autofib-1 and Autofib-1.5 in many respects. Generally the new instrument will be much smaller than its predecessors as it has only to access a field of approximately 180 mm in diameter. The robot positioner will be of a similar compact design as Autofib-1.5, but with the electromagnet pickup head replaced by a gripper (see chapter 5).

To avoid the restrictions on the performance of the servo loops encountered with both of the existing Autofib instruments, Autofib-2 will use a new type of DC servo loop for the X-Y carriage, where each motor is servoed from a rotary encoder mounted directly on the motor shaft. This will result in much faster and smoother movements of the X-Y carriage. Positional accuracy will be achieved as before by the use of linear encoders (to avoid ballscrew errors) which will be incorporated into the control system with the linear encoders providing the position feedback, and the rotary encoders the dynamic feedback.

The control of Autofib-2 will be provided by a VME bus microcomputer (for hardware compatibility with existing observatory instruments) running software

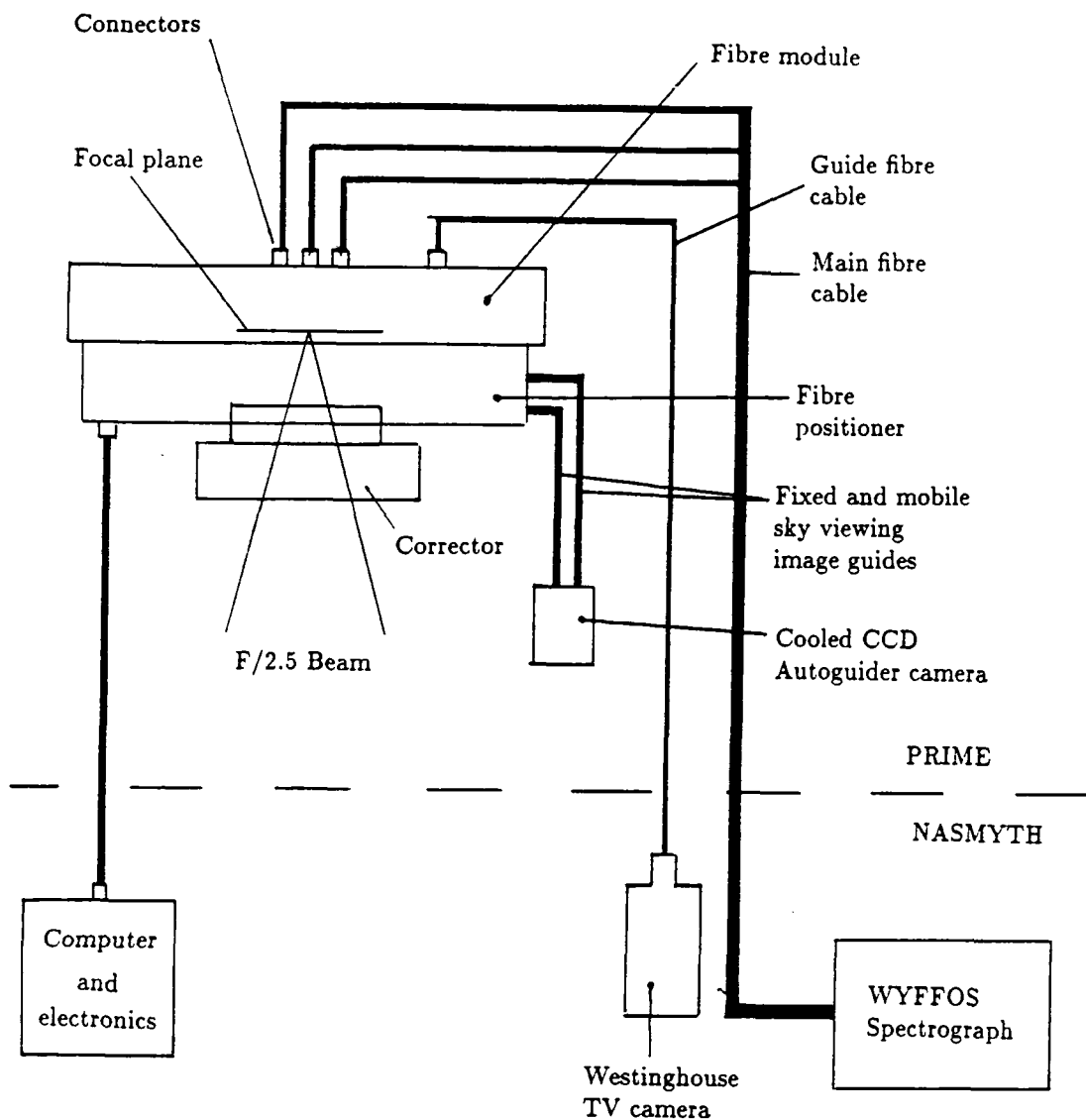


Figure 3.6 Block diagram of Autofib-2.

written in 'C', this will allow much of the software already written for Autofib-1.5 to be directly ported to the new computer. In addition the choice of 'C' allows the use of many software libraries supplied along with the intelligent motion control cards used in the Autofib design. Similar control techniques will be used for Autofib-2 as have been tried and tested on Autofib-1.5.

The multi-way fibre connectors were operationally a great success, although much more work is still required to improve their efficiency. Possible changes might include using a larger diameter fibre in the main fibre cable to remove alignment losses (but at a slight loss of resolution as the spectrograph now sees a larger fibre). The fibres in the main cable would have to be only 10  $\mu\text{m}$  larger in diameter to totally remove alignment losses at the connector.

While the viewing head idea has proved extremely useful, on Autofib-2 it will be replaced by two separate cameras. This will avoid the problem of matching the fibre illumination, or switching the coherent bundle from one camera to another (not a simple task at prime focus). The new design will use three separate TV cameras. The first of these will be for looking at the back illuminated fibres for positional measurements and to aid with fibre placement (see chapter 5). This 'fibre viewing' camera will be part of the fibre manipulation unit. A second TV camera will be dedicated to looking at the sky. This will be fed by two image guides, one of which will be fixed at a single point in the field and the other will be moved around the field by the X-Y carriage. Both image guides will feed a peltier cooled autoguider CCD TV camera. The third camera (a Westinghouse TV camera) will look at the output from the guide fibres as before.

In conclusion, Autofib-1.5 has been a very successful testbed instrument, enabling the testing of many new ideas for future instruments. It is unlikely that some of these ideas (for example the multi-way fibre connectors) would have been risked on a common user instrument without previous experience. While Autofib-1.5 did not achieve the required positional accuracy for a prime focus instrument, many of the causes of positioning errors were investigated. Although the new fibre probe design gave an improved performance in terms of being able to assign fibres to objects as will be discussed further in chapter 6, it would seem that the projection of the prism from the button may have reduced the positional accuracy

significantly. While this was not critical for Autofib-1.5, it is a matter to be looked at more closely for Autofib-2.

## **4 Observing with Autofib-1.5**

### **4.1 Introduction**

The main reason for building a complete working instrument as a prototype for Autofib-2, was that it was the best way to understand some of the new problems involved and to provide experience using fibres at the WHT. The previous chapter described the technical results from the two commissioning runs of Autofib-1.5 at the WHT, and this chapter presents some of the observations made during the two visits to the WHT. While Autofib-1.5 has been very successful in terms of the gaining of experience which will feed into the design for Autofib-2, it has also been shown to be a working scientific instrument.

During the two commissioning runs, the fibre output from Autofib-1.5 was fed to the Fibre Linked Experimental Spectrograph (FLEX). The resulting spectroscopic data provided a useful confirmation of the operation of the instrument. Following on from the second commissioning run, Autofib-1.5 and FLEX were scheduled for a PATT observing run. The observing procedures used when observing with Autofib-1.5 are now detailed, and some observational results presented.

### **4.2 Observations, March 1989**

#### **4.2.1 Motivation of observations**

The March 1989 commissioning run was never intended to be a scientific



observing run. However, sample spectra were taken to test the ability of the instrument to obtain spectroscopic data.

#### 4.2.2 Technical setup

The experimental setup for Autofib-1.5 has already been discussed in detail and requires no further description. The multiple fibre output from the fibre positioner was fed from the instrument at the cassegrain focus to the nasmyth platform where the FLEX spectrograph was situated. The light from the fibre slit was collimated using a F/8 parabolic mirror, then passed on to a reflection grating. The spectra were imaged onto a standard La Palma CCD detector using a reflecting Maksutov-Cassegrain camera (F/2.2, 197mm focal length). For most of the observations a low dispersion grating (150 lines/mm) was used to cover a wide spectral range, but for a few observations, a higher dispersion grating (400 lines/mm) was used. The 150 lines/mm grating gave a wavelength coverage from 3180 to 7216Å centered on 5200Å with a wavelength resolution of 19.6Å. The 400 lines/mm grating gave a wavelength coverage of 7612 to 9187Å centered on 8400Å with a wavelength resolution of 6.8Å. The WHT was still in an interim state at this time, no autoguider or calibration lamps were available within the interim A & G box at the cassegrain focus.

#### 4.2.3 The observations

As much of the testing of the fibre positioner was performed using open star clusters with accurately known positions, these clusters formed the first target for spectroscopic observations. The two clusters observed were Messier 35 (M35) and Messier 67 (M67). After setting up the target field configuration and acquiring the field using the guide probes, an exposure was started on the CCD. The telescope was guided by the observer who was able to watch the image of the guide stars in the guide fibres on a TV camera monitor. Several exposures of 1800 seconds were made to enable the removal from the image of cosmic ray events. Arc line

calibration exposures were made by dangling the arc lamps above the fibre probes inside the interim A & G box during a short exposure, as no calibration lamp facilities were available at that time.

Some results from these exposures are shown in figures 4.1 to 4.6. These results were rather disappointing as not many of the fibres yielded a result. Reasons for this were two fold. Firstly the positioning accuracy of the spectroscopic fibres was not very good at about 100–150  $\mu\text{m}$ , and the guide fibre probes were probably worse. This made acquiring the target field very difficult despite the fact that the positions of the stars in the cluster were very well known. Secondly, the seeing at the time of the observations was poor, approximately 2–3 arcseconds. This effectively reduced the amount of light through the 1.2 arcsecond fibres by a factor of between 4 and 9. However, the poor seeing did mean that we were getting some light through the badly placed fibres. During one exposure near dawn, the seeing improved suddenly to sub-arcsecond levels, and the exposure showed no photons from the target stars at all.

A second set of observations were made of the core of the Coma cluster of galaxies. The low dispersion grating was used for this work. Again, poor seeing and bad fibre placement accuracy meant that spectra for only the brightest galaxies were obtained despite the low dispersion used.

#### 4.2.4 Example results

Low dispersion (318 $\text{\AA}/\text{mm}$ ) spectra of stars in M35 and M67 are shown in figures 4.1 to 4.4. Several absorption lines are identified in each spectrum. As the stars in M67 are older and cooler than those in M35, it was expected that different absorption lines would be seen. For example, in the spectra of M35, the hydrogen Balmer lines are very strong with very few other features in the spectra. However, for the spectra obtained for M67, the hydrogen lines are weaker, and the Calcium II (H and K) lines are beginning to show. Other absorption lines

are also visible in the spectra. The cutoff at the blue end of the spectrum is due to a number of causes. Firstly, the atmosphere cuts off any light blueward of about 3200Å. Secondly, the CCD detector is very insensitive to blue radiation, and finally although the optical fibre is optimised for blue transmission, its transmission decreases rapidly at wavelengths of less than 4000Å.

Figure 4.5 shows a higher dispersion (124Å/mm) spectrum of a star in M67 before and after sky subtraction. The spectrograph grating has been chosen to select the red end of the spectrum. In the spectrum of the star and sky, several bands of emission lines due to OH in the atmosphere are visible. Identified absorption lines in the spectrum of the star include the Calcium triplet, and the atmospheric oxygen A band. It is the presence of sharp emission lines from the atmosphere at the red end of the spectrum that causes many problems during the sky subtraction process for faint objects.

Figure 4.6 shows two spectra of galaxies in the Coma cluster, for these observations the low dispersion grating was used. Several absorption lines are identified.

### 4.3 Observations, April 1990

#### 4.3.1 Astronomical results from the commissioning run, April 1990

The telescope time was divided into three nights for commissioning the instrument and four nights for a PATT observing run to look for evidence of the mass and extent of dark galactic halos. By the time of these observing runs, full cassegrain acquisition and guiding facilities were available.

No spectroscopic data was obtained as part of the commissioning run. The main aim of the commissioning run was to test the improvements made to the instrument since 1989, and perform various calibration procedures on the sky. Chief among these was to make a determination of the plate scale of the telescope at the cassegrain focus. For this purpose, the x,y coordinates of approximately 20

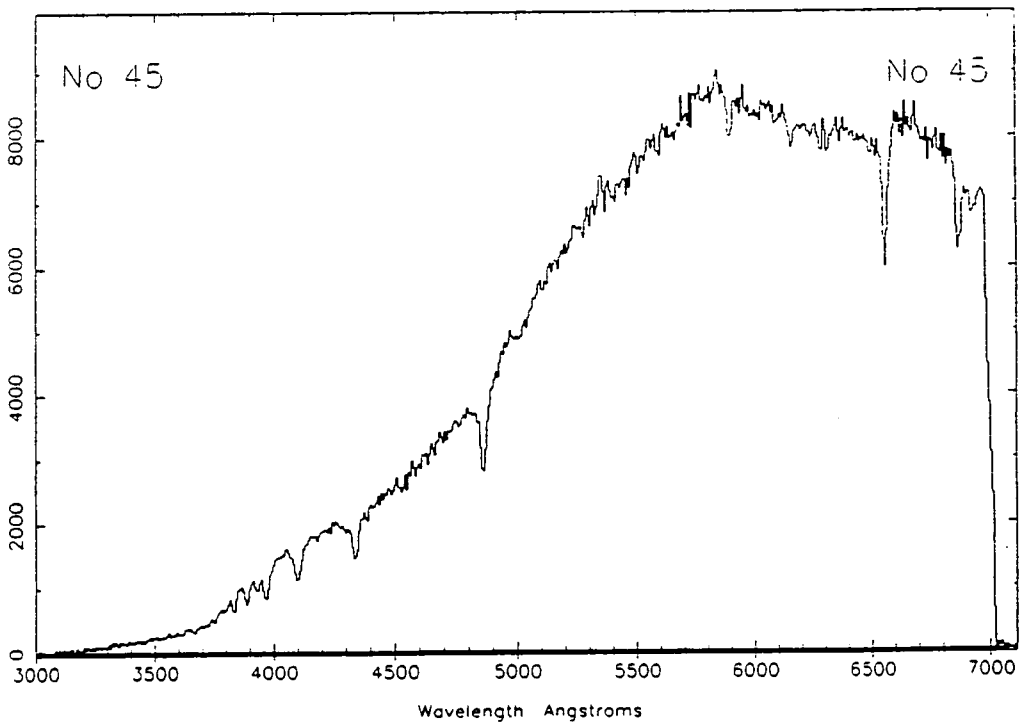
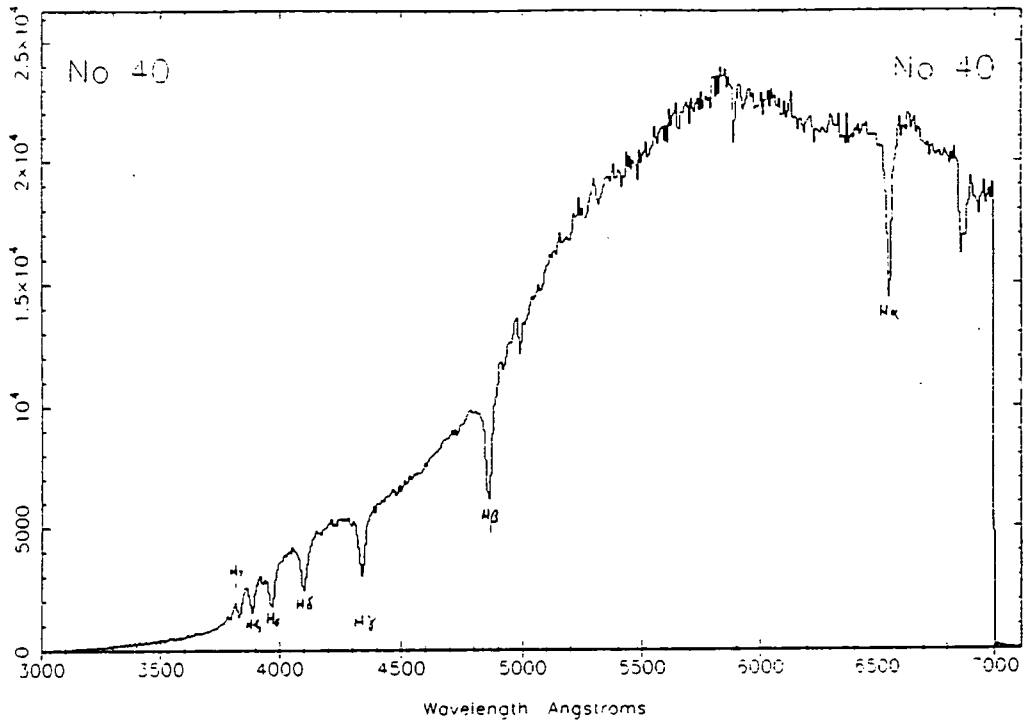


Figure 4.1 Spectra of stars in M35 from fibre numbers 40 and 45.

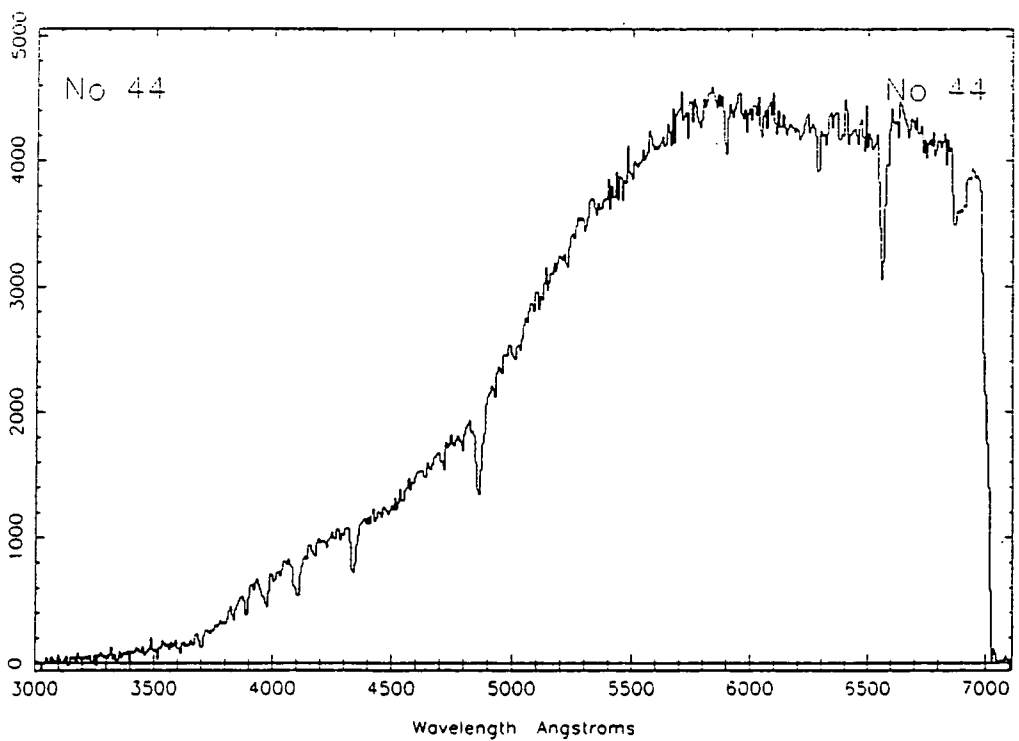
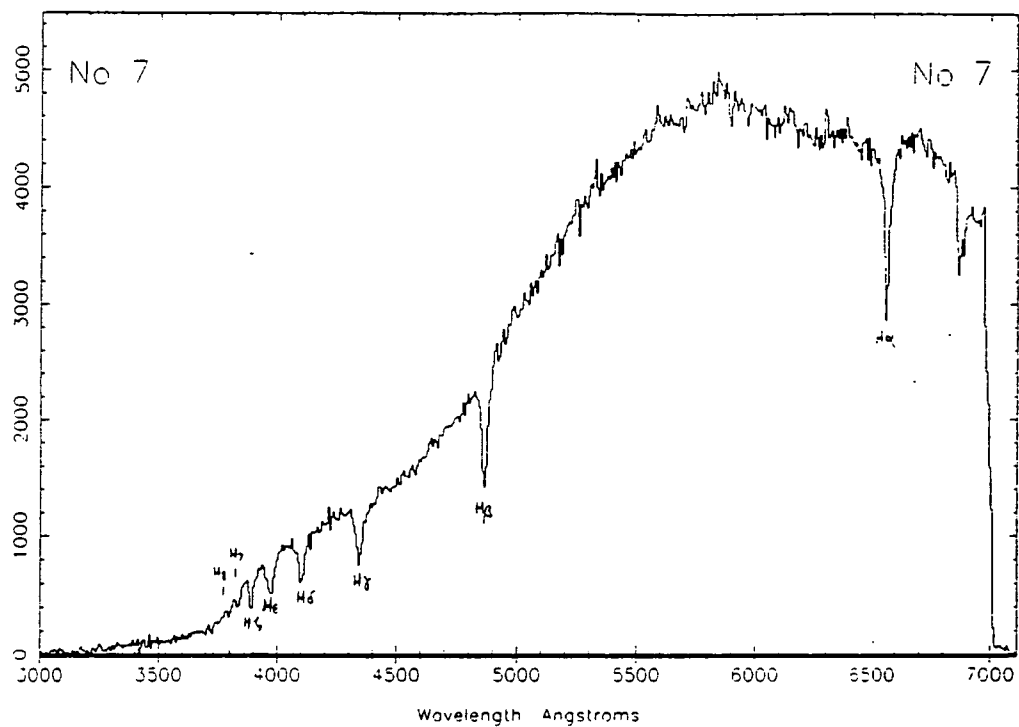


Figure 4.2 Spectra of stars in M35 from fibre numbers 7 and 44.

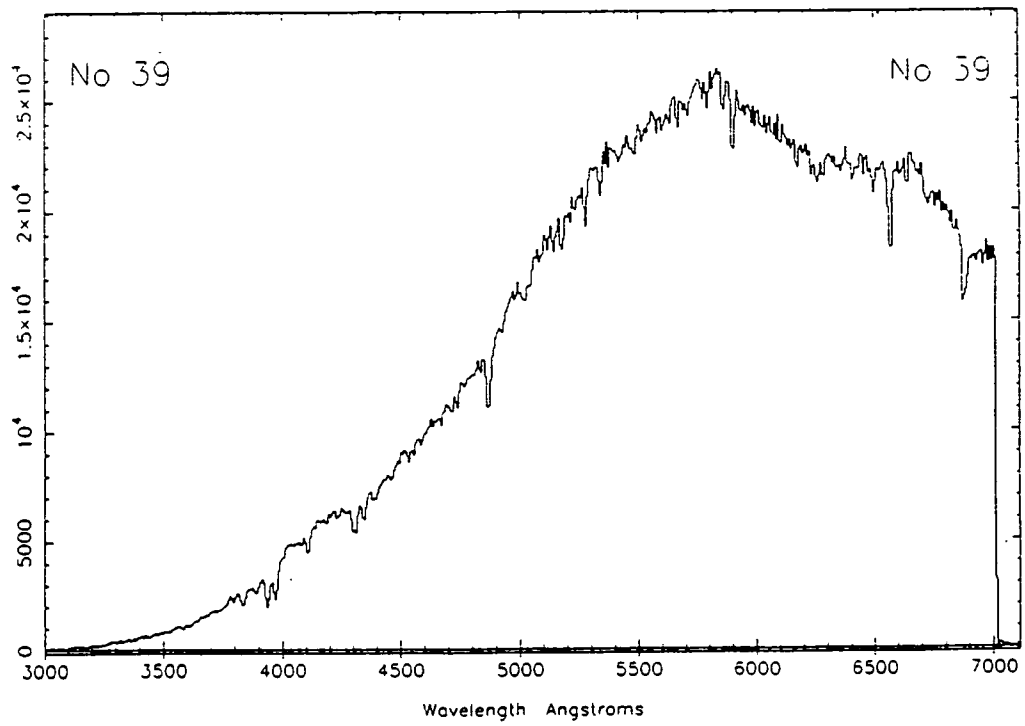
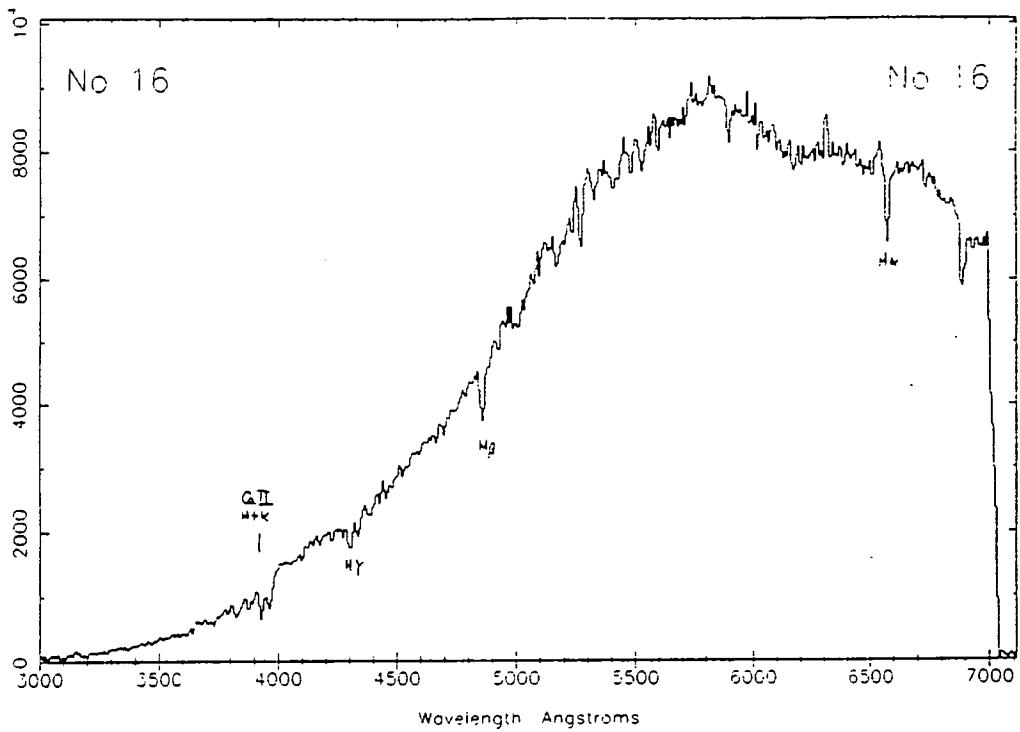


Figure 4.3 Spectra of stars in M67 from fibre numbers 16 and 39.

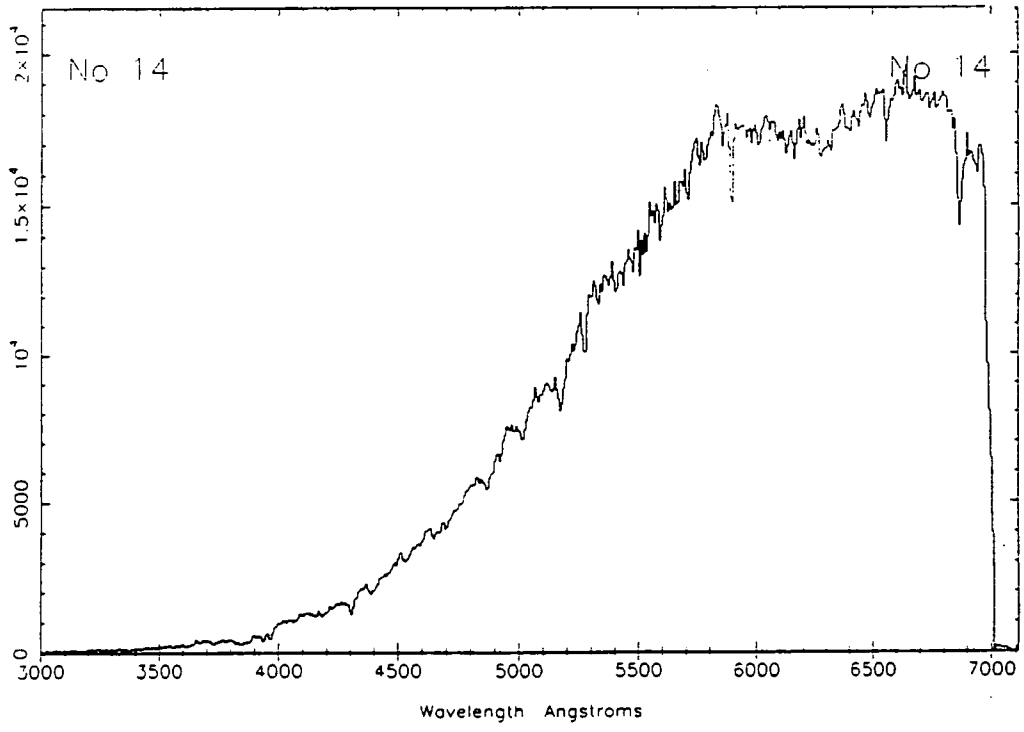
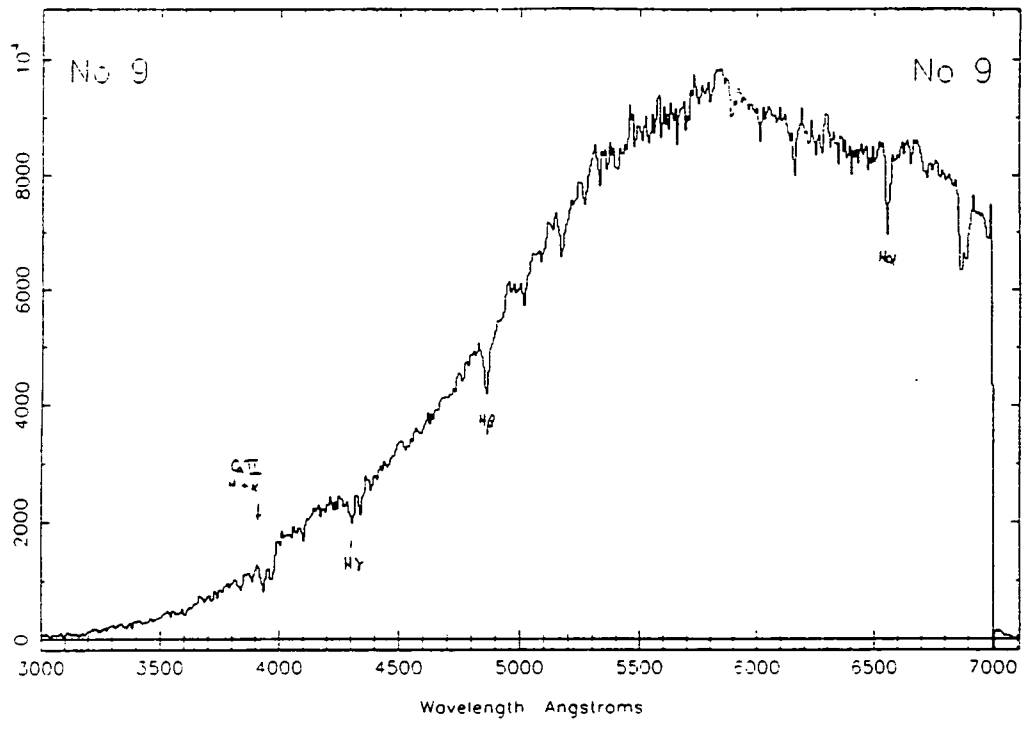


Figure 4.4 Spectra of stars in M67 from fibre numbers 9 and 14.

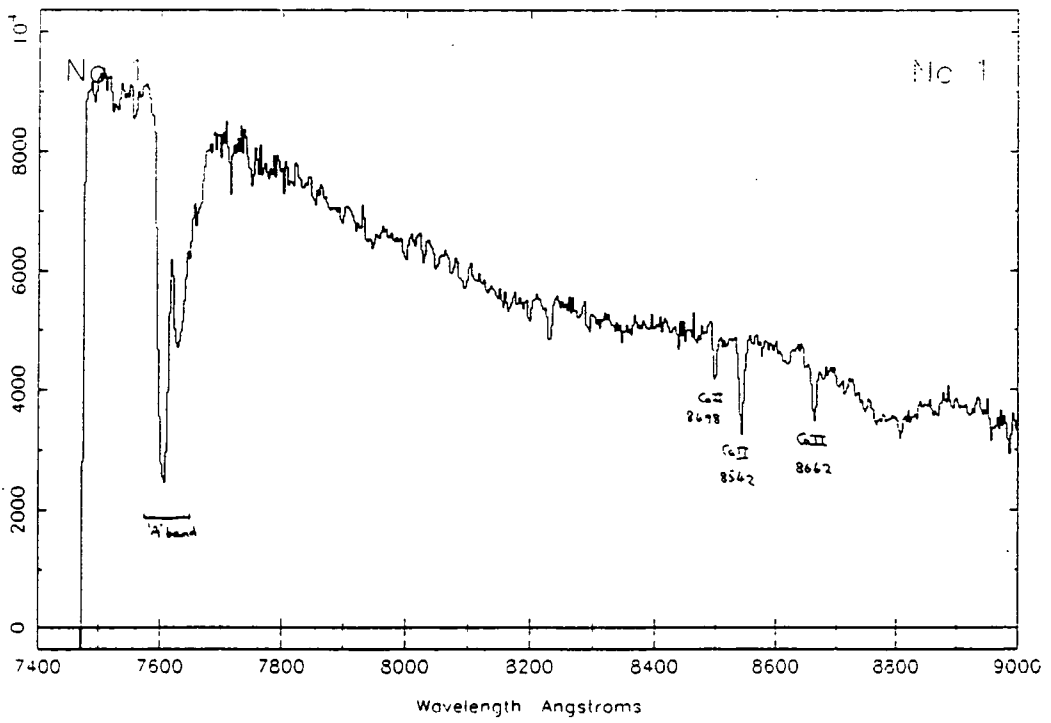
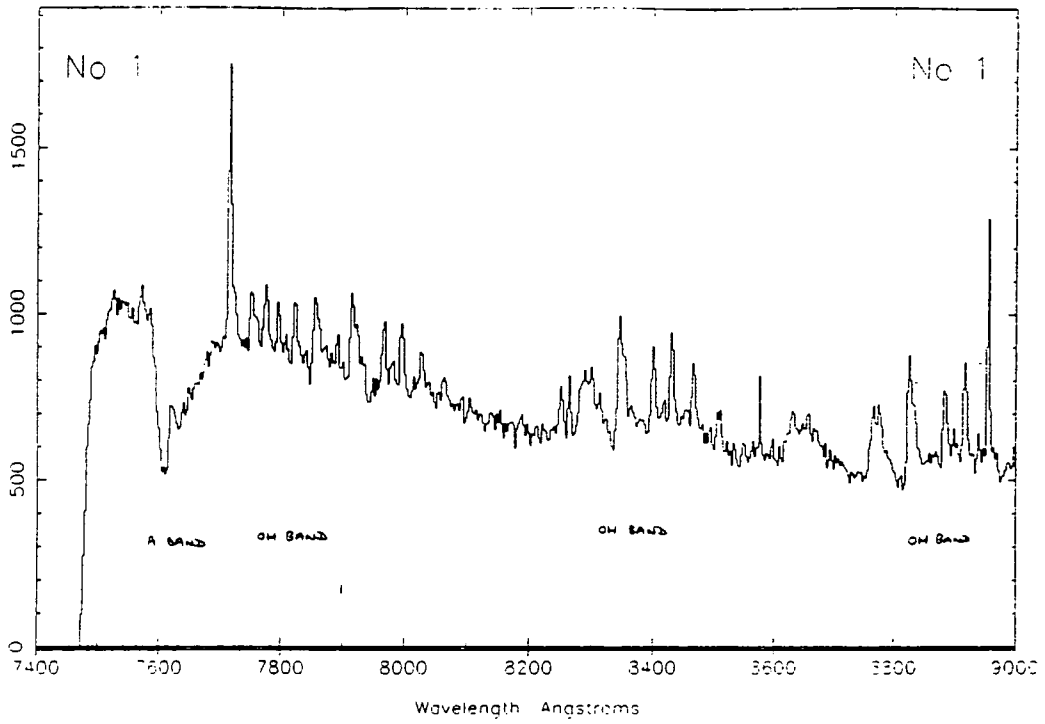


Figure 4.5 Spectrum of a star obtained through fibre number 1, top, before sky subtraction and below, after sky subtraction.



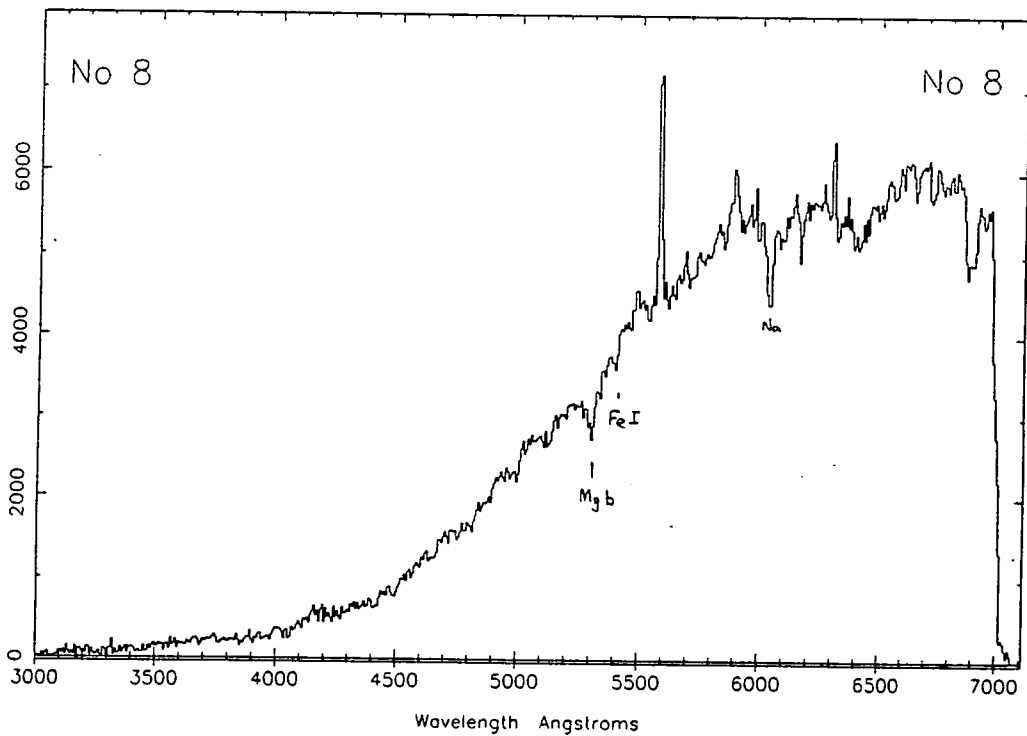
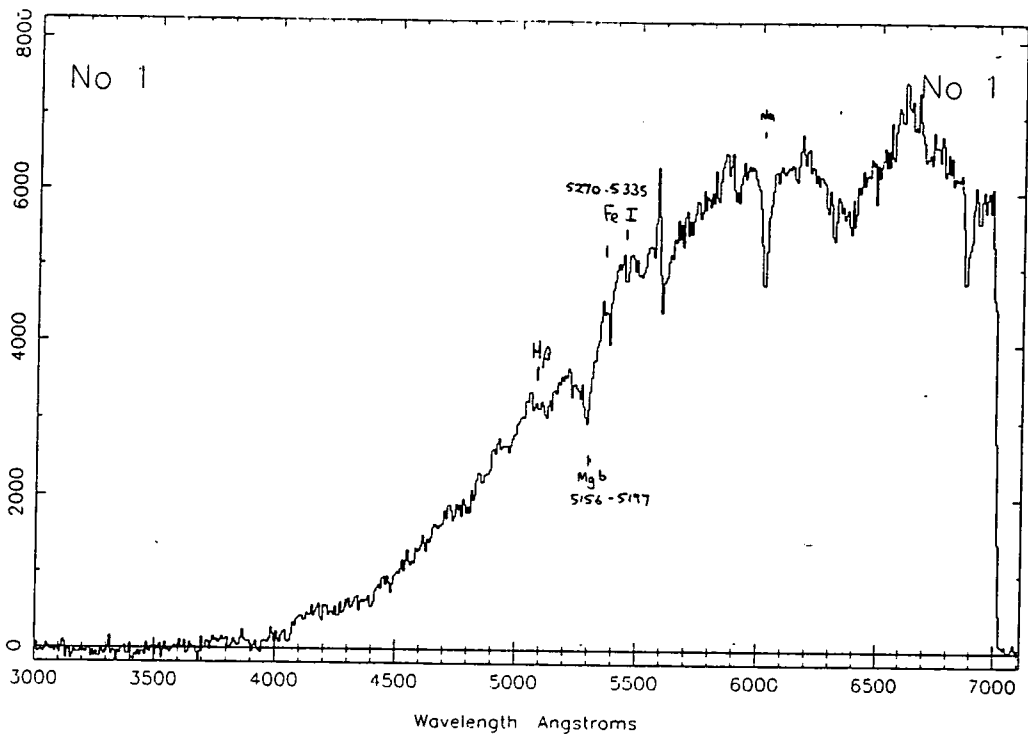


Figure 4.6 Spectra of two galaxies in the Coma cluster.

of the brightest stars in the outer regions of the globular cluster Messier 5 (M5) were measured using the viewing head of Autofib-1.5 whilst the telescope was under the control of the cassegrain autoguider. This procedure was repeated for two orientations of the instrument, the second 90° from the first. These measured positions of the stars were compared to their astronomical coordinates (RA and Dec) using the ASTROM software package. This procedure yielded information about the plate scale and the geometry of the X-Y carriage of Autofib-1.5.

Using the above method, the plate scale of the cassegrain focus was found to be 221.8277  $\mu\text{m}$  /arcsecond. The mean residuals from this process were approximately 0.3 arcsecond for the first attempt, and 0.15 arcsecond for the second attempt when the seeing had improved slightly. Although this did not agree with the plate scales used during the earlier commissioning run, the discrepancy was probably due to the fact that the telescope optics had been re-aligned when installing the new temperature compensated focus drive for the secondary mirror. The new plate scale determination agreed with that used for the FOS Multi-slit aperture mask as closely as might be expected as the back focal distance of FOS and Autofib-1.5 was only the same to an accuracy of 1mm.

A secondary result of the comparison of measured against actual coordinates of the stars was an estimate of the orthogonality of the X-Y carriage. On the first calculation, the deviation was found to be +0.5 arcminutes, and on the second attempt about -0.5 arcminutes. The true value probably lies somewhere between these values. In principle this effect could be taken account of in the configuration software. However, for Autofib-1.5, the magnitude of the non-orthogonality is approximately 50  $\mu\text{m}$  (or less than 0.25 arcsecond) across the diameter of the field and may simply be ignored

#### 4.3.2 The extent of massive dark halos, April 1990

The PATT observing run to look for evidence of massive dark halos around spiral galaxies followed directly after the commissioning run with Autofib-1.5. The main idea of the project was to try and identify satellite galaxies around carefully chosen spiral galaxies similar to the Milky Way. A number of candidate spiral galaxies were identified out to a radius of approximately 500 kpc from survey plates scanned using the APM machine at Cambridge.

These candidates formed the target objects for a series of Autofib target fields. Once redshifts for the candidates had been determined, background objects could be removed, and the velocity dispersion of the galaxy satellites calculated. The velocity dispersion would then give information about the mass distribution of the central galaxy to a larger radius than could be achieved by measuring the rotation curve of the central galaxy alone.

#### 4.3.3 Technical setup

Again the FLEX spectrograph located at the nasmyth platform was used. The absorption lines that the observations required were the H and K calcium lines at 3933.6 and 3968.5Å because these absorption lines would be visible in the spectra of almost all galaxies. To get the required velocity accuracy, a 1200B grating was used in conjunction with a dye coated (blue enhanced) GEC CCD. Unfortunately, during the commissioning run it was found that the GEC CCD was prone to picking up electrical noise thus making the observations useless. Therefore, the CCD was changed to an EEV uncoated CCD. As this CCD had a poor blue response, the grating was changed to a 900R to pickup any H $\alpha$  emission lines in the galaxy spectra. The disadvantage in using any H $\alpha$  emission lines to determine redshifts is that not all galaxies show this emission line, for example, elliptical galaxies have almost no interstellar gas and therefore no H $\alpha$  emission.

With the 900R grating the wavelength coverage was from 5800 to 7200Å. Flat fields were obtained through the fibres off the twilight sky before observing began each evening. Calibration exposures were taken using the arc lamps built into the A & G box, although care was required because the illumination of the arc lamps did not cover the whole focal plane. For this reason, arc exposures were made with the fibre probes in the target field locations, and also in a circle near the centre of the field.

#### 4.3.4 Target field acquisition

As mentioned in the previous chapter, the positioning accuracy of the fibres during this run was considerably better than on the earlier run. However, despite the fibres being at the required locations, it was difficult to unambiguously acquire the target fields. The problems arose because the target and fiducial star positions were obtained from Palomar Observatory Sky Survey (POSS) Schmidt plates. As these plates were rather old, the proper motions of the guide stars meant that they were no longer in the same positions relative to the galaxies.

An attempt to solve this problem was made by using the viewing head to check on the position of every known star in the field in addition to those with guide fibres assigned. With the telescope under the control of the autoguider, the viewing head was driven to the expected location of every star in the field, and the TV camera monitor marked with the position of the star in the field of view. After this procedure it was possible to divide the guide stars into two sets, a first in which the stars clearly had similar proper motions, and a set of stragglers with different proper motions. At this point, the assumption was made that the stragglers away from the consistent set of stars had high proper motions, and that the consistent set of stars had smaller proper motions. It was then only necessary to ensure that two of the guide fibres were used at the location of two of the stars with smaller proper motions. However, at this point it should be noted that if

the set of stars that appear together, each have large but similar proper motions, this method will not enable the observer to acquire the target field correctly. Of course, the alternative was to try acquiring the field using each fiducial object in turn, and see which gave the best result.

Experimentation with acquiring the field using different fiducial stars showed that using the consistent set of stars made for the best field acquisition, and gave the largest amount of signal through the fibres. Once the target field had been acquired, several exposures of 3000 seconds were made. This was the longest exposure that could be made before cosmic ray events became intolerable.

Despite the precautions taken to acquire the target fields, the results were not very satisfactory. Only two spectra yielded a  $H\alpha$  emission line from a total of three fields observed before bad weather ended the observing run. Although the FLEX spectrograph is not very efficient (the camera has a central obstruction and uncoated optics), this would not account for the lack of signal in the spectra. The seeing during the observations was extremely good, better than 1.5 arcseconds over the whole run, and sub-arcsecond for large parts of each night, so seeing was not a problem. A more likely explanation would be a large amount of extinction in the atmosphere. From outside the dome, very few stars were visible to the naked eye although the visible stars did cover the whole sky. Dawn revealed the sky above the observatory to be coloured light brown from dust in the atmosphere. From the numbers and magnitude of the stars visible during the night, the extinction was estimated to be approximately 4 magnitudes.

#### 4.3.5 Results

Figure 4.7 shows the only usable spectra that were obtained from the PATT observing run. The spectrum from the central galaxy and a candidate satellite are shown. On checking the log file for the fibre configuration however, it was found that the candidate satellite galaxy was very close to the central galaxy, and may

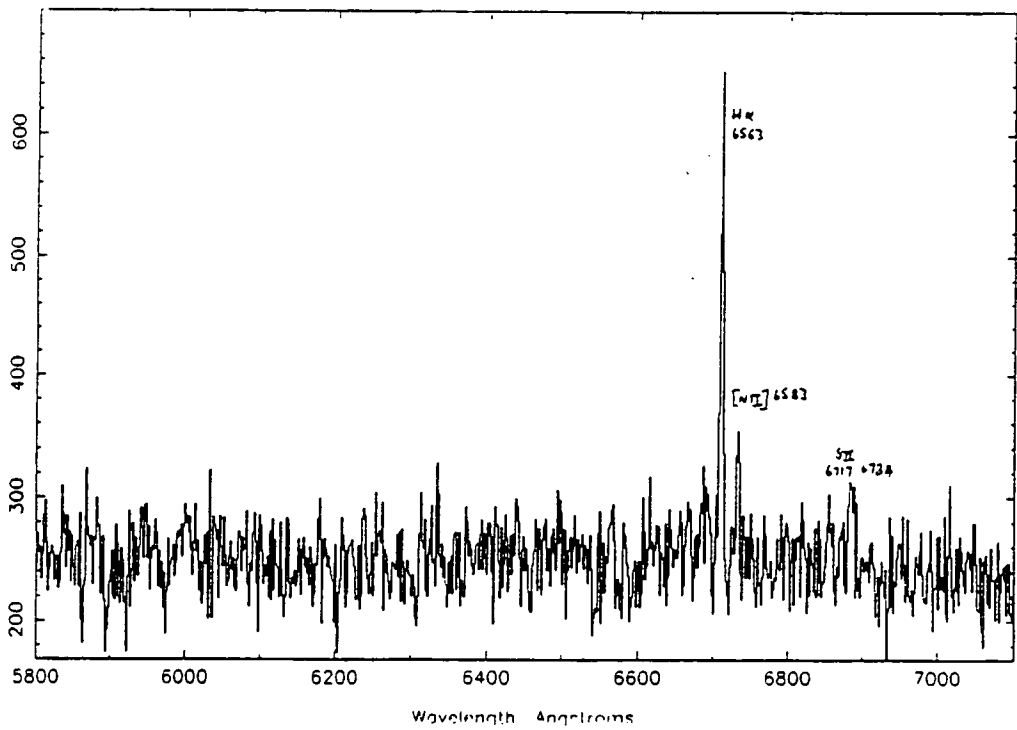
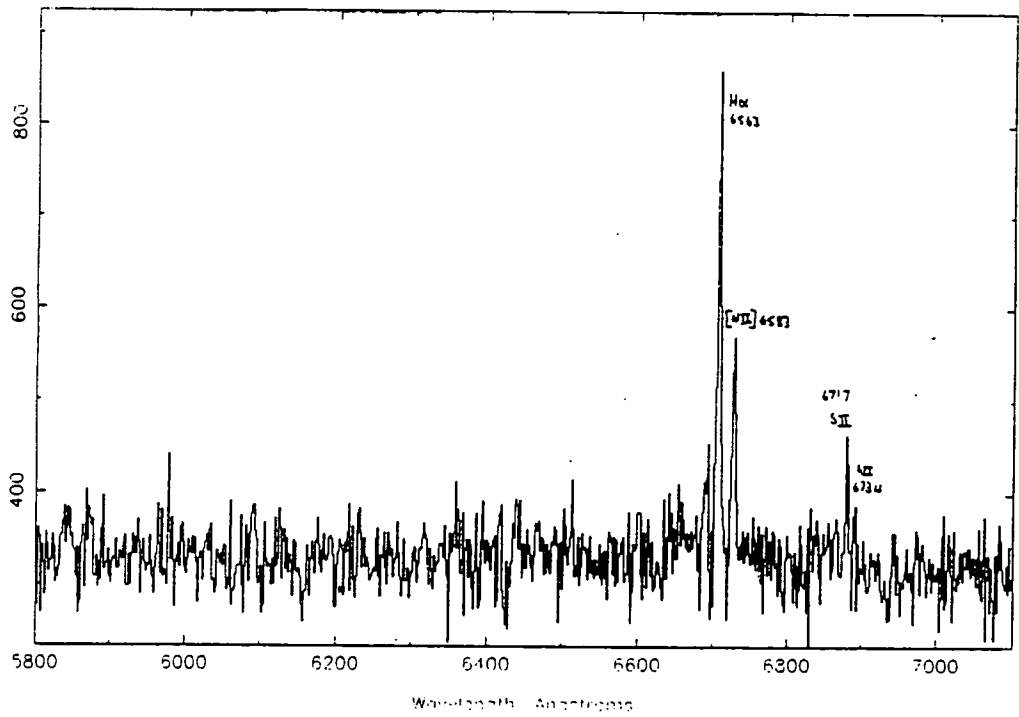


Figure 4.7 Spectra from the central galaxy (NGC 3154, upper) and a candidate satellite galaxy (lower).

have been a bright HII region. This is supported by the fact that the redshifts of the emission lines are almost identical in both cases. The emission lines identified have been redshifted from the rest frame by approximately  $145\text{\AA}$  in the case of the central galaxy, and approximately  $148\text{\AA}$  for the candidate satellite. The difference in the redshift is probably due to the rotation curve of the galaxy.

#### 4.4 Conclusions

From the two observing runs, some spectroscopic data has been acquired. Several technical problems and poor seeing reduced the quality of the data during the first commissioning run. For the second commissioning and observing run, the technical problems with Autofib-1.5 were almost completely eliminated and the fibre positioning process was achieved without any hitches. However, the observing run was still not as successful as might have been hoped, due to poor weather and astrometric problems.

For future observing runs with Autofib-1.5, or its successor Autofib-2, it will be important to ensure that the astrometry is more up to date. This should be possible as soon as the second POSS survey becomes available. Alternatively, plates taken at the prime focus of the WHT (when its corrector is commissioned) would also provide suitable astrometric data. It should be noted that the proper motion of guide stars has not been a problem with Autofib-1 at the AAT where the astrometric data comes from more recent UKST Survey plates.

A new spectrograph is currently under construction to replace FLEX as a fibre fed spectrograph. The new spectrograph (WYFFOS) will share the nasmyth platform of the WHT with the Ground based High Resolution Imaging Laboratory (GHRIL). WYFFOS will be much more efficient than FLEX and will also be optimised for use with fibres.



## 5 A new technique for automated fibre positioning

### 5.1 Introduction

The small plate scale at the prime focus of large telescopes has both advantages and disadvantages for multiple fibre spectroscopy. In particular, compared to secondary foci, one has access to much larger fields of view (given a suitable prime focus corrector). However, the spectroscopic fibres must be positioned with much greater precision in order to obtain sub-arcsecond accuracy similar to that obtained at cassegrain. The proposed new prime focus of the AAT, the 2dF facility (Taylor and Gray, 1990), has a plate scale of  $67 \mu\text{m} / \text{arcsec}$ , so to achieve a positioning accuracy of 0.2 arcseconds rms we must position fibres to better than  $15 \mu\text{m}$  rms.

Current experience at the cassegrain focus of the AAT with Autofib-1 and at the WHT with Autofib-1.5 has shown that it is possible to achieve approximately  $\pm 25 \mu\text{m}$  rms in positioning accuracy. However, this is only possible after a large amount of calibration in the laboratory, followed by a final tune up of the calibration for each field being observed. Obviously if we are to obtain even higher accuracy for much larger numbers of fibres (up to 400 fibres are planned), such calibration procedures must be improved and made less time consuming, or even eliminated.



A new prototype test instrument ( the 2dF prototype) has been developed which replaces the electromagnet of the original Autofib design with a pneumatic gripper. The key aspect of the operation of the 2dF prototype system is that while a fibre is being manipulated by the gripper it is back illuminated from the spectrograph end and viewed in high magnification by a TV system built into the gripper. As the fibre is being placed, any positional errors due to deficiencies in the manufacture of the gripper and fibre can be measured, and the fibre replaced with an equal and opposite error introduced into the X-Y carriage. The errors should then cancel out and, when viewed by the TV system with the X-Y carriage in the desired position, the fibre should appear central in the TV's field. Whilst this chapter contains work undertaken as research and development for the 2dF facility, the techniques are also directly applicable to the prime focus instrument for the WHT ( Autofib-2 ).

## 5.2 Description of the 2dF prototype

### 5.2.1 Mechanical description.

The prototype system is shown in figures 5.1 and 5.2. Figure 5.1 shows the whole mechanical system including the X-Y carriage, the fieldplate support frame and the fibre handling assembly. Figure 5.2 shows the fibre handling assembly in more detail, including the Z axis, pneumatic gripper, optical system and optical fibre. Note that no attempt has been made to make this an instrument for telescope use, it is solely a test rig for trying out new ideas.

The X-Y carriage is a relatively inexpensive proprietary unit driven by stepper motors with mini-stepping drives to obtain a resolution of  $2 \mu\text{m}$  per mini-step. Open loop motion control (there is no X-Y encoding) is obtained using a 3-axis PC based intelligent stepper control card.

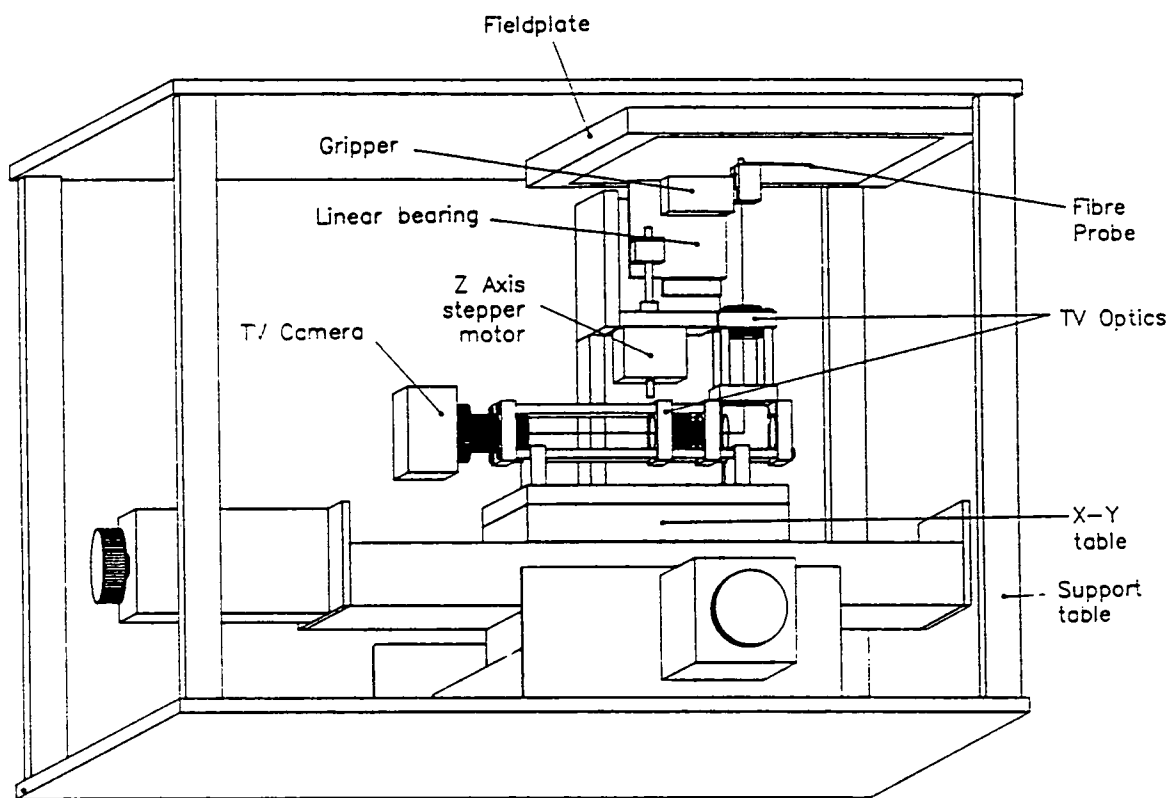


Figure 5.1 Complete mechanical assembly of the 2dF prototype.

The new techniques in fibre positioning involve the redesign of the fibre handling part of the robot. The previous system in Autofib-1 and Autofib-1.5 used an electromagnet to hold the individual fibre buttons, and a motor-leadscrew arrangement to raise and lower the button. The electromagnet has been replaced by a two finger pneumatic gripper manufactured by SMC. The gripper is mounted so that the fibre, when back illuminated from the spectrograph may be viewed via the optical system. The optical system used to view the fibres consists of a pair of achromats to transfer the image of the fibre to a more accessible point, a folding flat, a 10 $\times$  microscope objective and a CCD TV camera feeding a PC based frame

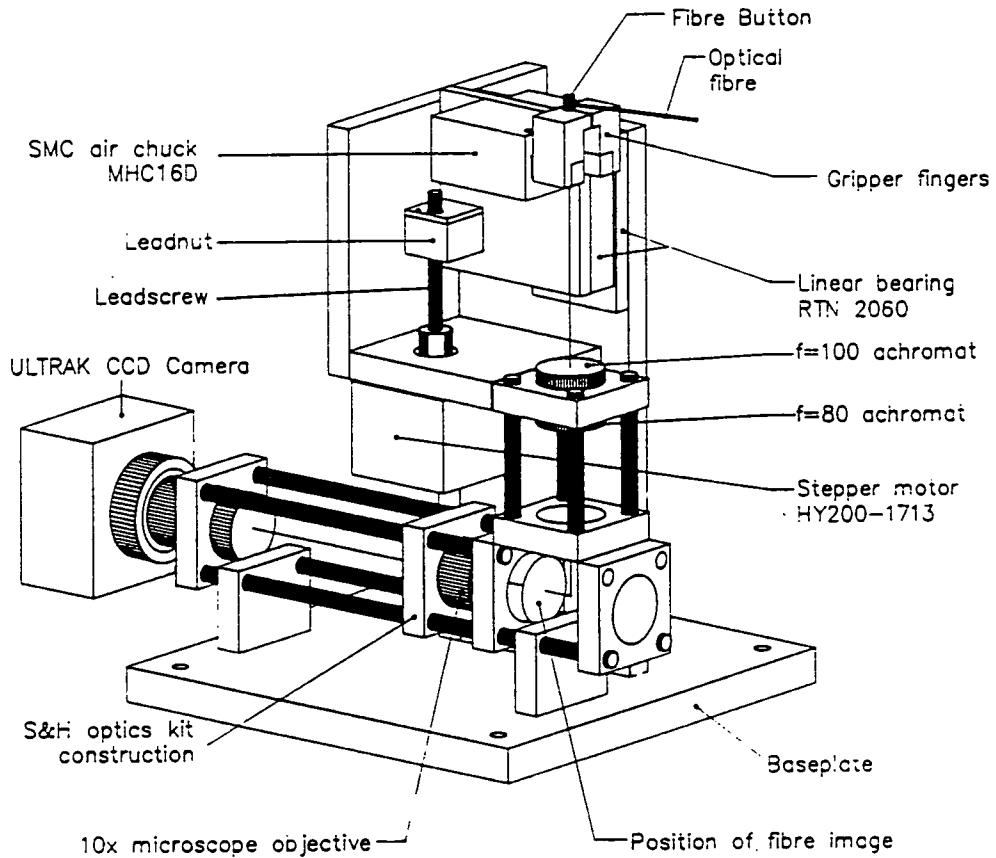


Figure 5.2 Gripper assembly for the 2dF prototype.

grabber. The entire optical system is mounted firmly to the X-Y carriage, but is mechanically decoupled from the moving parts of the Z axis.

The Z axis is also an open loop stepper system controlled by the 3rd axis of the PC control card. A similar design of linear bearing, leadscrew and lead nut to that on Autofib-1 is used. The fibre design is also similar to that of Autofib-1 except that now the conical hole for the electromagnet has been replaced by a short cylinder for the pneumatic fingers to hold (see figure 5.3).

Instead of encasing the optical fibre from the button to the pivot in a stainless steel tube, only the first 15 mm are encased in tubing to aid with polishing the

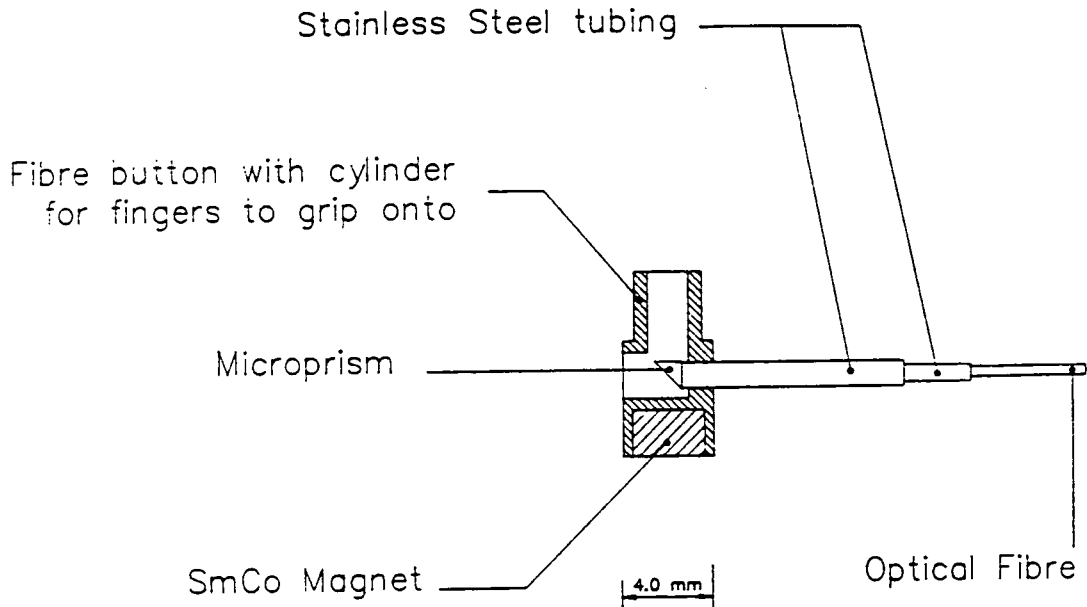


Figure 5.3 Cross section of fibre probe used with the 2dF prototype.

fibre and mounting inside the button. The remainder of the fibre remains bare for better fibre-fibre crossover characteristics.

### 5.2.2 Control of the prototype robot

The control of the prototype positioner is performed by a Compac 386/20e PC which acts as a host to both the 3-axis intelligent stepper control card and the frame grabber. The computer can accept interactive commands to perform simple functions, for example: move X-Y carriage, open gripper jaws, close gripper jaws, move Z axis, grab image, locate centroid of image and store the results. More complex instructions are simply built up from the basic commands, for example: pickup button, putdown button.

In a second mode of operation, the computer is able to receive commands from a file. This "batch" file enables repetitive testing of the robot without any

need for interaction. The robot automatically logs the positional accuracy of each fibre placement in a file for later inspection.

### 5.3 Testing of the 2dF prototype

#### 5.3.1 Centroiding accuracy

The position of a fibre within the field of view of the TV system is determined by digitising the TV image and applying a centroiding algorithm. The algorithm consists of background subtraction followed by a 2-dimensional determination of the mean position of the back illuminated fibre core. To determine the accuracy of this procedure, a back illuminated  $260\ \mu\text{m}$  fibre (approximately 4 arcseconds at the focus of 2dF) was viewed by the optical system and centroided 50 times without any mechanical motions. The distribution of the centroid positions is shown in figure 5.4.

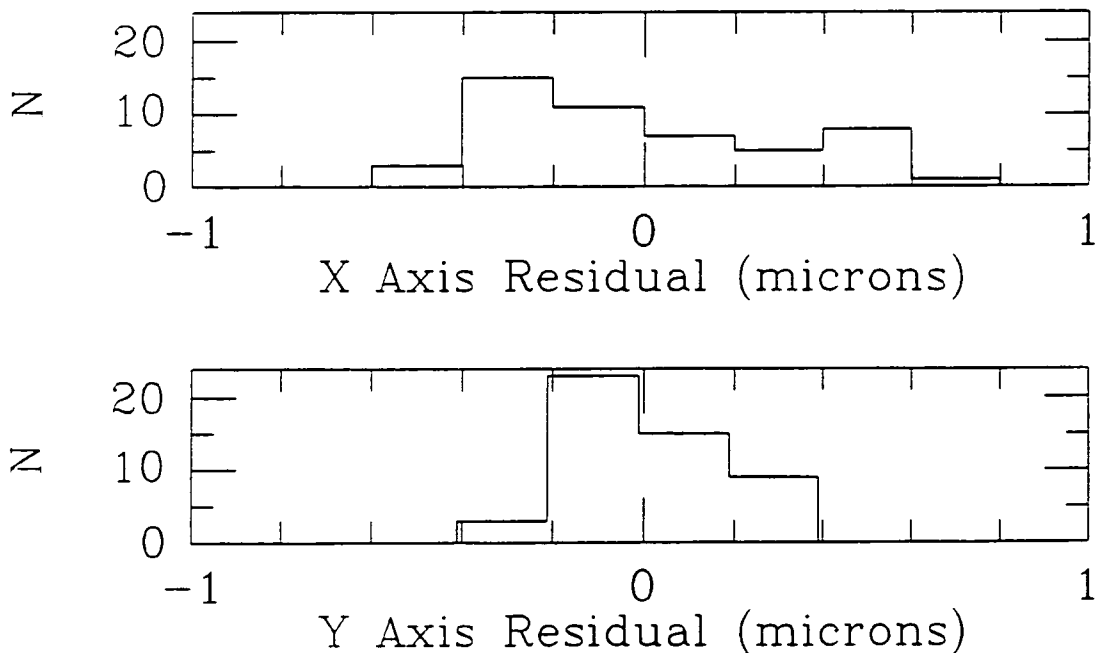


Figure 5.4 Results from fibre image centroiding tests.

The rms scatter in these distributions are  $\pm 0.32 \mu\text{m}$  in the X direction and  $\pm 0.16 \mu\text{m}$  in the Y direction. The image scale at the TV detector is 0.720 pixels/  $\mu\text{m}$  in the X direction and 1.007 pixels/  $\mu\text{m}$  in the Y direction, both scales being accurate to better than 1%.

### 5.3.2 Accuracy of the X-Y table

Determination of the accuracy of the X-Y table in terms of orthogonality of the axes, linearity of the screw pitch and straightness of travel has not been attempted because we are only concerned with the accuracy of the fibre placement with respect to the table's coordinate system. We therefore need only worry about the table's repeatability. To determine this, a fibre was left stationary on the field plate while the carriage was brought to it from various x,y positions. Each time the TV system returned and viewed the fibre, it centroided the image to determine the error. The distribution of these errors is shown in figure 5.5. The double peaked distributions show that there is  $7 \mu\text{m}$  of backlash in the X axis and  $14 \mu\text{m}$  of backlash in the Y axis. To eliminate backlash in further tests the 'X-Y move' software was modified so that wherever the carriage was asked to go, it would ensure that it always arrived at the destination point from the same direction. The error distribution using the modified software is shown in figure 5.6. The rms scatter of the distributions is  $3.1 \mu\text{m}$  in X and  $6.9 \mu\text{m}$  in Y. The results presented in figures 5.5 and 5.6 also confirm that the open loop stepper drives do not lose any steps.

### 5.3.3 Procedure for positioning fibres

The placement procedure for each fibre is as follows; pickup fibre and carry it to the x,y target position. Place the fibre on fieldplate and release jaws. Centroid the fibre image to determine the position error, close the gripper jaws and offset the X-Y carriage by equal and opposite error without moving the Z axis. Release

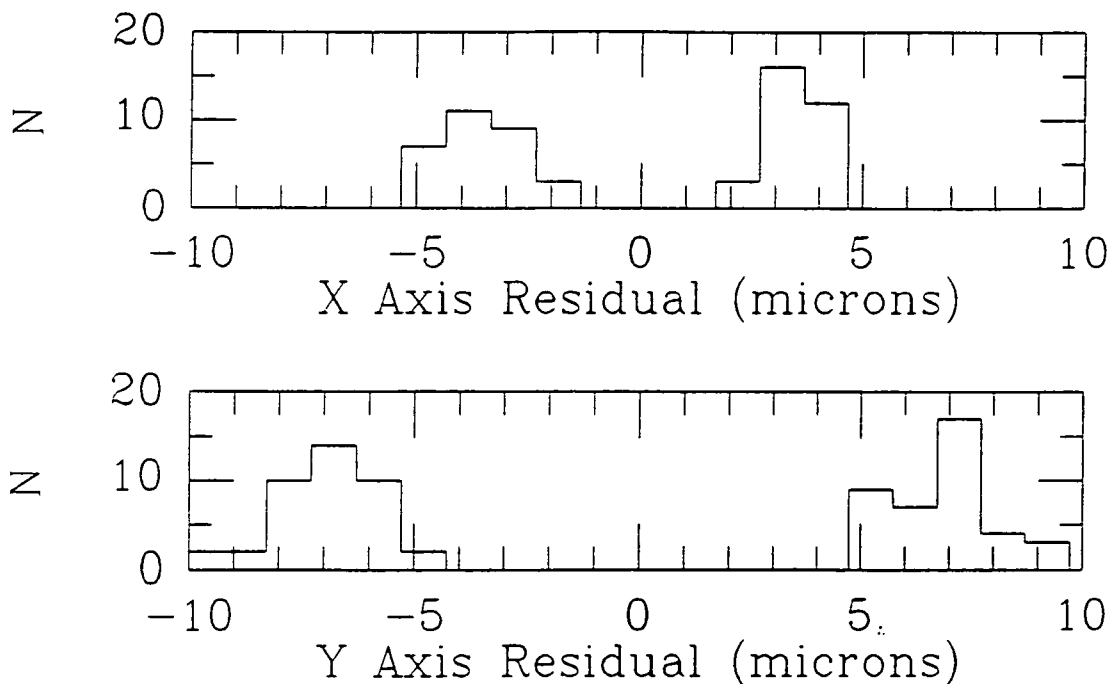


Figure 5.5 Repeatability tests of X-Y table showing evidence of backlash.

the gripper jaws and offset the carriage back to target position. Finally centroid the fibre image a second time and record any residual errors,  $\Delta x$  and  $\Delta y$ .

#### 5.3.4 Overall Positioning Accuracy

Figure 5.7 shows the distribution of the radial error  $\Delta r$  for 351 placements of a single fibre at various positions on the fieldplate, where:

$$\Delta r = \sqrt{\Delta x^2 + \Delta y^2}$$

The rms error was  $\pm 4.4\mu\text{m}$  and 97% of the positions were within  $10\mu\text{m}$  of the target position.

If necessary when  $\Delta x$  and  $\Delta y$  are not within the required accuracy then the last 5 operations outlined in the previous section, can be repeated until the required

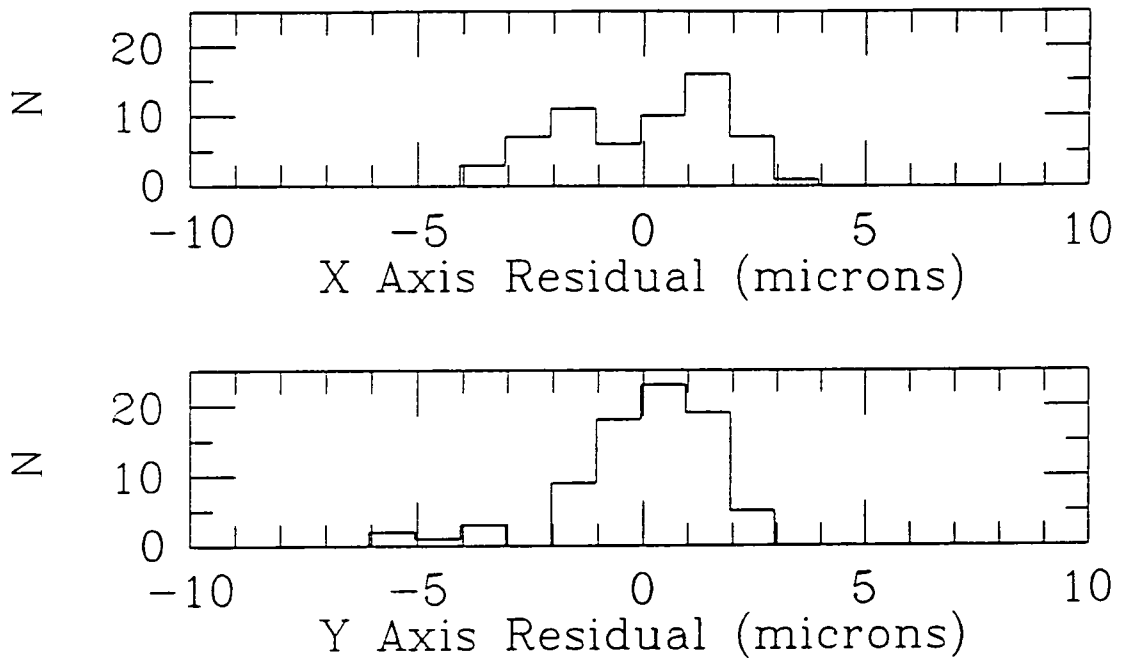


Figure 5.6 As previous figure, but with corrected backlash.

accuracy is obtained. In this way it is possible to trade-off setting up time against accuracy. Figure 5.8 shows similar results to figure 5.7 except that the robot would not accept positioning errors  $\Delta r$  greater than  $8\mu\text{m}$ . The experiment was run for 213 fibre placements.

Figure 5.9 shows the distribution of errors for 3 fibres being handled sequentially for a total of 80 fibre placements. The robot was not instructed to retry any bad placements. The rms error was  $\pm 7.9\mu\text{m}$  and 76% of the positions were within  $10\mu\text{m}$  of the target position. These results were not as good as those in figure 5.7 because the extra 2 fibres did not behave as well as the original fibre. It appears that some aspects of the fibre probes manufacture are critical. For example, if a button has a very slightly convex base it can rotate during the final correction stage and introduce slightly larger errors.



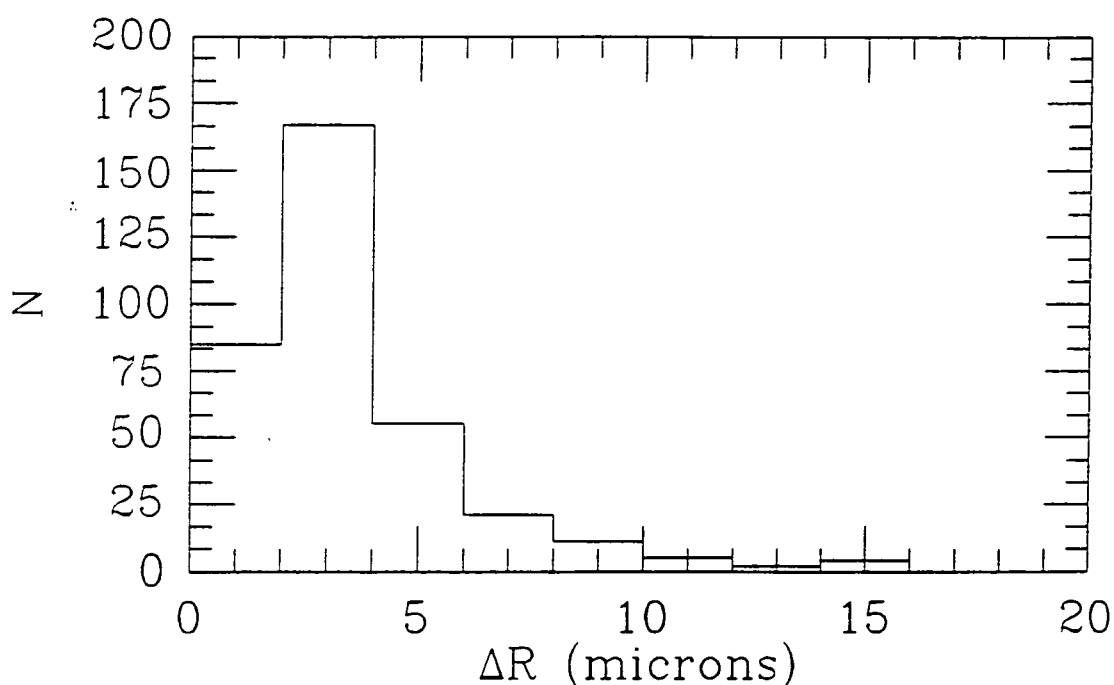


Figure 5.7 Positional accuracy results for a single fibre.

The above results show that aided by robot vision techniques, it is possible to achieve very high precision in the placement of a fibre probe. It should be noted that no special techniques were used in the manufacture of the fibre probes, and that no information about the manufacturing errors present in the fibre probe was required. The accuracy achieved is considerably better than is required for a prime focus instrument. However, the prototype described is not suitable for use on a telescope, and will require to be considerably improved in terms of reliability and speed. The rest of this chapter is dedicated to applying the above technique in a more practical implementation suitable for a telescope instrument.

### 5.3.5 Speed of operation

The duty cycle of the laboratory prototype system just described is very long at approximately 25 seconds per fibre placement. A large fraction of this time is

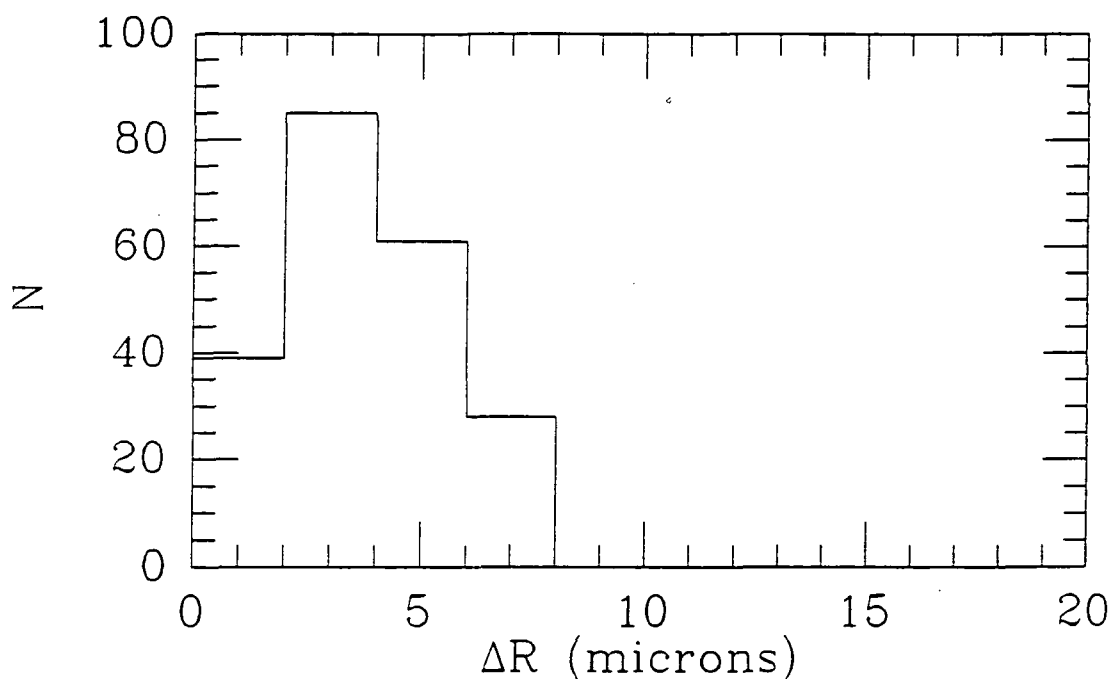


Figure 5.8 As previous figure, but with a tolerance of  $8\mu\text{m}$ .

taken centroiding the fibre image, this is currently about 6 seconds for each image centroid. As will be seen later in this chapter, the pickup-putdown cycle must be performed within approximately 3.5 seconds. With optimised software and possibly more powerful computer hardware, the centroiding of the fibre image should be performed much more quickly. Note that the second fibre position measurement is to provide data on the positioning accuracy and would not necessarily be needed in practice. The X-Y carriage, the Z-axis and the gripper can also be speeded up considerably.

### 5.3.6 Problems for future work

Whilst the principle of the 2dF prototype has proved to be very successful, there have been some problems. The gripper jaws grip the cylindrical button inside

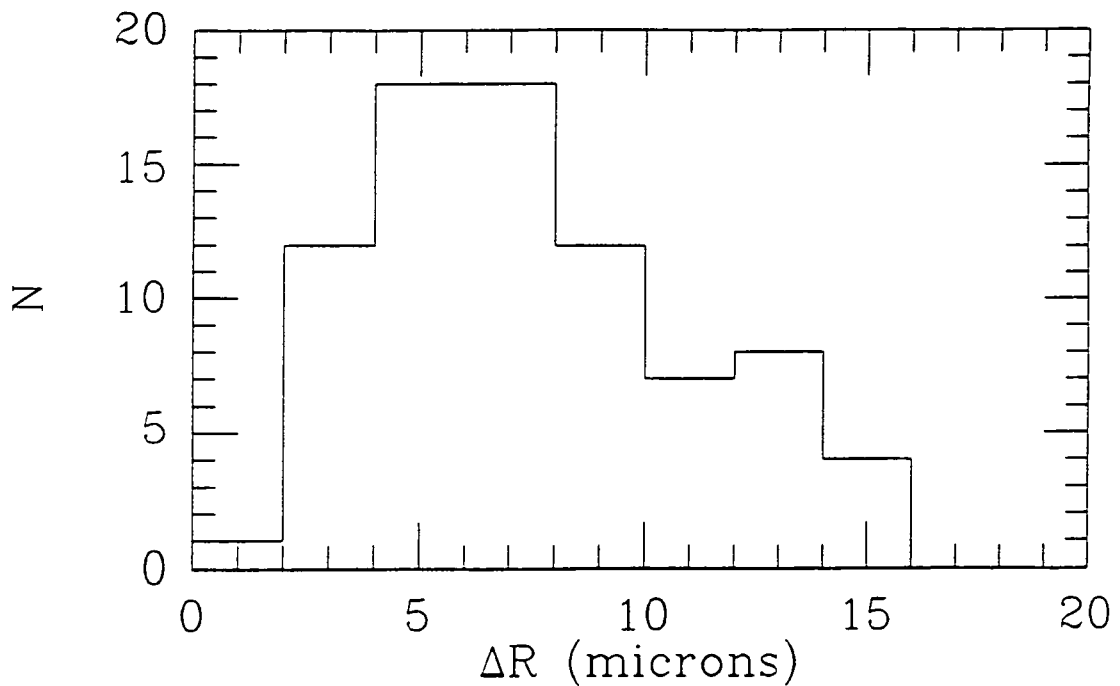


Figure 5.9 Positional accuracy results for 3 fibres.

two semicircular grooves in the jaws, and whilst this gave a very positive grip on the button, it did cause the button to be jolted severely as it was released from the jaws. This was caused by poor clearance between the jaws and the button as the jaws were pivoted a small distance away from the button. Whilst the release jolt of the button was fairly repeatable, it would appear that this was the main source of the remaining position errors. Also, as the fibre placement procedure was designed to remove the effect of this jolting, elimination of the jolt would simplify and speed up the putdown procedure.

During the tests so far, no fibre retraction system was used to keep the fibre in a straight line, this may have allowed the fibre to spin slightly as it was placed. Obviously for a telescope system, the fibre retraction mechanism must keep the individual fibres from tangling, and enable the software to predict accurately the position of each fibre along its length so that the anti-collision algorithms work

properly. However, it must not reduce the accuracy with which the fibres can be placed.

The centroiding algorithm as used in the initial prototype requires to be made faster and more robust. In particular if the fibre image is only partly visible to the camera, the centroiding algorithm must be robust enough to return a sensible position for the fibre. Due to the high magnification required to measure the position of the fibre accurately, the field of view of the camera is extremely small ( $\sim 600 \mu\text{m}$ ), this can result in a badly manufactured fibre not being visible to the camera when picked up by the gripper. Ideally a lower magnification TV system is required to give a larger field of view. This must be used with a new centroiding algorithm, but one which is still able to give positions accurate to approximately  $1 \mu\text{m}$  despite the lower magnification.

## 5.4 A new 2dF prototype

### 5.4.1 A new fibre probe design

The 4mm diameter button used so far, limits the closest approach of two fibres to approximately 1.2 arcminutes using appropriately shaped gripper jaws (the jaws used so far make no attempt to minimise the closest separation). Now that a large button surface area is no longer needed to maximise the grip of an electromagnet, we can afford to reduce the button diameter. Unfortunately, this will also reduce the force with which the button is held onto the fieldplate. However, if neodymium-iron-boron (NdFeB) magnets are used instead of the existing samarium-cobalt ones, the force of attraction to the fieldplate may be maintained despite the reduction in size.

Another possibility is to change the shape of the fibre buttons. The part of the button which is held by the gripper need not be concentric about the prism but offset a small distance. This 'handle' could be made much smaller as there

is no need for a hole for light to pass through. In addition the magnet could be elongated along the direction of the fibre to further minimise the profile of the fibre probe. The advantage of this design is that each fibre blocks a smaller section of the sky which could be viewed by other fibres (a very real problem when considering large numbers of fibres). An elongated fibre button was designed to conform to these ideas. Several practical constraints forced the final design of the button to be rather wider than originally anticipated. Chief amongst these was the selection of a suitable magnet, the smallest NdFeB magnets readily available in small quantities were 1.5mm×1.5mm in section and 6mm long. To use these magnets, a 2.0mm wide button was designed (figure 5.10), which encloses the magnet inside a slot in the base of the 'button' to try and reduce any magnetic crosstalk between individual buttons. A vertical 'fin' running the length of the button provides a handle for the gripper to grab hold of.

The new fibre probes were constructed with 100  $\mu\text{m}$  optical fibre, as this corresponds to the smallest fibre size (1.66 arcseconds) that is likely to be used. The buttons were machined from brass, taking extreme care to ensure that the brass handle remained perpendicular to the lower surface of the button. The NdFeB rare earth magnets were epoxied into the slot in the base of the finished button. Again the fibre remains bare for almost its entire length, and is terminated by three concentric stainless steel tubes 6mm long at one end. The tubing provides a point to handle the fibre during polishing and also a face to glue the microprism against. Once the microprism was glued in place, the tubing was inserted into the brass body of the fibre button and glued using a two-part epoxy (Araldite).

#### 5.4.2 A new design of gripping robot

A second gripping pickup head was designed in order to manipulate the new fibre probes. A section through the gripper unit is shown in figure 5.11. The gripper consists of two fingers driven pneumatically which grip the fibre button.

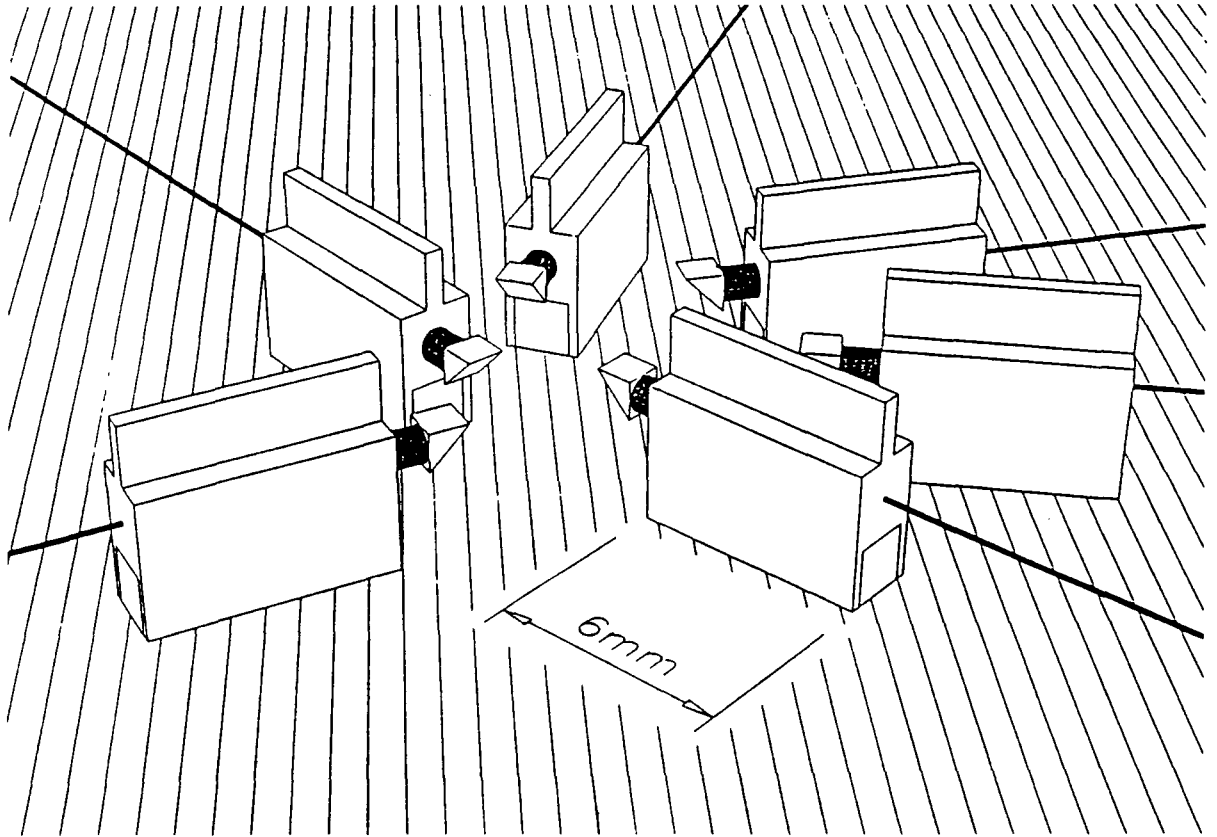


Figure 5.10 Conceptual design of new fibre probes.

The jaws are driven by a single acting piston, the jaws are closed by supplying compressed air to the piston, and opened by evacuating the piston chamber. To ensure that the jaws release the fibre probe cleanly, the two jaws are coupled together very strongly. This means that the forces present as the air pressure in the piston is released are balanced, and the release of the jaws remains repeatable. To manipulate the fibre probes, the fingers may be driven along the optical axis (the  $Z$  direction) and rotated about the optical axis (the  $\theta$  axis). A TV system is able to view a fibre probe held between the fingers through a central hole in the

gripper bodywork. The TV system uses a slightly lower magnification than the earlier system, and is able to see a field of view of  $1\text{mm}^2$  at scales of  $2.461\ \mu\text{m}/\text{pixel}$  (X axis) and  $1.424\ \mu\text{m}/\text{pixel}$  (Y axis).

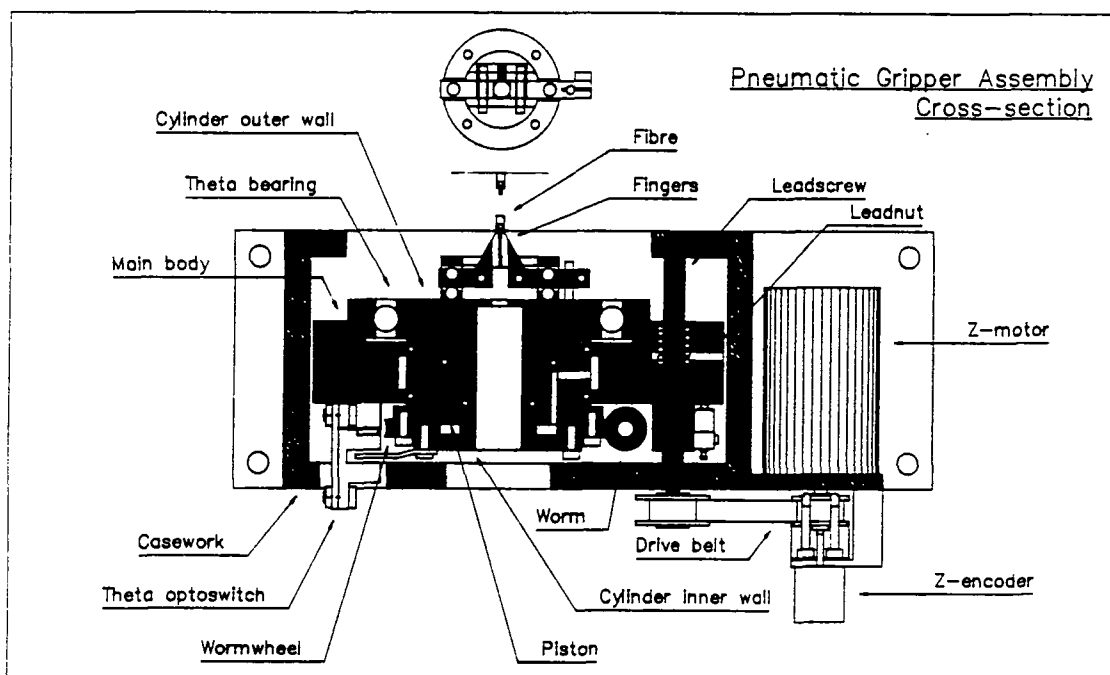


Figure 5.11 Section through the new gripper unit.

The  $\theta$  axis allows rotation of the fibre button to avoid twisting the fibres as they are moved from one position to the next. The rotation is driven by a motor

via a worm gear. The Z axis has been designed in a similar way to Autofib-1.5, as this offers a more compact device. However, the spur gears of the Autofib-1.5 design have been replaced by a timing belt between pulleys as this should be smoother and quieter. The gripper body slides on four linear bushings which allow it to move in the Z direction.

The new gripper is powered by two dc servo motors of the same type used on the Z axis of Autofib-1.5 and uses optical encoders to complete the servo loops. The initialisation of the Z and  $\theta$  axes uses similar opto-switches to those used successfully on the X and Y axes of Autofib-1.5. The gripper has specially designed jaws to improve access to closely packed fibres, and enable the picking up of a fibre whose 'handle' is off axis with respect to the grippers rotation and optical axis (figure 5.12). This new design of gripper jaw means that it is possible to measure the position of the fibre whilst gripping the off axis handle. Note that as the fibre handle is now offset from the optical/rotational axis, each fibre now has a defined position angle which the rotation stage will have to match before the fibre can be picked up. The maximum opening of the gripper jaws can easily be adjusted to aid in picking up tightly packed fibre probes.

The new gripping pickup head was tested on the same X-Y table in the same way as the earlier prototype. The only change was to lower the fieldplate closer to the X-Y table, because the new pickup head was considerably smaller than its predecessor.

#### 5.4.3 Fibre retraction mechanisms

During the initial testing of the 2dF prototype, no attempt was made to provide any form of fibre retraction mechanism for the flexible fibres. All other telescope instruments based on the Autofib concept use stainless steel hypodermic tubing surrounding the optical fibre to maintain each fibre on a known path



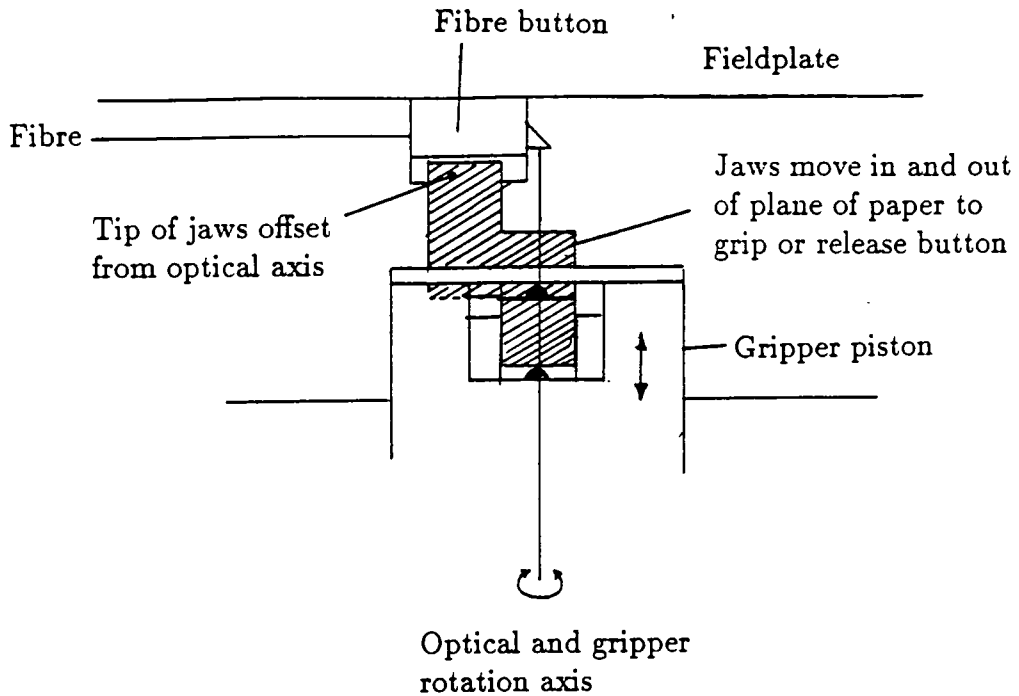


Figure 5.12 Gripper jaw design, showing a side view of the off axis jaw tip.

between pivot and prism thus enabling the anti-collision software to correctly predict the path of the fibre from the button to the pivot. Whilst this approach is suitable for cassegrain systems with relatively small numbers of fibres, as soon as the number of fibres is increased to those proposed for prime focus systems, there is a very real risk of the fibres tangling outside the pivot circle as the fibres are moved around inside the field area. Also for future fibre probe designs, we wish to remove the need for the stainless steel tubing so as to improve the ability of the fibre probe to cross each other. If this is to be possible, some other method must be found to tension the fibre to avoid any slack fibre tangling with other fibre probes.

A fibre retraction system must exhibit several properties:

- It must not induce any extra focal ratio degradation in the fibre.
- It must be extremely reliable.
- It must be easy to produce and simple to assemble.
- It must continue to function at all times and be able to recover from a non-operating state, for example when the instrument is removed from the telescope and stored.

One such system has been proposed (Gray and Taylor, 1990) which relies on a series of pulleys for each fibre probe, the fibre being tensioned around the first pulley by a piece of elastic cord (figure 5.13). This system has the advantage of being fairly simple and it will work even when the instrument is removed from the telescope, but it has several drawbacks, namely the effect of the attachment of the elastic cord to the optical fibre on the focal ratio degradation induced in the fibre, and also that it is very difficult to quantify the reliability of such a system. In particular, the effect of an elastic cord becoming unattached, or breaking would be disastrous. The complexity of the system is increased by the fact that the length of the elastic is necessarily long in order to reduce the effect of the increase in tension as the fibre is moved towards the centre of the field plate.

An alternative fibre retractor design using air pressure to provide constant tension on the fibre is shown in figure 5.14. In this design, the fibre enters the retractor through a small hole, and passes around a nylon wheel which is free to move along a slot. The fibre then exits in a second small hole above the entry hole. Air under pressure is fed into the retractor between the entry points of the fibre and the nylon wheel, and serves to keep the wheel forced as far back in its slot as the fibre will allow. The fibre is retained in a narrow slot around the wheels rim to avoid any possibility of the fibre slipping from the rim and releasing the

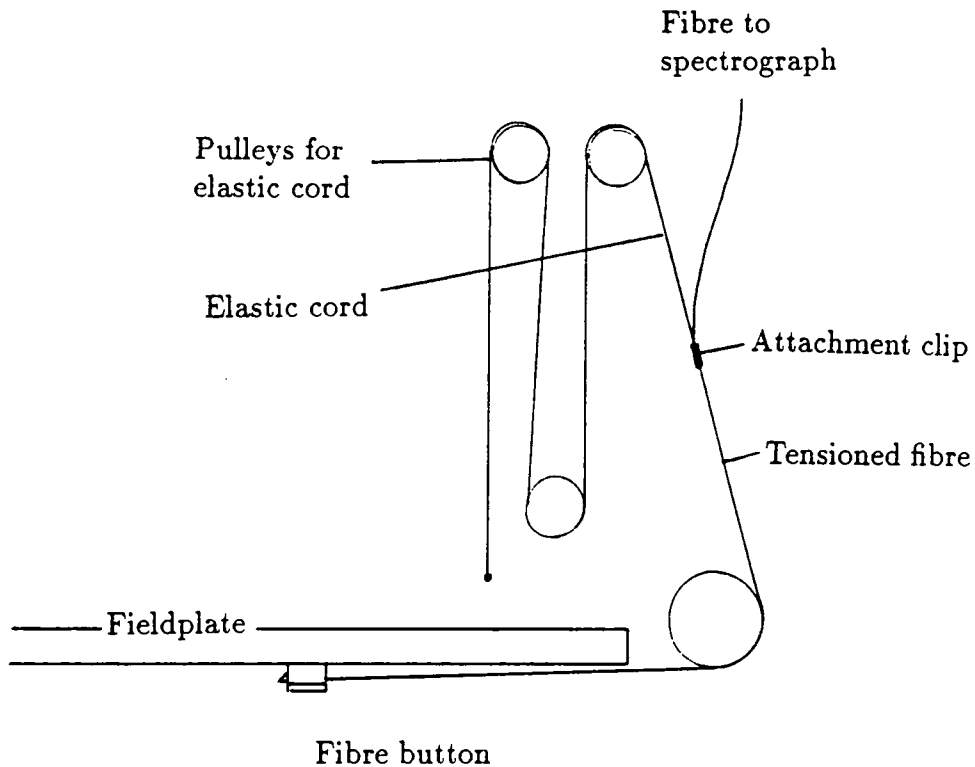


Figure 5.13 Elastic cord fibre retraction mechanism.

wheel. As the fibre probe is moved around the field, the wheel moves backwards and forwards in its slot. The pressure difference between the air supply and the open end of the retractor ensure that the wheel remains forced against the fibre, thus providing a constant tension in the fibre irrespective of the fibres position in the field.

This fibre retraction system has the advantage that it is simple to make and has no moving pieces that might fail. Also stress on the fibre can be reduced to a minimum by the use of a reasonably large nylon wheel to avoid any sharp radii of curvature of the fibre. A possible disadvantage of this type of retraction system is that it no longer functions if the compressed air supply is removed. This might occur during the day when the instrument is not being used, or when the

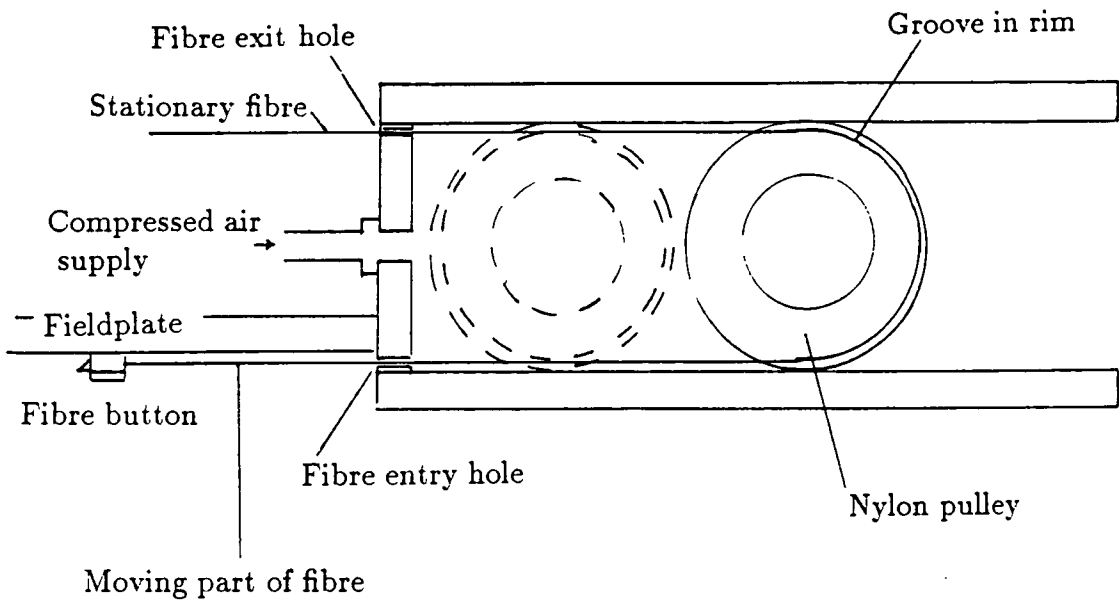


Figure 5.14 Air pressure fibre retraction system.

instrument is being mounted on or removed from the telescope. By making the groove in the rim of the nylon wheel for the fibre as deep as possible it should be possible for the retractor to recover and continue working upon resumption of the air supply with the minimum of difficulty.

#### 5.4.4 Experimental setup

The aim of the second prototype was to develop the techniques already investigated into a design suitable for a telescope instrument. The new prototype was designed to be able to handle 20 fibres in an  $18^\circ$  sector corresponding to the 400 fibres planned for the final instrument. The 20 fibres were manipulated by the robot on a fieldplate which was supported above the robot on four legs. The fibre pivots were arranged on a circle of radius 302mm. Behind the pivots a prototype of the air pressure retraction system was used to provide tension on each individual fibre

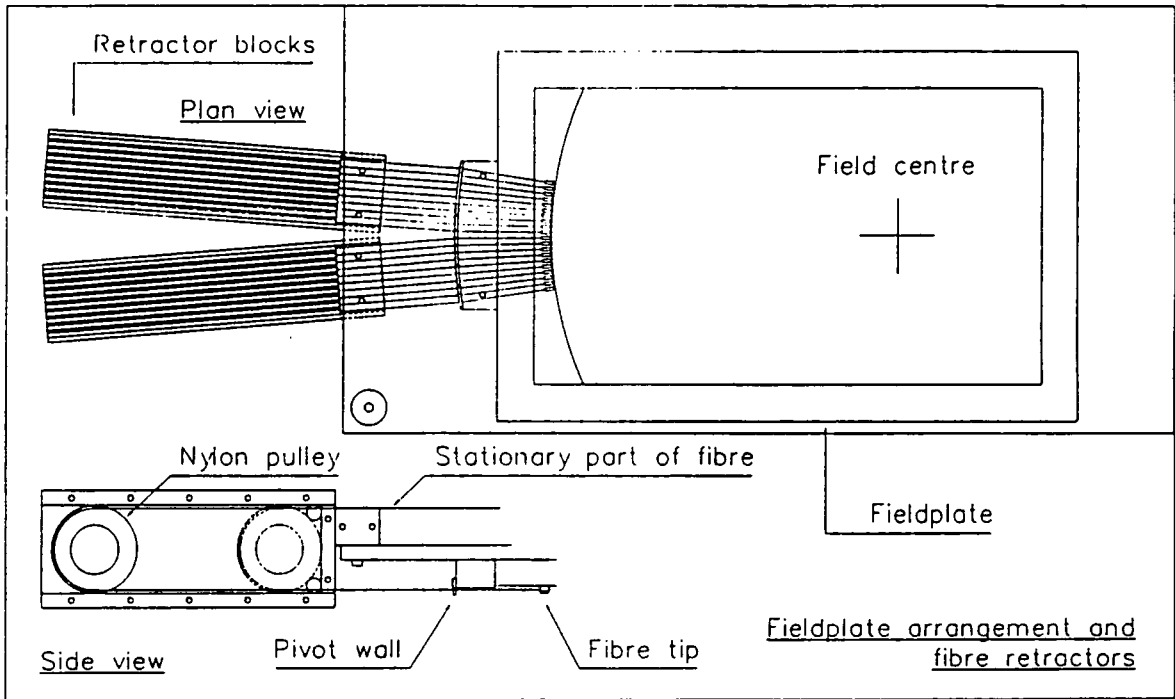


Figure 5.15 Experimental layout of the 20 fibre test fieldplate.

as in figure 5.15. The basic design shown in figure 5.14 was adapted to provide two banks of ten retraction mechanisms to facilitate easy modular assembly.

The stepper driven X-Y carriage remained unchanged and was again controlled from a PC. The new pickup head was powered by two DC servo motors with rotary encoders (the Z axis and  $\theta$  rotary stage), and controlled by the same PC as the X-Y carriage but using the Galil card already used for the WHT Autofib Prototype. As before the optical processing of the gripper CCD TV camera was

achieved using a PC based framegrabber. The control software for the testing of the new pickup head was adapted from the control software used on Autofib-1.5, with changes made to include the  $\theta$  axis motion and the new fibre probe design.

During the testing of the new pickup head, two different modes of operation were defined, 'zero' iterations, and 'one or more' iterations. The 'zero' iteration mode is that used before, where the robot has a single attempt to place the fibre. The 'one or more' iteration mode is where the robot attempts to place the fibre probe, and if the position error is too large, tries the fibre placement again. As before, there is a trade off between fibre placement accuracy and the average time taken to place a fibre probe

The fibre placement procedure was based on that used for the earlier prototype. For a simple case (zero iterations) the fibre was centroided whilst in the gripper jaws and the appropriate correction made to the X-Y carriage before placing the fibre on the fieldplate and measuring the final position error. If further iterations to the putdown procedure are required, the jaws are closed on the fibre button, and the last position errors used to impart a further correction to the fibre probe. This last movement is normally small, therefore the button is simply dragged across the fieldplate with no further Z movements. After opening the jaws, another centroid of the fibre image allows a second determination of the fibre position errors.

#### 5.4.5 Initial results

Three critical areas of the operation of a positioning system can be identified as requiring evaluation. These are the overall positioning accuracy, the reliability and the speed of operation. The initial testing served to give an idea as to likely performance and identify points requiring further attention.

Measurements of the repeatability of the fibre positioner were made for a subset of 9 fibres at different points in the field. After each fibre placement, the position error as determined by the TV system was recorded, then the operation repeated a total of 15 times to determine the spread in the position errors. A series of five different positioning tests were carried out to determine several properties of the fibre probes and the positioning robot. The tests were as follows:

1. At a single position near the centre of the field.
2. At a fixed position near the edge of the field.
3. At random positions along the radial direction.
4. At various non radial positions.
5. With different crossover points between two fibres.

The first test gives information about the accuracy of the gripper, largely independent of the fibre retraction mechanism and other fibres. The second test should also be independent of the retraction mechanism, but as the fibres were in close proximity (typically 1mm) of other fibres, any fibre-fibre interaction should be evident. The third and fourth tests were designed to show up any interaction between the fibre positioner and the retractor in a radial direction (test 3) and in a non-radial direction due to twisting of the fibre button due to the tension (test 4). The final test was to determine if there was any detrimental effect on the repeatability of the fibre positioning when a fibre was placed so as to cross another fibre at different points. Each of these tests was repeated for zero and one iterations of the putdown procedure.

The results of the tests are shown in table 5.1 and figures 5.16 to 5.24. There was only a small improvement in the scatter of the errors when using repeat iterations. The scatter of the errors when the fibres are at the edge of the field

for zero iterations is consistently larger than for zero iterations at any other point in the field. Together with the fact that on several occasions the gripper failed to pickup the fibre probe due to it having twisted, might indicate that magnetic crosstalk between the fibre probes is having an effect. The positioning test with the fibre at the edge of the field, but using a repeat iteration, shows some improvement in the scatter of the residuals, as might be expected. All of the remaining tests were carried out with the fibre under test being placed well away from other fibres.

Position	Iterations	$\langle \sigma_x \rangle$	$\langle \sigma_y \rangle$	$\langle \sigma_r \rangle$	Results
Radial centre	0	11.3	6.7	13.2	Fig 5.16
Radial edge	0	11.6	9.4	15.5	Fig 5.17
Radial random	0	9.4	7.5	12.2	Fig 5.18
Radial centre	1	8.8	6.7	11.3	Fig 5.19
Radial edge	1	9.9	7.7	12.7	Fig 5.20
Radial random	1	10.7	8.5	14.0	Fig 5.21
Non-radial	0	8.8	8.5	12.5	Fig 5.22
Non-radial	1	5.7	9.2	10.7	Fig 5.23
Crossover	1	4.8	7.4	8.9	Fig 5.24

Table 5.1 Summary of fibre positioning tests.

The residuals in the Y direction are typically 75% of that in the X direction. The geometry of the fieldplate sector under test may contribute to this effect, because the fibres were placed so that they were aligned almost parallel with the X axis. This geometry means that the fibre retractors are applying tension along the fibre in the X direction. Further work is presented later to investigate and try and reduce this extra scatter.

Figures 5.22 and 5.23 show that the fibre probes and gripper continue to perform well in a non-radial direction with no increase in the scatter of the residuals. The effect on the positioning of a fibre probe when it is crossing a second fibre



is shown in figure 5.24. Fibre #9 was tested crossing Fibre #5 at a point 40mm from the tip of Fibre #5. The distance of the crossover point from the tip of Fibre #9 was varied from 15mm to 40mm. A control run with Fibre #9 in the same positions, but not crossing Fibre #5 was also carried out. Again, there was no increase in the scatter of the residuals due to the crossing of another fibre compared with previous results. Tests with the point of crossover less than 40mm from the tip of Fibre #5 were attempted, but were unsuccessful as the fibre buttons had to be placed in such close proximity that magnetic crosstalk made the placement of the second fibre impossible.

Despite the problems encountered, the position error of less than 15  $\mu\text{m}$  rms found in almost all of the above tests is a factor of 2 improvement over existing electromagnetic pickup head designs. However, further work is required to solve some of the problems, and try to improve on these results.

## 5.5 Improvements and fine tuning

### 5.5.1 A new fibre centroiding software routine

The first task of the original centroiding routine was to improve the contrast of the fibre image. This requirement was removed by the use of a Look Up Table (LUT) on the camera input to the framegrabber. A threshold LUT is used to remove any background and increase the intensity of the fibre image. As this operation is performed in real time on each frame acquired by the frame grabber, there is no time penalty involved.

To improve on the existing centroiding routine, a new approach was used involving a hybrid algorithm. A very fast determination of the fibre location is used to roughly locate the fibre, then a slower but more accurate centroiding routine is applied to a small window containing the fibre image. Using this algorithm,

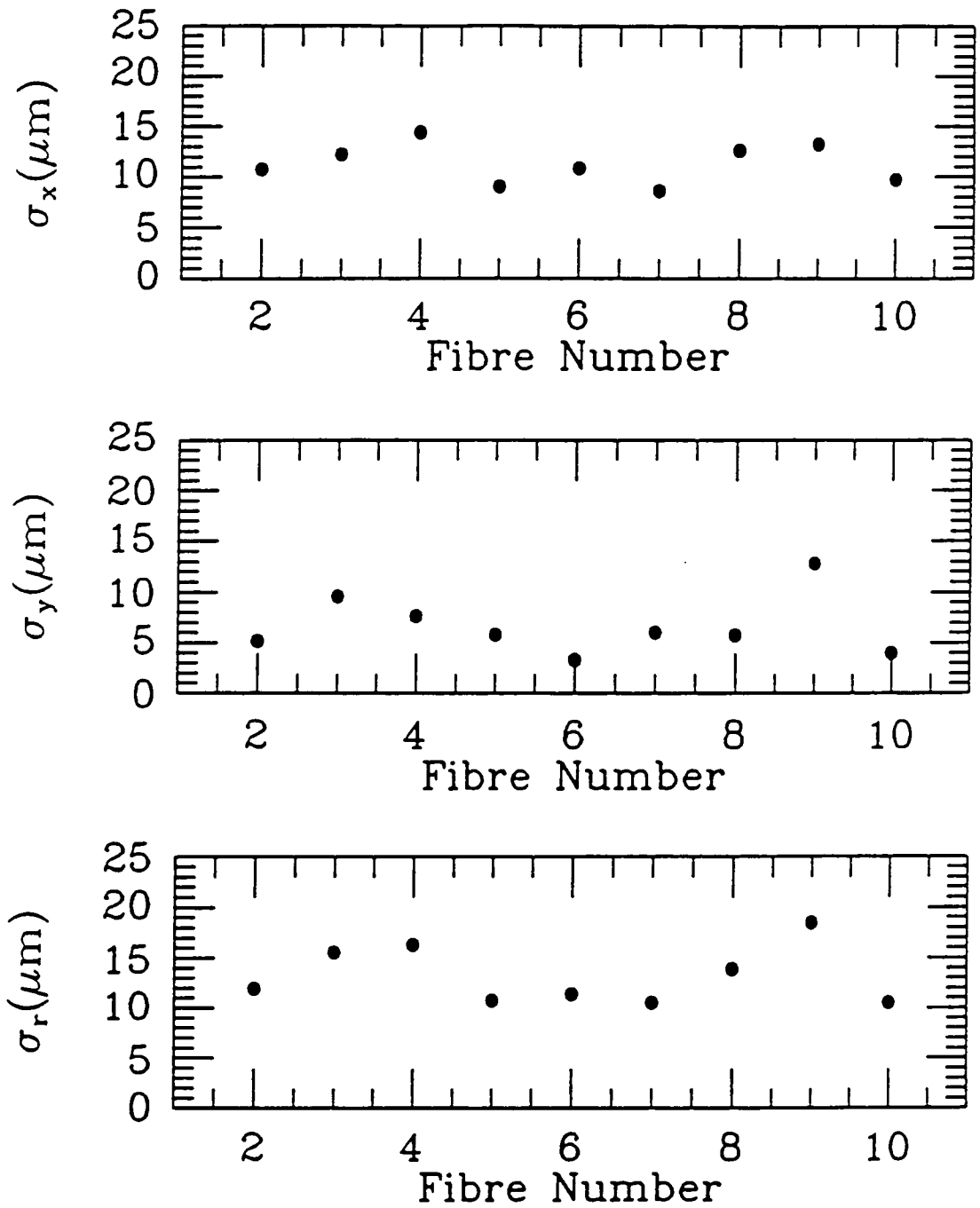


Figure 5.16 Results from placing the fibres at the centre of the fieldplate, zero iterations.

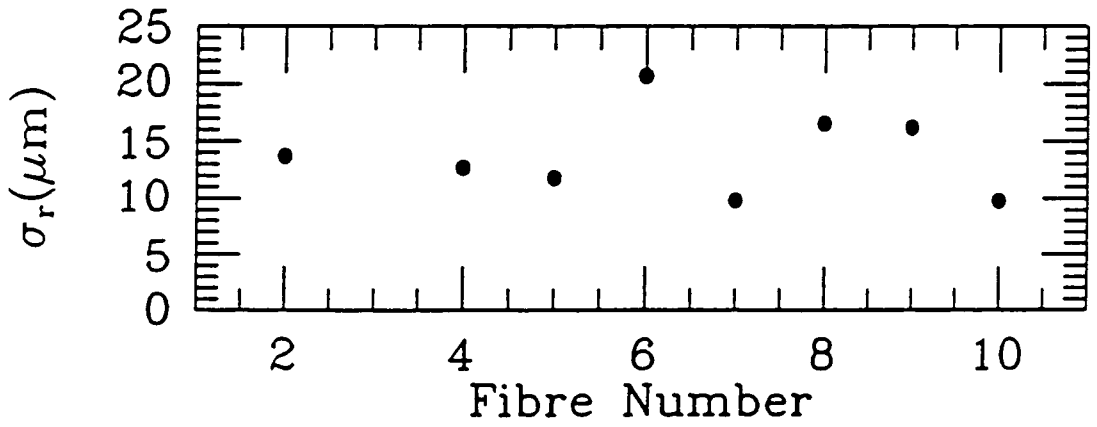
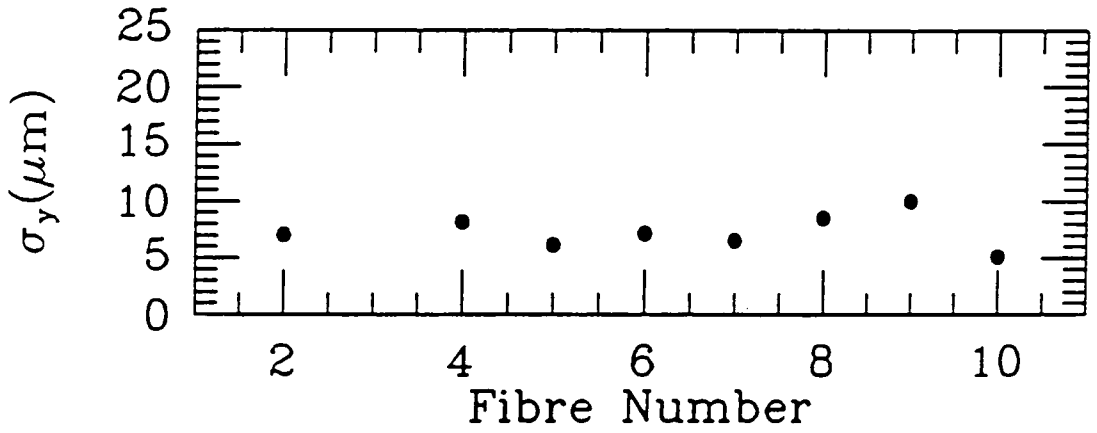
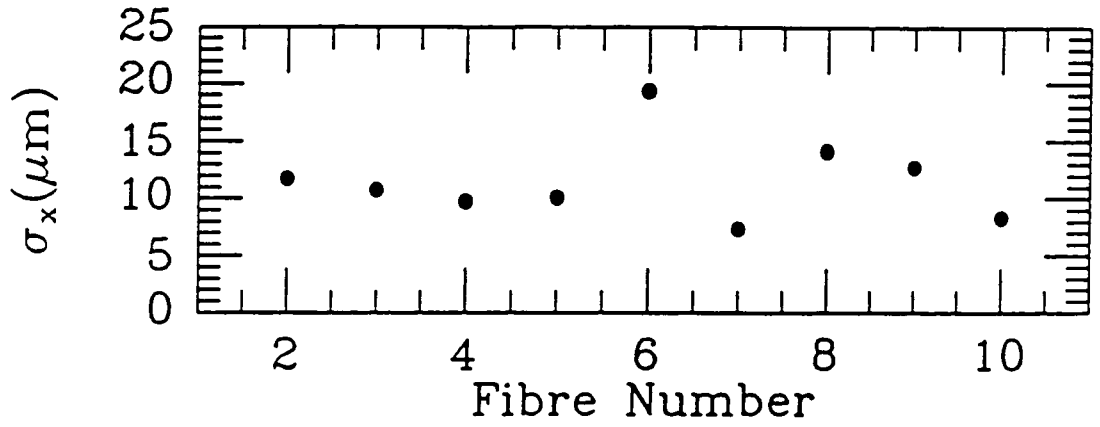


Figure 5.17 Results from placing the fibres in their parked locations, zero iterations.

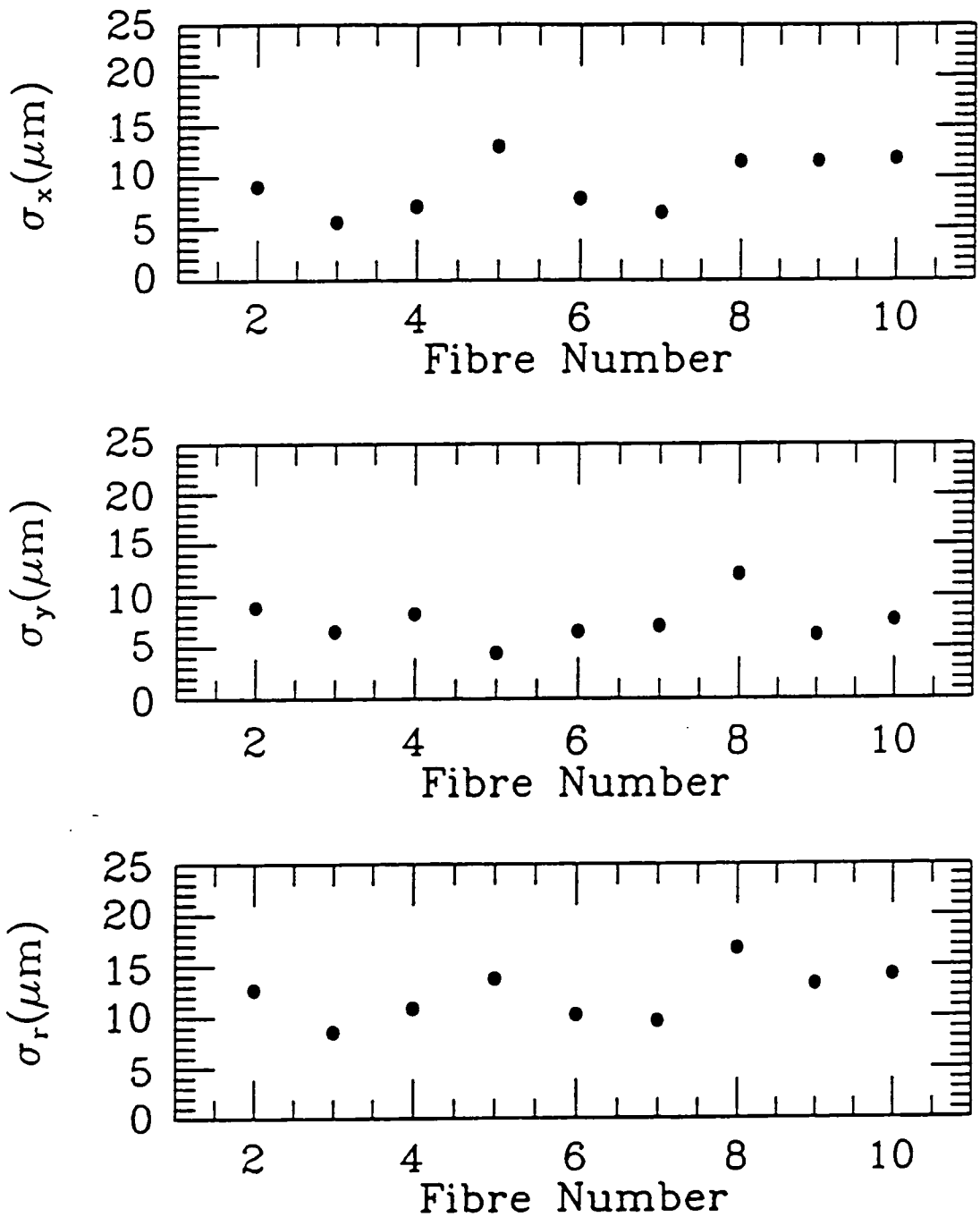


Figure 5.18 Results from placing the fibres in random radial positions, zero iterations.

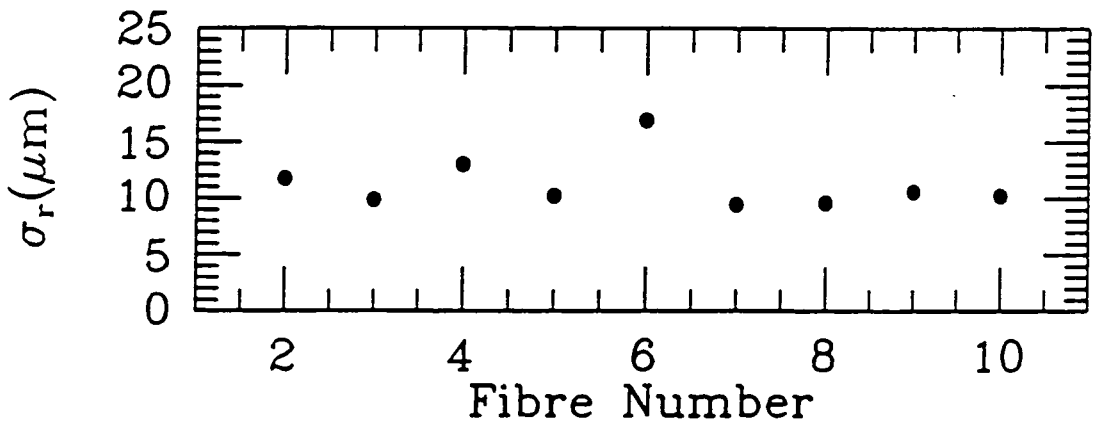
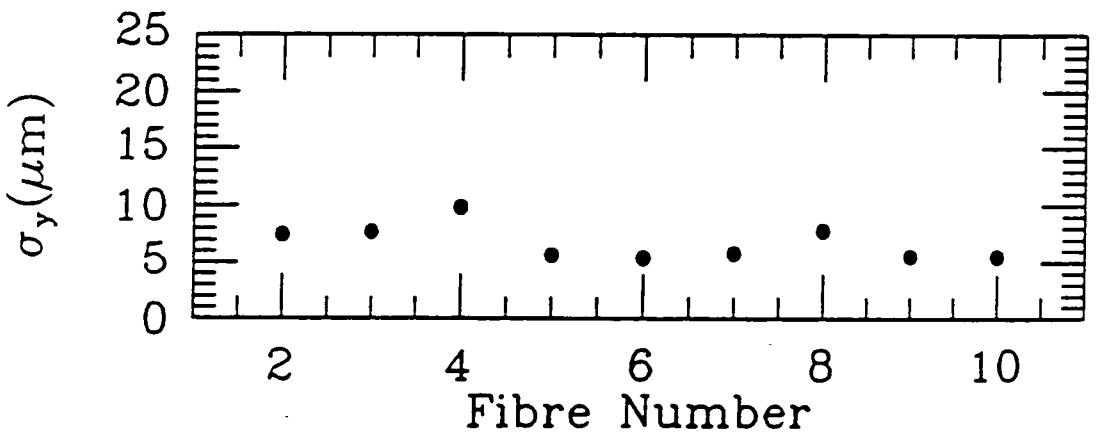
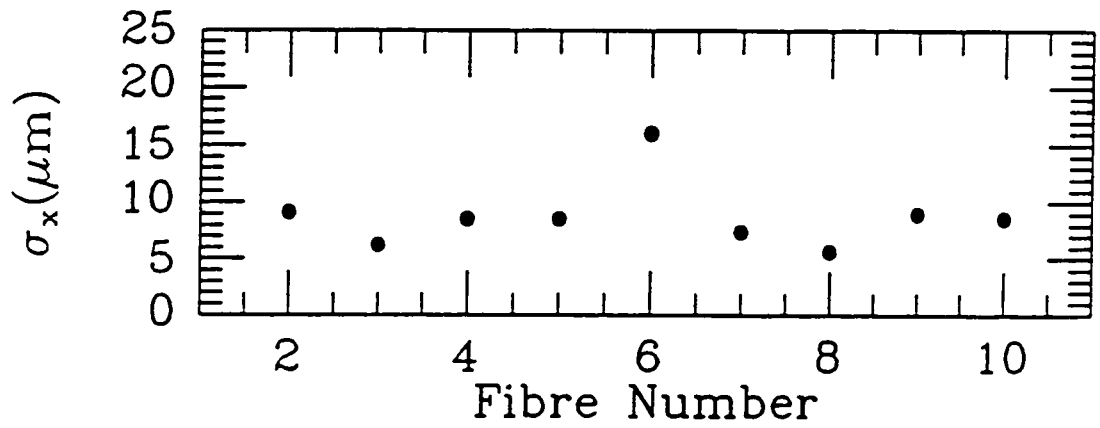


Figure 5.19 Results from placing the fibres at the centre of the fieldplate, one iteration.

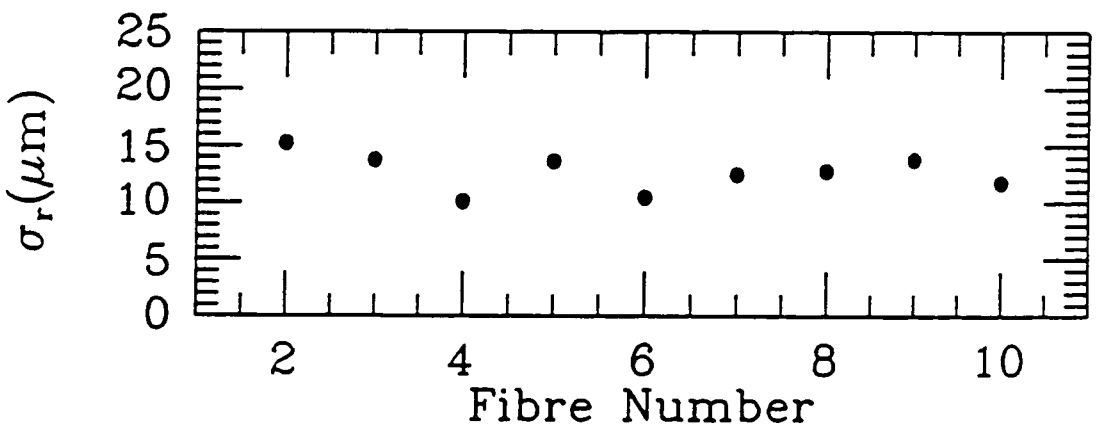
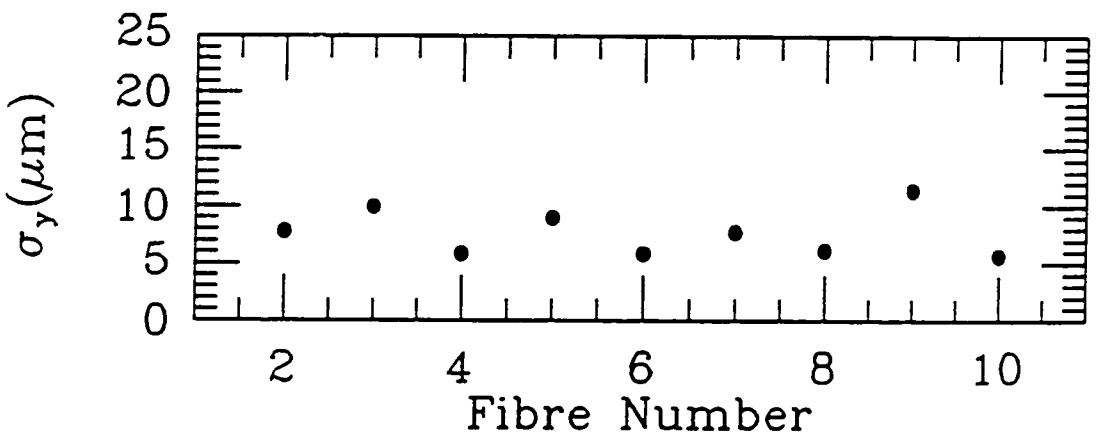
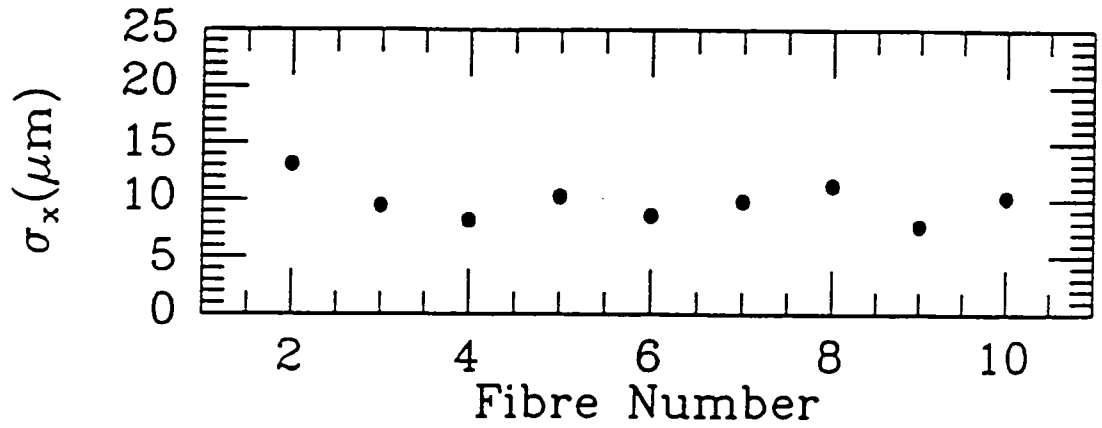


Figure 5.20 Results from placing the fibres in their parked locations, one iteration.

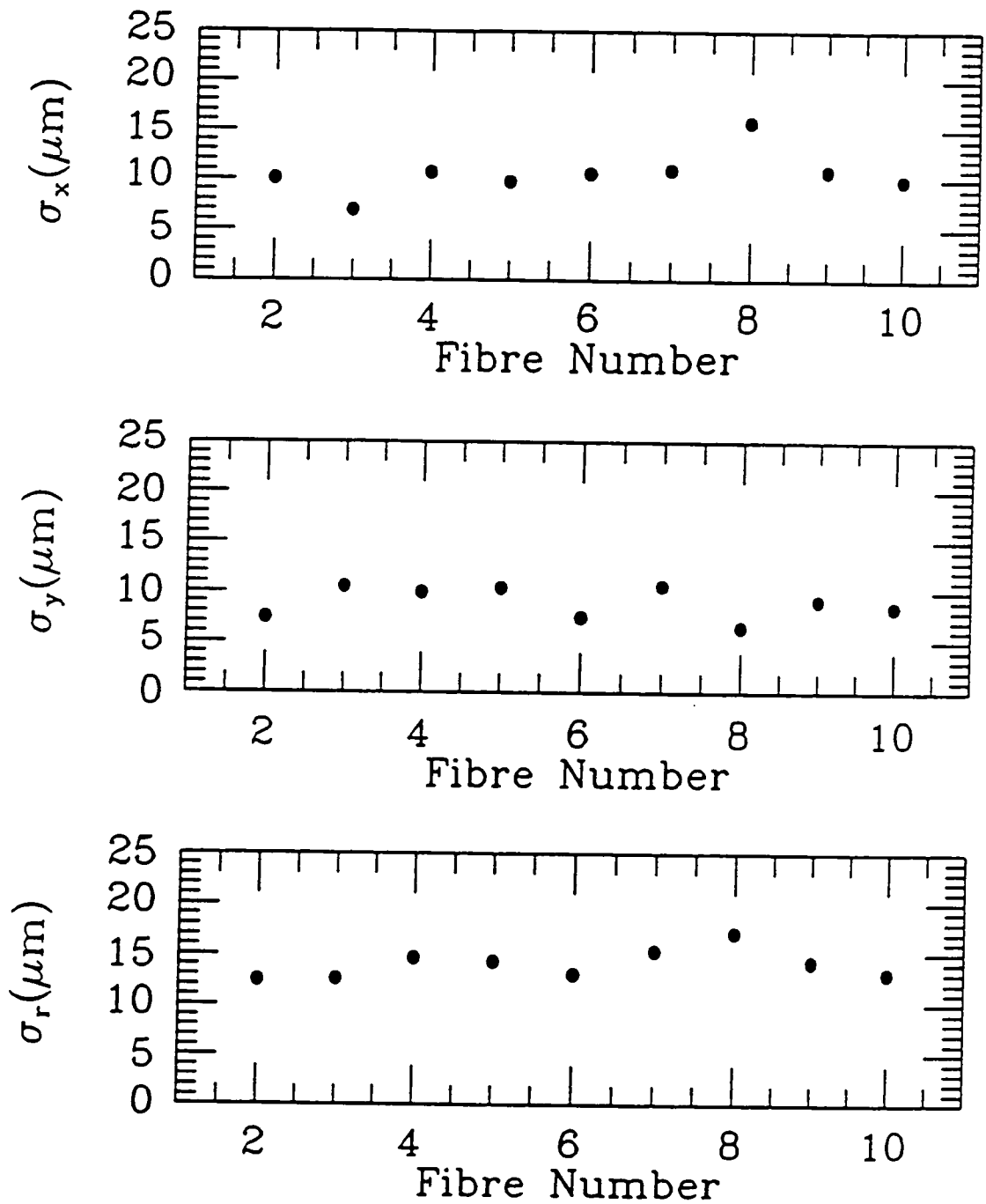


Figure 5.21 Results from placing the fibres in random radial positions, one iteration.

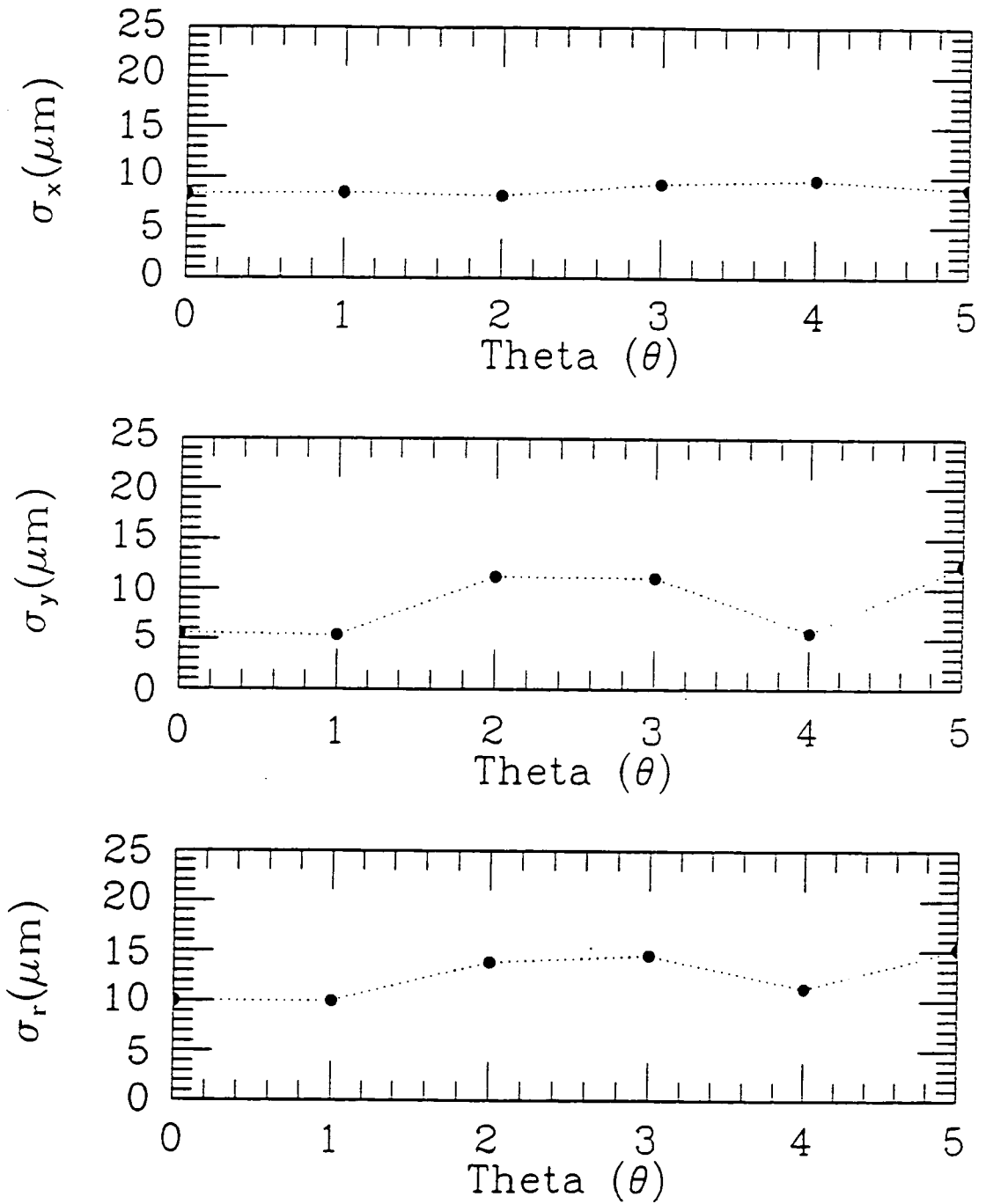


Figure 5.22 Results from placing the fibres in random non-radial positions, zero iterations.



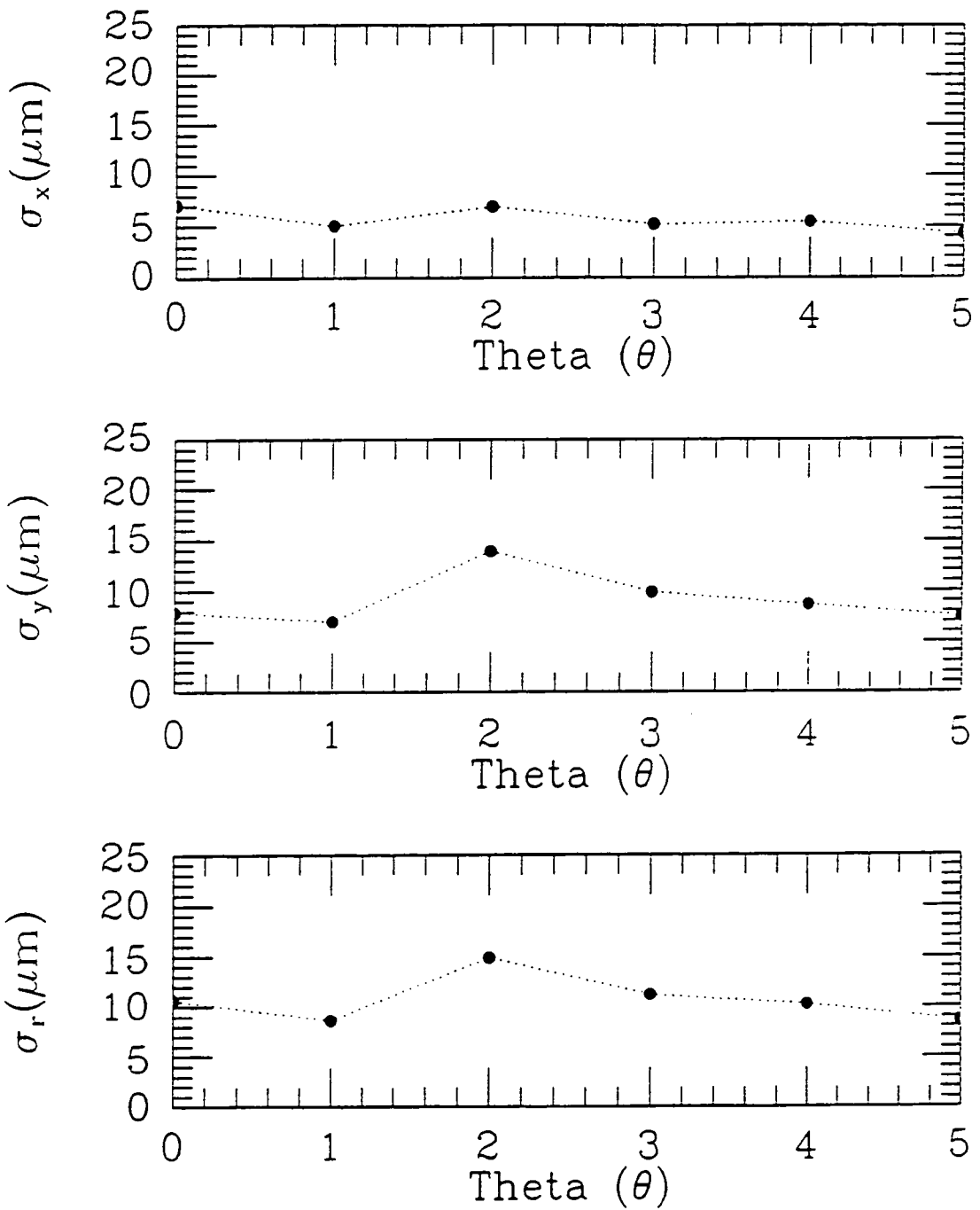


Figure 5.23 Results from placing the fibres in random non-radial positions, one iteration.

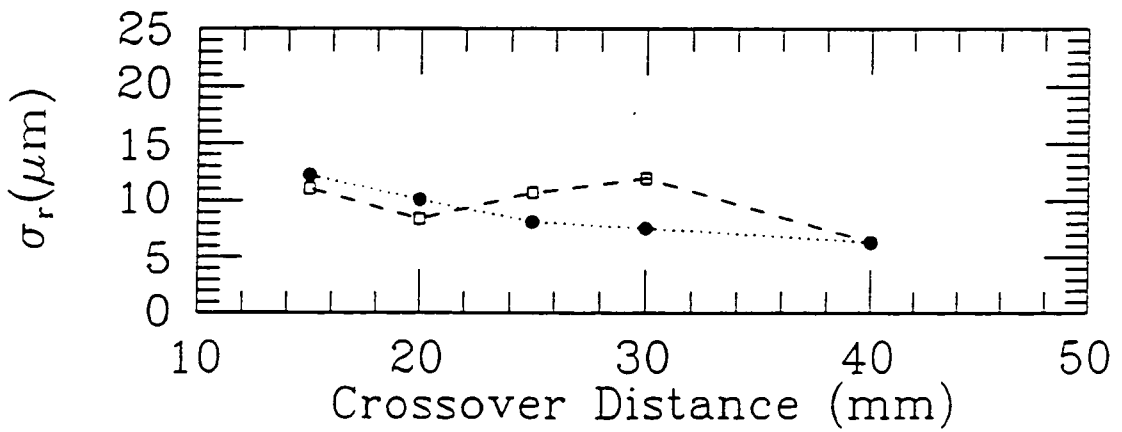
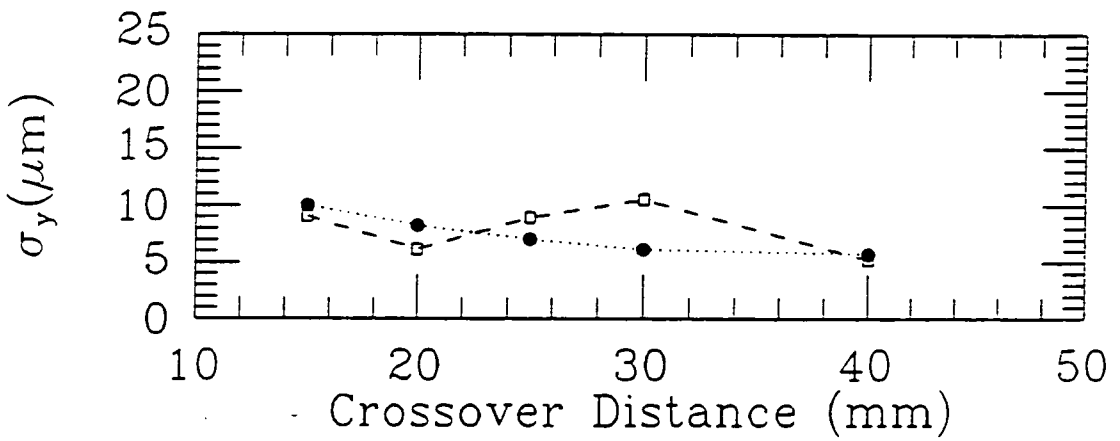
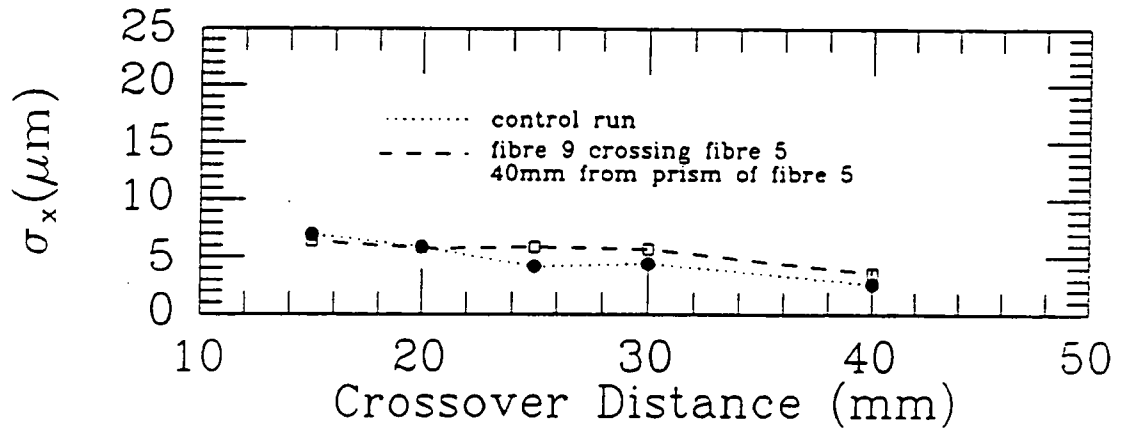


Figure 5.24 Results from two fibres crossing, one iteration.

the time taken to centroid the fibre image is reduced from 5.8 seconds to approximately 0.2 seconds, using exactly the same hardware as before. As a check on the repeatability of the centroiding routine, a fibre image was repeatedly centroided with no X-Y carriage motions between each centroid. In over 500 centroids, the result was identical to within one pixel (less than  $2.4 \mu\text{m}$  ).

### 5.5.2 Fine tuning of the gripper release

Testing the positional accuracy of the robot with no pressure applied to the fibre retractor gave no improvement in the scatter of the residuals in the X direction. Therefore the retractor was eliminated as a cause of the extra scatter of the residuals seen in the X direction. The action of the gripper jaws was observed closely under a microscope and a distinct kick was seen to be given to the gripper body on both pickup and release. If both kicks were identical, no overall effect was noticed, but in general the kick during the pickup operation was not identical to that during the putdown operation. The movement of the gripper body was seen to be due to the reaction to the initial movement of the pneumatic piston at the start of the opening or closing cycle of the jaws.

To remedy this effect, the jaws were modified slightly to improve the coupling between them. Also, the system of valves and regulators used to either pressurise or evacuate the gripper piston was modified to slow down the initial operation of the gripper jaws. This had the effect of reducing the reactive impulse felt by the main body of the gripper.

Testing the quality of the release of the gripper jaws after these modifications was performed by measuring the size and repeatability of the jolt as the fibre probe was released. This jolt is due to the handle on each fibre probe not being perfectly perpendicular to the field plate. The scatter on the released position for all of the fibres was measured to be less than  $4 \mu\text{m}$  rms at any point in the field.

### 5.5.3 A new fibre placement procedure

Timings for the original putdown procedure for zero and one iteration (using the original centroiding routine) are shown in table 5.2. These timings were obtained by interrogating the CMOS clock in the control computer during repeated pickup and putdown operations.

Operation	Time(secs)	
	One Iteration	Zero Iterations
<b>Pickup</b>		
$\theta$ move	1.15	1.15
Open jaws	0.70	0.70
Z move to plate	0.24	0.24
Close jaws	0.70	0.70
Z move	0.24	0.24
File update	0.11	0.11
<b>TOTAL</b>	<b>3.14</b>	<b>3.14</b>
<b>Putdown</b>		
Safety checks	0.82	0.82
$\theta$ move	1.15	1.15
Z move to (plate-50)	0.72	0.72
Centroid	5.80	5.80
Move to corrected (x,y)	1.62	1.62
Z move to plate	0.24	0.24
Open jaws	0.70	0.70
Z move to (plate-1000)	0.40	0.40
Move to wanted (x,y)	1.64	1.64
Centroid	5.80	5.80
Move to fibre (x,y)	1.59	
Z move to plate	0.44	
Close jaws	0.70	
Move to corrected (x,y)	1.53	
Open jaws	0.70	
Z move to (plate-1000)	0.44	
Move to wanted (x,y)	1.54	
Centroid	5.80	
Z move and close jaws	1.21	1.21
File update	0.11	0.11
<b>TOTAL</b>	<b>32.95</b>	<b>20.25</b>

Table 5.2 Current pickup and putdown operation timings.

Note that many of the steps of the putdown operation are included for development purposes. In particular the repeated movement back to the required x,y position for the fibre in order to measure the fibre position error is an unnecessary movement. Also, because the operation of the gripper jaws is extremely repeatable, it should be possible to use a form of error table to estimate the appropriate point at which to release the fibre in order to place the fibre at the required x,y position on the first attempt.

The theta movement required to place the fibre at the correct position angle for its x,y location can be performed in parallel with the X-Y carriage movement in that plane. Also the initial image centroid can be obtained during the time taken to carry the fibre probe to its new location and the destination position incremented to allow for the image offsets provided that the image is grabbed as part of the pickup procedure. The safety checks performed as part of the putdown operation are not absolutely necessary as the robot can perform these before any fibre movement is initiated. Timings for the restructured pickup and putdown operations are shown in table 5.3.

#### 5.5.4 Results using the modified prototype

The following results were obtained while manipulating the same subset of nine fibres as in the previous section. No repeat iterations were used to improve the fibre position errors. The fibre probes were tested at randomly generated positions both radially and non-radially in the field. Tests were not performed at each fibres park location due to the known problem of magnetic crosstalk between fibre probes. The error table used in the putdown procedure was generated automatically by the robot.

The mean residuals for each fibre ( $\langle dx \rangle$  and  $\langle dy \rangle$ ) indicate that the error table values derived by the robot are not quite right at present. Indeed it was found to be extremely difficult to fine tune the error table at the 5  $\mu\text{m}$  level. Further

Operation	Time(secs)	
	One Iteration	Zero Iterations
<b>Pickup</b>		
Open jaws	0.70	0.70
Z move to plate	0.24	0.24
Close jaws	0.70	0.70
Z move	0.24	0.24
File update	0.11	0.11
<b>TOTAL</b>	<b>1.99</b>	<b>1.99</b>
<b>Putdown</b>		
Z move to plate	0.24	0.24
Open jaws	0.70	0.70
Centroid	0.20	0.20
Close jaws	0.70	
Move to corrected (x,y)	1.62	
Open jaws	0.70	
Centroid	0.20	
Z move and close jaws	1.21	1.21
File update	0.11	0.11
<b>TOTAL</b>	<b>4.98</b>	<b>2.46</b>

Table 5.3 Restructured pickup and putdown operation timings.

Fibre #	$\langle dx \rangle$ $\mu\text{m}$	$\langle dy \rangle$ $\mu\text{m}$	$\sigma_x$ $\mu\text{m}$	$\sigma_y$ $\mu\text{m}$	$\sigma_r$ $\mu\text{m}$
2	-2	7	3.7	4.5	5.8
3	-6	-6	6.7	3.3	7.5
4	-9	4	5.3	1.8	5.6
5	-5	3	4.3	4.5	6.2
6	0	-5	6.2	3.5	7.1
7	0	-2	3.3	4.5	5.6
8	-6	-1	4.9	6.3	8.0
9	-4	3	4.5	6.3	7.7
10	-1	1	5.4	6.9	8.7

Table 5.4 Further results showing accuracy and repeatability for 9 fibres. A total of more than 100 operations on each fibre in different positions were performed.

tests on methods for measurement of the error table are under way. However, it

seems likely that as the fibre is placed at a particular point, it relaxes slightly due to the tension of the fibre retractor. If the error table is measured at the same point, the fibre and retractor system is already relaxed, and therefore the error table values measured do not include this effect.

Despite the difficulties in fine tuning the error table mentioned above, the results are very encouraging, with the repeatability better than  $9\ \mu\text{m}$  for all the test fibres. Since these results are for zero iterations, it should be possible to include a first iteration for the small percentage of fibre placements that are still outside of the required tolerance with very little overhead on the timings. Figure 5.25 shows the radial error distribution of the above results.

#### 5.5.5 Reliability

The fibre positioner performed very reliably with no failures in over 24 hrs total operation. Operation of the fibre positioner was interrupted on one occasion due to one of the fibre retractors becoming jammed, this was the only failure during the testing procedure.

It would appear that this type of fibre positioner is extremely reliable as well as accurate. The only problems seem to arise from the fibre retraction system and the design of the fibre probes. The fibre probes had a slight tendency to twist when placed in close proximity to another fibre probe. The gripper jaws only have a very limited clearance, and it became impossible for the robot to get hold of the fibre probe handle once the fibre button had twisted. Once this problem was identified, further testing was performed with each fibre probe at points remote from the other fibre probes

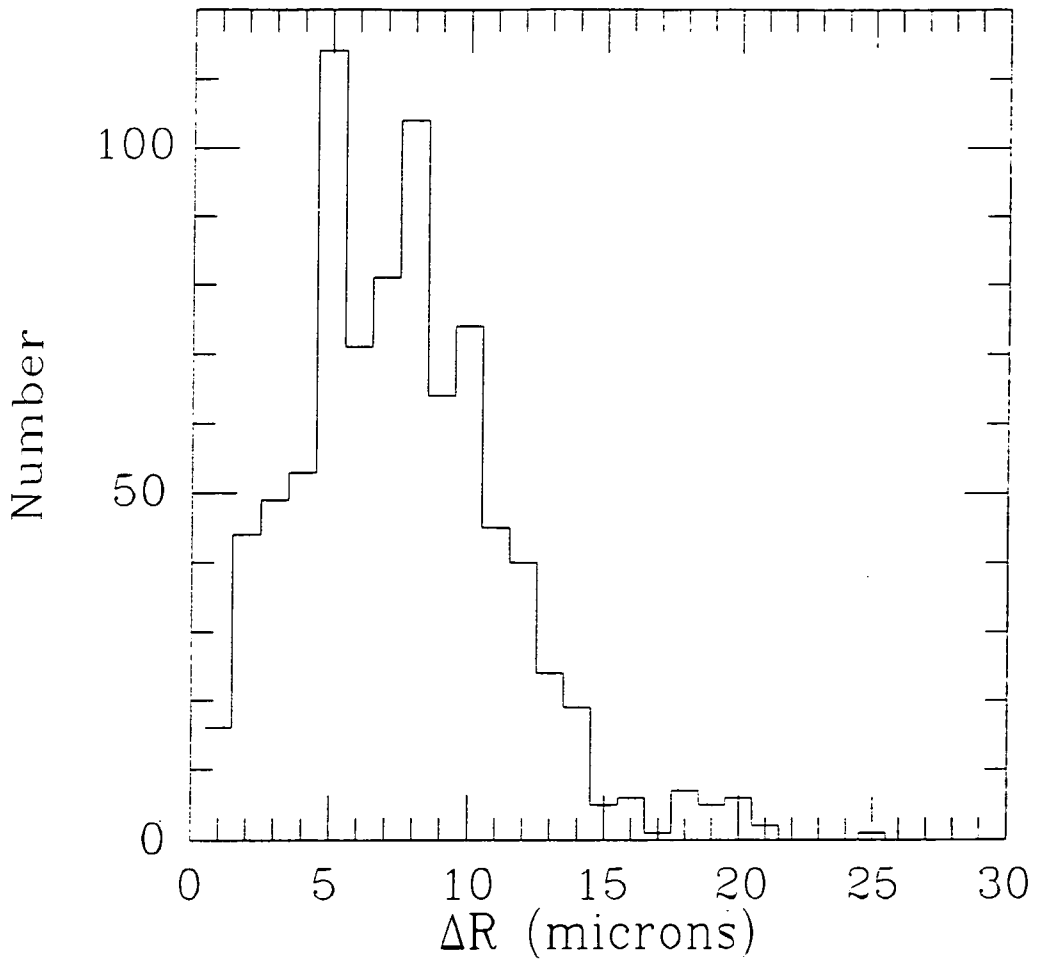


Figure 5.25 Radial error distribution for the results shown in table 5.4.

## 5.6 Further work

### 5.6.1 Reliability

While the current 2dF prototype has been very successful, there is still some room for improvement. Further work on the 2dF prototype is currently underway to improve on some aspects of the systems operation. In particular the reliability and speed of operation are under consideration.



A new design of fibre retractor based on a hybrid of the 'air pressure' and 'elastic pulley' designs is currently being manufactured. A constant tension spring instead of air pressure is used to tension a pulley (figure 5.26). This type of spring provides a constant tension over all of its working length. Since the fibre is acted on by a pulley and not an elastic cord, the focal ratio degradation properties should not be affected significantly. As air pressure is not being used to tension the pulley, very high tolerances in the parts of the fibre retractor are not required, making the retractor less likely to jam.

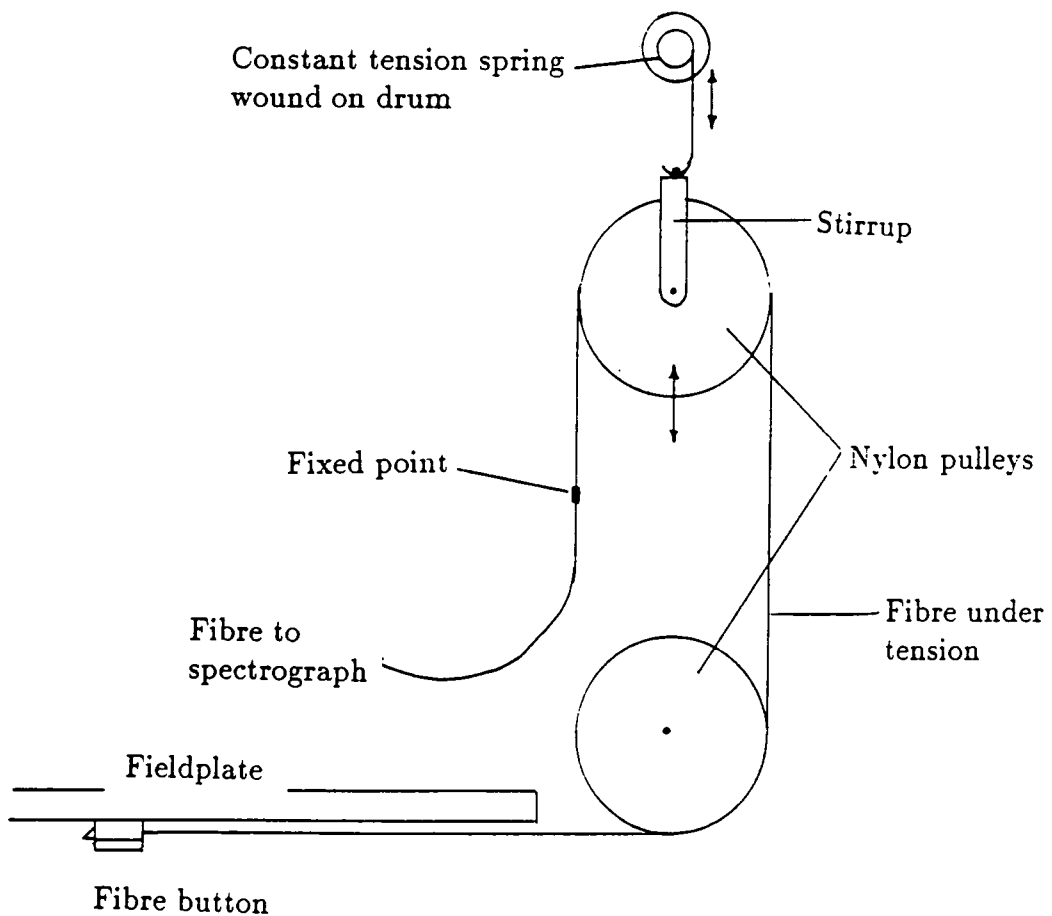


Figure 5.26 Hybrid design of fibre retractor based on a constant tension spring.

The problem of magnetic crosstalk between fibre probes prevents the assigning of fibres to closely separated target objects, as well as affecting the reliability of the fibre positioner. A second set of fibre probes are currently under construction using an identical design but with the body of the fibre probe manufactured from mild steel. In the new fibre probes, great care has been taken to ensure that the permanent magnets in the base of each button are aligned in the same orientation, ie. all have their north pole against the fieldplate, and the south pole at the top. The mild steel button then completes a magnetic circuit from the south pole back to the fieldplate.

Initial tests of the new fibre probes indicate that the attractive force with which they grip the fieldplate is almost a factor of two better at over 500g. Also, (and more importantly) the magnetic crosstalk between two fibre buttons is almost zero. It is possible to slide one button to within 200  $\mu\text{m}$  of another without affecting the position of either button.

### 5.6.2 Operating speed

Even using zero iterations, the current pickup and putdown operations are currently too slow for use on the 2dF instrument. With a target reconfiguration time of 30 minutes, each fibre must be moved in about 4.5 seconds. If we ignore the timings for the stepper driven X-Y carriage and use probable timings based on experience with the X-Y carriages on Autofib-1 and 1.5, then the pickup and putdown operations must be achieved in about 3.5 seconds to allow time to move the fibres around the field.

Further improvements in the timing of the centroid routine are probable with more powerful hardware. Also a total of 1.4 seconds is spent opening the jaws to pick up a fibre, and closing them after placing a fibre. There is no real reason why the jaws cannot be left open all of the time when they are not being used. The only reason for not doing this at present is that the vacuum ejector used to evacuate

the gripper piston is very noisy. A design already exists for a double acting piston version of the gripper unit that would be more controllable and quieter.

The  $Z$  and  $\theta$  servo loops are not yet fully tuned, it should be possible to improve the speed of the  $Z$  axis by at least a factor of two. Using these projections, it will be possible to reduce the current duty cycle of 4.45 seconds to approximately 2.5 seconds for zero iterations. This is well within the required 3.5 seconds, and would allow for the occasional iteration on the putdown procedure.

## 5.7 Summary

To summarise the work in this chapter, the basic idea of a robot equipped with robot vision being used to place the fibre probes in an Autofib type fibre positioning system has been tested and shown to be feasible. The technique has then been extended from a lab prototype to a fully engineered system which has a level of performance in terms of positional accuracy that exceeds that required for both the prime focus instruments planned for the AAT and WHT. Further testing is currently underway to evaluate the reliability and operational speed of the system.

## **6 Handling large numbers of fibres**

### **6.1 Introduction**

The configuration software described in section 2.5 has been found to be adequate for dealing with 72 fibres in a 17 arcminute field at the WHT and a 40 arcminute at the AAT. Under these circumstances it is usually possible to assign approximately 80% of the fibres to target objects in an unclustered field, the limitations being the closest approach between fibres allowed with the current fibre design, and the dead space created in the field as a fibre is placed on an object. The remaining 20% of the fibres are often used by placing them on remaining 'blank' areas of 'sky' to provide additional information when reducing the data. It should be noted that this latter procedure is somewhat risky, as it is possible to get contamination of a 'sky' fibre by a field star or galaxy.

For both of the prime focus developments at the WHT and AAT already mentioned, much larger fields will be available. While chapters 2,3 and 5 deal with the practical difficulties of working at a much smaller plate scale, this chapter considers how large numbers of fibres might usefully be used over such wide fields of view.

At the heart of the problem lies the algorithm used to assign fibres to objects. Is it still efficient in the situation of a large number of fibres or large numbers of objects case? What are the effects of different geometries of fibre button, and also

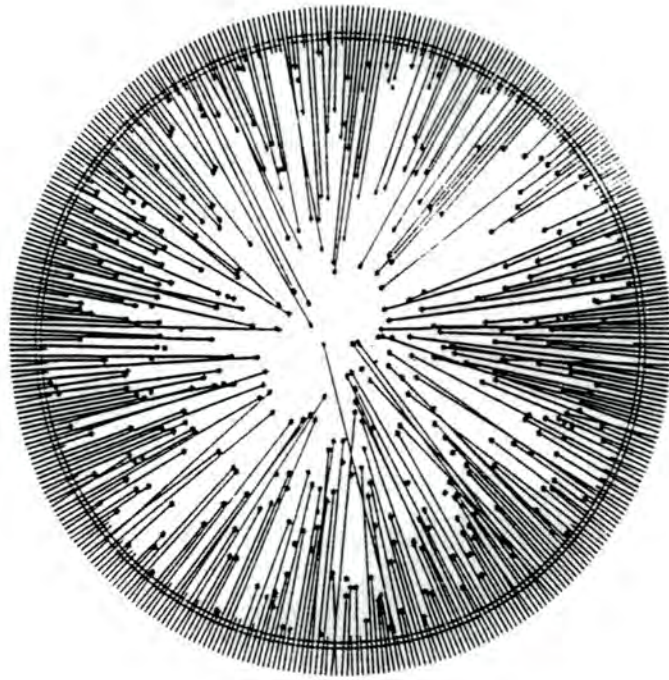
different geometries of arrays of fibre probes. Also if a new algorithm is devised, will it be possible to improve upon the 80% success rates already achieved at cassegrain focus.

## 6.2 Specifying the problem

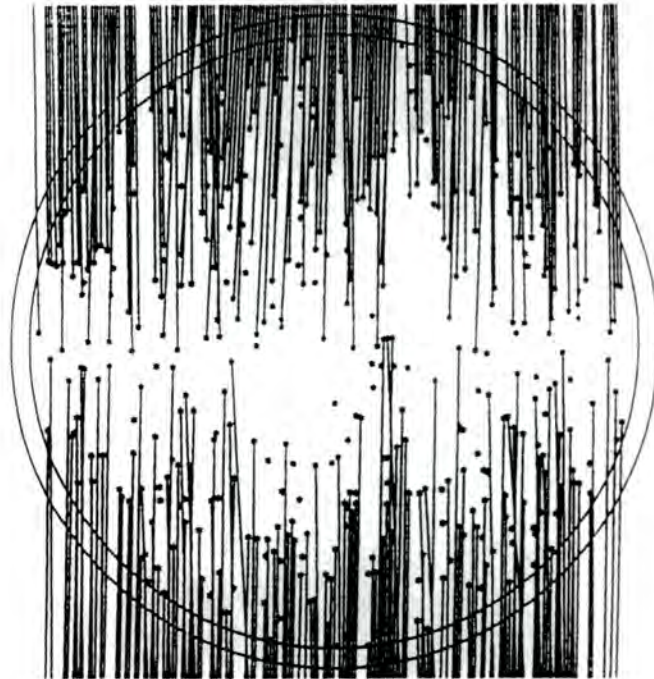
To date two different geometries of fibre array have been put forward, the original Autofib case, with fibres parked radially around the field, and the Norris case (Hamilton 1990) where the fibres are parked in two parallel banks on either side of the field (see figure 6.1).

All of the current Autofib type instruments use a magnetic cylindrical fibre button, either housing the fibre prism, or in the case of Autofib-1.5, offset slightly from the prism. However, in the case of Autofib-1.5, the only constraint on the size and shape of the button is the requirement that it be picked up by the electromagnet. When the pickup mechanism was changed from an electromagnet to a gripper (chapter 5) there was no longer any need to retain a cylindrical button. Therefore some thought was given to new fibre button designs that minimised the footprint of the button, thus reducing the dead area in the target field and the closest approach allowed for two fibres. In particular a design where the button is elongated along the direction of the fibre is considered.

In existing instruments, the fibres are held to a straight line inside a rigid stainless steel tube, however the necessary width of such a tube is a significant fraction of the footprint of the fibre probe. Obviously if the decision is made to dispense with the stainless steel tubes around the fibre, then the footprint of the fibre is reduced significantly. Also it may be possible to allow multiple fibre-fibre crossovers, thus increasing the number of fibres allocated to objects. With less mechanical restrictions on the fibre, it might also be possible to increase the maximum non-radial angle allowed in order to acquire more objects without reducing the accuracy of the fibre placement.



AUTOFIB GEOMETRY 400 fibres, 400 objects.



NORRIS GEOMETRY 400 fibres, 400 objects

Figure 6.1 Fibre probe array geometries in example configurations, where the number of objects in an unclustered field equals the number of fibres.

The problem of deciding how many fibres may be usefully used in covering a given physical field size may be determined using simulations to model the parameter space, the result being an ideal design for the fibre module component of the automated fibre positioning system. By including practical engineering constraints it should be possible to model a realistic example, and predict how efficiently the astronomer can expect to acquire a given number of objects in his target field.

### 6.3 Current techniques

Current configuration algorithms at the AAT can usually acquire 80% of the specified objects in the target field, the remaining 20% are lost due to obscuration by fibres on other objects, or remain inaccessible due to the fibre–fibre anti-collision constraints. The modified fibre probe design on Autofib–1.5 makes it slightly easier to acquire objects in the field, with only 15–20% of objects remaining after the configuration procedure (using the same plate scale and field size as at the cassegrain focus of the AAT). Both of these instruments have 72 pivots, and a similar working area (the WHT field only covers a small part of the working area of Autofib 1.5 as it was designed to be large enough to cover the AAT cassegrain field). The current algorithms used to assign fibres either disallow fibre crossovers (WHT instrument) or only allow simple crossovers (AAT instrument).

A possible reason for the better performance of the WHT configuration software is the smaller fibre probe tip size. If we consider the area blocked by a fibre probe lying near the centre of the field, a second fibre tip contained within a button (as at the AAT) may only be placed to within a button radius of the exclusion zone of the first fibre. However a fibre tip of the design used in Autofib–1.5 may be placed only a prism dimension away from the first fibre. In this way the effective area blocked by a fibre is determined by the width of the fibre added to the radius of the fibre probe tip, this is approximately 6.5mm on the AAT Autofib, but only 3.0mm on the WHT instrument. For this reason consideration is only given to new

button designs with a prism that protrudes from the button or fibre probe handle (a cylindrical button is no longer required). This effect is in practice compounded by the fact that the WHT plate scale is slightly larger, and the field size smaller, giving lower densities of objects for fibres to acquire.

#### **6.4 Description of the simulations for the 2dF facility**

In parallel with the work for the 2dF facility described in chapter 5, a standard fibre probe with fibre diameter 0.25mm, and button dimensions 10mm long by 1mm wide was chosen to investigate several aspects of the problem, as well as acting as a standard benchmark to compare other fibre probe designs against. The simulations are intended to look at the following:

- Norris vs Autofib fibre probe array geometry
- Target surface density
- Fibre crossing restrictions
- Target clustering
- Maximum allowed non-radial angle
- Pivot geometries
- Object priority distributions
- Fibre probe design

Test target fields were generated randomly using a program which allowed the specification of the number, and the clustering scale of the objects in a test field. Priorities are assigned to the objects on a radial distance basis, those near the centre of the field having the highest priority. This priority distribution was chosen in preference to the random priority distribution following experience gained with



Autofib-1.5, where it was found to make it easier to access the objects near the centre of the field with fibres.

The test fields are written to a file in the correct format for the configuration software. Clustered fields are produced using a radial gaussian form, the standard deviation being specified. Each simulation was repeated ten times, the result being the mean of the ten attempts. This was to minimise the effect of any unusually good or bad attempts, and to give an idea of the likely spread of the results. The simulations were performed using the configuration algorithm described in chapter 2, the configuration software being slightly modified for the increased number of fibres and to allow multiple crossovers.

The concept of the fibre positioner for the 2dF facility is of a single positioner servicing two fieldplates (Gray and Taylor, 1990) each with 400 individual fibre probes arranged around a field with a physical diameter of 440mm. The fibre pivots were equi-spaced around a circle of radius 300mm for the Autofib case and in two parallel banks, each at a tangent to a circle of radius 300mm, for the Norris case. The fibre length was set to 315mm in both cases to avoid any fibres passing too far beyond the centre of the field. The fibre probe set consisted of 390 spectroscopic fibres and 10 guide fibres, no attempt being made to assign the guide fibres to guide stars at this point.

Figure 6.2 shows the results of some preliminary simulations where the performance of the configuration software has been tested for a large number of object densities. The number of fibres placed on objects is a smoothly increasing function of the number of objects in the field for both a cylindrical button, as currently used, and a rectangular button as described in chapter 5. There is an obvious shortfall in the number of fibres able to be assigned to objects when the number of objects is equal to the number of fibres. This shortfall disappears for larger numbers of objects at the expense of objects near the centre of the field, as the

additional fibres are all placed on objects at the edge of the field. Figure 6.2 also shows the benefit of minimising the footprint of the fibre probe, in that the performance of the rectangular button with smaller footprint is superior to that of the modified cylindrical one based on those used on Autofib-1.5. Also shown is the theoretical upper limit of the performance of the configuration software where the number of assigned fibres is equal to the number of objects (until the number of objects exceeds the number of fibres).

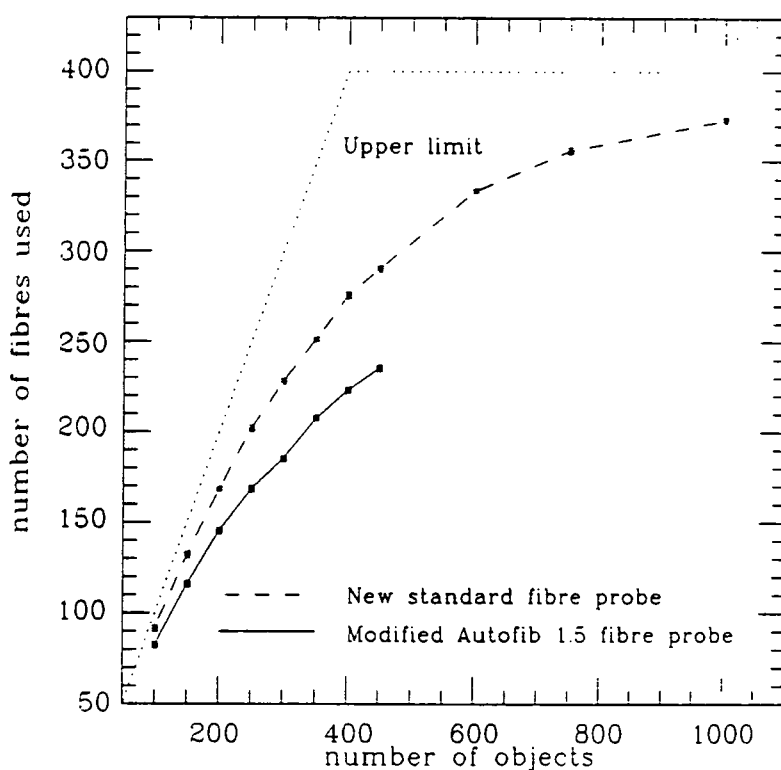


Figure 6.2 Example of a full simulation for a fibre probe with a cylindrical button (diameter 3.5mm) and a rectangular button (10mm by 1mm). Simulations were run for unclustered target objects and a maximum non-radial angle of the fibre probes of 5°.

By choosing the three cases of 200,400 and 800 objects for the majority of the simulations it was possible to assess the results in three different regimes:

- Number of objects  $<$  number of fibres.
- Number of objects  $=$  number of fibres.
- Number of objects  $>$  number of fibres.

There are many useful astronomical applications in these three regimes. Observations at low object densities include surveys of high redshift quasars using colour selected candidates, the internal dynamics of clusters of galaxies and the spectroscopic follow up of radio sources. At medium densities of objects, projects include deep surveys of all quasars. High object densities are found in projects such as redshift surveys of faint galaxies for large scale structure studies and the study of Galactic structure by observing the kinematic properties of stars.

## 6.5 Results for the fibre array geometry simulations

### 6.5.1 Initial results for a simple case

The results of the first simulations are shown in figure 6.3 where  $\sigma$  is the field clustering scale ( $\sigma = 10.0^\circ$  is larger than the field size and represents an unclustered field),  $\theta$  is the maximum allowed non-radial angle, the simulations being run for  $\theta = 1, 10$  and  $20$  degrees.

Comparison of the Norris and Autofib fibre array geometries shows that for both cases (no crossovers allowed and crossovers allowed), the Autofib geometry is marginally better in terms of the number of objects acquired in the field for the unclustered fields. However if we consider the case where the objects in the field exhibit some clustering (figure 6.4), then for  $\sigma < 2.0^\circ$ , the Autofib geometry is far superior to the Norris case. It is worthwhile noting that  $\sigma = 0.5^\circ$  corresponds to 66% of the objects within the central  $1^\circ$  of the field. From this result, it was

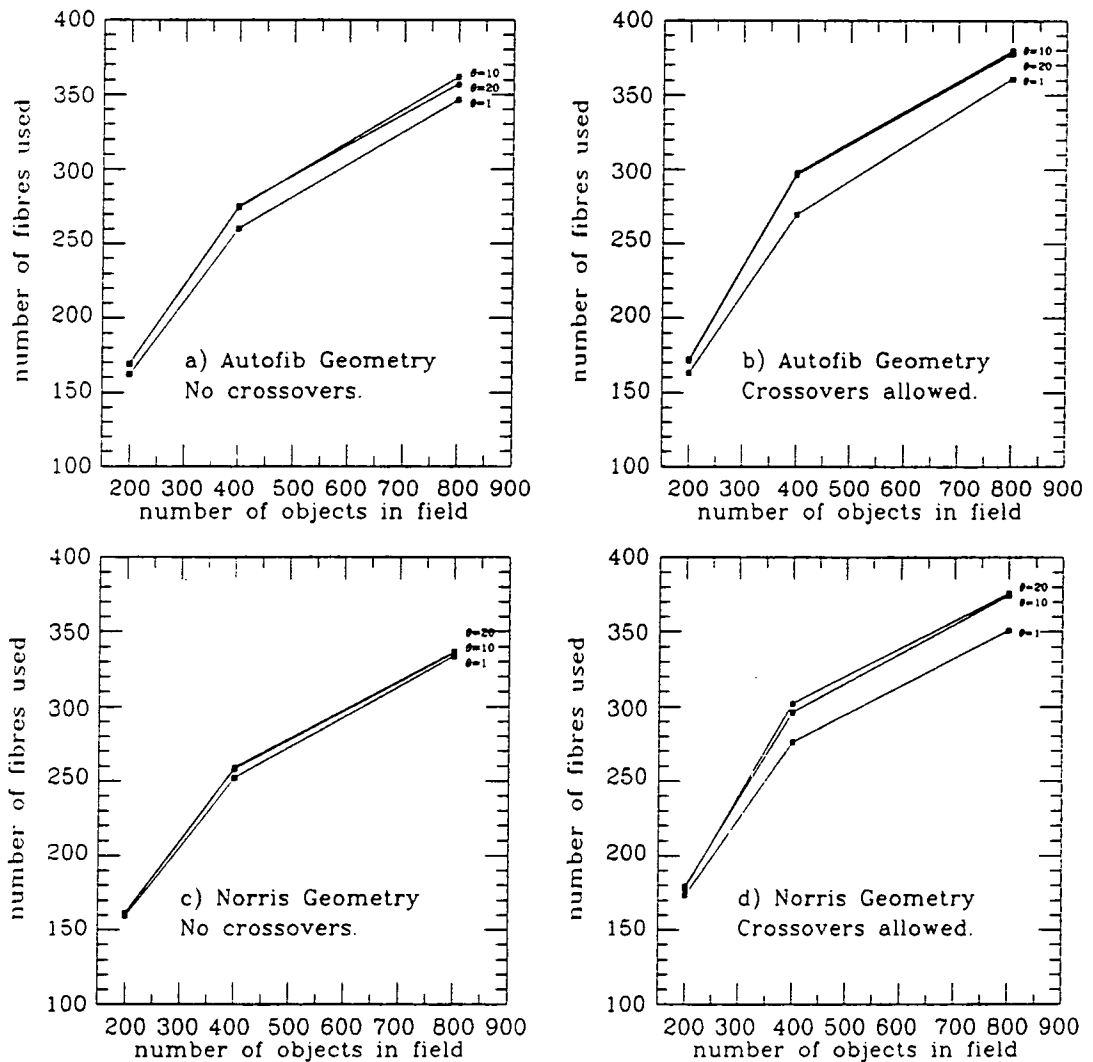


Figure 6.3 Graphs showing efficiency of configuration software for Norris and Autofib geometries at different object surface densities. Simulations are for a standard fibre probe with button 1mm wide by 10mm long, and fibre width 0.25mm, at non-radial angles of 1,10 and 20 degrees.

decided to exclude the Norris design from any further simulations, because it held no advantages over the Autofib design, and in some cases performed significantly worse.

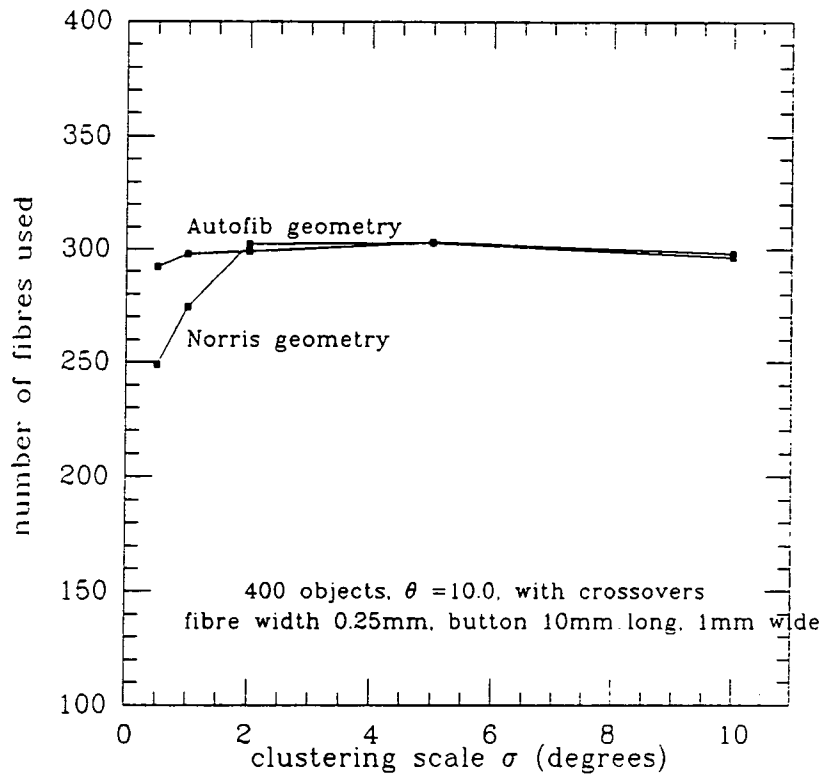


Figure 6.4 A comparison of the Norris and Autofib geometries as the clustering scale of the target objects is varied. The simulations are for a field containing 400 objects in a gaussian distribution of standard deviation  $\sigma$ .

Examination of the effect of increasing the maximum allowed non-radial angle of each fibre shows that simply increasing  $\theta$  as much as possible does not increase

the number of objects acquired beyond a certain point, in particular there seems to be no significant advantage in increasing  $\theta$  from  $10^\circ$  to  $20^\circ$  (figure 6.3b) as this results in a slight decrease in the number of fibres used. This is because it becomes progressively more difficult for a fibre to cross over other fibres at large angles to the first one. Another point to consider is that we cannot allow the number of fibre–fibre crossovers to increase indefinitely. If we are to be able to go from one configuration directly to the next without parking all of the fibres, we should attempt to minimise the number of fibre crossovers. Figure 6.5a shows the number of fibre–fibre crossovers as a function of  $\theta$ .

Having noted that it is worth restricting the value of  $\theta$  to less than  $10^\circ$ , it would be instructive to find out if there is an optimum value for  $\theta$  which will maximise the number of objects acquired, but keep the number of crossovers to a minimum. Figure 6.5b shows the data of figure 6.3b supplemented with more data at different values of  $\theta$  and plotted in a different way. As can be seen, there is no increase in the number of fibres assigned to objects beyond  $\theta = 3^\circ$ , thus in reducing the non-radial angle from  $10^\circ$  to  $3^\circ$  we reduce the number of crossovers significantly, from approximately 400 to 150, but at the same time the yield from the configuration software is not degraded. For any geometry (pivot radius, number of fibres etc.) we would expect there to be an optimum value of  $\theta$  which maximises the number of fibres assigned to objects, but keeping the number of fibre–fibre crossovers to a minimum.

### 6.5.2 Pivot geometries

The pivot circle radius used in the simulations so far was chosen using experience gained from the original fibre probe design where the fibre was encased in a rigid stainless steel tube. However with the flexible fibre probes and retractor described in chapter 5 we are no longer constrained to the large pivot circle that rigid fibre probes require. The following simulations show the effect of changing

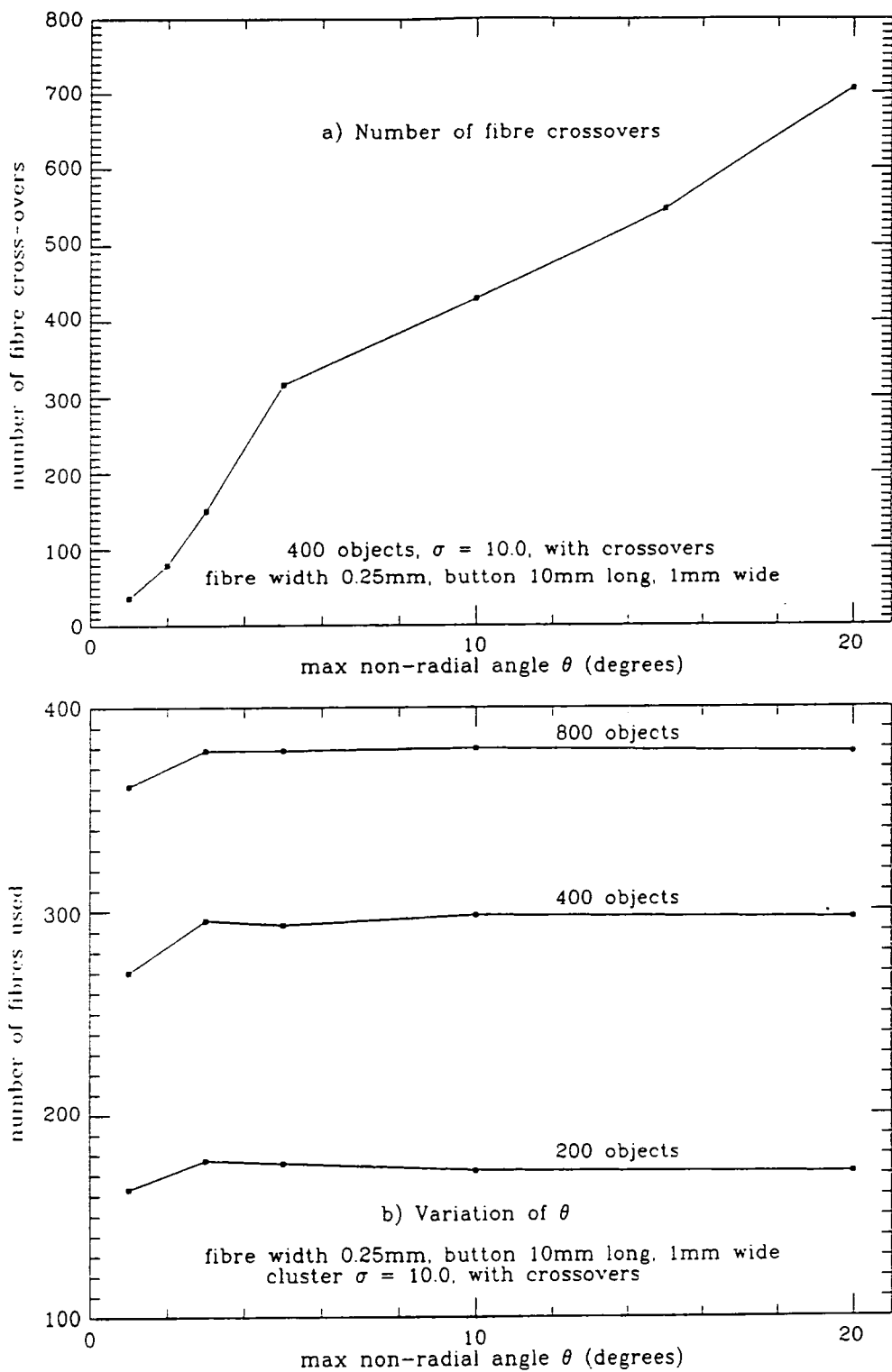


Figure 6.5 This figure shows in more detail the effect of increasing the maximum allowed non-radial angle ( $\theta$ ). a) shows the number of fibre-fibre crossovers, and b) the number of fibres assigned, both as a function of  $\theta$ .

the pivot circle radius, as a function of the number of fibres assigned to objects, and the number of fibre-fibre crossovers.

It can be seen from figure 6.6a that increasing the radius of the pivot circle gives a slight increase in the number of the fibres assigned to objects, however this is at the expense of a huge increase in the number of fibre-fibre crossovers (figure 6.6b). At this point one must decide on what is an acceptable number of crossovers, and whether the small increase in objects acquired is worth the extra problems incurred. This may be compared with the alternative option of decreasing the radius of the pivot circle, and reaping the benefit of the substantial decrease in the number of crossovers, but at a slight loss in the number of objects acquired. A pivot radius of  $R=300\text{mm}$  gives a suitable compromise, allowing over 90% of the objects available with  $R=350\text{mm}$  to be acquired, but with a factor of two reduction in the number of crossovers.

Another option for the fibre pivot geometry might be to stack the 400 pivots in two layers, one above the other. The reason for this would be to increase the possibilities for fibre crossovers. If a fibre from the upper layer of pivots is placed on an object within the central part of the field, the fibre will make an angle with the fieldplate large enough for a fibre from the lower layer of pivots to pass under the first fibre. In addition, if the lower fibre is outside of a certain radius, its fibre button might be located directly below the fibre of the upper button. Of course the lower fibre may be vignetted slightly, and this scheme will impose extra constraints during the field setup procedure, but it is worth considering as it has the potential to remove the large amount of dead space created by the placing of a fibre on an object near the centre of the field.

Examination of figure 6.7 shows that there is no real gain from the increased complexity of two layers of pivots. This result is surprising, although it may be that the current algorithm used in the configuration software is unsuited to a



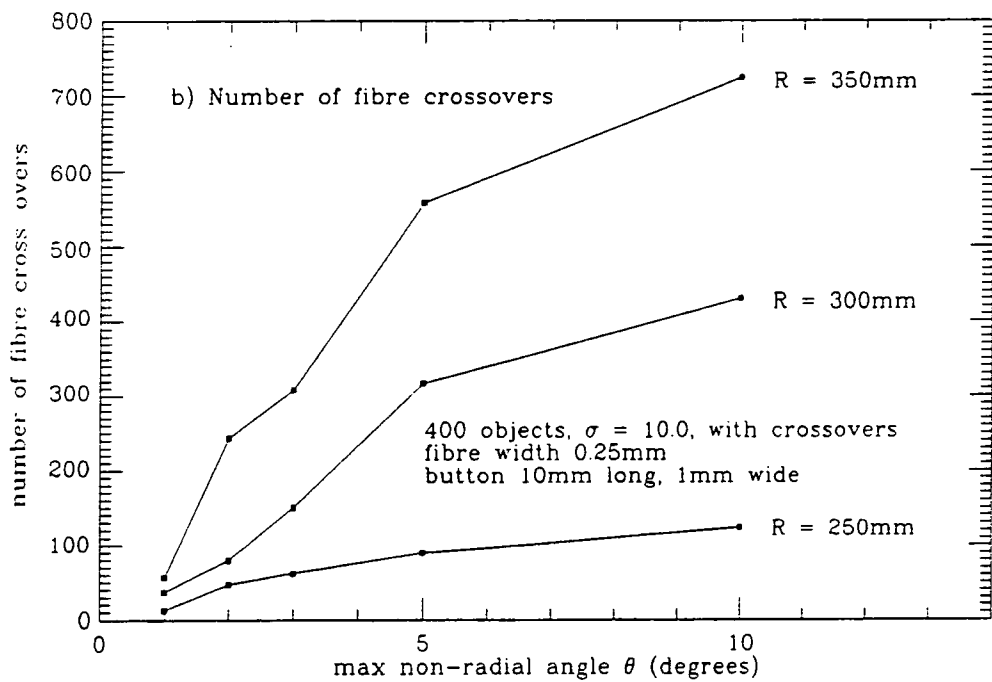
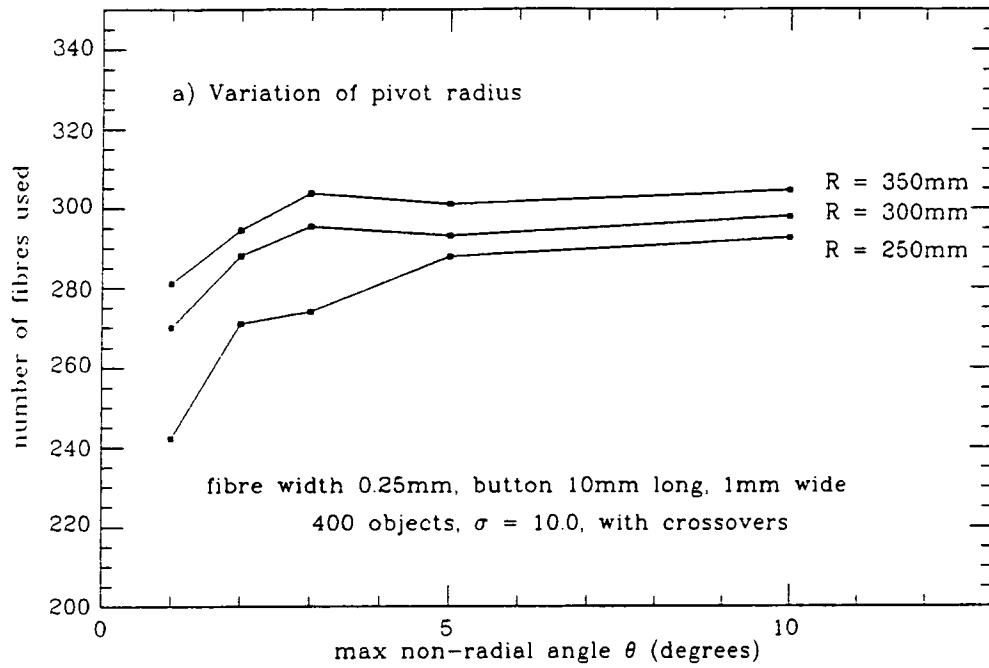


Figure 6.6 Figures showing the effect of varying the radius of the pivot circle, a) in terms of the number of fibres assigned to objects, and b) the effect on the number of fibre-fibre crossovers.

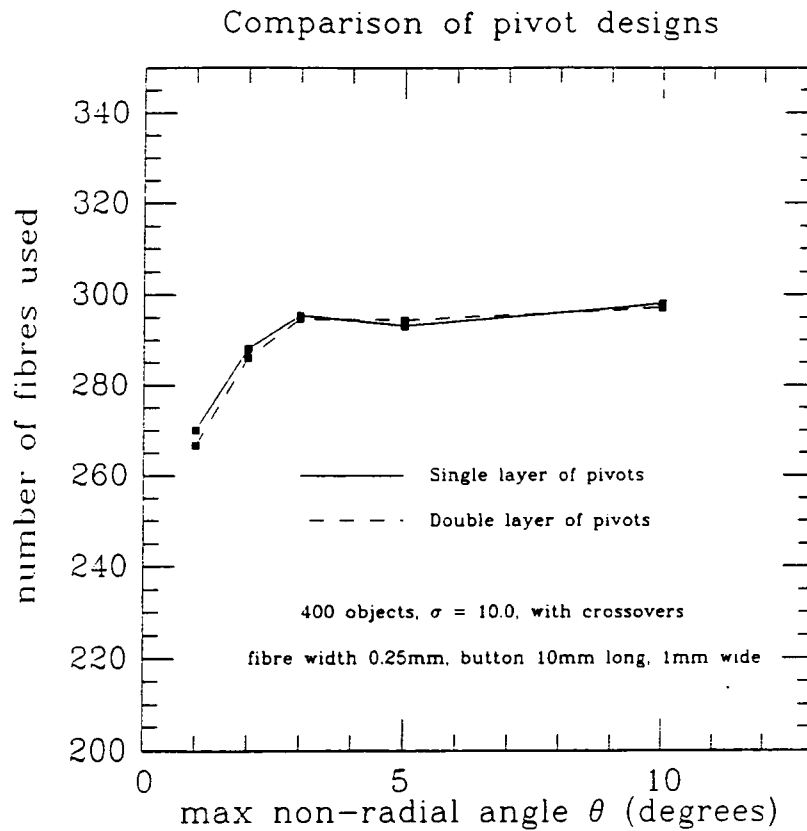


Figure 6.7 Comparison of a double layer pivot design and conventional single layer of pivots.

pivot geometry of this form. Given that this approach does not immediately give a significant improvement in the yield of objects, and has the added disadvantages of variable vignetting of the fibres and extra complexity required in the field setup procedure, this is a poor solution to the problem and it is not taken any further. Of course if a suitable configuration algorithm is devised that can give a significant improvement in the yield of objects, then the disadvantages of this approach may be deemed acceptable.

### 6.5.3 Object priority distributions

As mentioned earlier, previous experience with Autofib-1.5 led to the initial choice of a radial distribution of object priorities for the simulations. However with a much larger field and uniformly distributed objects (as is quite possible for a typical survey project) it might be useful to consider a target field where objects of the same priority are distributed evenly over the field. Figure 6.8 shows a comparison between the two cases of radial and uniform object priority distributions for an unclustered field, and the corresponding number of fibre crossovers.

The above figure shows the unexpected result that the adoption of a uniform object priority distribution significantly increases the yield of objects, and at the same time decreases the number of fibre crossovers. As the original reason for choosing a radial object priority distribution was to match non uniform distributions of objects, it would be useful at this point to compare the effect of field clustering on both radial and uniform object priority distributions.

Figure 6.9 shows how field clustering affects the different object priority distributions. Increased clustering of the field affects the efficiency of the configuration program more severely for the uniform priority distribution as expected, but does not fall to the lower level of the radial priority distribution. It should be noted that the use of a uniform priority distribution may lead to adverse selection effects, for instance, if the number of objects is greater than the number of fibres, then the fibres will be placed preferentially on objects at the edge of the field.

## 6.6 Design of fibre probes

### 6.6.1 Expected losses

The standard fibre probe design used so far in the simulations is an ideal case. However, in designing a fibre probe for production, we must consider the problems of manufacturing such a fibre probe. In chapter 5, a modified form of

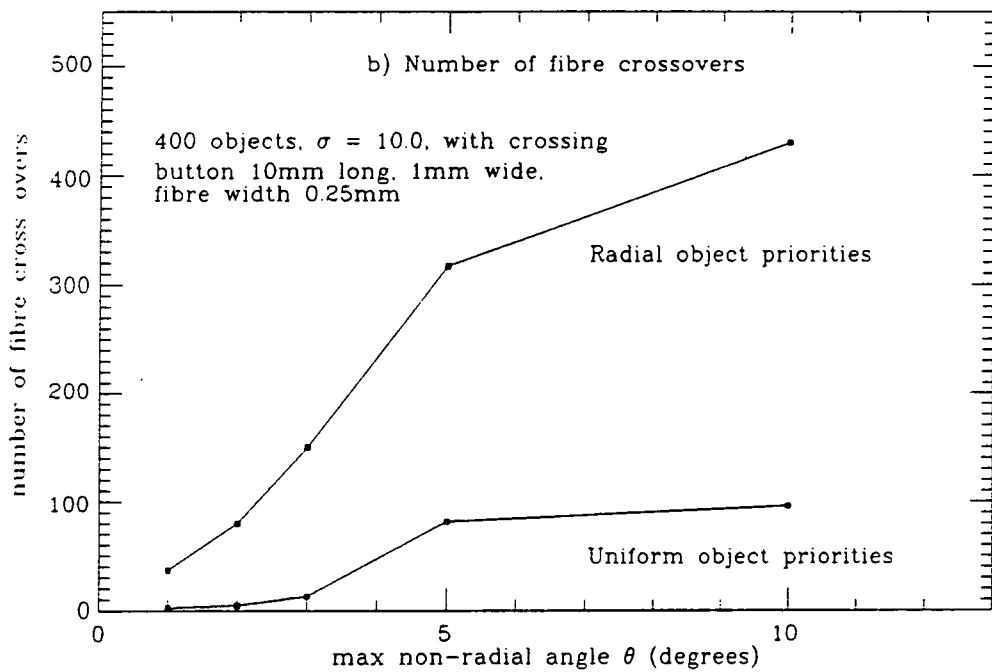
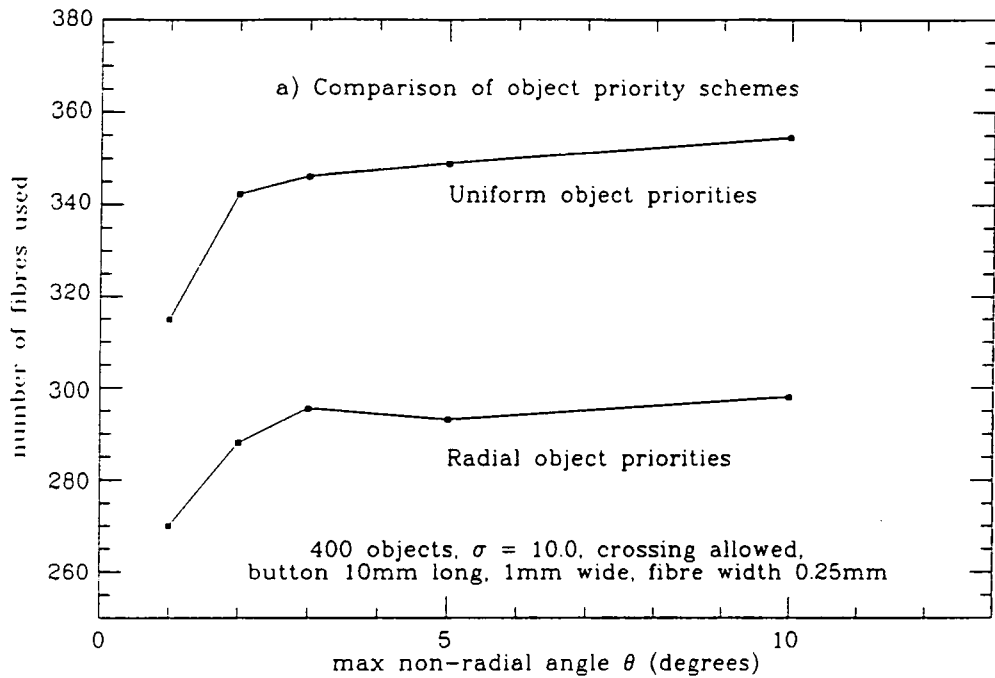


Figure 6.8 Radial vs Uniform object priority distributions, a) compares the efficiency in terms of number of fibres assigned to objects, and b) compares the number of fibre-fibre crossovers.

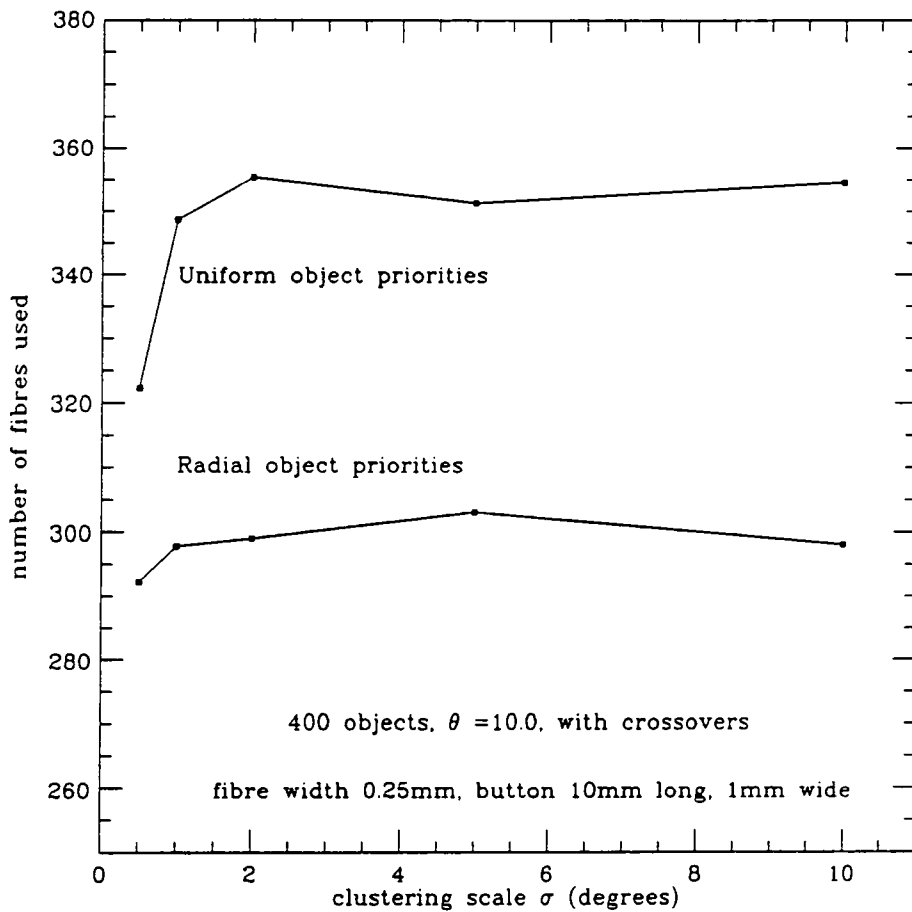


Figure 6.9 Comparison of the radial and uniform object priority distributions for different clustering scales.

the elongated fibre button was put forward, in order to get around some of the problems of fibre probe manufacture. This button was 2mm wide by 6mm long in order to have a similar base area and hence a similar magnetic attractive force. As the manufacture of such a fibre probe is feasible, it would be instructive to simulate it to determine the effect of the fibre probe design on the efficiency of the configuration software.

Another point to note is that during the simulations, the width of the bare fibre was considered to be only its physical diameter, but in a real case, we should have a reasonable tolerance on this 'width' as we cannot tension the fibre highly enough to be able to predict the exact position of every point along the length of the fibre. In fact focal ratio degradation of the light passing through the fibre may limit the tension to only 0.1N (Taylor and Gray, 1989), resulting in an uncertainty of the position of the fibre of  $\pm 0.5\text{mm}$ , thus a realistic 'width' of the fibre would be 1mm.

As the size of the fibre and button increase, so does the fraction of the field obscured by the fibres themselves. When testing the software algorithm we should bear in mind what fraction of the objects we might expect to be obscured naturally by the placement of fibres on other objects. If we consider  $N$  objects in a  $2^\circ$  field, assuming that they exhibit no clustering, we can calculate the object density in the field. The area of the field obscured by the fibre probes is equal to the number of fibres times the area obscured by a fibre extended from its pivot by an average amount. Performing this calculation for the ideal case, it can be shown that we would expect to obscure approximately 7% of the objects in the field.

However for the more realistic case where the fibre width is taken to be 1mm, almost 21% of the objects are lost due to obscuration by other fibres, the extra area of the button having only a marginal effect compared to the extra width of the fibre. Thus if we can acquire 320 of 400 possible objects for a realistic fibre probe design, then the process of assigning fibres is not being limited by the configuration algorithm. However, it is worth noting that a more intelligent algorithm may be able to reduce the effect of object obscuration by careful choice of which fibre to place on a given object.

## 6.6.2 Results

Figure 6.10 shows simulations of the 2mm by 6mm fibre probe with 1mm wide fibre, for both the radial and uniform priority schemes, compared with the standard fibre probe used for the previous simulations. As can be seen the more realistic of the two (in that it is much simpler to manufacture) does not perform as well as the longer and thinner standard probe. The reason for the degraded performance is simply that the new button has a larger footprint, both in the more realistic fibre width, and in the area of the fibre button that extends beyond the fibre.

To determine the individual effect of the increased fibre width and increased button size, two further fibre probe designs were simulated, one with the standard fibre button, but a large fibre width, and the second with the realistic fibre button and the small fibre width (figure 6.11).

In the interpretation of figure 6.11, it is worth separating the effects of button size and fibre width. The smaller the width of the fibre button the higher the yield of the configuration software, as expected. However the effect of the fibre width is more subtle. At small non-radial angles, the fibres tend not to cross each other as frequently, and the minimum separation between fibre tip and fibre is important, the smaller fibre width giving a slightly improved yield in terms of number of objects acquired. However as the non-radial angle is allowed to increase, crossovers become more common, and the minimum separation between fibre tip and fibre becomes less important. In this case it is usually possible to assign the same numbers of fibres to objects for both the thin and thick fibre case. Obviously if fibre-fibre crossovers are to be disallowed, then the small non-radial angle case applies, meaning that we must try to reduce the effective width of the fibres as much as is possible.

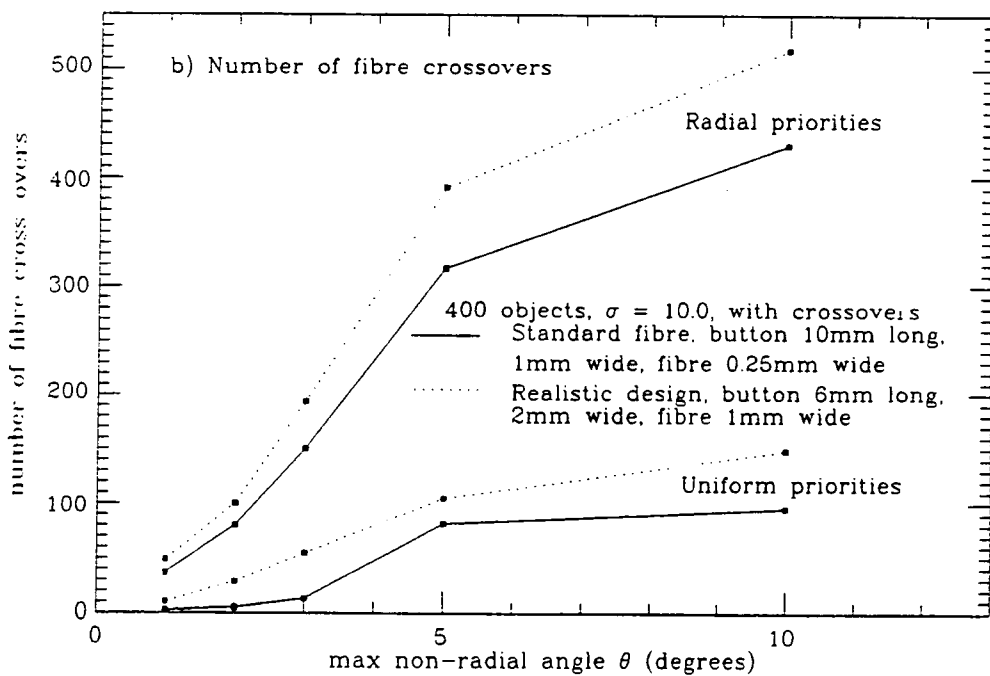
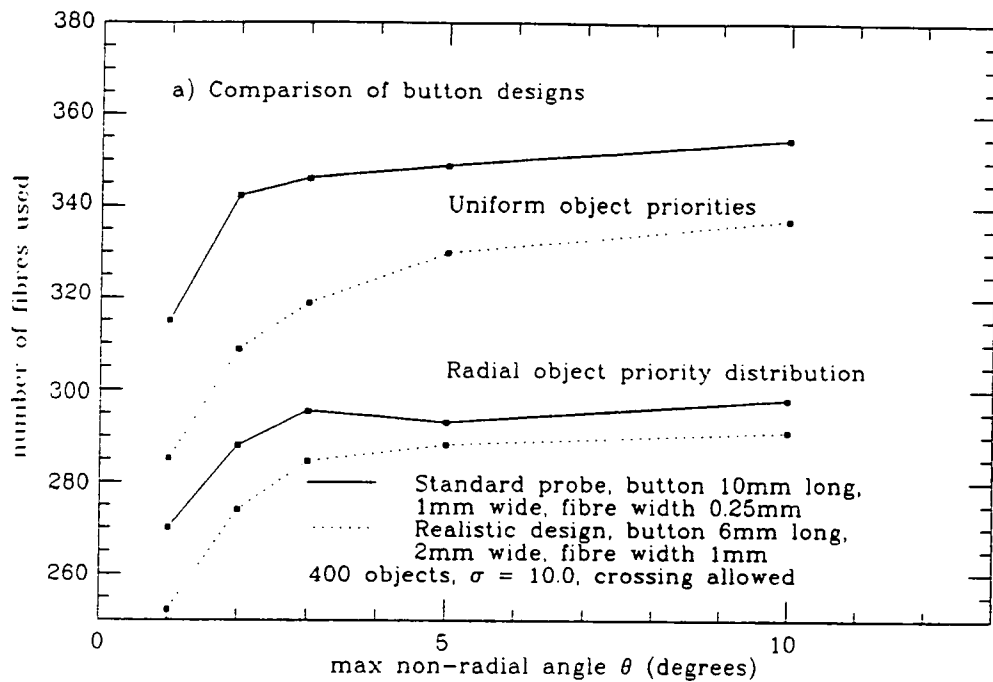


Figure 6.10 A comparison of a manufactured design with the standard fibre probe, a) efficiency in terms of fibres assigned to objects, and b) number of fibre-fibre crossovers.



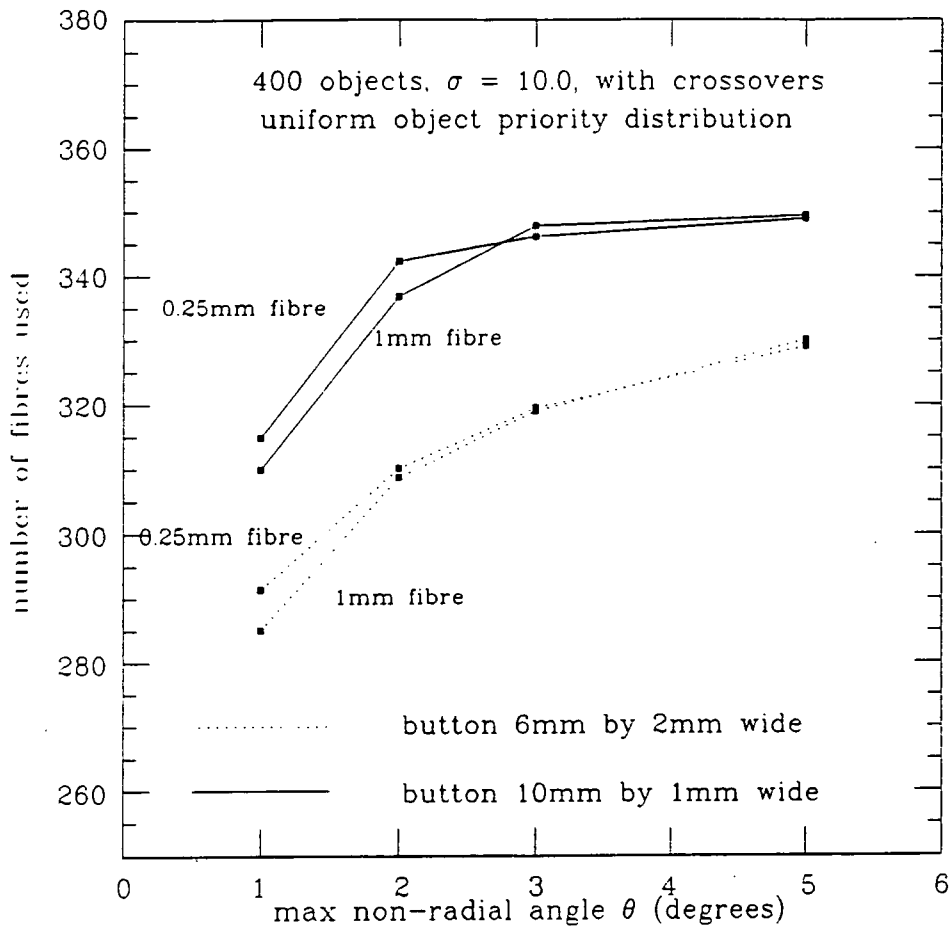


Figure 6.11 Simulations of a combination of fibre designs to determine the individual effects of changes to the fibre probe design

## 6.7 Simulations for the WHT prime focus instrument, Autofib-2

### 6.7.1 Differences between 2dF and Autofib-2

The main difference between the two instruments is that of available field size, the field for 2dF being  $2^\circ$  whereas it is only  $1^\circ$  for Autofib-2. Both prime foci have a similar plate scale ( $67$  and  $57 \mu\text{m}/\text{arcsec}$ ) which means that the physical

size of the field area is four times smaller for the WHT prime focus case. This will obviously have a large effect on the number of fibre probes chosen for the design of Autofib-2. For the 2dF instrument, potential fibre geometries have been discussed earlier in this chapter, similar simulations are now required for the WHT instrument. The main difficulties which occur in the Autofib-2 case arise from the smaller physical field size, and from the fact that the fibre probes cannot be made any smaller than those for the 2dF case. Thus for the WHT instrument the field size is a factor of four smaller, while the area blocked by the fibre probes does not decrease at all.

The original specification for Autofib-2 was to include up to 300 fibres to access the  $1^\circ$  field, however experience from the simulations for 2dF has shown that perhaps 150 fibre probes feeding a single spectrograph is a more realistic goal. A fibre probe array of 160 fibre pivots in a radial pattern containing 150 spectroscopic fibres and 10 guide fibres matches the WYFFOS spectrograph design quite well (the slit length can contain approximately  $150 \times 1.5$ arcsecond fibres).

The rigid fibre probe approach has been retained (with its inherent limitations on crossovers) as it is not clear how developed the flexible fibre retractors proposed for the 2dF will be by the time the fibre module design for Autofib-2 has to be finalised. The rectangular fibre “button” is retained however, as this offers obvious advantages in a small footprint and minimal fibre-fibre separation.

The maximum allowed non-radial angle is now defined by the need to avoid the fibres colliding or tangling outside of the pivot circle, as well as preventing collisions inside the field. This restraint is in turn heavily dependent on the overall geometry of the array of fibre probes. To maximise the allowed value of the non-radial angle ( $\theta$ ), the radius of the pivot circle should be as large as possible, a radius of 350mm giving a maximum  $\theta$  of approximately  $4^\circ$  with no danger of collision outside the field. Naturally if no crossovers are allowed, then it is the position of

other fibres inside the field that will ultimately constrain the allowed positions of a fibre within this  $\theta$  limit.

In order to maximise the allowed non-radial angle between parked fibres, the park radius of the fibre probes should be as large as possible ( the constraint on reliability imposed by the use of an electromagnetic pickup head no longer applies with the use of a pneumatic gripper). However the larger the park radius of the fibres, the larger the overall size of the fibre module. The maximum size of the fibre module is defined by the allowed space envelope for the instrument at the prime focus of the WHT. If the length of each fibre probe is equal to the pivot radius plus 15mm (to allow for slight travel past the centre of the field), the approximate required radius of the fibre module is given by:

$$\text{fibre module radius} = \text{pivot radius} + \text{park radius} + 15\text{mm} + 150\text{mm}$$

Where the additional 150mm is required to allow the fibres to curve from the fibre probe to a conduit below the fieldplate, the amount of space required being a result of experience gained from the construction of Autofib-1.5.

Obviously the minimum park radius is defined by the desire that parked fibres should not obscure any of the usable field (as is the case with Autofib at the AAT) which is of 105mm (or 30 arcminutes) radius. As the field of the WHT PFC continues past 30 arcminutes (albeit strongly vignetted (Bingham, 1984)) it was decided to increase the park radius from 105mm to 136mm (39 arcminutes). This allows the use of the field beyond 30 arcminutes for spectroscopy of bright field objects, and also decreases the chance of a bright star falling on a parked fibre.

Using these fibre module parameters we obtain a fibre module radius of about 550mm, well within the allowed space envelope of  $R=600\text{mm}$  defined by the central obstruction of the primary mirror.

### 6.7.2 Results of the Autofib-2 simulations

Using the above parameters for the fibre module, and the realistic button design already modelled above (button 6mm long, 2mm wide and fibre 1mm diameter), simulations similar to those for the 2dF facility were performed. The maximum non-radial angle was restricted to less than  $4.0^\circ$  and crossovers were not allowed. Test fields were generated containing 150 target objects, this being the most difficult case in which the number of objects equals the number of fibres.

From figure 6.12a we see that the fibres are so crowded at the edge of the field in their parked locations that when placed on objects they are forced to follow an almost radial direction (by the no crossovers constraint). Hence increasing the maximum allowed non-radial angle ( $\theta$ ) does not improve the efficiency of the configuration software. As before, the uniform object priority distribution performs better than the radial one.

For clustered fields with a uniform object priority distribution the yield of the configuration software is unaffected until the objects are strongly clustered ( $\sigma = 0.25^\circ$ ) where a 13% drop in yield occurs. This compares with a 10% drop in yield for the 2dF case with  $\sigma = 0.5^\circ$  (ie field diameter/4).

For the case where the objects have a radial priority distribution, the drop in yield is smaller (approximately 10% for the Autofib-2 case and 5% for the 2dF case), but it is not until even shorter clustering scales (of order field diameter/8) that the two priority distributions are comparable.

The overall efficiency of the configuration algorithm for the Autofib-2 case is approximately 70% for all but the most strongly clustered fields. While this compares favourably to the 2dF case (approximately 80%), it must be remembered that we are trying to use a higher density of fibres per unit area of sky.

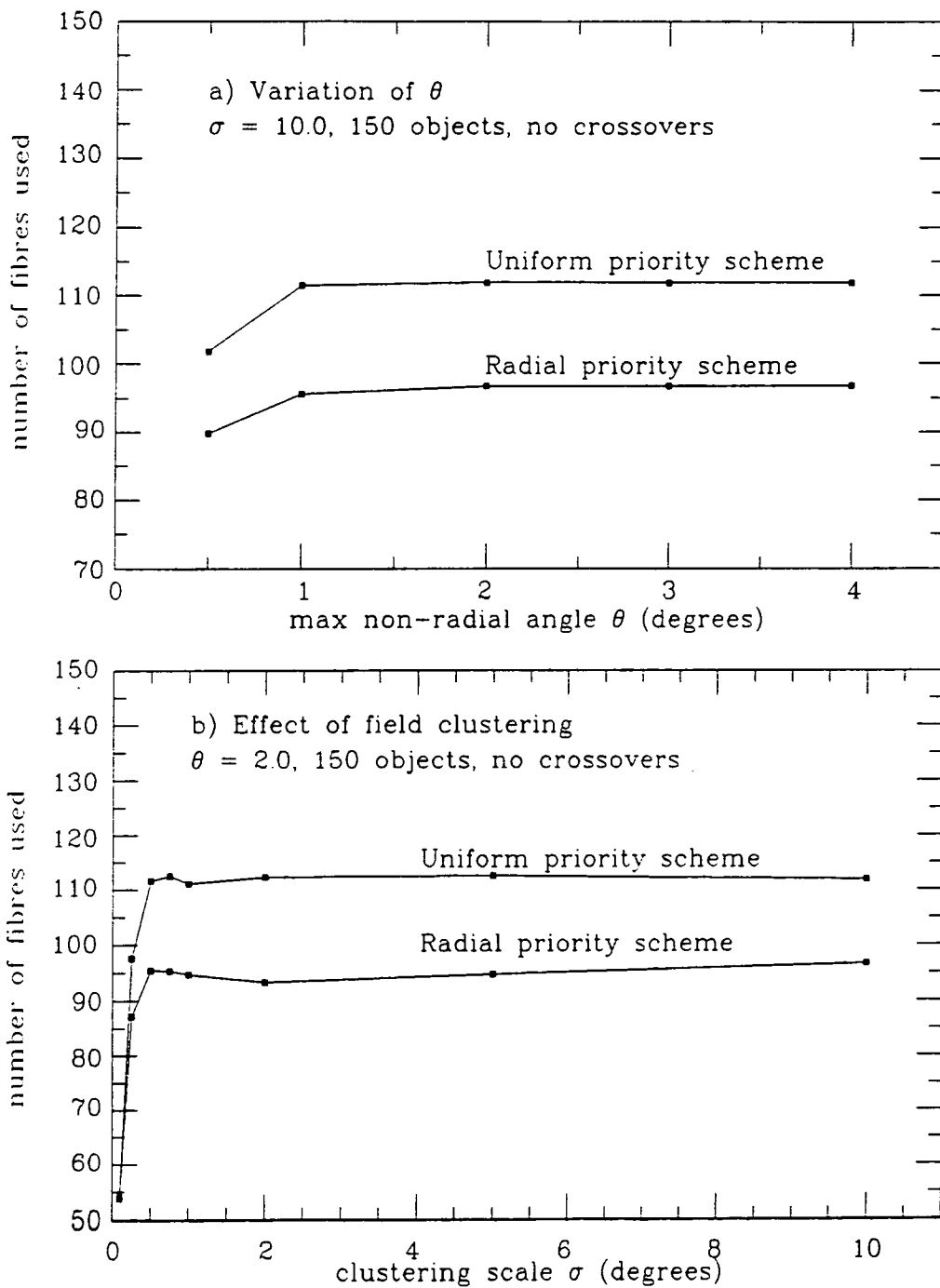


Figure 6.12 Simulations for Autofib-2, a) shows the effect of varying  $\theta$ , and b) the effect of field clustering.

## 6.8 Summary

In the above work it has been shown that with modifications, the techniques currently employed at cassegrain may be used with some success at both the prime foci of the WHT and AAT. In practice however, the efficiency of these techniques may not reach that achieved in these simulations. This may be due to non-random clustering effects, preferential choice of objects (due to the observers personal preference or due to a brightness cutoff) or simply the difficulty in acquiring sufficient guide stars (normally 2 or 3). The latter effect may be substantially reduced by the inclusion of additional guide fibres in order that none has to move far from the radial direction to acquire a guide star. Commissioning tests with Autofib-1.5 using fibre modules containing both 6 and 8 guide fibres showed that increasing the number of guide fibres improved the ability to acquire sufficient guide stars significantly. Consequently the design for Autofib-2 has provision for 10 guide fibres equi-spaced among 150 spectroscopic fibres.

Whilst it has been shown that for almost all randomly generated fields a uniform object priority distribution out-performs a radial distribution, this is not a very realistic case. For a real astronomical field the astronomer is likely to have his own priorities, based on scientific importance, magnitude, or previous observations. To allow for a non-standard list of object priorities it is probable that a great deal of trial and error will be required to achieve a satisfactory fibre configuration.

However, for the prime foci developments described, a large amount of interactive fibre-object assignments will be difficult and tedious given the large numbers of fibres involved. For this reason a new fibre configuration algorithm is required. Such an algorithm must possess several properties which have been highlighted by the above work:

- The ability to take account of complex object priority schemes.

- To preferentially choose fibre-object assignments that minimise the dead area in the field.
- To attempt to reduce the amount of interactive fibre assignment to a minimum.

It is toward these aims that the next generation of “*optimising*” configuration algorithms are being developed. This work is currently at a very early stage, but it is worthwhile describing the general principles and some initial results.

For each object in the field a list is made of all the fibres that may legally acquire it. Starting with the object that may be acquired by the least number of fibres (to avoid losing a ‘difficult’ object) a fibre is chosen from its list and assigned to the object. It is the method of choice of the fibre at this point that is critical, currently the fibre chosen is that fibre that occurs the least frequently in the lists for the other objects. Once a fibre is assigned, the process starts again with the construction of the lists of allowed fibres for the remaining objects.

Early tests of the algorithm with 64 fibres and objects (in the cassegrain case) are encouraging, with over 90% of objects acquired when crossovers are allowed. However, due to the necessity to reconstruct the ‘list of fibres’ for each object every time a fibre is assigned, the algorithm is extremely slow. If the number of target objects is equal to the number of fibres, then the amount of CPU time taken to arrive at a configuration by this method scales as  $N^4$  where  $N$  is the number of fibres. A practical implementation has not yet been made for 64 fibres, let alone expanded to 150 or 400 fibres.

In summary, current techniques applied to the prime focus case are a sufficient (if not ideal) solution to the fibre configuration problem. However a more complete solution to the problem might be achieved by the development of a new optimising configuration algorithm together with an increase in computing power.

## 7 Conclusions

### 7.1 Overview

The work contained in chapters 2,3 and 4 dealt with the investigation into some new techniques for constructing and operating an automated fibre positioning system at the William Herschel Telescope. Many new techniques were tried out on an experimental instrument, Autofib-1.5. This test bed instrument was commissioned on the telescope twice, and both times proved itself capable of obtaining astronomical data.

Chapter 5 contained a description of the work into developing a new technique for accurately placing the fibre probes of an automated fibre positioner to much higher accuracies than had been achieved before. Other aspects considered were the speed and reliability of operation, both of which are critical for future instruments at the prime focus of the WHT and AAT.

Methods of usefully increasing the number of fibres available for use in an automated fibre positioner were investigated in chapter 6. Rather than constructing a series of experiments, the problem was examined by exploring the parameter space using a series of computer simulations.



## 7.2 Design and operational experience

The prototype fibre positioner for the WHT (Autofib-1.5) contained many new design features. While it is probable that a few of these new ideas will be used in the common user instrument (Autofib-2), the rest will require modification or complete redesign to improve their performance or function before they can be used in Autofib-2. A good example of the latter case is the fibre and sky viewing head. While both modes of operation were individually very successful, combining the two modes was not such a success. Therefore a future instrument will be built to include both of these features as separate devices.

Many of the operational tests performed with Autofib-1.5 showed that although existing techniques were improved upon, for example reliability and ease of packing fibres closely together, the improvements were not always enough to extend the work to prime focus. Features such as the multi-way fibre connector were designed as a result of experience with the prototype instrument during testing at the telescope.

A different approach to the problem of positioning fibre probes was tried in the work described in chapter 5. This involved the use of robot vision techniques to improve the calibration of the robot in real time as each fibre probe was placed in position. This technique has proved to be extremely powerful and has been adopted for Autofib-2. In particular this technique allows for much more accurate positioning of the fibre probes and 'intelligent' software that allows for automatic calibration of the instrument. A second result of this work was a new design of fibre probe. Through the simulations of chapter 6 this new design has been shown to be much more flexible when large numbers of fibres are used in crowded fields.

### 7.3 Applications to future work

The result of the work contained in this thesis has been the accumulation of a large amount of experience in operating an automated fibre positioning system under observing conditions and also in the development of high speed and precision positioning robots.

This experience is now being put to use in the design of Autofib-2, and in the near future, the design of the fibre positioner for the 2dF facility. These two future instruments require the high precision fibre positioning systems developed in chapter 5 as well as the improved reliability and error recovery resulting from the work of chapters 2 and 3.

In the future, it is probable that large telescopes will become available dedicated to spectroscopic survey science with a fibre fed spectrograph (for example the 3.5m WIYN telescope). For such instruments, the techniques described in this thesis for the building of more reliable instruments for prime focus will be of considerable use. If remote observing becomes the norm, then high reliability and ease of possible error recovery becomes essential.

Future 8 metre class telescopes already are planned which include multiple fibre feeds for spectrographs at the secondary foci. The plate scale at such a focus is very large, so positioning accuracy is not a problem. However the use of robotic vision techniques allows for the automatic calibration if an automated fibre positioner, this may become extremely important if the numbers of available fibres increases to use the physically large fields available.

Of course, if larger numbers of fibres are planned, the fibre configuration techniques discussed in chapter 6 must be improved considerably. This is one area of work that will benefit existing instruments with no additional instrument hardware upgrades.

## References

- Allington-Smith, J.R., Breare, J.M., Ellis, I.R., Parry, I.R., Shaw, G.D., Webster, J., Gellatly, D.W., and Worswick, S.P., *Proc. SPIE*, **1235**, 691, (1990)
- Atherton, P.D., Taylor, K., Pike, C.D., Harmer, C.F.W., Parker, N.M., Hook, R.N., *Mon. Not. R.A.S.*, **201**, 661, (1982)
- Baranne, A., in "Instrumentation for Ground-Based Astronomy: Present and Future" (ed Lloyd B. Robinson), 296, (1987)
- Barden, S.C., and Massey, P., in "Fibre Optics in Astronomy" (ed S.C. Barden), *ASP Conf. Series*, **3**, 140, (1988)
- Barden, S.C., and Rudeen, A.C., *Proc. SPIE*, **1235**, 729, (1990)
- Breare, J.M., Ellis, R.S., Purvis, A., Miller, M., and Webb, D.A., *Proc. SPIE*, **627**, 278, (1986)
- Breare, J.M., Cox, G.C., Ellis, R.S., Martin, G.P., Parry, I.R., Purvis, A., Waltham, N.R., Webster, J., Fosbury, R.A.E., Gellatly, D.W., Jorden, P.R., Lowne, C.M., Lupton, W.F., Powell, J.R., Thorne, D.J., van Breda, I.G., Worswick, S.P., and Wynne, C.G., *Mon. Not. R.A.S.*, **227**, 909, (1987)
- Bingham, R., RGO/La Palma Technical Notes No. 9, (1984)
- Brodie, J.P., Bixler, J.V., Craig, W.W., Donnelly, R.H., Hailey, C.J., and Seppala, L.G., *Proc. SPIE*, **1235**, 722, (1990)

- Buzzoni, B., Delabre, B., Dekker, H., D'Odorico, S., Enard, D., Focardi, P., Gustafsson, B., and Reiss, R., *ESO Messenger*, **38**, 9, (1984)
- Cohen, J.G., Oke, J.B., Carr, M., Harris, F.H., and Hamilton, D., in "Fibre Optics in Astronomy" (ed S.C. Barden), ASP Conf. Series, **3**, 190, (1988)
- Fort, B., CFH Information Bulletin No. 16
- Craig, W.W., Stewart, R.E., Blaedel, K.L., and Brodie, J.P., in "Fibre Optics in Astronomy" (ed S.C. Barden), A.S.P. Conf. Series, **3**, 153, (1988)
- D'Odorico, S., *ESO Messenger*, **40**, 11, (1985)
- Dressler, A., and Gunn, J.E., *Ap.J.*, **263**, 533, (1982)
- Dupin, J.P., Fort, B., Mellier, Y., Picat, J.P., Soucail, G., Dekker, H., and D'Odorico, S., *ESO Messenger*, **47**, 55, (1987)
- Ellis, R.S., Couch, W.J., Parry, I.R., and Purvis, A., *Multislit User Manual for the INT*, RGO Publications, (1986)
- Ellis, R.S., and Parry, I.R., in "Instrumentation for Ground-Based Astronomy: Present and Future" (ed Lloyd B. Robinson), 192, (1987)
- Enard, D., and Delabre, B., Proc. SPIE, **445**, 522, (1983)
- Felenbok, P., Guerin, J., Fernandez, A., Tournassoud, P., and Vailant, R., in "Fibre Optics in Astronomy" (ed S.C. Barden), ASP Conf. Series, **3**, 174, (1988)
- Fordham, J.L.A., Bone, D.A., Norton, T.J., and Read, P.D., Proc. SPIE, **1235**, 636, (1990)
- Fort, B., Mellier, Y., Picat, J.P., Rio, Y., and Lelievre, G., Proc. SPIE, **627**, 321, (1986)

- Geary, J.C., Huchra, J.P., and Latham, D.W., Proc. SPIE, **627**, 509, (1986)
- Gray, P.M., Proc. SPIE, **445**, 57, (1983)
- Gray, P.M., and Sharples, R.M., *Focap User Manual*, AAO User Manual. (1985)
- Gray, P.M., Proc. SPIE, **627**, 96, (1986)
- Gray, P.M., and Taylor, K., Proc. SPIE, **1235**, 709, (1990)
- Hamilton, D., Proc. SPIE, **1235**, 673, (1990)
- Hill, J.M., Angel, J.R.P., Scott, J.S., Lindley, D., and Hintzen, P., Proc. SPIE, **331**, 279, (1980)
- Hill, J.M., Angel, J.R.P., Scott, J.S., Lindley, D., and Hintzen, P., *Ap. J. Lett.*, **242**, L69, (1980)
- Hill, J.M., Angel, J.R.P and Richardson, E.H., Proc. SPIE **445**, 85, (1983)
- Hill, J.M., and Lesser, M.P., Proc. SPIE, **627**, 303, (1986)
- Hill, J.M., and Lesser, M.P., in "Instrumentation for Ground-Based Astronomy: Present and Future" (ed Lloyd B. Robinson), 233, (1987)
- Hubbard, E.N., Angel, J.R.P., and Gresham, M.S., *Ap. J.*, **229**, 1074, (1979)
- Ingerson, T.E., Schommer, R. and Suntzeff, N., NOAO Newsletter, **16**
- Ingerson T.E., in "Fibre Optics in Astronomy" (ed S.C. Barden), ASP Conf. Series, **3**, 99, (1988)
- Kernighan B.W., and Ritchie D.M., "The C Programming Language, 2<sup>nd</sup> Edition", Pub. Prentice Hall

- Lund, G., and Enard, D., *Proc. SPIE*, **445**, 65, (1983)
- Parry, I.R., Ph.D Thesis, Univ. of Durham, (1986)
- Parry, I.R., and Gray, P.M., *Proc. SPIE*, **627**, 118, (1986)
- Parry I.R., and Sharples R.M., in "Fibre Optics in Astronomy" (ed S.C. Barden), *ASP Conf. Series*, **3**, 93, (1988)
- Parry, I.R., and Carrasco, B.E., *Proc. SPIE*, **1235**, 702, (1990)
- Powell, J.R., *Proc. SPIE*, **445**, 77, (1983)
- Powell, J.R., *Proc. SPIE*, **627**, 125, (1986)
- Robertson, J.G., *PASP*, **98**, 1220, (1986)
- Taylor, K., and Atherton, P.D., *Mon. Not. R.A.S.* **191**, 675, (1986)
- Taylor, K., and Gray, P.M., "Design Study for the 2dF", AAO internal report, (1989)
- Taylor, K., and Gray, P.M., *Proc. SPIE*, **1236**, 290, (1990)
- Watson, F.G., *Proc. SPIE*, **627**, 787, (1986)
- Watson, F.G., in "Fibre Optics in Astronomy" (ed S.C. Barden), *ASP Conf. Series*, **3**, 125, (1988)
- Wynne C.G., and Worswick S.P., *Mon. Not. R.A.S.*, **220**, 657, (1986)

## Appendix A

Appendix A contains information relevant to the operation of the WHT Prototype instrument (Autofib-1.5) and also forms a brief description of the control software. This information is grouped into four sections:

- A list of commands for the control of the WHT Prototype.
- Technical procedures for Autofib-1.5.
- Control software error messages.
- A description of the control software.

### List of control commands

The commands available to control the WHT Autofib Prototype may be divided into three classes of command. The first class consists of those commands which may be entered at the keyboard in 'INTERACTIVE' control mode. These involve changes to the information displayed on the mimic display, initialisation of the robot positioner, and high level commands involving the movement of the robot that do not affect the fibre configuration. The second class of commands are those generated by the Command Generating Program (CGP) part of the control software to move the fibres from one configuration to the next. The astronomer has no direct access to these commands, and as they are potentially dangerous for the fibre probes, several software checks are made before these commands are executed from the 'AUTOMATIC' mode of control. The final class of command are those available from 'ENGINEERING' mode, these include all of the first two

classes of command as well as additional commands. These extra commands include those necessary for calibration and initial configuration of the instrument, as well as some very low level commands to control individual functions of the robot for testing or extricating the robot from an error situation.

On starting up the control software by typing 'CONTROL', the astronomer is prompted to hit the return key, on doing this the astronomer enters the basic control level. The prompt shown on the mimic display asks the astronomer to select the control mode (Interactive, File or Quit) by entering I, F or Q. Entering 'Q' allows the astronomer to exit the program, 'I' or 'F' starts up the required mode of control. A further choice that is not advertised on the screen is to enter 'E' to enter the engineering mode.

#### Interactive commands

Here follows a list of commands available in the interactive control mode. Note that for all commands with numerical parameters, a space should separate the different parameters.

- EM** Enable the motors of all three axes in software, and energise the relay to apply power to the X, Y motors. Finally remove friction brake from X axis. The motors remain energised at all times until they are actively disabled by issuing a disable motors command (below) or exiting from the control software.
- DM** Disables all three motors. Firstly the brake is applied to the X axis, then the motors are disabled in software. Finally power is removed from the X and Y axes by de-energising the relay.
- GO** Initialise all three axes, Z axis first to ensure that it is clear of the fieldplate, then the X and Y axes simultaneously. No movements



of the robot are possible until this command has been issued as the optical encoders will not have been initialised.

- PK** Park the pickup head at a safe location. The park location is defined in software and is clear of the observing area.
- Q** Quit from interactive mode and return to the basic control level.
- TP** Display the current position of the X,Y carriage in the status window.
- TF n** Display the current x,y of the button of fibre n in the status window.
- VW x y** Position viewing head at the specified x,y. This command automatically allows for the offset of the viewing head from the pickup head.
- VF n** Position the viewing head above the location of fibre n.
- VA** Position the viewing head above each spectroscopic fibre in turn, pausing at each. Can be used to eyeball each fibre to confirm that it is at its correct location. Alternatively if no back illumination is present, each of the target objects may be observed in turn.
- VG** As above, but checking each of the guide fibres in turn.
- PP** Display the pickup head position x,y,z in the position window of the mimic display. This is the default position display, the alternative is selected by the VP command (below).
- VP** Display the current viewing head x,y in the position window, this is most useful when using the viewing head to check locations of fibres or objects.

- JO** Enter the 'jogging' mode of the X-Y carriage. The step size is selected using the F1-F4 keys (10, 30, 100, 300  $\mu\text{m}$  respectively) and the movement of the carriage by the arrow keys. The x,y offset from the position of the carriage on entry to the jogging mode is continuously displayed in the status window. Once finished, 'Q' returns back to interactive mode.
- ME n** Measure the position error on fibre n, store the results in a temporary file on disk. Before exiting from the control software, the astronomer is prompted for a filename for permanent storage of the results if not already done using the SM command (below).
- MA** Measure the position errors of all of the fibres in turn, store the results as for the above command.
- SM** Rename the temporary error measurements file to avoid over-writing the data next time the software is started up, or if several sets of measurements are required to be stored separately.
- MN** Select the manual mode for centroiding the fibre images, this uses the arrow keys in the same way as the JO command described above.
- CM** Select the automatic centroiding mode. In this mode the manual mode is retained for the guide fibres (due to the more complex image), but the centroiding of the spectroscopic fibres is performed automatically using the frame grabber image.
- CI n** Centroid fibre n and display the offsets of the fibre from the TV centre on the mimic display. The actual operation of this function depends on the mode selected using the CM or MN commands. In the automatic centroiding mode this command will only generate a

sensible answer if the viewing head is feeding a camera connected to the frame-grabber.

**CS** Display a cursor at the centre of the frame-grabber image to enable the centre of the screen to be marked. This is extremely useful as it provides a reference mark for centering the guide fibres. Once the screen has been marked, hit return and the screen will display its normal image.

#### File or automatic commands

The following commands may be generated by the automatic command generating program part of the control software. These commands are used to move fibres around using the robot, and as they will change the configuration, must only be generated in software where the necessary anti-collision checking can be performed.

**PU** Pickup fibre probe at the current x,y.

**PD** Putdown fibre probe at the current x,y.

**MO x y** Move the X-Y carriage to the specified x,y. No movement in Z is performed when this command is executed.

**PF n** Command to park fibre n at its location in the park circle.

**MF n** Move the X-Y carriage to the current x,y of the button of fibre n.

**UP x y** Update the fibre probe tip coordinates of the fibre about to be put-down.

**AB** Test to see if space bar has been struck, abort automatic field setup if necessary.

**PS** Pause the field setup, wait for the return key to be struck before continuing.

#### Additional commands available in engineering mode

The following commands are available in engineering mode in addition to all those already described. Extreme care is required when using some of the low level commands as it is not possible to completely prevent an illegal fibre configuration when using this mode of control.

**PA** Park all of the spectroscopic fibres in their park locations.

**PG** Park all of the guide fibres in their park locations.

**LF n** Load fibre n, a procedure to enable the software to determine the exact position of a fibre after initial loading of the fibre module, or if a fibre has been moved manually. Actual execution depends on the centroid mode selected using MN or CM.

**LA** Load all of the fibres in turn.

**ZM z** Move the Z axis to encoder position z.

**MG n** Control of the electromagnet is achieved using this command, n = 0 turns the magnet off, n = 1 energises the electromagnet. The current status of the magnet may be determined from the mimic display.

**ER n** Generate an error offset l,b for fibre n. As for LF, actual execution depends on the centroiding mode selected.

**ET** Generate an error offset for each fibre in turn (ie generate an error table).

- SE** Save the error table data under a filename (prompted for) to avoid over-writing at a later date, or to keep different sets of data separate.
- RE** Resets the error flag, On occurrence of an error an error flag is set to prevent further operation. To extract the robot from an error situation, the error flag must be reset in engineering mode, before trying to correct the error.
- SP n** Reduce the maximum speed of the X-Y carriage. Useful if the DC servo-loops are causing concern.
- OP** Override the pressure sensor for future pickup or putdown operations by setting  $P1 = 5000$  and  $P2 = 0$ . (The normal operating values for  $P1$  and  $P2$  are contained in CONTROL.DAT)
- RP** Reset the pressure sensor to normal operational values after using the **OP** command to override the pressure sensor.
- CF n** Check the position error of fibre  $n$  and if it is outside a given tolerance (specified in the data file CONTROL.DAT) try and correct it by moving the fibre slightly. The positions in the current status file CURRENT.FIB are updated.
- CA** Correct the positions of all the fibres.
- SC** Copy current.fib to a given filename in order that a corrected (using **CF n** or **CA**) configuration may be saved.
- OB x y** Software prompts for a fibre number ( $n$ ). This command moves the tip of fibre  $n$  to be at the specified  $x,y$  after checking that this is not an illegal fibre location.

## Technical procedures

Unless care is taken when powering up the instrument, it is possible to cause a large amount of damage both to the robot and the fibre module. A safe procedure for switching on and off is detailed below to eliminate any risk to the instrument (or operator if the instrument is being operated off the telescope). In particular the control computer should not be switched off whilst the instrument remains powered up.

### Power up procedure

1. Boot up the control computer.
2. Start control software and enter into 'Interactive' mode.
3. Switch on power to Power and Distribution (P&D) box.
4. Ensure that the X,Y disable switch (on right of P&D box) is up and that the red light is on. If this cannot be achieved then there is an electrical problem and no attempt should be made to power up the instrument until it has been rectified.
5. Switch on the DC servo-amplifier.
6. Close the X,Y motor disable switch. The red light should extinguish, with no movement from the instrument.
7. Enter the **EM** command to enable the motors, there should be an audible click from the instrument as the brake releases and the X,Y relay closes.
8. Issue a **GO** command to initialise all three axes, movement should be smooth and slow during the initialisation.
9. The instrument is now powered up, and awaits further commands.

## Shutdown procedure

1. Park the robotic positioner using the **PK** command.
2. Issue a disable motors (**DM**) command. There should be an audible click as the relay opens and the brake engages.
3. Open the X,Y motor disable switch on the P&D box, the red light should come on.
4. Switch off the servo-amplifier.
5. Switch off the P&D box.
6. Exit from the control software by issuing a **Q** command to return to the basic command level, then a second **Q** to exit from the software completely.

## Control software error messages

### General error messages

The following section contains general error messages that may be displayed in the 'error message' window of the mimic display. These messages generally are to inform the astronomer that a piece of input information is invalid or that the command entered is illegal in some way.

If an error occurs, an **RE** command must be issued in 'Engineering' mode in order to proceed. The **RE** command resets the error flag condition. If an error condition occurs during an automatic configuration setup, all subsequent commands in the file will not be carried out as an **RE** command will not have been given. The operator must first respond to the 'Interactive, File or Quit' prompt by entering engineering mode and then entering **RE**. After this the fault

must be corrected in some way (which may require manual intervention) before the field setup can be continued.

**UNKNOWN FIBRE** Supplied fibre number is outside of allowed values. ie. it is less than one, or greater than the number of fibres available.

**UNUSED FIBRE** The particular fibre number chosen is missing or broken.

**ERROR:MAGNET TOO LOW** The X-Y carriage cannot be moved when the Z axis is at too low a position.

**CANT PARK FIBRE** Cannot park the fibre as requested without a collision occurring at the park position.

**ILLEGAL POSITION** The destination position of a move command is outside the allowed software or hardware limits.

**ILLEGAL MOVEMENT A** The pickup head cannot move outside of the park circle when carrying a fibre.

**ILLEGAL MOVEMENT B** The pickup head cannot move more than one fibres length from the appropriate pivot when carrying a fibre.

**SERVO WARNING!** A warning message to indicate that the X-Y carriage did not arrive to within 25  $\mu\text{m}$  of the required position at the end of a move.

**TIMED OUT DURING MOVE** No motion completed signal received from the Galil card within a reasonable length of time. Most likely cause is that a movement was requested without power being switched on to the P&D box or the DC servo amplifier.

**CANT MOVE FIBRE** Supplied position for fibre in an OB command would cause a collision and therefore the movement is prohibited.



**CANT OPEN ETABLE.DAT** The file containing the error table information is missing. Program aborts safely as no assumptions may be made about the error table.

**CANT OPEN CURRENT.FIB** The file containing the current fibre configuration is missing, no further action is possible without this information so the program terminates safely.

**REPLY NOT UNDERSTOOD** An incorrect response was given at the basic command level, only 'I,E,F' or 'Q' in upper case are recognised.

**CANT OPEN SETUP FILE** Error opening the configuration setup file, this file containing the necessary instructions to setup the new configuration must be generated in file mode.

**INSTRUMENT ERROR** An error has occurred during an automatic field setup, subsequent commands were ignored thus leaving the field configuration incomplete.

**COMMAND UNKNOWN** The command entered was not recognised, it may have been spelt incorrectly or entered in lower case.

**CURRENT SPEED UNKNOWN** An attempt to change the operating speed of the X-Y carriage can only be made after the robot has been initialised (**GO**) as it is during the initialisation that the operating speed is defined.

**ERROR: MOTORS DISABLED** Command that requires a movement was issued before the motors had been enabled (**EM**).

**ERROR: INITIALISATION?** Command that required a movement was issued before the robot had been initialised (**GO**).

**ERROR HAS OCCURRED** Cannot process a command as a previous error has already occurred. The error flag must be reset and the error corrected before any new commands may be given.

**FIELD SETUP ABORTED** During the automatic setup of a fibre configuration the 'SPACE' bar was struck, thus aborting the field setup at a safe point.

**CANT OPEN E\_DATA.DAT** Could not open temporary file to store measurements of error table values.

**CANT OPEN M\_DATA.DAT** Could not open temporary file to store position error measurements.

**CANT OPEN DATA FILE** During an initialisation (GO) the software was unable to open CONTROL.DAT, the file containing all of the operating parameters for the robot.

**CANT OPEN CONFIG FILE** During an automatic field setup, the configuration file (\*.FIB) requested could not be opened, probably missing or spelt incorrectly.

**UNABLE TO OPEN FILE** While generating the sequence of commands needed to setup a field configuration the software could not open the file to write the list of commands into.

**ERROR IN # OF PIVOTS** The number of pivots specified in a \*.FIB file does not agree with the current software values.

**TIMEOUT ON CHAR IN** Handshaking routine failing to communicate with the Galil card.

**TIMEOUT ON CHAR OUT** Handshaking routine failing to communicate with the Galil card.

Pickup and putdown error messages

The following fibre pickup and putdown error messages are listed in sequential order for both the pickup and putdown operations. This means that if an error occurs, the checks listed above it must have been completed successfully.

Pickup error messages

**CANT PICKUP 2ND BUTTON** The control software thinks that the pickup head is already carrying a button so will not allow the picking up of a second button.

**NO BUTTON AT THIS X-Y** The control software is not aware of any button at the x,y co-ordinate that the pickup command was issued.

**LOW PICKUP** The pickup head has travelled too far (ie further than expected if button present). This means the button is not at the expected position. To recover from this error the fibre must be placed manually in the load ring. The load ring coordinates are automatically entered in the CURRENT.FIB file and in memory. The mimic display is also updated to show the fibre in the load ring.

**BUTTON BADLY PLACED** The pressure sensor indicates that the fibre button is not seated properly on the pickup head when the electromagnet first contacts the button. The magnet is turned off automatically and the pickup operation aborted. Since the fibre is not far from its expected position, recovery is possible by issuing a **LF n** (load fibre n) command and searching for the back illuminated fibre.

**PICKUP FAILED** The pressure sensor has indicated the absence of the fibre button after raising the Z axis to its carrying height. (NB The software automatically attempts a second pickup operation before issuing this error message) The fibre is in the correct location but is not being picked up. Check the pickup operation on the same fibre and other fibres to find out if the problem is that particular fibre or the electromagnet.

Putdown error messages

**NO BUTTON TO PUTDOWN** The pressure sensor indicates that there is no button on the electromagnet when a putdown command is issued. In file mode this almost certainly means that the fibre has fallen off the electromagnet in transit.

**CANT IDENTIFY BUTTON** The control software does not know the number of the fibre button on the electromagnet. This condition is probably due to the careless use of engineering commands.

**POSITION ILLEGAL** The position at which the putdown operation is requested is illegal in that it is either outside the range of the fibre or it may cross-over or collide with other fibres.

**BUTTON DROPPED** The pressure sensor indicates that there is no button on the electromagnet after it has descended to the fieldplate. The button must have gone away during the Z movement.

**LOW PUTDOWN** After the electromagnet has descended to the fieldplate the Z encoder indicates that it has gone further than would be expected if a button were present on the electromagnet. This message may occur when the pressure sensor has been effectively disabled using the **OP** command. The memory and **CURRENT.FIB** are updated to show the fibre in its pickup location.

## A brief description of the control software

The following section includes a very brief description of the control software that operates the WHT Autofib Prototype. There are four data files essential to the operation of the instrument, these contain the control parameters for the instrument, the parameters for the fibre module and fibre probes, the current locations of each of the fibres and the error table values for each of the fibres.

### CONTROL.DAT

This data file contains the various parameters required to operate the fibre positioner, including the software settings for the DC servo loops for the X,Y and Z axes, and default settings for pressure sensor.

VZ 15000	Max vertical speed
VM 50000	Max x-y speed
AZ 200000	Z axis acceleration
AC 400000	X-Y axis acceleration
KX 1	Integrator for x axis
KY 3	Integrator for y axis
GZ 55	Gain for z axis
GX 32	Gain for x axis
GY 55	Gain for y axis
P1 5000	Pressure limit
P2 0	Pressure limit
X0 -700	X centre mark mark offset
Y0 -1750	Y axis centre mark offset
NS 30	Default nudge size for jogging mode
VX -508	Viewing head X offset
VY 50658	Viewing head Y offset
SX 1.0000	Scale for x axis of camera (microns/pixel)
SY 1.0000	Scale for y axis of camera (microns/pixel)
FD 260	Fibre diameter in microns
UN 2	Under sampling factor in centroiding routine

## PARAMS.DAT

This data file contains a complete description of the fibre module at the present time. The physical dimensions of each fibre probe (as relevant to the anti-collision software) and their allowed patrol area in terms of maximum extension from the pivot and maximum non-radial angle allowed. The fibre probe array is described by the number of pivots, the number of guide fibres and the number of unused fibre pivots. The geometry of the array being specified by the fibre pivot radius and the radius of the circle of parked fibres.

72	Number of pivots
300000	Pivot circle radius
180000	Park circle radius
2000	Tube diameter (microns)
5000	Button diameter (microns)
2500	Prism diameter (microns)
4.0	Fibre theta (degrees)
310000	Fibre length (microns)
6000	Button/Prism centre to centre spacing (microns)
500000	Min distance from pivot for crossover
300000	Min distance from button for crossover
8	Number of guide bundles
1 10 19 28 37 46 55 64	Guide pivot numbers
0	Number of unused pivots
	Unused/Dead pivot numbers

## CURRENT.FIB

This file contains the current coordinates of each fibre probe. As a probe is moved, its entry in the file is automatically updated on the control computer hard disk. If the control software should be interrupted for some reason, it should be

possible to recover the instrument using the information maintained in the CURRENT.FIB file. The following excerpt from CURRENT.FIB shows the header information present in the data file, and the format of the fibre probe coordinates.

AUTOFIB CURRENT CONFIGURATION

72 pivots 56 spectral fibres 8 guide probes 8 unused:

Piv#	type	XPIV	YPIV	XBUT	YBUT	XOBJ	YOBJ
1	2	0	300000	-11540	70148	-11847	64066
2	1	-26146	298858	-18901	102070	-18772	95992
3	1	-52094	295442	-16755	17973	-16129	12429
4	1	-77645	289777	-27557	44468	-26328	38488
5	1	-102606	281907	-31592	38945	-29840	33212
6	1	-126785	271892	-56411	90534	-54211	84886
.....							

ETABLE.DAT

The file etable.dat contains a list of the error offsets for each fibre. This information is in the form of three numbers for each fibre probe, the fibre number, and the *l,b* error offsets. If the robot is being used without any error table, ETABLE.DAT should be replaced with a similar file containing zero values for *l,b*. The control software will not start up unless it can find this file.

Flow diagram of control code

Figure A-1 shows a flow diagram of the control software, the point of entry is gained at the top when the command 'CONTROL' is typed at the control

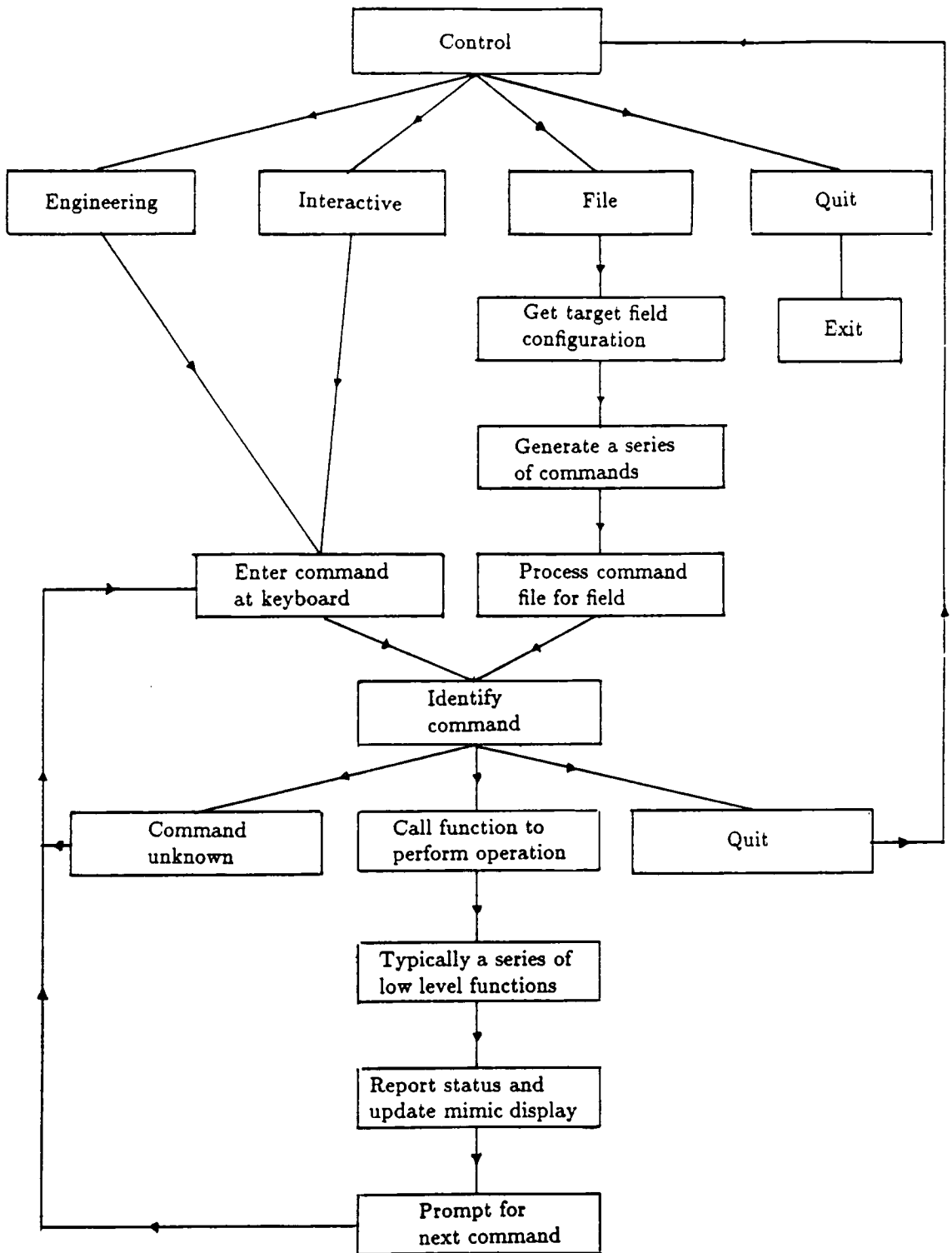


Figure A-1 Flow diagram for the control software for Autofib-1.5.



computer. The second row shows the four options at the basic command level: Interactive, File, Engineering or Quit.

#### Example section of code

An example function from the control code is reproduced below, this is the function *move(x,y)* which is responsible for the movement of the X-Y carriage. This is a typical function from the control code. The *move(x,y)* function may be used by itself from a **MO x y** command or from within numerous other commands. for example **VF n** which places the viewing head at the location of fibre n.

The first section of the code deals entirely with preventing any errors from occurring, checks are made to ensure that the motors have been enabled and initialised. Next, checks are made to ensure that the movement requested is a legal one. Finally, if the movement of the X-Y carriage is allowed, the necessary calculations are made (acceleration and maximum speed of each axis) and instructions sent to the Galil motion control card. Once the motion has been started, the software waits until the Galil card indicates that the motion has been completed, then updates the instrument status and returns a status flag to indicate that the motion has been completed successfully.

```
/* function to move the pickup head to a point X,Y in a straight line */

move(newx,newy)

long newx,newy;                                /* newx,newy is the destination point */

{
  extern long x,y,z;                            /* current coordinates of the pickup head */
  extern long piv_r,park_r;                    /* pivot circle and park circle radii */
  extern long butx[],buty[];                  /* arrays containing button coordinates */
  extern long pivx[],pivy[];                  /* arrays containing pivot coordinates */
  extern long vmax,acmax; /* maximum translational speed and acceleration */
```

```

extern long fibre_length;      /* maximum extension of fibre from pivot */

extern char status_message[];
extern char error_message[];
extern char cmd[16];

extern int idn;                /* identification number of fibre being carried */
                                /* if idn = 99 then no fibre is on electromagnet */
                                /* else if (idn.ge.1.or.idn.le.npivs) then */
                                /* fibre idn is on electromagnet */

extern int npivs;              /* number of pivots in fibre module */
double dx,dy,fract;
double r,x2,y2;

long vx,acx;
long vy,acy;
long i;

if (error_check() == NOT_OK) { /* check error status of instrument */
    return(ERROR);            /* if error has already occurred, */
                                /* then abort this movement */
}

if (check_status() == NOT_OK) { /* check that motors are enabled */
    return(ERROR);            /* and that robot has been initialised */
}

getpos();                      /* update current x,y,z position */

if (z > (UPPER +100)) { /* prevent movement when p/u head near plate */
    sprintf(error_message,"ERROR: MAGNET TOO LOW!");
    output_err();            /* if necessary write error message to screen */
    return(ERROR);
}

                                /* check position against x,y limits */
if ((labs(newx) > XMAX) || (newy > YMAX) || (newy < YMIN)) {
    sprintf(error_message,"ILLEGAL POSITION ");
    output_err(); /* if destination is outside of limits, display error */
    return(ERROR); /* message and abort move */
}

                                /* limit movement when button present on electromagnet */

```

```

if ( (button_off() != TRUE) || ( (idn > 0) && (idn <= npivs) )) {
    x2 = (double)newx *(double)newx;
    y2 = (double)newy *(double)newy;
    r = sqrt(x2 +y2);
    if (r > (double)(park_r +100) ) { /* cant move outside park circle */
        sprintf(error_message,"ILLEGAL MOVEMENT A ");
        output_err();
        return(ERROR);
    }
    r = distance(pivx[idn],pivy[idn],newx,newy);
    if (r > fibre_length) { /* cant move > fibre length from pivot */
        sprintf(error_message,"ILLEGAL MOVEMENT B ");
        output_err();
        return(ERROR);
    }
}

/* if have got this far then destination position is legal */

sprintf(status_message,"MOVE %07ld %07ld ",newx,newy);
output_stat(); /* display status message indicating about to start move */

if ((newx == x) && (newy == y)) { /* if already at new pos. do nothing */
    sprintf(status_message," ");
    output_stat(); /* movement completed successfully */
    return(FINISHED); /* return finished flag */
}

dx = fabs( (double)(newx -x) ); /* calculate shift in position */
dy = fabs( (double)(newy -y) ); /* for x and y */

/* calculate relative speeds and accelerations so that the x and y */
/* movements start and finish at the same time */

if ( dx > dy) { /* if x shift > y shift */
    fract = dy /dx;
    vx = vmax; /* x velocity = maximum */
    vy = (long)(fract *(double)vmax); /* y velocity = fraction of maximum */
    acx = acmax; /* x acceleration = max */
    acy = (long)(fract *(double)acmax); /* y acceleration = fraction */
}
else if (dy > dx) { /* if y shift > x shift */

```

```

    fract = dx /dy;
    vy = vmax;                               /* y velocity = maximum */
    vx = (long)(fract *(double)vmax); /* x velocity = fraction of maximum */
    acy = acmax;                             /* y acceleration = max */
    acx = (long)(fract *(double)acmax);      /* x acceleration = fraction */
}
else {                                       /* x and y shifts are equal */

    vx = vmax;                               /* set x and y velocities = max */
    vy = vmax;
    acy = acmax;                             /* set x and y accelerations = max */
    acx = acmax;
}
/* write commands to Galil card using com_out()
function to do communication */

sprintf(cmd,"SP %ld",vx);                   /* issue speed commands to x,y axes */
com_out(cmd,X_ADDR);
sprintf(cmd,"SP %ld",vy);
com_out(cmd,Y_ADDR);
sprintf(cmd,"AC %ld",acx);                  /* issue acceleration commands to x,y axes */
com_out(cmd,X_ADDR);
sprintf(cmd,"AC %ld",acy);
com_out(cmd,Y_ADDR);
sprintf(cmd,"PA %ld",newx);                 /* issue position commands to x,y axes */
com_out(cmd,X_ADDR);
sprintf(cmd,"PA %ld",newy);
com_out(cmd,Y_ADDR);
strcpy(cmd,"BG");                          /* issue begin commands to x/y axes */
com_out(cmd,X_ADDR);
strcpy(cmd,"BG");
com_out(cmd,Y_ADDR);

if (wait() == ERROR)
    return(ERROR);                          /* wait until motion in x and y is complete */

strcpy(cmd,"ST");                          /* issue stop commands to x,y axes */
com_out(cmd,X_ADDR);
strcpy(cmd,"ST");
com_out(cmd,Y_ADDR);

for (i=0; i < 10; i++)                     /* update pickup head position */
    getpos();                               /* several times */

```

```
if (button_on()) {                /* if button present on pickup head */
    butx[idn] = x;                /* then update button coordinates as well */
    buty[idn] = y;
}
sprintf(status_message,"          ");
output_stat();                   /* clear status window on mimic display */
return(FINISHED); /* move completed successfully, return finished flag */

}
```

## Appendix B

Appendix B contains some information about the configuration software used with Autofib-1.5. The first file reproduced below is an example of the input data file for the configuration software. The first letter of each record is an identifier which tells the software how to process the information on the rest of the line.

- L** Is a label for the target field (optional)
- D** The date of that the observations are to be made. This is optional, the default being the current date.
- E** The equinox of the coordinates.
- O** The sky position angle for the instrument. This is the 'Demand Sky PA' at the WHT, or the instrument rotator angle at the AAT. Again this information is optional, the default being 90°.
- H** The hour angle the observations are to be made at, this information is optional, the default being zero hours.
- C** The coordinates of the centre of the field. This information must be supplied in the input file. This will be the final telescope pointing position for the target field.
- S** The record contains information about a sky position.
- F** The record contains information about a fiducial object.
- P** The record contains information about a target (or program) object.



P	15	15	44.43	2	12	50.7	1.0	*	35	260	15.41	9.99	99
F	15	15	44.40	2	13	4.2	1.0	*	36	259	12.78	9.99	99

The configuration software reads in the above input file and converts the sky program and fiducial object positions to x,y coordinates relative to the supplied centre of the field. The software then reports any defaults used, and starts to assign the fibres to objects. Once the program has completed this stage, it prompts the observer to ask if it is required to plot the result on the IKON image display. If this option is used, the fibre configuration is plotted on the image display and the observer has the opportunity to interactively change the configuration. This option is not followed in the example below.

After reporting on the success of the fibre configuration procedure, the program asks if the observer wishes to change the rotator angle. This option can be quite useful in order to align any fiducial objects with the guide fibres.

```
$ run configure
```

```
Input file? > m5
```

```
Opening config and log files
Reading through field datafile
```

```
Default hour angle used (0.0)
Crossing of fibres disabled
```

```
Fibre park configuration got from PARK.FIB
Processing 19 objects, 7 skys & 64 fibres.
How many sky fibres are required ? 7
```

```
Median position = 69461.09 -32142.80
Pivot nearest median point = 50
Objects sorted into order from median point
Placing first fibre
```



Trying object No. 1  
Trying object No. 2  
First fibre done

Returning to try and place all unused fibres

Configuration has 53 fibres, 7 objects and 0 skys unassigned  
Display on screen ? (Args,Ikon etc ) : n

Final configuration has 53 fibres 7 objects and 0 skys unassigned

Rotator angle is currently 90.0  
Change the rotator angle ?: n

Take hardcopy of final configuration ?: n

Fibre configuration in M5.fib  
Fibre log file in M5.log

The last option is to request a hard copy of the final fibre configuration. The output of the program is in the form of two files. The \*.FIB (where \* is the field name) is not shown below, but is identical in form to the CURRENT.FIB file shown in Appendix A, except that the coordinates of the fibres refer to the new fibre configuration. The \*.LOG file is for the information of the observer, and is reproduced below. The original information contained in the input file for each object is retained, and appended with the corresponding x,y instrument coordinates and the fibre and spectrograph slit numbers of any fibres that have been assigned.

Lastly, some final information about the fibre configuration is contained in the log file. In case any spare fibres were placed randomly on 'sky' during the

interactive configuration procedure, the x,y locations of such fibres are listed in the log file.

Field file = M5  
 Rotator angle = 90.0 degrees  
 Demand Sky PA (WHT April 1990) = 102.1 degrees  
 Field centre = 15 16 0.000 2 15 15.00  
 Hour angle = 0.00 hours  
 Date of observation = 1989.1670  
 Equinox of coordinates = 1950.0

RA	DEC	X	Y					Piv	Slit
Fiducial stars									
F 15 15 42.96	2 10 16.7	56.458	-66.303	1.0	*	18	253		
F 15 15 33.48	2 12 56.3	88.069	-31.003	1.0	*	23	210		
F 15 15 32.75	2 14 3.6	90.541	-16.088	1.0	*	24	206	B	
F 15 15 42.57	2 14 7.5	57.899	-15.131	1.0	*	30	252		
F 15 15 39.84	2 13 46.5	66.965	-19.813	1.0	*	32	238		
F 15 15 44.40	2 13 4.2	51.778	-29.150	1.0	*	36	259		
Program objects									
P 15 15 26.74	2 15 13.0	110.563	-0.755	1.0	*	10	185	II21	56 44
P 15 15 27.15	2 14 57.6	109.191	-4.166	1.0	*	11	188	II21	
P 15 15 38.42	2 8 25.4	71.474	-91.024	1.0	*	14		C3	44 35
P 15 15 36.93	2 9 5.0	76.458	-82.258	1.0	*	15		C1	45 36
P 15 15 36.37	2 9 47.8	78.349	-72.773	1.0	*	16	219		
P 15 15 40.81	2 10 24.5	63.613	-64.594	1.0	*	17		C5	47 37
P 15 15 44.73	2 10 43.9	50.589	-60.255	1.0	*	19	263		43 34
P 15 15 41.61	2 11 24.2	60.991	-51.349	1.0	*	20		C6	48 38
P 15 15 39.07	2 12 0.9	69.461	-43.235	1.0	*	21		C4	50 39
P 15 15 33.37	2 12 13.9	88.413	-40.406	1.0	*	22	209		
P 15 15 36.17	2 14 40.5	79.196	-7.874	1.0	*	25	218	V29	
P 15 15 38.36	2 15 24.4	71.942	1.880	1.0	*	26	227	V2	
P 15 15 39.54	2 15 5.7	68.007	-2.255	1.0	*	27	234		57 45
P 15 15 38.54	2 14 26.7	71.307	-10.912	1.0	*	28	228		54 43
P 15 15 40.73	2 14 4.8	64.023	-15.747	1.0	*	29	242		
P 15 15 40.44	2 13 50.6	64.973	-18.899	1.0	*	31	241		53 42
P 15 15 39.58	2 13 1.3	67.798	-29.838	1.0	*	33	235		52 41
P 15 15 42.27	2 12 16.7	58.833	-39.702	1.0	*	34	251		
P 15 15 44.43	2 12 50.7	51.671	-32.143	1.0	*	35	260		51 40

Sky positions

S 15 15 44.43	2 15 41.6	51.778	5.751 1.0 *	1 261	II-1	58 46
S 15 15 54.18	2 11 13.1	19.193	-53.692 1.0 *	2 377		38 29
S 15 16 20.54	2 14 47.4	-68.314	-5.922 1.0 *	3 929		18 14
S 15 16 17.65	2 17 56.1	-58.578	35.890 1.0 *	4 911	I-74	11 99
S 15 16 2.85	2 20 24.4	-9.274	68.630 1.0 *	5 630		72 56
S 15 15 28.55	2 18 4.8	104.652	37.355 1.0 *	8 192	II42	60 48
S 15 15 27.10	2 17 19.2	109.452	27.230 1.0 *	9 187	II37	59 47

Fibres on unmarked positions

X	Y	Piv#	Slit#
---	---	------	-------

None assigned

